JAERI-M
90-172

THYDE-W: RCS (Reactor Coolant System) ANALYSIS CODE

October 1990

Yoshiro ASAHI, Kiyoshi MATSUMOTO
and Masashi HIRANO

日本原子力研究所
Japan Atomic Energy Research Institute

JAERI-Mレポートは，日本原子力研究所が不定期に公刊している研究報告書です。
入手の問合わせは，日本原子力研究所技術情報部情報資料課（〒319-11茨城県那珂郡東海村）あて，お申しこしください。なお，このほかに財団法人原子力弘済会資料センター（〒319-11 茨城県那珂郡東海村日本原子力研究所内）で複写による実費頒布をおこなっております。

JAERI-M reports are issued irregularly.
Inquiries about availability of the reports should be addressed to Information Division Department of Technical Information, Japan Atomic Energy Research Institute, Tokai-mura, Naka-gun, Ibaraki-ken 319-11, Japan.

編集兼発行　日本原子力研究所
印　　刷　いばらき印刷㈱

JAERI-M 90-172

THYDE-W: RCS (Reactor Coolant System) Analysis Code

Yoshiro ASAHI, Kiyoshi MATSUMOTO[+] and Masashi HIRANO[+]

Department of Reactor Engineering
Tokai Research Establishment
Japan Atomic Energy Research Institute
Tokai-mura, Naka-gun, Ibaraki-ken

(Received September 10, 1990)

THYDE-W is applicable not only to transient analyses, but also to steady state analyses of RCS behaviors. In a steady state analysis, the code generates a solution satisfying the transient equations without external disturbances. In a transient analysis, the code calculates temporal RCS behaviors in response to various external disturbances. One of the most important features of THYDE-W is the fact that mass, momentum and energy conserve.

The first half of the report is the description of the methods and models for use in the THYDE-W code, i.e., (1) the thermal-hydraulic network model, (2) the various RCS components models, (3) the heat sources in fuel, (4) the heat transfer correlations, (5) the mechanical behavior of clad and fuel, and (6) the steady state adjustment. The second half of the report is the user's manual for the THYDE-W code (version SV05L07) containing the items; (1) the program control, (2) the input requirements, (3) the execution of THYDE-W jobs, (4) the output specifications and (5) the sample input data set and the sample calculation.

Keywords: THYDE-W Code, RCS, Methods, Models, Heat Transfer, Control, Thermal-Hydraulic Network, Clad, Fuel, LOCA, RCS Transients, Version SV05L07, Sample Problem, User's Manual

---

+ Department of Reactor Safety Research

JAERI－M 90－172

THYDE－W：RCS（原子炉冷却材系）解析コード

日本原子力研究所東海研究所原子炉工学部
朝日　義郎・松本　　潔[+]・平野　雅司[+]

（1990年9月10日受理）

THYDE －Wコードは，RCSのふるまいの過渡解析だけでなくその定常解析にも応用できる。本コードは，定常解析では外乱なしの過渡方程式を満足する解を生成し，過渡解析では各種外乱に対するRCSの応答を求める。THYDE－Wの最も重要な特長は質量，運動量，エネルギが保存することである。

本報告書の前半には，THYDE－Wで使われている諸方法と諸モデル；(1) 熱水力回路網，(2) RCSの諸要素，(3) 燃料中の熱源，(4) 熱伝達相関式，(5) 被覆材と構造材の機械的ふるまい，(6) 定常状態の調整，について述べてある。後半は，THYDE－Wコード（SV05L07版）の使用手引書であって，以下の項目からなっている：(1) プログラム制御，(2) 入力仕様，(3) ジョブの実行，(4) 出力仕様，(5) サンプル入力データとサンプル計算結果。

東海研究所：〒319－11　茨城県那珂郡東海村白方字白根2－4
＋ 原子炉安全工学部

Contents

目　　次

LIST OF TABLES *PAGE*

LIST OF FIGURES *PAGE*

1. Introduction

The subject matter of this document is the description of the computer code, THYDE-W, to be applicable not only to transient analyses, but also to steady state analyses of reactor coolant system (RCS) of water reactors. Especially, THYDE-W is applicable to a large break loss-of-coolant accident (LB-LOCA), which can be considered to be the most critical for testing methods and models[2)-10)] for plant dynamics, since thermal-hydraulic conditions in the system drastically change during the transient. Therefore, THYDE-W has intensively been applied to LOCA analysis to verify its methods and models.

There are three major problems in thermal-hydraulic analysis, which appear typically in an LB-LOCA. First of all, imbalance of mass or momentum or energy may result if improper space differencing is applied to the conservation equation. If space differencing is incorrect, mass imbalance in a LOCA analysis could be so large that a large amount of mass comparable to injected ECC water could "disappear" from the system. Secondly, even if the space differencing is correct, imbalance still could occur unless the equations thus spatially differenced are solved "exactly" by applying a non-linear implicit scheme. Thirdly, various mode transitions, e.g., coolant phase change may bring about numerical instabilities. These problems predominate especially at low pressure. This fact is the main reason why the secondary system of a PWR or the neiborhood of the turbine of a BWR, which is at low pressure already at a steady state, has not been adequately included in a transient analysis. In a LOCA analysis, in particular, to avoid numerical instability induced by condensation ("water packing") and to somehow

continue a reflood calculation, it is customary either to raise the ECC water enthalpy or to neglect the time derivatives in the conservation equations. These assumptions are not only unconvincing, but also are likely to lead to erroneous conclusions.

The main features of THYDE-W are (1) the steady state adjustment, (2) the new thermal-hydraulic network model, (3) the non-linear implicit scheme for thermal-hydraulics, (4) the non-equilibrium models, (5) the automatic time step width control and (6) vectorization of the program :

(1) THYDE-W carries out steady state adjustment, which is complete in the sense that the state obtained is the set of exact solutions to the null transient problem, i.e., the transient problem without an external disturbance. Originally, this capability was developed to obtain a well defined initial state from which a transient calculation by THYDE-W can start. From a different point of view, it provides THYD-W with another capability, that is, what is called thermal-hydraulic design of RCSs.

(2) A new representation of a control volume has made it possible to develop a new thermal-hydraulic network model, which well matches our physical intuitions. The model reduces the flow equations by three steps, each of which is closely related to topological features of the hydraulic network. The new model does not depend on specific forms for the conservation equations, but is quite general.

(3) To solve the equations of a network "exactly", an iterative method which may be referred to as a non-linear implicit method is applied based on the new network model. Since a linear implicit method does not yield an "exact" solution, its applicability is questionable especially at low pressure when non-linearity of the flow equations

predominates.

(4) The non-linear implicit scheme for use in the thermal-hydraulic network requires continuity of all the parameters involved in the flow equations. Physically, this amounts to taking into consideration non-equilibrium effects arising from various mode transitions.

(5) THYDE-W determines the time step width automatically as the calculation proceeds. The non-linear implicit method, the non-equilibrium model and the steady state adjustment are all combined to materialize the automatic time step width control of THYDE-W.

These features have enabled THYDE-W to perform a through calculation [43] of LB-LOCAs without an artificial change of the methods and models.

Chapters 2 to 6 describe the methods and model for use in THYDE-W, while chapters 7 to 10 are the user's mannual. Chapter 11 presents the results of a PWR LB-LOCA calculated with THYDE-W. Whenever it is found necessary to refer to input specifications in the discussions in chapters 2 to 6, this will be done by referring to the relevant input data block as BBXX, where XX is the identification number of input data blocks described in section 8.4.

What is improved with THYDE-W as compared to THYDE-P2[45] is ; (1) analyses of a plural number of disjoint loops or nets are possible, (2) the control system simulation model is included, (3) the trip model is better, (4) heavy water as a coolant is allowed, (5) the effect of drift flux is accounted for in the steady state adjustment, (6) boron transport is included and (7) to obtain loop heat balance, the option of adjusting the enthalpy distribution is prepared in addition to that of adjusting heat exchanger areas.

2. *Thermal-Hydraulics*

In this chapter, we will discuss the thermal-hydraulic network model of the THYDE-W code. Starting from the three conservation equations for a two-phase mixture, we will develop the new calculation scheme for thermal-hydraulics such that mass, momentum and energy conserve. If we stay within the framework of the three conservation equations for two-phase mixture, however, it will be difficult to explain two major problems; (1) phase separation and (2) phase change. In order to solve these problems, we are obliged to resort to what is called UV (unequal velocity) and UT (unequal temperature) models. In THYDE-W, the UV effect will be accounted for on the basis of the drift flux model (see section 2.2.2), while the UT effect will be incorporated by taking into consideration two other conservation equations (section 2.2.3).

In section 2.1, nodes and junctions for use in the THYDE-W thermal-hydraulic network model are defined. It is the special node-and-junction representation of a thermal-hydraulic system that will enable us to construct the new thermal-hydraulic network model described in sections 2.2 and 2.3. In section 2.2, we will derive the equations for nodes and junctions from the conservation equations. In section 2.3, the new algorithm for a thermal-hydraulic system is presented. The accumulator and steam separator models are described in section 2.4 along with the hydraulic machine model. In section 2.5 , we will discuss loss coefficients, valves and critical flows.

2.1 Network Components

In the THYDE-W code, a coolant network is represented by nodes and junctions shown in Tables 2-1 and 2-2. THYDE-W has a special model for accumulators (refer to section 2.4.2). In such a representation of a coolant network, a node and a junction appear alternately.

A normal node is a volume element to which the one-dimensional flow model may be applicable (see Fig.2-1-1). It is the new representation of the conservation laws in such a volume element, i.e., a normal node, that will enable us to construct the new thermal-hydraulic network model to be described in sections 2.2 and 2.3. We will see later that even a pump can be represented by a normal node. Let the positive direction of a flow be that of the steady state flow. For a node, the inlet and outlet of the steady state flow will be referred to as points A and E, respectively.

A normal junction serially connects two normal nodes possibly with a sudden area change (see Fig.2-1-2). Among nodes and junctions in Table 2-1 and 2-2, only mixing junctions are multiple-branched (see Fig.2-1-3). Owing to this very feature, they play an essential role in forming a complex coolant network such as a reactor coolant system (see Fig.2-3-1). In THYDE-W, a steam separator is simulated by a mixing junction (refer to section 2.4.3).

A boundary junction (Fig.2-1-4) will be placed at an interface between our thermal- hydraulic network and its exterior. A dead end of a duct can be simulated by a boundary junction through which no interaction with the exrerior takes place. Boundary junctions can be classified into two groups, i.e., pressure sources (p-sources) and mass flux sources (G-sources). We call a normal node adjacent to a boundary

junction a boundary node, exemplified by a guillotine break node, a dead end node and an injection node. Depending on the situation, they can be either p-sources or G-sources. A dead end is a special case of G-sources. The boundary conditions of the system will be incorporated in the model by modifying the node equations of the boundary node.

The duct connecting a boundary junction to a mixing junction of the network is called a linkage duct which is composed of a number of normal nodes called the linkage nodes (see Fig.2-1-4). Whether the coolant may be initially flowing or not, we let point E of a linkage duct be the end adjacent to the boundary junction, whereas point A be the other end adjacent to the mixing junction. Accordingly, points A and E of each node in the linkage duct can be determined. For a stagnant chain of nodes from a mixing junction to another, one can arbitrarily decide points A and E of the chain. Accordingly, points A and E of each node of the stagnant chain can be determined. It should be noted that prior to a double-ended break, the break point is regarded as a normal junction, but after an occurence of a break the break point will become a boundary junction. Finally, we note that a node and a mixing junction have volume whereas a normal or boundary junction is volumeless. We also note that in a power plant the thermal-hydraulic network can be regarded as a medium which combines thermal-hydraulically the thermal, mechanical and neutronic behaviors of the system.

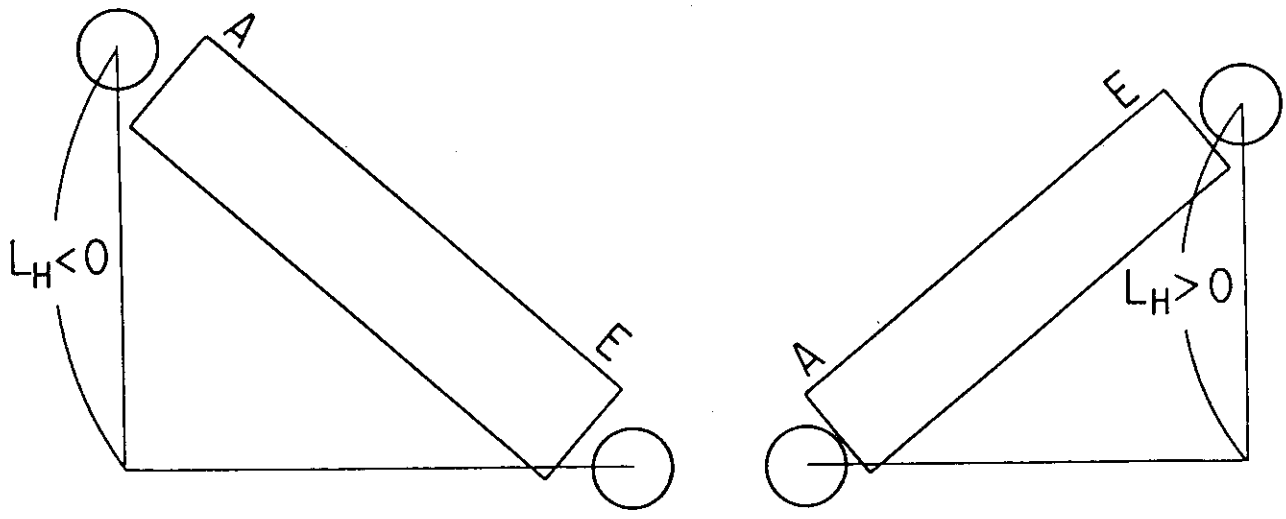

Fig.2－1－1　Normal Node

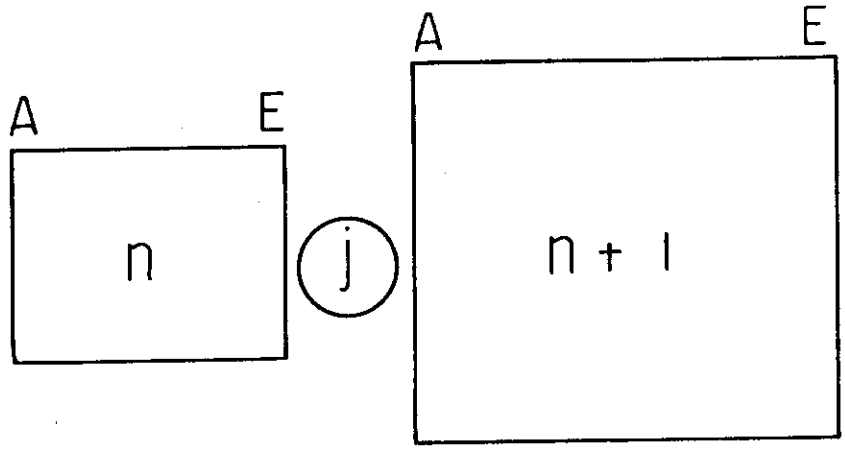

Fig.2－1－2　Two Successive Normal Nodes Connected by Normal Junction

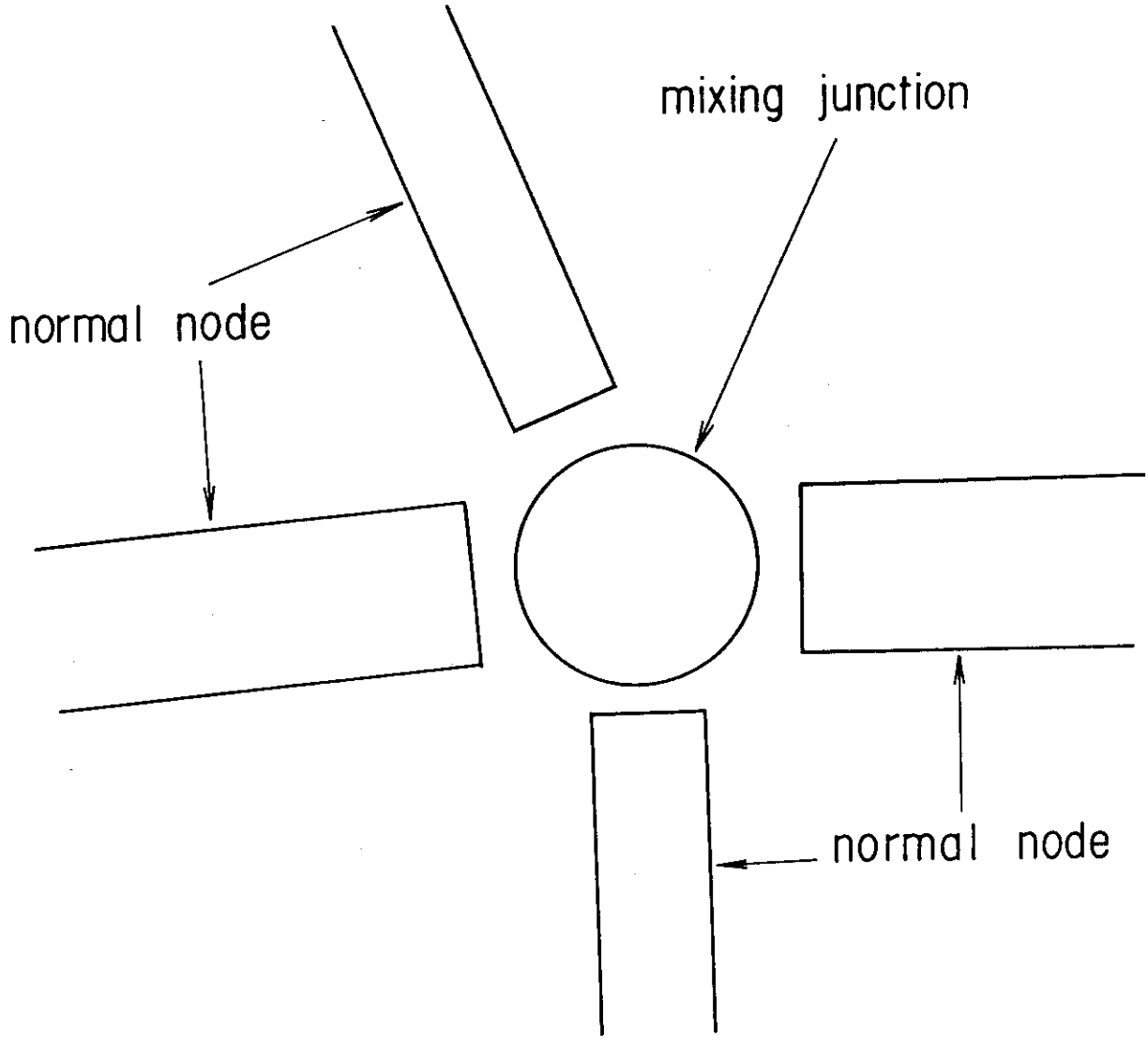

Fig.2-1-3 Mixing Junction

Table 2-1 Nodes

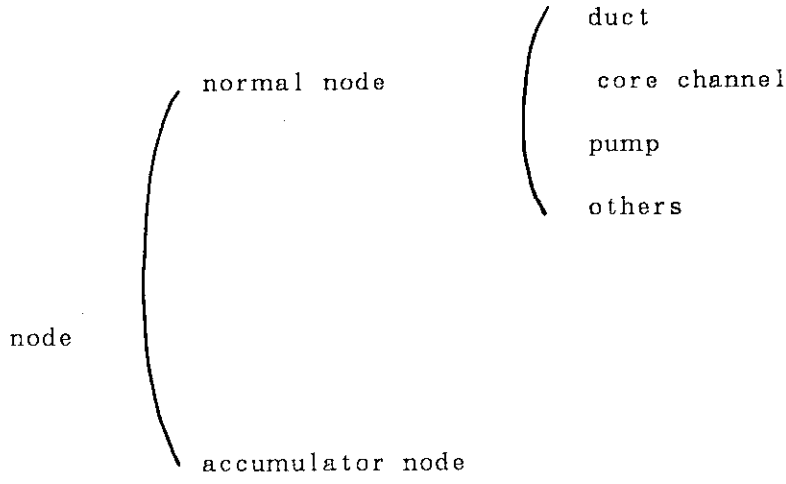

Table 2-2 Junctions

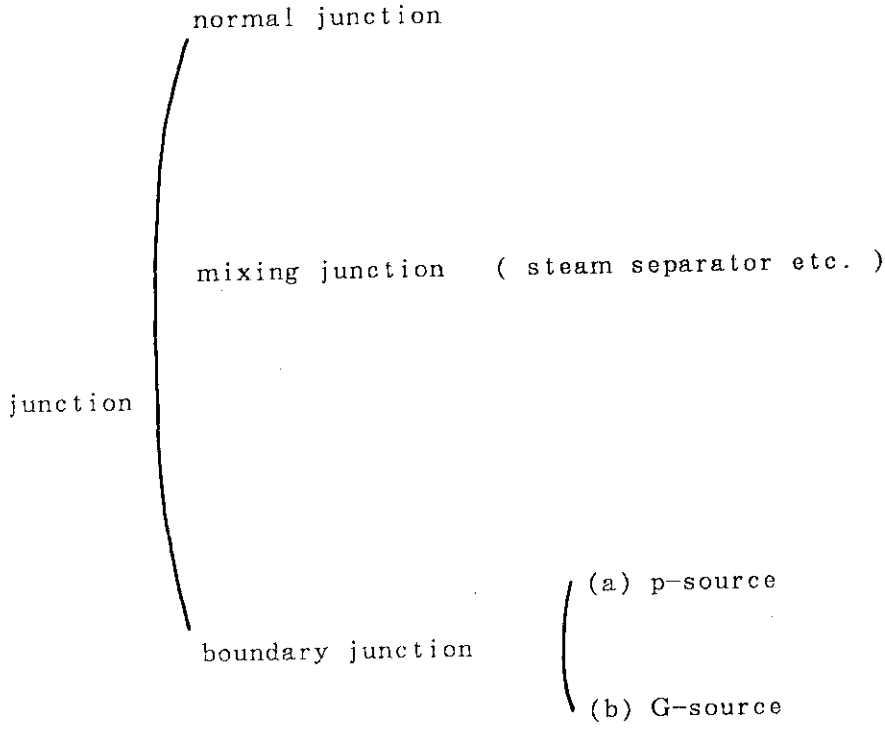

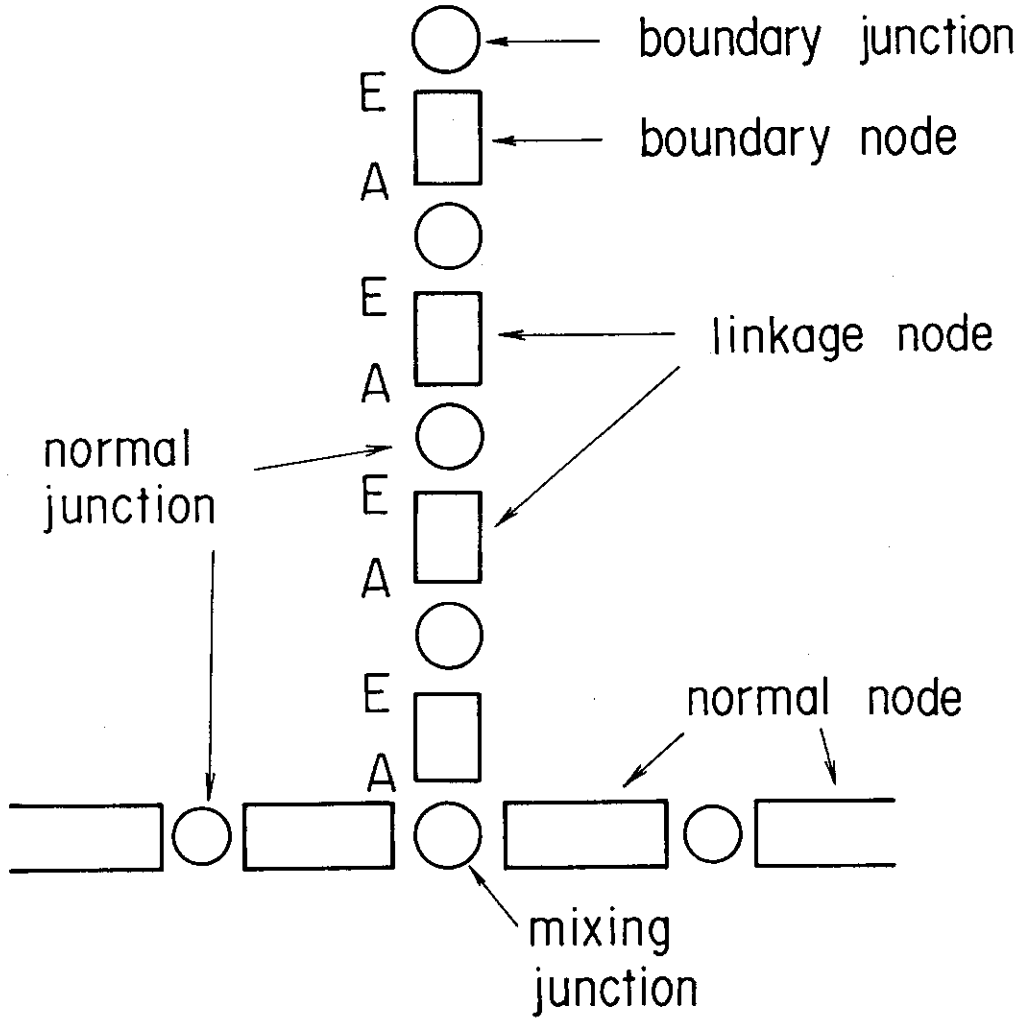

Fig.2－1－4 Linkage Nodes and Boundary Junction

2.2 *Derivation of Network Equations*

In this section, we will derive the equations for the network.

2.2.1 *Conservation Equations for Two-Phase Mixture*

The one-dimensional mass, energy and momentum equations for a two-phase mixture[2-6] are given by

$$\frac{\partial}{\partial t}A\rho+\frac{\partial}{\partial z}AG=0 \tag{2-2-1}$$

$$\frac{\partial}{\partial t}A\rho h+\frac{\partial}{\partial z}A\Lambda=Aq''' \tag{2-2-2}$$

and

$$\frac{\partial}{\partial t}AG+A\frac{\partial p}{\partial z}+\frac{\partial}{\partial z}A\Psi=-A\rho g-\frac{A}{2}\left(\frac{\kappa}{L}+\frac{f}{D}|G|G\right)\frac{\Phi^2}{\rho_f} \tag{2-2-3}$$

where

$$\kappa=kG|G| \qquad Re\geq Re_t$$
$$=(k\mu/D)Re_tG \qquad Re\leq Re_t \tag{2-2-4}$$

$$\rho=\alpha\rho_g+(1-\alpha)\rho_f \tag{2-2-5}$$

$$G=\alpha\rho_g u_g+(1-\alpha)\rho_f u_f \tag{2-2-6}$$

$$\Psi=\alpha\rho_g u_g^2+(1-\alpha)\rho_f u_f^2 \tag{2-2-7}$$

$$\Lambda=\alpha\rho_g h_g u_g+(1-\alpha)\rho_f h_f u_f \tag{2-2-8}$$

$$\rho h=\alpha\rho_g h_g+(1-\alpha)\rho_f h_f \tag{2-2-9}$$

We consider in the following way. The solution (p, h) to the conservation equations for the mixture, i.e., Eqs.(2-2-1) to (2-2-3) defines the equilibrium state. And non-equilibrium density ρ in Eqs.(2-2-1) to (2-2-3) will be obtained from equilibrium density ρ with a time lag. The equation to govern the lag will be described in subsection 2.2.3. The actual (non-equilibrium) state will asymptotically approach the equilibrium by transferring energy between

the phases, if the mixture is left without external disturbances.

2.2.2 *Thermal-Hydraulic Quantities*

We eliminate u_g and u_f in Eqs.(2-2-7) and (2-2-8) with the help of

$$u_f=\frac{G-\alpha\rho_g u_{rel}}{\rho}$$

and

$$u_g=\frac{G+(1-\alpha)\rho_f u_{rel}}{\rho}$$

Then, we obtain

$$\Psi=\frac{G^2}{\rho}+B \tag{2-2-10}$$

and

$$\Lambda=Gh+I \tag{2-2-11}$$

where

$$B=\frac{\alpha(1-\alpha)\rho_g\rho_f}{\rho}u_{rel}^2 \tag{2-2-12}$$

and

$$I=\frac{\alpha(1-\alpha)\rho_g\rho_f h_{gf}}{\rho^2}u_{rel}. \tag{2-2-13}$$

The relative velocity u_{rel} may be given by the drift flux model[11] as

$$u_{rel}=\frac{u_{gj}}{1-\alpha} \tag{2-2-14}$$

where u_{gj} is the drift velocity[12][13], and

$$u_{gj}=1.14\left[\frac{\sigma g(\rho_{fs}-\rho_{gs})}{\rho_{fs}^2}\right]^{1/4}S_\alpha^2 \tag{2-2-15}$$

for the "churn-turbulent" bubbly flow. Factor S_α is defined such that

$$S_\alpha=1-e^{(1-\alpha)/(1-\alpha_c)} \tag{2-2-16}$$

with $\alpha_c=0.8$, in order to avoid divergence of u_{rel} when α approaches unity. When α is large, the flow pattern becomes annular or stratified flow so that u_g and u_f could change independently. Momentum flux B has been found usually not effective, while enthalpy flux I may play an important

role, for example, in phase separation under a vertical low flow condition.

Next, we consider a parameter x_1 defined such that

$$x_1 = \frac{h - h_{fs}(p)}{h_{gf}(p)} \quad , \tag{2-2-17}$$

where $h_{gf} = h_{gs} - h_{fs}$. Equation (2-2-17) can be transformed to

$$h = h_{gs}x_1 + h_{fs}(1 - x_1) \quad , \tag{2-2-17a}$$

which implies that x_1 is the mass fraction of the vapor phase in a two-phase mixture, that is , mass quality. Parameter x_1, however, can become either greater than unity or less than zero. Therefore, we might define mass quality such that

$$\begin{aligned} x_c &= 1 && h > h_{gs} \\ &= x_1 && h_{fs} \leqq h \leqq h_{gs} \\ &= 0 && h < h_{fs} \quad . \end{aligned}$$

But, since the derivatives of mass quality defined above are not continuous at $x_1 = 0$ or 1, we may fail to obtain a solution such that mass, energy and momentum conserve. This is one of the problems associated with phase change.

In order to overcome the difficulty, we will define x_c to be referred to as equilibrium mass quality which is a smooth function of p and h and bounded between zero and unity such that

$$\begin{aligned} x_c &= a e^{-(a - x_1)/a} && x_1 < a \\ &= x_1 && a \leqq x_1 \leqq b \\ &= 1 - (1-b) e^{-(x_1 - b)/(1-b)} && x_1 > b \end{aligned} \tag{2-2-18}$$

where $0 < a < b < 1$. In terms of x_c, we can define

$$\alpha_c = \frac{x_c \rho_f^c}{x_c \rho_f^c + (1 - x_c)\rho_g^c} \quad , \tag{2-2-19}$$

which is $0 < \alpha_c < 1$. In Eq.(2-2-19), $\rho_g^c = \rho(p, h_g^c)$ and $\rho_f^c = \rho(p, h_f^c)$, where equilibrium specific enthalpies h_g^c and h_f^c are yet to be defined in the

following. We will call the quantity α_c the void fraction in what is called the equilibrium model (see subsection 2.2.3).

Next, we discuss the implications of the modifications of x_1 for $x_1 < a$ and $x_1 > b$, i.e., Eq.(2-2-18). Consider the equilibrium state so that for example $\alpha = \alpha_c$. Then Eq.(2-2-9) gives

$$h = x_c h_g^c + (1-x_c) h_f^c \quad , \tag{2-2-20}$$

since Eq.(2-2-19) gives

$$x_c = \frac{\alpha_c \rho_g^c}{\rho^c} = \frac{\alpha_c \rho_g^c}{\alpha_c \rho_g^c + (1-\alpha_c)\rho_f^c} \quad .$$

Equation (2-2-20) should be compared with another expression for h;

$$h = x_1 h_{gs} + (1-x_1) h_{fs} \quad , \tag{2-2-21}$$

that is Eq.(2-2-17a).

For $a \leqq x_1 \leqq b$, x_1 is equal to x_c so that we can define

$$h_g^c = h_{gs} \tag{2-2-22}$$

and

$$h_f^c = h_{fs} \quad . \tag{2-2-23}$$

For $x_1 < a$, assuming $h_g^c = h_{gs}$ in Eq. (2-2-20), we obtain

$$h_f^c = \frac{h - x_c h_{gs}}{1-x_c} \tag{2-2-24}$$

and

$$h_g^c = h_{gs} \quad . \tag{2-2-25}$$

For $x_1 > b$, assuming $h_f^c = h_{fs}$, we similarly obtain

$$h_g^c = \frac{h - h_{fs}(1-x_c)}{x_c} \tag{2-2-26}$$

and

$$h_f^c = h_{fs} . \tag{2-2-27}$$

Equation (2-2-24) implies that for a two-phase mixture whose specific enthalpy h is nearly equal to h_{fs}, h_f^c is less than h_{fs}, while Eq.(2-2-26) implies that for a two-phase mixture whose specific enthalpy h is nearly

equal to h_{gs}, h_g^c is greater than h_{gs}. Equilibrium specific enthalpies h_g^c and h_f^c thus obtained can be used to obtain gas and liquid densities.

In transient analyses, it has been found that smoothing of equilibrium void fraction α_e defined by Eq.(2-2-19) as well as equilibrium specific enthalies h_g^c and h_f^c defined by Eqs.(2-2-22) to (2-2-27) does not suffice to overcome difficulties such as "water packing" encountered near $x_1 = 0$ at low pressure. In the next subsection, we intend to deal with this problem.

2.2.3 Relaxation Equation for Void Fraction

In this subsection, we will derive the relaxation equation for void fraction, which is closely related to what is called the UT model or the non-equilibrium model. The assumptions and comments concerning this derivation are listed below:

(1) In this subsection, we will assume that mixture specific enthalpy h has already been obtained by solving Eq.(2-2-2) . It should be reminded that mixture specific enthalpy h contains the effects of heat trasferred from the wall and enthalpy transported by the two-phase mixture flow. Therefore, these effects do not present themselves in the following discussion, but only heat flow between the phases is involved

(2) Given any pair of p and h, we can uniquely define the (fictitious) equilibrium state with $\alpha_e(p,h)$ $h_f^c(p,h)$ and $h_g^c(p,h)$ as described in the previous subsection. In a saturated equilibrium state, vapor and liquid temperatures are equal to the saturation temperature $T_s(p)$ so that there is no heat flow between the phases. (Strictly speaking, this is not correct for "unsaturated" equilibrium state with

$x_1 < a$ or $b < x_1$.)

(3) A non-equilibrium state can be defined by p, h and a non-equilibrium void fraction, say, α. In a non-equilibrium state, $T_g \neq T_f$ so that there will be heat flow between the phases.

(4) In view of comment (2), to each actual state with p, h and α, there corresponds an equilibrium state defined by p and h. An equilibrium state actually exists at a steady state.

(5) Evaporation is accounted for as a change of α_e, regardless of equilibrium or non-equilibrium. Thus, evaporation in a non-equilibrium state is taking place as much as in the corresponding equilibrium state. The deviation from the equilibrium state contributes not to evaporation, but to heat flow between the phases leading to thermal-equilibrium.

(6) Consider a non-equilibrium state with constant p and constant h. Then, no evaporation occurs in the corresponding equilibrium state, and hence neither in the non-equilibrium state. But, non-equilibrium void fraction α can still change such that α asymptotically approaches to $\alpha_e(p,h)$ due to energy transfer (or heat flow) between the phases, if the mixture is left without external disturbances.

In the following, under several assumptions, we will derive the equation which governs the dynamic behavior of non-equilibrium void fraction α.

Let the incremental values with δ mean the deviation from the equilibrium value. Then, any quantity such as void fraction α and vapor generation rate Γ can be divided into two parts such that

$$\alpha = \alpha_e + \delta\alpha \quad , \tag{2-2-28}$$

and

$$\Gamma = \Gamma_e + \delta\Gamma \quad . \tag{2-2-29}$$

Since it is assumed that the rate of phase change in a nonequilibrium state is the same as in the corresponding equilibrium state, we have $\delta\Gamma = 0$ so that Eq.(2-2-29) gives

$$\Gamma = \Gamma_c \quad . \tag{2-2-30}$$

Similarly, heat input to the vapor phase can be set such that

$$q_g''' = (q_g''')^c + \delta(q_g''') \tag{2-2-31}$$

where the first term accounts for the portion of the external heat input to the vapor phase to be used for phase change at the corresponding equilibrium state, while the latter acconts for interfacial heat transfer. The latter may be expressed as

$$\delta\ (q'''_g) = \frac{S_{int}\varphi_{int}}{V} \tag{2-2-32}$$

where V is the total volume of the mixture of interest, while S_{int} is the total interfacial area in V. The interfacial heat flux φ_{int} may be expressed as

$$\varphi_{int} = h_{tr}^{int}(T_f - T_g) \tag{2-2-33}$$

which vanishes at a saturated equilibrium state where $T_f = T_g = T_s$.

Specific enthalpy of the mixture given by Eq.(2-2-9) can be expressed as

$$xh_g + (1-x)h_f = h \tag{2-2-34}$$

where

$$x = \frac{\alpha\rho_g}{\alpha\rho_g + (1-\alpha)\rho_f} \quad . \tag{2-2-35}$$

Equation (2-2-35) defines non-equilibrium mass quality x in terms of the non-equilibrium quantities, α, ρ_f and ρ_g, where

$$\rho_f = \rho_f(p, h_f) \tag{2-2-36}$$

and

$$\rho_g = \rho_g(p, h_g) \quad . \tag{2-2-37}$$

We assume the ideal gas law for the vapor phase so that

$$\rho_g = \frac{p}{R_g T_g} \tag{2-2-38}$$

which leads to

$$\frac{\delta \rho_g}{\rho_g} + \frac{\delta T_g}{T_g} = 0 \tag{2-2-39}$$

since $\delta p = 0$. Neglecting $\delta \rho_f$ and using Eq.(2-2-39), we obtain from Eq.(2-2-35)

$$\delta x = \frac{\rho_g \rho_f}{\rho^2} \left[\delta \alpha - \alpha(1-\alpha) \frac{\delta T_g}{T_g} \right] . \tag{2-2-40}$$

Since $\delta h = 0$, we obtain from Eq.(2-2-34),

$$h_{gf} \delta x + (c_p)_g x \delta T_g + (1-x)(c_p)_f \delta T_f = 0 . \tag{2-2-41}$$

Substituting Eq.(2-2-40) into Eq.(2-2-41), we obtain

$$\delta \alpha + \left[\frac{(c_p)_g \alpha \rho}{h_{gf} \rho_f} - \frac{\alpha(1-\alpha)}{T_g} \right] \delta T_g + \frac{(c_p)_f (1-\alpha) \rho}{h_{gf} \rho_g} \delta T_f = 0. \tag{2-2-42}$$

The energy conservation equation for the vapor phase is given by

$$\frac{\partial}{\partial t} \alpha \rho_g h_g + \frac{\partial}{\partial z} \alpha \rho_g h_g u_g = q_g''' = (q_g''')^c + \delta (q''')^c , \tag{2-2-43}$$

which is the vapor phase part of the energy conservation equation (2-2-2). In Eq.(2-2-43), cross section A was dropped. For the corresponding equilibrium state, we have

$$\frac{\partial}{\partial t} \alpha_c \rho_g^c h_g^c + \frac{\partial}{\partial z} \alpha_c \rho_g^c h_g^c u_g = (q_g''')^c . \tag{2-2-44}$$

Subtracting Eq.(2-2-44) from Eq.(2-2-43) and using Eq.(2-2-32), we obtain

$$\frac{\partial}{\partial t} \delta (\alpha \rho_g h_g) + \frac{\partial}{\partial z} \delta (\alpha \rho_g h_g) u_g = \frac{S_{int} \varphi_{int}}{V} . \tag{2-2-45}$$

The mass conservation equation for the vapor phase is given by

$$\frac{\partial}{\partial t} \alpha \rho_g + \frac{\partial}{\partial z} \alpha \rho_g u_g = \Gamma , \tag{2-2-46}$$

which is the vapor phase part of the mass conservation equation (2-2-1). In Eq.(2-2-46), cross section A was dropped. For the corresponding equilibrium state, we have

$$\frac{\partial}{\partial t}\alpha_c\rho_g^c+\frac{\partial}{\partial z}\alpha_c\rho_g^c u_g = \Gamma_c \quad . \tag{2-2-47}$$

Subtracting Eq.(2-2-48) from Eq.(2-2-47) and using Eq.(2-2-30), we obtain

$$\frac{\partial}{\partial t}\delta(\alpha\rho_g)+\frac{\partial}{\partial z}\delta(\alpha\rho_g)u_g = 0 \quad . \tag{2-2-48}$$

In the following, we will make several assumptions to derive the relaxation equation for void fration α from Eqs.(2-2-45) and (2-2-48). First of all, assuming $\rho_g h_g \sim \rho_g^c h_g^c \sim constant$ in Eq.(2-2-45), we obtain,

$$\frac{\partial}{\partial t}\delta\alpha+\frac{\partial}{\partial z}(\delta\alpha)u_g = \frac{S_{int}\varphi_{int}}{V\rho_g^c h_g^c} \quad . \tag{2-2-49}$$

Next, we consider a solution to Eq.(2-2-48) such that

$$\delta(\alpha\rho_g) = 0 \quad , \tag{2-2-50}$$

which, with the help of Eq.(4-2-39), gives

$$\frac{\delta\alpha}{\alpha} = \frac{\delta T_g}{T_g} \quad . \tag{2-2-51}$$

Substituting Eq.(2-2-51) into Eq.(2-2-42), we obtain

$$\left[\frac{h_{gf}\alpha\rho_f}{\rho}+(c_p)_g T_g\right]\rho_g\delta\alpha + (1-\alpha)\rho_f(c_p)_f\delta T_f = 0. \tag{2-2-52}$$

Now, in Eqs.(2-2-51) and (2-2-52), assuming that the equilibrium state is saturated, we set

$$\begin{aligned}\delta T_f &= T_f - T_s \\ \delta T_g &= T_g - T_s \\ \delta\alpha &= \alpha - \alpha_c\end{aligned} \tag{2-2-53}$$

to obtain

$$T_g - T_s = \frac{\alpha-\alpha_c}{\alpha}T_g \tag{2-2-54}$$

and

$$T_f - T_s = \frac{(h_{gf}\alpha\rho_f/\rho+(c_p)_g T_g)\rho_g}{(1-\alpha)\rho_f(c_p)_f}(\alpha_c-\alpha) \quad . \tag{2-2-55}$$

Substituting Eqs.(2-2-54) and (2-2-55) into Eq.(2-2-42), we obtain

$$\varphi_{int} = h_{tr}^{int}\left[\frac{T_g}{\alpha}+\frac{h_{gf}\alpha\rho_f\rho_g/\rho+(c_p)_g T_g\rho_g}{(1-\alpha)\rho_f(c_p)_f}\right](\alpha_c-\alpha) \quad . \tag{2-2-56}$$

Equation (2-2-49) with Eq.(2-2-56) describes void propagation with relaxation. In THYDE-W, it will be further transformed to obtain the void relaxation equation without the propagation term. Substituting Eq.(2-2-56) into Eq.(2-2-49), approximating $T_g \sim T_f \sim T_s$ and neglecting $\partial \alpha_c / \partial t$ and the second term of the left hand side, we obtain

$$\frac{\partial \alpha}{\partial t} = \frac{\alpha_c - \alpha}{\tau(\alpha)} \quad . \tag{2-2-57}$$

In Eq.(2-2-57), time constant τ is a function of void fraction α, among other things, such that

$$\tau = \frac{\rho_g^c h_g^c \rho A_\alpha}{h_{tr}^{int} T_s \rho_{fs} B_\alpha} \tag{2-2-58}$$

where

$$A_\alpha = \frac{V\alpha(1-\alpha)}{S_{int}} \tag{2-2-59}$$

and

$$B_\alpha = \frac{\rho}{\rho_f}\left[1+\left(\frac{(c_p)_g \rho_{gs}}{(c_p)_f \rho_{fs}}-1\right)\alpha+\left(\frac{h_{gf}\rho_{gs}}{T_g \rho (c_p)_f}\right)\alpha^2\right]$$

$$\sim (1-\alpha)^2 + \frac{h_{gf}\alpha^2}{(c_p)_f T_s} \quad . \tag{2-2-60}$$

Factor A_α can further be transformed as follows. For a bubbly flow, we note:

$$\frac{\alpha V}{S_{int}} = \frac{V_g}{S_{int}}$$

$$= (volume\ of\ single\ bubble)/(surface\ area\ of\ single\ bubble)$$

$$= \frac{d_g}{6} .$$

A similar manipulation is possible for a dispersed flow. Thus, we obtain ;

$$\frac{\alpha V}{S_{int}} = \frac{d_g}{6}(1-\alpha) \qquad ;bubbly \quad flow \ (\alpha \ll 1)$$

$$\frac{d_f}{6}\alpha \qquad ;dispersed \quad flow \ (\alpha \sim 1)$$

where Taylor instability[45] gives

$$d_g = d_f = 2\left(\frac{\sigma}{g(\rho_f-\rho_g)}\right)^{1/2} \equiv d \ .$$

We interpolate $\alpha V/ S_{int}$ smoothly between bubbly and dispersed flows to obtain

$$A_a = \frac{d}{6}(1-\alpha+\alpha^2) \ . \qquad (2-2-61)$$

In THYDE-W, the interfacial heat transfer coefficient h_{tr}^{int} in Eq.(2-2-58) is chosen to be

$$h_{tr}^{int} = c_{eff}\frac{d\rho_g(c_p)_g}{6}(1-\alpha)exp(\frac{p-b}{a}) \qquad (2-2-62)$$

where :

c_{eff} = 1.0 for p > 10.0 ata

= 0.1 for p < 5.0 ata

p = pressure in ata,

a = 17.3 ata

and

b = 30 ata .

In Eq.(2-2-61), the interfacial heat transfer coefficient h_{tr}^{int} is assumed (1) to have the same pressure dependence as of nucleate boiling (refer to Eq.(3-5-6), (2) to be large for bubbly flow and small for dispersed flow and (3) for τ given by Eq.(2-2-58) to be of order of 5 seconds at 30 ata. The factors exp(p/a), $(1-\alpha)$ and $d\rho_g(c_p)_g$exp(-b/a)/6 account for items (1), (2) and (3), respectively. Substituting Eqs.(2-2-60), (2-2-61) and (2-2-62) into Eq.(2-2-58), we obtain

$$\tau = \frac{(1-\alpha+\alpha^2)h_{gs}}{c_{eff}(c_p)_g T_s B_a exp((p-b)/a)} \ . \qquad (2-2-63)$$

Equation (2-2-57) will be referred to as the relaxation equation for the void fraction. We now let p and h vary, following the conservation equations for the mixture. We here note that the effect

of changes of p and h on the relaxation equation presents itself mainly through α_c. As h includes the contribution of external heat source (see Eq.(2-2-2)) , so does α_c.

2.2.4 *Normal Node Equations*

We assume that a normal node has uniform cross section A, length L, height L_H and external heat source q'''. It should be noted that height L_H is signed as shown in Fig.2-1-1 and that L_H must be the height between the centers of the two adjacent junctions. Therefore, a summation of inputted L_H's along any closed path in a coolant network should vanish. Since we assume a uniform cross section for a normal node, the symbol A in Eqs.(2-2-1) to (2-2-3) entirely drops.

In THYDE-W, the number of parallel channels, the flow area per channel A and the hydraulic diameter D are to be inputted. For a core flow associated with a fuel rod whose pitch and outer radius are l_p and r_R, respectively , A and D to be inputted may be given as follows ;

$$A = l_p^2 - \pi r_R^2$$

and

$$D = \frac{2A}{\pi r_R} \quad .$$

In this report, the super- or sub-scripts A, E, av, new and old will be used to refer to point A, point E, node average point, time $t+\Delta t$ and time t, respectively. Symbols new and av, however, will frequently be dropped. For a variable f(p,G,h), its node average f^{av} will be defined as

$$f^{av} = f(p^{av}, h^{av}, G^{av})$$

where

$$p^{av} = (p^A + p^E) / 2$$

$$G^{av} = (G^A+G^E)/2$$

and h^{av} is given as the solution of Eq(2-2-65).

Differencing Eqs.(2-2-1),(2-2-2) and (2-2-3), spatially between points A and E within a normal node and temporally between $t+\Delta t$ (new) and t (old), we obtain, respectively

$$(f_1)_n = -L_n\frac{\rho_n-\rho_n^{old}}{\Delta t}+G_n^A-G_n^E = 0 \quad , \tag{2-2-64}$$

$$(f_3)_n = -L_n\frac{\rho_n h_n-\rho_n^{old}h_n^{old}}{\Delta t} +\Lambda_n^A-\Lambda_n^E+q_n\cdots L_n = 0 \quad , \tag{2-2-65}$$

and

$$(f_4)_n = -L_n\frac{G_n^A+G_n^E-G_n^{Aold}-G_n^{Eold}}{2\Delta t} + p_n^A-p_n^E+\Psi_n^A-\Psi_n^E$$

$$-\frac{1}{2}(\kappa+\frac{fL}{D}\,|G|G)_n(\frac{\Phi^2}{\rho_f})_n - \rho_n^{av}g(L_H-L_{head})_n = 0 \quad . \tag{2-2-66}$$

In THYDE-W, it is assumed that

$$\frac{\Phi^2}{\rho_f} = \frac{1}{\rho} \quad . \tag{2-2-67}$$

In order to define specific enthalpies h_n^A and h_n^E for normal nodes (see Eqs.(2-2-69) and (2-2-70)) and h_j^+ for normal junctions (see subsection 2.2.5), we define time constants $(\tau_h^A)_n$, $(\tau_h^E)_n$ and $(\tau_h^+)_j$, respectively, for enthalpy mixing such that

$$(\tau_h^A)_n = (\tau_h^E)_n = 1.\times10^{-5}\,\mathrm{sec} \quad ,$$

and

$$(\tau_h)_j^+ = 1.\times10^{-5}\,\mathrm{sec} \quad . \tag{2-2-68}$$

Similarly, τ_h^E can be determined. Then, we will define h_n^A and h_n^E such that

$$h_n^A = h_{from}^+ \qquad \textit{if from-junc is normal and open (not a break)}$$

$$= h_n^{Aold} \qquad \textit{else if from-junction is closed,}$$

$$= \frac{h_n^{Aold}(\tau_h)_n^A+h_{from}^+\Delta t}{(\tau_h)_n^A+\Delta t} \qquad \textit{else if } G_n^A>0 \ .$$

$$= \frac{h_n^{Aold}(\tau_h)_n^A + h_n \Delta t}{(\tau_h)_n^A + \Delta t} \qquad else\ if\ G_n^A \leqq 0$$

(2-2-69)

and

$$h_n^E = h_{to}^+ \qquad if\ to\text{-}junc\ is\ normal\ and\ open\ (not\ a\ break)$$

$$= h_n^{Eold} \qquad else\ if\ to\text{-}junction\ is\ closed$$

$$= \frac{h_n^{Eold}(\tau_h)_n^E + h_{to}^+ \Delta t}{(\tau_h)_n^E + \Delta t} \qquad else\ if\ G_n^E < 0$$

$$= \frac{h_n^{Eold}(\tau_h)_n^E + h_n \Delta t}{(\tau_h)_n^E + \Delta t} \qquad else\ if\ G_n^E \geqq 0 \quad .$$

(2-2-70)

If the to-junction is a boundary junction, then $h_{to}^+(t)$ in Eq.(2-2-70) should be given as a boundary condition. This is also the case with $h_{from}^+(t)$ in Eq.(2-2-69), if the from-junction is a boundary junction.

In Eq.(2-2-65), we note that

$$A = Gh + I$$

(see Eq.(2-2-11)). The relative enthalpy fluxes I_n^A and I_n^E must carefully be defined to ensure its continuity at junctions. In the following, we will use parameters ξ_n^A, ξ_n^E, γ_n^A and γ_n^E to be defined in section 2.5. Let $\mathcal{I}^+$ and $\tilde{I}$ be the total relative enthalpy flux through a normal junction and the coordinate independent relative enthalpy flux, respectively. Then, $\mathcal{I}^+$ can be expressed such that

$$\mathcal{I}^+ = A_{opn}^+(\xi^E \tilde{I})_{from} \qquad if\ (c_{VH})_{to} = 1.\ and\ (c_{VH})_{from} \neq -1 \quad .$$

$$= -A_{opn}^+(\xi^A \tilde{I})_{to} \qquad if\ (c_{VH})_{to} \neq 1.\ and\ (c_{VH})_{from} = -1 \quad .$$

Then, we set

$$I_c^E = \frac{\mathcal{G}_{to}^+}{A} \quad , \tag{2-2-71}$$

and

$$I_c^A = \frac{\mathcal{G}_{from}^+}{A} \quad . \tag{2-2-72}$$

Equation (2-2-71) applies if the to-junction is normal, while Eq.(2-2-72) applies if the from-junction is normal. Next, we consider the cases when the to-junction or the from-junction is a mixing junction. If the to-junction is a mixing junction, we obtain

$$\begin{aligned} I_c^E &= \gamma^E \xi^E \tilde{I} && c_{VH} > 0 \\ &= -\gamma^E \xi^E \tilde{I}^+ && c_{VH} < 0 \quad . \end{aligned} \tag{2-2-73}$$

If the from-junction is a mixing junction, we obtain

$$\begin{aligned} I_c^A &= \gamma^A \xi^A \tilde{I}^+ && c_{VH} > 0 \\ &= -\gamma^A \xi^A \tilde{I} && c_{VH} < 0 \quad . \end{aligned} \tag{2-2-74}$$

Thus, with the help of Eqs.(2-2-71) to (2-2-74), we can obtain effective I^A or I^E such that

$$\frac{d}{dt} I^A = \frac{I_c^A - I^A}{\tau} \tag{2-2-75}$$

and

$$\frac{d}{dt} I^E = \frac{I_c^E - I^E}{\tau} \quad . \tag{2-2-76}$$

Here, we note that the time constants in Eqs.(2-2-75) and (2-2-76) must be identical for a given normal junction so that the relative enthalpy flux can have continuity. Physically, Eqs.(2-2-75) and (2-2-76) describe the enthalpy transport due to relative velocity u_{rel} given by Eq.(2-2-14). Since the drift velocity u_{gj} given by Eq.(2-2-15) is related to the terminal velocity of a bubble, it is necessary to take into account the transition process in which the bubble tends to attain the terminal

velocity. Time constant τ in Eqs.(2-2-75) and (2-2-76) could be obtained by considering how the transition process evolves. But, it is set to be 0.05 sec in the present version of THYDE-W.

Next, we define the momentum coupling equation between a junction and a normal node such that

$$p^{+}_{from} - \left[p^{A}_{n} + \frac{\kappa^{+}_{from}}{2\rho^{A}_{n}} \right] = 0 \qquad (2\text{-}2\text{-}77)$$

and

$$\left[p^{E}_{n} - \frac{\kappa^{+}_{to}}{2\rho^{E}_{n}} \right] - p^{+}_{to} = 0 \quad . \qquad (2\text{-}2\text{-}78)$$

For a turbulent flow, we have

$$\kappa^{+}_{from} = k^{A}_{n} G^{+}_{from} \mid G^{+}_{from} \mid = k^{A}_{n} \left(\frac{A_n}{A^{+}_{from}} \right)^{2} G^{A}_{n} \mid G^{A}_{n} \mid = \frac{k^{A}_{n}}{(\xi_n{}^{A} r^{A}_{n})^{2}} G^{A}_{n} \mid G^{A}_{n} \mid$$

$$= \frac{\kappa^{A}_{n}}{(\xi^{A}_{n})^{2}} \quad , \qquad (2\text{-}2\text{-}79)$$

where Eq.(2-2-4) was used. If quantity κ^{A}_{n} is used, the same expression can be obtained for a laminar flow. The condition for a turbulent flow, $(\mid G \mid D/\mu)^{+}_{from} > Re_t$ can be expressed such that

$$Re^{A}_{n} / \sqrt{\gamma^{A}_{n} \xi^{A}_{n}} > Re_t ,$$

since

$$(\mid G \mid D/\mu)^{+}_{from} = \sqrt{A^{A}_{n} / A^{+}_{from}}\, Re^{A}_{n} = Re^{A}_{n} / \sqrt{\gamma^{A}_{n} \xi^{A}_{n}}$$

where we set

$$\mu^{+}_{from} \sim \mu^{A}_{n} \quad .$$

The similar expression can be obtained for κ^{+}_{to}. In summay, we have

$$\kappa^{i}_{n} = \frac{k^{i}_{n}}{(\gamma^{i}_{n})^{2}} G^{i}_{n} \mid G^{i}_{n} \mid \qquad Re^{i}_{n} / \sqrt{(\gamma\xi)^{i}_{n}} > Re_t \quad (i = A, E) \qquad (2\text{-}2\text{-}80)$$

$$= \frac{k^{i}_{n}}{(\gamma^{i}_{n})^{2}} \left(\frac{\mu}{D} \right)^{i}_{n} Re_t G^{i}_{n} \qquad Re^{i}_{n} / \sqrt{(\gamma\xi)^{i}_{n}} \leq Re_t \quad (i = A, E). \qquad (2\text{-}2\text{-}81)$$

Substituting Eq.(2-2-79) into Eq.(2-2-77), we obtain

$$(f_2)_n = (\xi_n^A)^2(p_{from}^+ - p_n^A) - \frac{\kappa_n^A}{2\rho_n^A} = 0 \quad . \qquad (2\text{-}2\text{-}77a)$$

Similarly, substituting $\kappa_{to}^+ = \kappa_n^E/(\xi_n^E)^2$ into Eq.(2-2-78), we obtain

$$(f_3)_n = (\xi_n^E)^2(p_n^E - p_{to}^+) - \frac{\kappa_n^E}{2\rho_n^E} = 0 \quad . \qquad (2\text{-}2\text{-}78a)$$

2.2.5 *Junction Equations*

We note that only a single normal node is involved in all the conservation equations discussed in the preceding subsection, i.e., Eqs. (2-2-64), (2-2-65), (2-2-66), (2-2-77a) and (2-2-78a). In this subsection, we will consider the conservation equations in which a plural number of normal nodes are involved. They are the conservation equations for mass and energy at a normal or mixing junction.

For a mixing junction j, we have

$$(f_1^+)_j = \frac{(\rho_j^+ - \rho_j^{+old})}{\Delta t} - (\sum_{from} A_n G_n^E - \sum_{to} A_n G_n^A)/V_j^+ = 0 \qquad (2\text{-}2\text{-}82)$$

and

$$(f_2^+)_j = \frac{(\rho_j^+ h_j^+ - \rho_j^{+old} h_j^{+old})}{\Delta t}$$

$$- (\sum_{from} A_n \Lambda_n^E - \sum_{to} A_n \Lambda_n^A)/V_j^+ - q_j^{'''+} = 0 \qquad (2\text{-}2\text{-}83)$$

where $\sum_{to}$ and $\sum_{from}$ are the summations over the to- and from-nodes of junction j, respectively.

If junction j is normal , Eq. (2-2-82) reduces to

$$(f_1^+)_j = -A_{from} G_{from}^E + A_{to} G_{to}^A = 0 \quad . \qquad (2\text{-}2\text{-}84)$$

The energy equation for normal junction j is assumed to be

$$(f_2^+)_j = h_j^+ - \frac{h_j^{+old}(\tau_h)_j^+ + h_c \Delta t}{(\tau_h)_j^+ + \Delta t} = 0 \qquad (2\text{-}2\text{-}85)$$

where $(\tau_h)_j^+$ has been defined in Eq.(2-2-68) and

$$h_c = h_{from}^{av} \qquad if\ G_{to}^A \geqq 0,$$

$$= h_{to}^{av} \qquad if\ G_{to}^A < 0.$$

2.2.6 *Boundary Node Equations*

Within the framework of our thermal-hydraulic network, what connects our network to its exterior is the boundary nodes, i.e., injection nodes, dead end nodes and break nodes. Accumulators to be described in subsection 2.4.2 are regarded as exterior and are connected to our network by the boundary junctions. Within the framework of our network theory, the boundary conditions of our network should be specified by those equations of the boundary node.

First of all, we note that the boundary condition for enthalpy can be given by specifying h_{from}^+ in Eq.(2-2-69) or h_{to}^+ in Eq.(2-2-70) for a boundary node.

The boundary conditions may be classified into two; p-sources and G-sources. Generally speaking, however, a hydraulic boundary condition usually is a p-source boundary condition. For a p-source boundary, the boundary condition will be given by specifying p_{to}^+ in Eq.(2-2-78a) and by specifying h_{to}^+ in Eq.(2-2-70) for a boundary node. For example, in case of an open accumulator, h_{from}^+ and p_{to}^+ are given by h_L and p_x to be obtained from Eqs.(2-4-69) and (2-4-71), respectively. It should be reminded that a boundary junction (except a guillotine break junction) is situated next to the point E of an outermost linkage node.

For a G-source boundary, we have instead of Eq.(2-2-78a),

$$(f_3)_n = G_n^E - G(p_n^E, h_n^E, t) = 0 \qquad (2\text{-}2\text{-}86)$$

where G(p,h,t) is a given function. For example, a behavior of the pumped injection subsystems can be simulated by a G-source (it can also be simulated by a p-source).

Next, we discuss the break boundary condition. Consider the from-node of the break junction. When the discharge flow is inertial, p_{to}^{+} and ξ_n^E in Eq.(2-2-78a) for the break node will be given by

$$\frac{dp_{to}^{+}}{dt} = \frac{p_{ref}-p_{to}^{+}}{\tau} \qquad (2\text{-}2\text{-}87)$$

and

$$\xi_n^E = 1 \quad .$$

Here, it should be noted that loss coefficient k_n^E to be used in Eq.(2-2-77a) must be the one " after the break " . Time constant τ in Eq.(2-2-87) is an input of THYDE-W (BB17). If the network calculation with Eq.(2-2-87) results in

$$|G_n^E| > G_M(p_n^E, h_n^E) \quad , \qquad (2\text{-}2\text{-}88)$$

then instead of Eq. (2-2-78a), we use the critical flow condition

$$(f_3)_n = f_B(p_n^E, G_n^E, h_n^E) = |G_n^E| - G_M(p_n^E, h_n^E) = 0 \qquad (2\text{-}2\text{-}89)$$

where G_M is given in subsection 2.5.3. Equation (2-2-89) is a special case of Eq.(2-2-86) which defines G-source boundary conditions. Suppose that the break flow is in the region of critical flow. And let G_N be the solution to Eq.(2-2-78a) with p_n^E, p_{to}^{+} and ρ_N^E being the old values. If the calculation with Eq.(2-2-89) turns out to be

$$|G_n^E| < G_N$$

then, we return to the inertial flow, that is, Eq. (2-2-78a) with Eq.(2-2-87). The equations for the from-node of the break can similarly be given. When the break flow is an inertial flow, it may become an inflow. Then, it will be assumed that $h^{+} = h_{gs}$ in Eqs.(2-2-69) and (2-2-70).

2.3 Algorithm for Thermal-Hydraulic Network

2.3.1 Overall Strategy

In this section, we will develop the algorithm for a thermal-hydraulic network which can be represented in terms of nodes and junctions defined and discussed in the preceding section. Accumulator nodes will be treated separately in subsection 2.4.2. An example of thermal-hydraulic networks is shown in Fig.2-3-1, which represents the nuclaer steam supply system (NSSS) of a PWR. We note that in such a representation, any two neighboring normal nodes will be connected via a junction. In the following, some of the points which we should keep in mind when reticulating a coolant system are listed in order:

(a) A mixing junction has a volume and is multiple-branched.

(b) For a double-ended break, we set a normal junction at the place where the break will be assumed to occur. Prior to the occurrence of the break, the junction will be regarded as a normal junction with which the steady state adjustment for the entire network will be performed.

(c) A split break may be simulated to occur at the end of a fictitious linkage node placed at the point where the break is assumed to take place.

(d) Whenever there are parallel channels, the entire flow area and

the flow area per channel must be distinguished. If this were not taken into account, we would have pressure and flow rate changes at the inlet and outlet of the parallel channels.

Other requirements are cited in Chapter 8.

The computational procedure for use in THYDE-W is shown in Fig. 2-3-2. For the calculation of a steady state, reference should be made to chapter 6. Looking over Fig.2-3-2, we can see that the network and its exterior are coupled to each other with a time lag Δt. At step 1 in Fig.2-3-2, the state of the exterior such as the pump head, the heat input to the network , the degree of openings of the valves and the thermal-hydraulic condition at the boundary junctions will be specified. The present section corresponds to step 2. In this section, we will present a new algorithm for a hydraulic network, which is an implicit scheme for the system described by the node-and-junction equations derived in the previous section. It is due to the entirely new node-and-junction representation of a hydraulic network that such an implicit integration technique can yield the algorithm which may well coincide with our physical intuition, as can be seen in the discussions that follow. Step 3 is discussed in chapters 3 and 5. For step 4, reference should be made to section 7.3.

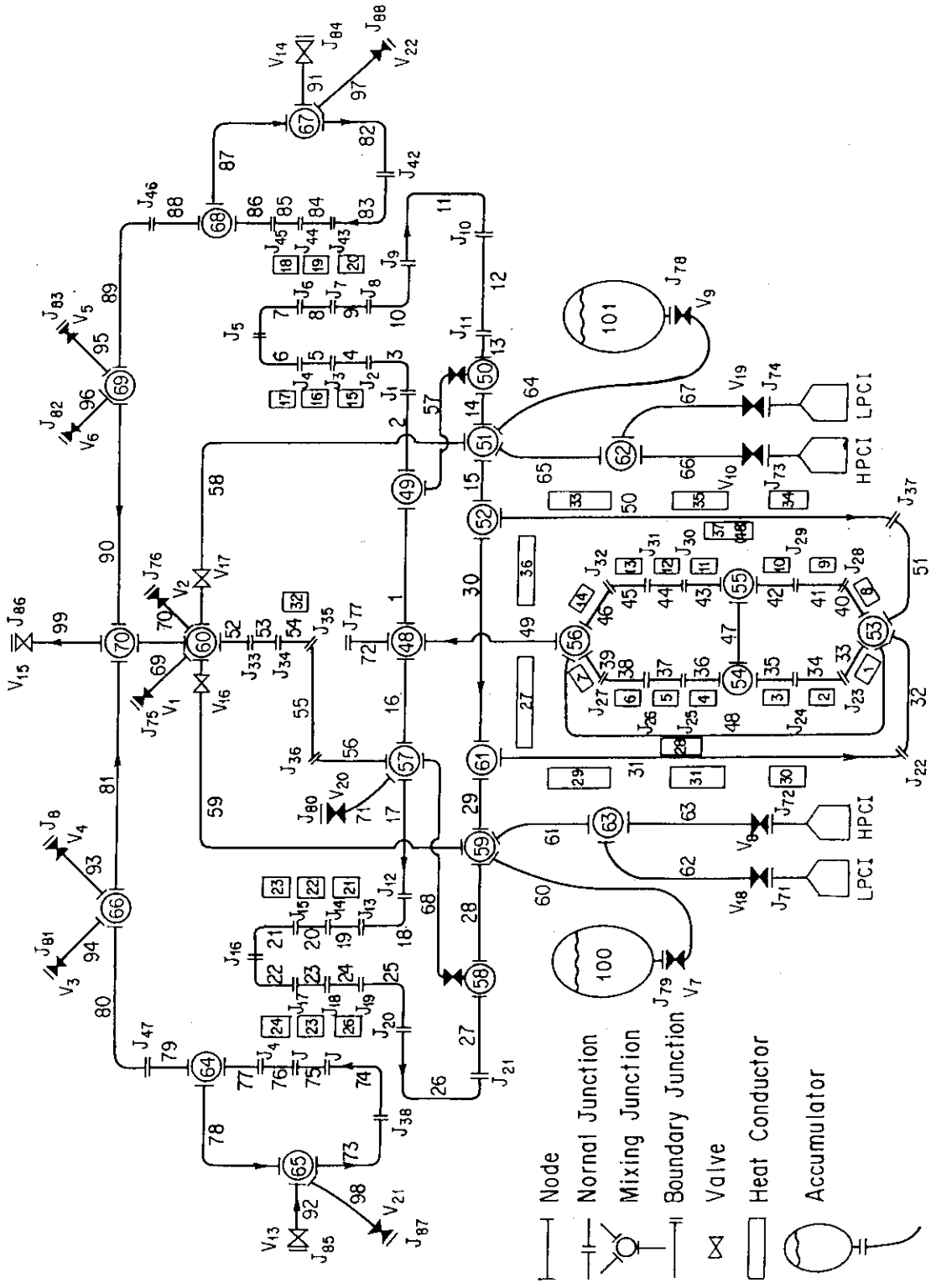

Fig. 2－3－1 Example of Noding : NSSS of a PWR

1. Obtain new states of boundary junctions, hydraulic machines, control systems, valves, accumulators and hydraulic sources.

2. Solve the simultaneous equation of order 5N+2J for the thermal-hydraulic network by means of the non-linear implicit method. Simultaneously obtain coolant state. Use old heat inputs to coolant flow.

3. Obtain new states of heat conductors along with their heat fluxes under a new coolant condition. Obtain a new distribution of boron concentration.

4. Check the time step width. If its reduction is necessary, go back to step 1 and repeat the calculation all over again with the halved time step width. Otherwise, proceed to the calculation for the next time step.

Fig. 2-3-2 Overall Transient Computation Procedure

2.3.2 Vector Representation of Network Equations

By casting the equations discussed in section 2.2 into the vector forms, we can develop the solution procedure for thermal-hydraulics, which is the second step in Fig.2-3-2. In this section, only for the sake of clarity, we assume that the hydraulic network is composed of a single disjoint subnetwork. Looking over the discussions that follow, we can see that the procedure in this section is quite general, independent of the thermal-hydraulic model as long as the Jacobian has a structure of the same kind.

For a hydraulic system we will define the unknown state vector of the system which is (5N+2J)-dimensional such that

$$\boldsymbol{x}=\begin{bmatrix} \boldsymbol{x}_1 \\ \boldsymbol{x}_2 \\ \boldsymbol{x}_3 \\ \cdot \\ \cdot \\ \cdot \\ \boldsymbol{x}_N \\ \boldsymbol{x}_{N+1} \end{bmatrix} \tag{2-3-1}$$

where

$$\boldsymbol{x}_n=\begin{bmatrix} (x_1)_n \\ (x_2)_n \\ (x_3)_n \\ (x_4)_n \\ (x_5)_n \end{bmatrix} = \begin{bmatrix} G_n^A \\ p_n^A \\ G_n^E \\ p_n^E \\ h_n^{av} \end{bmatrix} \qquad (1 \leqq n \leqq N) \tag{2-3-2}$$

and

$$\boldsymbol{x}_{N+1}= \begin{bmatrix} x_1^+ \\ x_2^+ \\ x_3^+ \\ x_4^+ \\ \cdot \\ \cdot \\ x_J^+ \end{bmatrix} = \begin{bmatrix} p_1^+ \\ h_1^+ \\ p_2^+ \\ h_2^+ \\ \cdot \\ \cdot \\ p_J^+ \\ h_J^+ \end{bmatrix} \tag{2-3-3}$$

so that x_n is 5 dimensional for $1 \leqq n \leqq N$ and 2J dimensional for n = N + 1. In the above, J and N are the numbers of junctions (excluding boundary

junctions) and nodes (including boundary nodes, but excluding accumulator nodes), respectively. We note that J includes the normal junction where a double-ended break may be assumed to occur. Vector $\boldsymbol{x}_n$ $(1 \leqq n \leqq N)$ is associated with node n, while vector $\boldsymbol{x}_{N+1}$ is the collection of state vectors of the entire junctions except the boundary junctions. It should be noted here again that the states of the boundary junctions are not unknown, but are given as the boundary conditions. In order for the problem to be soluble, as many relationships as 5N+2J are needed.

There are 5 relationships associated with each normal node n, that is, (1) the mass equation within node n, $(f_1)_n$, i.e., Eq.(2-2-64), (2) the equation of pressure linkage with the from-junction, $(f_2)_n$, i.e., Eq.(2-2-77a), (3) the equation of pressure linkage with the to-junction, $(f_3)_n$, i.e., Eq.(2-2-78a), (4) the momentum equation within node n, $(f_4)_n$, i.e., Eq.(2-2-66), and (5) the energy equation within node n, $(f_5)_n$, i.e., Eq.(2-2-65). We reproduce them in the following :

$$(f_1)_n = G_n^A - G_n^E - L_n \frac{\rho_n^{av} - \rho_n^{avold}}{\Delta t} = 0 \qquad (2\text{-}3\text{-}4)$$

$$(f_2)_n = (\xi_n^A)^2 (p_{from}^+ - p_n^A) - \frac{\kappa_n^A}{2\rho_n^A} = 0 \qquad (2\text{-}3\text{-}5)$$

$$(f_3)_n = (\xi_n^E)^2 (p_n^E - p_{to}^+) - \frac{\kappa_n^E}{2\rho_n^E} = 0 \qquad (2\text{-}3\text{-}6)$$

$$(f_4)_n = p_n^A - p_n^E + \Psi_n^A - \Psi_n^E - \frac{1}{2\rho_n^{av}} \left[\kappa + \frac{fL}{D} \mid G \mid G \right]_n^{av}$$

$$- \rho_n^{av} g (L_H - L_{head})_n - L_n \frac{G_n^A + G_n^E - G_n^{Aold} - G_n^{Eold}}{2\Delta t} = 0 \qquad (2\text{-}3\text{-}7)$$

and

$$(f_5)_n = \frac{\Lambda_n^A - \Lambda_n^E}{L_n} + q_n''' - \frac{\rho_n^{av} h_n^{av} - \rho_n^{av,old} h_n^{av,old}}{\Delta t} = 0 \quad . \qquad (2\text{-}3\text{-}8)$$

Specific enthalpies h_n^A and h_n^E are given by Eqs.(2-2-69) and (2-2-70), respectively. Quantities κ, Ψ and Λ are defined by Eqs.(2-2-4), (2-2-7)

and (2-2-8), respectively.

If node n is a boundary node, then $(f_3)_n$ (or $(f_2)_n$) will be given as described in subsection 2.2.6 . For example, if the to-junction is a break under a critical mass flow condition, we have

$$(f_3)_n = f_B(p_n^E, G_n^E, h_n^E) = |G_n^E| - G_M(p_n^E, h_n^E) = 0 \quad , \tag{2-3-6a}$$

while if the to-junction is a G-source , then we have Eq.(2-2-86), i.e.,

$$(f_3)_n = G_n^E - G(p_n^E) = 0 \quad . \tag{2-3-6b}$$

There are two equations associated with each junction. For any normal junction j, we have Eqs.(2-2-80) and (2-2-81), i.e.,

$$(f_1^+)_j = -A_{from} G_{from}^E + A_{to} G_{to}^A = 0 \quad . \tag{2-3-9}$$

and

$$(f_2^+)_j = h_j^+ - \frac{h_j^{+old} \tau_{hj}^+ + h_c \Delta t}{(\tau_h)_j^+ + \Delta t} = 0 . \tag{2-3-10}$$

After a break occurs at junction j, it might no longer be regarded as a normal junction, but as a boundary junction so that the number of the unknowns as well as the dimension of the system Jacobian would change after the break. But, in order to retain the same dimension and structure of the system Jacobian even after an initiation of a break at a normal junction, we keep allocating the dummy unknown variables p_j^+ and h_j^+ for this junction j such that, after its initiation,

$$(f_1^+)_j = p_j^+ - p_j^{+old} \tag{2-3-11}$$

and

$$(f_2^+)_j = h_j^+ - h_j^{+old} \quad . \tag{2-3-12}$$

For a mixing junction j, we have Eqs.(2-2-82) and (2-2-83)

$$(f_1^+)_j = \sum_{to} A_k G_k^A - \sum_{from} A_l G_l^E + V_j^+ (\rho_j^+ - \rho_j^{+old}) / \Delta t = 0 \tag{2-3-13}$$

and

$$(f_2^+)_j = \sum_{to} A_k \Lambda_k^A - \sum_{from} A_l \Lambda_l^E + V_j^+ (\rho_j^+ h_j^+ - \rho_j^{+old} h_j^{+old}) / \Delta t - q_j'''^+ = 0 \quad . \quad (2\text{-}3\text{-}14)$$

Eq.(2-3-9) is the special case of Eq.(2-3-13), when $V_j^+=0$ and there is no branching at junction j.

Thus, we have 5N+2J equations which can be cast into a function vector f such that

$$f = \begin{bmatrix} f_1 \\ f_2 \\ \cdot \\ \cdot \\ \cdot \\ f_N \\ f_{N+1} \end{bmatrix} \qquad (2\text{-}3\text{-}15)$$

where

$$f_n = \begin{bmatrix} (f_1)_n \\ (f_2)_n \\ (f_3)_n \\ (f_4)_n \\ (f_5)_n \end{bmatrix} \qquad (1 \leqq n \leqq N) \qquad (2\text{-}3\text{-}16)$$

and

$$f_{N+1} = \begin{bmatrix} f_1^+ \\ f_2^+ \\ \cdot \\ \cdot \\ \cdot \\ f_J^+ \end{bmatrix} = \begin{bmatrix} (f_1^+)_1 \\ (f_2^+)_1 \\ (f_1^+)_2 \\ (f_2^+)_2 \\ \cdot \\ \cdot \\ \cdot \\ \cdot \\ \cdot \\ (f_1^+)_J \\ (f_2^+)_J \end{bmatrix} \qquad (2\text{-}3\text{-}17)$$

It should be noted that the 5-dimensional function vector f_n associated with node n is related to only one pair of junctions, i.e., the from- and to-junctions, but not directly to the other normal nodes. In other words, nodes are decoupled to each other. Function vector f_{N+1} is the collection of the junction equations $(f_1^+)_j$ and $(f_2^+)_j$, so that it is 2J dimensional.

We now have to solve the thermal-hydraulic network equation

$$f(x(t), t) = 0 \quad , \qquad (2\text{-}3\text{-}18)$$

where only for the sake of clarity Δt is dropped. In order to solve a thermal-hydraulic network equation such as Eq.(2-3-18), it has been common to use what may be called a linear implicit method [2),(3),(7),(18)]. But, as long as a linear implicit method were used, mass, momentum and energy would not conserve, even if the space difference were correct. In THYDE-W, we use an iterative procedure that may be called the nonlinear implicit method to solve Eq.(2-3-18) with a strict convergence criterion. A linear implicit method is equivalent to performing no iteration in the nonlinear implicit method without paying an attention to convergence of any kind. In other words, it is equivalent to the nonlinear implicit method under a very weak convergence criterion so that no iteration is needed.

2.3.3 Method for Solution to Themal-Hydraulic Network Equation

This subsection corresponds with step 2 in Fig.2-3-2. Suppose that we have obtained the solution of Eq.(2-3-18) up to time t and now wish to solve it for new time $t+\Delta t$, i,e.,

$$f(x(t+\Delta t), t+\Delta t)=0 \qquad (2\text{-}3\text{-}19)$$

Step 1 in Fig.2-3-2 can be regarded as specifying the form of functions vector f at time $t+\Delta t$. We now set the unknown state vector $x^{new}=x(t+\Delta t)$ to be

$$x^{new}=x_g+\Delta x \qquad (2\text{-}3\text{-}20)$$

where x_g is an appropriate guess vector. Substituting Eq.(2-3-20) into Eq.(2-3-19), we obtain

$$f(x_g+\Delta x)=0 \qquad (2\text{-}3\text{-}21)$$

where the argument $t+\Delta t$ has been dropped. Expanding Eq.(2-3-21) around x_g and retaining only the terms up to the first order in Δx, we obtain

$$f(x_g)+J\Delta x=0 \qquad (2\text{-}3\text{-}22)$$

where J is (5N+2J)x(5N+2J) Jacobian matrix such that

$$J=\frac{\partial f}{\partial x}\Big|_{x=x_g} \quad .$$

By solving the linear equation Eq.(2-3-22), we could claim to have obtained the solution. But, it should be noted that the solution to Eq.(2-3-22) does not satisfy the conservation laws, i.e. Eq.(2-3-19). In THYDE-W, we try to obtain the solution of Eq.(2-3-19) with an iteration procedure as closely as possible so that mass, energy and momentum do conserve.

The procedure to solve Eq.(2-3-19) or (2-3-21) is shown in Fig. 2-3-3, which is a nonlinear implicit method. Such a nonlinear implicit method is needed especially at low pressure where non-linearity of the flow equations predominates. The non-linear implicit method imperatively requires continuity of the various parameters involved in the flow equations, e.g., Eq.(2-2-18), which, in turn, makes the automatic time step width control possible. Reference should be made to section 7.3 for the time step width control (TSWC) with respect to the nember of iterations.

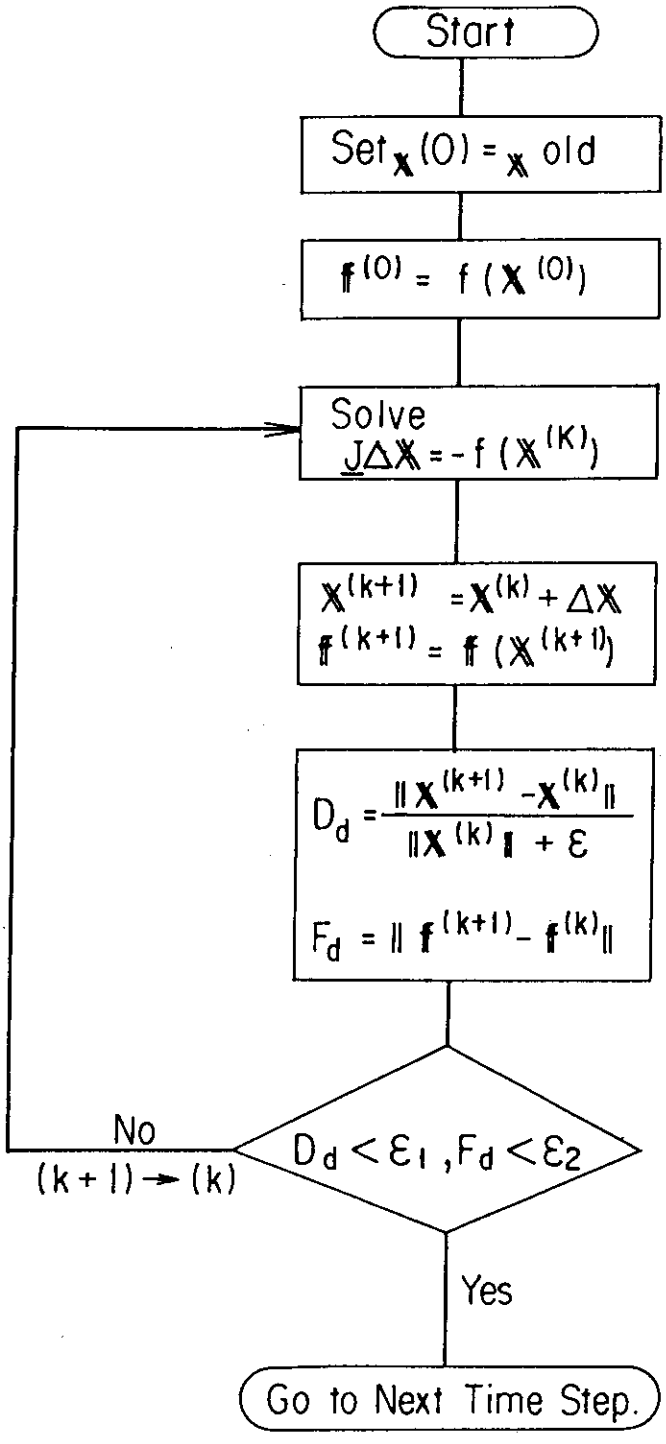

Fig. 2-3-3 Nonlinear Implicit Scheme for Thermal-Hydraulic System

The Jacobian matrix J has the following form

$$J=\begin{bmatrix} J_1 & 0 & 0 & \cdots & R_1 \\ 0 & J_2 & 0 & \cdots & R_2 \\ 0 & 0 & J_3 & \cdots & R_3 \\ 0 & 0 & 0 & \cdots & R_4 \\ \vdots & \vdots & \vdots & \cdots & \vdots \\ L_1 & L_2 & L_3 & \cdots & M \end{bmatrix} \qquad (2\text{-}3\text{-}23)$$

where J_n, R_n, L_n and M are also the following (5x5), (5x2J), (2JX5) and (2Jx2J) jacobian matrices such that

$$J_n=\frac{\partial f_n}{\partial x_n}$$

$$R_n=\frac{\partial f_n}{\partial x_{N+1}}$$

$$L_n=\frac{\partial f_{N+1}^{+}}{\partial x_n}$$

and

$$M=\frac{\partial f_{N+1}^{+}}{\partial x_{N+1}}$$

whose components are given in Appendix A.2. We note that all the other elements of matrix J vanish due to node-node decoupling.

With the help of Eq.(2-3-23), Eq(2-3-22) can be decomposed to the following set of equations.

$$J_n\Delta x_n+R_n\Delta x_{N+1}=-f_n \qquad (n=1,2,\ldots,N) \qquad (2\text{-}3\text{-}24)$$

and

$$\sum_{n=1}^{N} L_n\Delta x_n+M\Delta x_{N+1}=-f_{N+1} \qquad (2\text{-}3\text{-}25)$$

From Eq.(2-3-24), we obtain

$$\Delta x_n=-J_n^{-1}R_n\Delta x_{N+1}-J_n^{-1}f_n \qquad (2\text{-}3\text{-}26)$$

which is substituted into Eq.(2-3-25) to obtain

$$B\Delta x_{N+1}=F \qquad (2\text{-}3\text{-}27)$$

where B and F are (2Jx2J) and (2Jx1) matrices, respectively, such that

$$B=\sum_{n=1}^{N}\mathcal{B}_n-M \qquad (2\text{-}3\text{-}28)$$

$$\mathcal{B}_n = L_nJ_n^{-1}R_n \qquad (2\text{-}3\text{-}28a)$$

and

$$F = f_{N+1} - \sum_{n=1}^{N} L_n J_n^{-1} f_n \quad . \tag{2-3-29}$$

Thus, the node-and-junction equation (2-3-22) has been reduced to the junction equation (2-3-27).

For a given branch, we number the junctions from upstream to downstream successively in the direction of the steady state flow. Then, for a given node, (5x2J) matrix $\mathbf{R}_n$ and (2Jx5) matrix $\mathbf{L}_n$ are made to have the following simple block structures whose non-zero elements correspond to the from- and to-junctions of node n ;

$$R_n = [\ o\ o\ \ldots\ r_n\ \ldots\ o\ o\ ] \tag{2-3-30}$$

and

$$L_n = \begin{bmatrix} o \\ o \\ \cdot \\ \cdot \\ l_n \\ \cdot \\ \cdot \\ o \\ o \end{bmatrix} \tag{2-3-31}$$

where r_n and l_n are (5x4) and (4x5) matrices respectively such that

$$r_n = \quad (\partial f_n / \partial x^{+}_{from}, \partial f_n / \partial x^{+}_{to}) \tag{2-3-32}$$

and

$$l_n = \quad \begin{bmatrix} \partial f^{+}_{from} / \partial x_n \\ \partial f^{+}_{to} / \partial x_n \end{bmatrix} \quad . \tag{2-3-33}$$

With the help of Eqs.(2-3-30) and (2-3-31), the elements of matrices B and matrix F can further be manipulated. First, we deal with matrix F. With the help of Eq.(2-3-31), we obtain

$$L_n J_n^{-1} f_n = \begin{bmatrix} o \\ o \\ \cdot \\ \cdot \\ l_n J_n^{-1} f_n \\ \cdot \\ \cdot \\ o \end{bmatrix} \tag{2-3-34}$$

where non-zero element $l_n J_n^{-1} f_n$ corresponds to the from- and to- junctions of node n. It can be expressed with the help of Eq.(2-3-33) as

$$l_n J_n^{-1} f_n = \begin{bmatrix} \partial f_{from}^{+} / \partial x_n \; J_n^{-1} f_n \\ \partial f_{to}^{+} / \partial x_n \; J_n^{-1} f_n \end{bmatrix} . \tag{2-3-35}$$

We set

$$F = \begin{bmatrix} F_1 \\ F_2 \\ \cdot \\ \cdot \\ F_{J-1} \\ F_J \end{bmatrix} \tag{2-3-36}$$

where $F_j (1 \leqq j \leqq J)$ is a 2-dimensional vector. Substituting Eq.(2-3-34) with Eq.(2-3-35) into Eq.(2-3-29) and comparing the resultant equation with Eq.(2-3-36), we obtain

$$F_j = f_j^{+} - \sum_{to\text{-}nodes} F_{j,to} - \sum_{from\text{-}nodes} F_{j,from} \tag{2-3-37}$$

where

$$F_{j,from} = \frac{\partial f_j^{+}}{\partial x_{from}} J_{from}^{-1} f_{from} , \tag{2-3-37a}$$

and

$$F_{j,to} = \frac{\partial f_j^{+}}{\partial x_{to}} J_{to}^{-1} f_{to} . \tag{2-3-37b}$$

The explicit forms of $F_{j,to}$ and $F_{j,from}$ are given in Appendix A.5.

Substituting Eqs.(2-3-30) and (2-3-31) into Eq.(2-3-28a), we obtain

$$\mathcal{B}_n = \begin{bmatrix} o & o & o & \cdots & o & o \\ o & o & l_n J_n^{-1} r_n & \cdots & o & o \\ o & o & o & \cdots & o & o \\ o & o & o & \cdots & o & o \end{bmatrix} . \tag{2-3-38}$$

In Eq.(2-3-38), non-zero element $l_n J_n^{-1} r_n$, corresponding to the from- and to- junctions of node n, is given as

$$l_n J_n^{-1} r_n = \begin{bmatrix} (b_{from,from})_n & (b_{from,to})_n \\ (b_{to,from})_n & (b_{to,to})_n \end{bmatrix} \tag{2-3-39}$$

where

$$(b_{ij})_n = \frac{\partial f_i^+}{\partial x_n} J_n^{-1} \frac{\partial f_n}{\partial x_j^+} \qquad (i,j = from \ \ or \ \ to) \tag{2-3-40}$$

which is a (2x2) matrix given in Appendix A.3. The non-zero elements of $\mathcal{B}_n$ correspond, as shown in Eq.(2-3-39), to the to- and from-junctions of node n. Matrix $J_n^{-1} r_n$ and vector $J_n^{-1} f_n$ are obtained in subroutine IVJACB, while matrix $l_n J_n^{-1} r_n$ and vector $l_n J_n^{-1} f_n$ are obtained in subroutine REDUCJ.

Matrix M can be expressed as

$$M = \begin{bmatrix} m_1 & 0 & \cdots & 0 \\ 0 & m_2 & \cdots & 0 \\ 0 & 0 & \cdots & m_j \end{bmatrix} \tag{2-3-41}$$

where

$$m_j = \frac{\partial f_j^+}{\partial x_j^+} \tag{2-3-42}$$

which is given in Appendix A.4.

Substituting Eqs.(2-3-38) and (2-3-41) into Eq.(2-3-28), it can be seen that (2Jx2J) matrix B can be represented as a (JxJ) matrix, whose components are 2x2 matrices. The (i,j) component of matrix B does not vanish when either (1) i=j or (2) i and j corresponds to two neiboring junctions, that is,

$$\sum_n (b_{ii})_n - m_i \qquad for \quad i = j \tag{2-3-43}$$

and

$$(b_{ij})_{n_{ij}} \qquad for\ two\ neighboring\ junctions\ i\ and\ j$$

where the summation for i=j should be made over all from- and to- nodes of junction j, while n_{ij} is the number of the node between two neighboring

junctions i and j.

Consider the hydraulic network shown in Fig.2-3-4 where N = 9 and J = 7. In this case, the (14x14) matrix **B** can be obtained as follows. First, we obtain matrices $\mathcal{B}_n$ (n= 1,2,..9) given by Eq.(2-3-38) as follows :

$$\mathcal{B}_1=\begin{bmatrix} (b_{11})_1 & 0 & 0 & (b_{14})_1 & 0 & 0 & 0 \\ 0 & 0 & 0 & 0 & 0 & 0 & 0 \\ 0 & 0 & 0 & 0 & 0 & 0 & 0 \\ (b_{41})_1 & 0 & 0 & (b_{44})_1 & 0 & 0 & 0 \\ 0 & 0 & 0 & 0 & 0 & 0 & 0 \\ 0 & 0 & 0 & 0 & 0 & 0 & 0 \\ 0 & 0 & 0 & 0 & 0 & 0 & 0 \end{bmatrix}$$

$$\mathcal{B}_2=\begin{bmatrix} (b_{11})_2 & (b_{12})_2 & 0 & 0 & 0 & 0 & 0 \\ (b_{21})_2 & (b_{22})_2 & 0 & 0 & 0 & 0 & 0 \\ 0 & 0 & 0 & 0 & 0 & 0 & 0 \\ 0 & 0 & 0 & 0 & 0 & 0 & 0 \\ 0 & 0 & 0 & 0 & 0 & 0 & 0 \\ 0 & 0 & 0 & 0 & 0 & 0 & 0 \\ 0 & 0 & 0 & 0 & 0 & 0 & 0 \end{bmatrix}$$

$$\mathcal{B}_3=\begin{bmatrix} 0 & 0 & 0 & 0 & 0 & 0 & 0 \\ 0 & (b_{22})_3 & 0 & 0 & 0 & (b_{26})_3 & 0 \\ 0 & 0 & 0 & 0 & 0 & 0 & 0 \\ 0 & 0 & 0 & 0 & 0 & 0 & 0 \\ 0 & 0 & 0 & 0 & 0 & 0 & 0 \\ 0 & (b_{62})_3 & 0 & 0 & 0 & (b_{66})_3 & 0 \\ 0 & 0 & 0 & 0 & 0 & 0 & 0 \end{bmatrix}$$

$$\mathcal{B}_4=\begin{bmatrix} 0 & 0 & 0 & 0 & 0 & 0 & 0 \\ 0 & 0 & 0 & 0 & 0 & 0 & 0 \\ 0 & 0 & 0 & 0 & 0 & 0 & 0 \\ 0 & 0 & 0 & 0 & 0 & 0 & 0 \\ 0 & 0 & 0 & 0 & 0 & 0 & 0 \\ 0 & 0 & 0 & 0 & 0 & (b_{66})_4 & (b_{67})_4 \\ 0 & 0 & 0 & 0 & 0 & (b_{76})_4 & (b_{77})_4 \end{bmatrix}$$

$$\mathcal{B}_5=\begin{bmatrix} 0 & 0 & 0 & 0 & 0 & 0 & 0 \\ 0 & 0 & 0 & 0 & 0 & 0 & 0 \\ 0 & 0 & (b_{33})_5 & 0 & 0 & 0 & (b_{73})_5 \\ 0 & 0 & 0 & 0 & 0 & 0 & 0 \\ 0 & 0 & 0 & 0 & 0 & 0 & 0 \\ 0 & 0 & 0 & 0 & 0 & 0 & 0 \\ 0 & 0 & (b_{37})_5 & 0 & 0 & 0 & (b_{77})_5 \end{bmatrix}$$

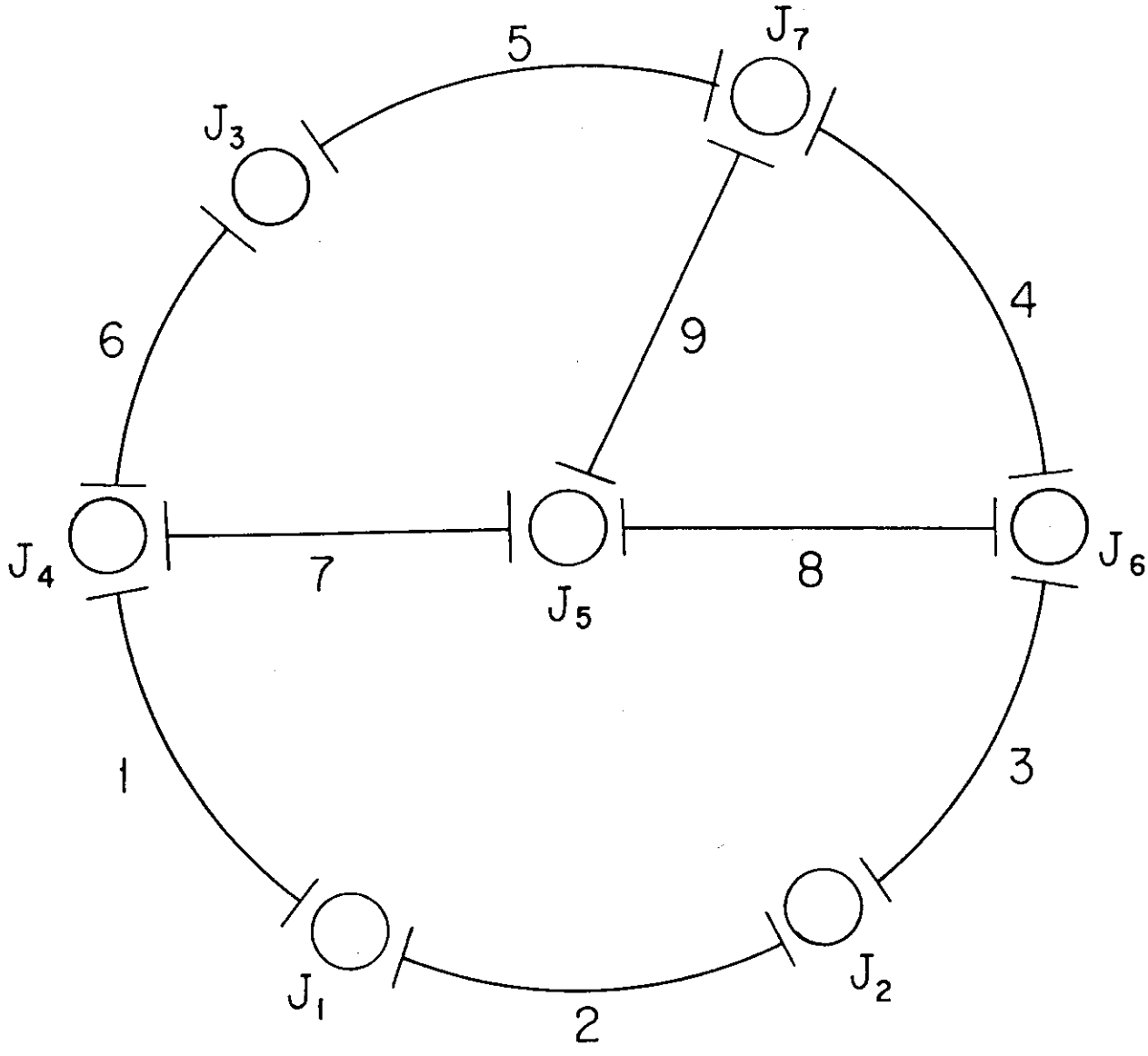

Fig. 2-3-4 Example of Thermal-Hydraulic Network

$$\mathfrak{B}_6=\begin{bmatrix} 0 & 0 & 0 & 0 & 0 & 0 & 0 \\ 0 & 0 & 0 & 0 & 0 & 0 & 0 \\ 0 & 0 & 0 & 0 & 0 & 0 & 0 \\ 0 & 0 & (b_{33})_6 & (b_{34})_6 & 0 & 0 & 0 \\ 0 & 0 & (b_{43})_6 & (b_{44})_6 & 0 & 0 & 0 \\ 0 & 0 & 0 & 0 & 0 & 0 & 0 \\ 0 & 0 & 0 & 0 & 0 & 0 & 0 \end{bmatrix}$$

$$\mathfrak{B}_7=\begin{bmatrix} 0 & 0 & 0 & 0 & 0 & 0 & 0 \\ 0 & 0 & 0 & 0 & 0 & 0 & 0 \\ 0 & 0 & 0 & 0 & 0 & 0 & 0 \\ 0 & 0 & 0 & (b_{44})_7 & (b_{45})_7 & 0 & 0 \\ 0 & 0 & 0 & (b_{54})_7 & (b_{55})_7 & 0 & 0 \\ 0 & 0 & 0 & 0 & 0 & 0 & 0 \\ 0 & 0 & 0 & 0 & 0 & 0 & 0 \end{bmatrix}$$

$$\mathfrak{B}_8=\begin{bmatrix} 0 & 0 & 0 & 0 & 0 & 0 & 0 \\ 0 & 0 & 0 & 0 & 0 & 0 & 0 \\ 0 & 0 & 0 & 0 & 0 & 0 & 0 \\ 0 & 0 & 0 & 0 & 0 & 0 & 0 \\ 0 & 0 & 0 & 0 & (b_{55})_8 & (b_{56})_8 & 0 \\ 0 & 0 & 0 & 0 & (b_{65})_8 & (b_{66})_8 & 0 \\ 0 & 0 & 0 & 0 & 0 & 0 & 0 \end{bmatrix}$$

and

$$\mathfrak{B}_9=\begin{bmatrix} 0 & 0 & 0 & 0 & 0 & 0 & 0 \\ 0 & 0 & 0 & 0 & 0 & 0 & 0 \\ 0 & 0 & 0 & 0 & 0 & 0 & 0 \\ 0 & 0 & 0 & 0 & 0 & 0 & 0 \\ 0 & 0 & 0 & 0 & (b_{55})_9 & 0 & (b_{57})_9 \\ 0 & 0 & 0 & 0 & 0 & 0 & 0 \\ 0 & 0 & 0 & 0 & (b_{75})_9 & 0 & (b_{77})_9 \end{bmatrix}$$

Thus, we obtain matrix **B** defined by Eq.(2-3-43) as

$$B=\begin{bmatrix} Z_1 & (b_{12})_2 & 0 & (b_{14})_1 & 0 & 0 & 0 \\ (b_{21})_2 & Z_2 & 0 & 0 & 0 & (b_{26})_3 & 0 \\ 0 & 0 & Z_3 & (b_{34})_6 & 0 & 0 & (b_{37})_5 \\ (b_{41})_1 & 0 & (b_{43})_6 & Z_4 & (b_{45})_7 & 0 & 0 \\ 0 & 0 & 0 & (b_{54})_7 & Z_5 & (b_{56})_8 & (b_{57})_9 \\ 0 & (b_{62})_3 & 0 & 0 & (b_{65})_8 & Z_6 & (b_{67})_4 \\ 0 & 0 & (b_{73})_5 & 0 & (b_{75})_9 & (b_{76})_4 & Z_7 \end{bmatrix}$$

where

$$Z_1=(b_{11})_1+(b_{11})_2-m_1$$

$$Z_2=(b_{22})_2+(b_{22})_3-m_2$$

$$Z_3=(b_{33})_5+(b_{33})_6-m_3$$

$$Z_4 = (b_{44})_1 + (b_{44})_6 + (b_{44})_7 - m_4$$

$$Z_5 = (b_{55})_7 + (b_{55})_8 + (b_{55})_9 - m_5$$

$$Z_6 = (b_{66})_3 + (b_{66})_4 + (b_{66})_8 - m_6$$

and

$$Z_7 = (b_{77})_4 + (b_{77})_5 + (b_{77})_9 - m_7 \quad .$$

Junction equation (2-3-27) can further be reduced to what may be called the mixing junction equation. To this end, we use the following numbering convention for junctions. Let q be the number of branches in the network with at least one normal junction. Then partitioning the normal junctions branch-wise into q groups and collecting the mixing junctions as one group (group q+1), we have q+1 junction groups. Let $l_k (1 \leqq k \leqq q+1)$ be the size of junction group k.

Then we can cast Eq.(2-3-27) to the following form.

$$B = \begin{bmatrix} B_{d_1} & 0 & \cdots & 0 & B_{R_1} \\ 0 & B_{d_2} & \cdots & 0 & B_{R_2} \\ 0 & 0 & \cdots & B_{d_q} & B_{R_q} \\ B_{L_1} & B_{L_2} & \cdots & B_{L_q} & B_{d_{q+1}} \end{bmatrix} \qquad (2\text{-}3\text{-}44)$$

$$\Delta x_{N+1} = \begin{bmatrix} \Delta \tilde{x}_1 \\ \Delta \tilde{x}_2 \\ \cdot \\ \cdot \\ \Delta \tilde{x}_{q+1} \end{bmatrix} \qquad (2\text{-}3\text{-}45)$$

and

$$F = \begin{bmatrix} \tilde{F}_1 \\ \tilde{F}_2 \\ \cdot \\ \cdot \\ \tilde{F}_{q+1} \end{bmatrix} \qquad (2\text{-}3\text{-}46)$$

where the tilde refers to a junction group.

The matrices B_{R_k} and B_{L_k}, which are $2l_k \times 2l_{q+1}$ and $2l_{q+1} \times 2l_k$ respectively, show how junction group k ($1 \leqq k \leqq q$) and q+1 are coupled to each other such that

$$B_{R_k} = \begin{bmatrix} \cdot & (b_{k_A^+, k_f})_{k_A} & \cdot & \cdots & \cdot & \cdot \\ \cdot & \cdot & \cdot & \cdots & \cdot & \cdot \\ \cdot & \cdot & \cdot & \cdots & \cdot & \cdot \\ \cdot & \cdot & \cdot & \cdots & (b_{k_E^+, k_t})_{k_E} & \cdot \end{bmatrix} \qquad (2\text{-}3\text{-}47)$$

(k_f) (k_t)

and

$$B_{L_k} = \begin{bmatrix} \cdot & \cdots & \cdot & \cdot \\ (b_{k_f, k_A^+})_{k_A} & \cdots & \cdot & \cdot \\ \cdot & \cdots & \cdot & \cdot \\ \cdot & \cdots & \cdot & \cdot \\ \cdot & \cdots & \cdot & (b_{k_t, k_E^+})_{k_E} \\ \cdot & \cdots & \cdot & \cdot \end{bmatrix} \qquad (2\text{-}3\text{-}48)$$

(1) (l_k)

where $k_a, k_e, k_a^+, k_e^+, k_f$ and k_t are the most upstream node , the most downsteam node, the from-junction and the to-junction for junction group k ($1 \leqq k \leqq q$), respectively. Eq.(2-3-47) shows that the non-zero 2×2 elements of matrix B_{R_k} are $(1, k_f)$ and (l_k, k_t), while Eq.(2-3-48) shows that the non-zero 2×2 elements of matrix B_{L_k} are $(k_f, 1)$ and (k_t, l_k). These mean that, for a given junction group k ($1 \leqq k \leqq q$), the most upstream junction in group k is linked to from-mixing junction k_f, while the most downstream junction to to-mixing junction k_t.

In case of Fig.2-3-4, noting that

$q = 2$

$l_1 = 2$ (j=1 and 2)

$l_2 = 1$ (j=3)

and

$l_3 = 4 \quad (j=4,5,6,7)$,

we obtain matrices B_{L_k} and B_{R_k} (k= 1 and 2) and B_{d_k} (k = 1,2,3) as follows :

$$B_{L_1}=\begin{bmatrix} (b_{41})_1 & 0 \\ 0 & 0 \\ 0 & (b_{62})_3 \\ 0 & 0 \end{bmatrix}$$

$$B_{L_2}=\begin{bmatrix} (b_{43})_6 \\ 0 \\ 0 \\ (b_{37})_5 \end{bmatrix}$$

$$B_{R_1}=\begin{bmatrix} (b_{14})_1 & 0 & 0 & 0 \\ 0 & 0 & (b_{26})_3 & 0 \end{bmatrix}$$

$$B_{R_2}=\begin{bmatrix} (b_{34})_6 & 0 & 0 & (b_{73})_5 \end{bmatrix}$$

$$B_{d_1}=\begin{bmatrix} Z_1 & (b_{12})_2 \\ (b_{21})_2 & Z_2 \end{bmatrix}$$

$$B_{d_2}=Z_3$$

and

$$B_{d_3}=\begin{bmatrix} Z_4 & (b_{45})_7 & 0 & 0 \\ (b_{54})_7 & Z_5 & (b_{56})_8 & (b_{57})_9 \\ 0 & (b_{65})_8 & Z_6 & (b_{67})_4 \\ 0 & (b_{75})_9 & (b_{76})_4 & Z_7 \end{bmatrix}$$

Substituting Eqs.(2-3-44), (2-3-45) and (2-3-46) into Eq.(2-3-27), we obtain

$$B_{d_k}\Delta\tilde{x}_k+B_{d_{q+1}}\Delta\tilde{x}_{q+1}=\tilde{F}_k \qquad (1 \leqq k \leqq q) \qquad (2\text{-}3\text{-}49)$$

and

$$\sum_{k=1}^{q} B_{L_k}\Delta\tilde{x}_k+B_{d_{q+1}}\Delta\tilde{x}_{q+1}=\tilde{F}_{q+1} \qquad (2\text{-}3\text{-}50)$$

We obtain from Eq.(2-3-49),

$$\Delta\tilde{x}_k=-B_{d_k}^{-1}B_{R_k}\Delta\tilde{x}_{q+1}-B_{d_k}^{-1}\tilde{F}_k \qquad (1 \leqq k \leqq q) \qquad (2\text{-}3\text{-}51)$$

which is substituted into Eq.(2-3-50) to obtain

$$C\Delta\tilde{x}_{q+1}=G \tag{2-3-52}$$

where

$$C=B_{d_{q+1}}-\sum_{k=1}^{q}B_{L_k}(B_{d_k})^{-1}B_{R_k} \tag{2-3-53}$$

and

$$G=\tilde{F}_{q+1}-\sum_{k=1}^{q}B_{L_k}(B_{d_k})^{-1}\tilde{F}_k \tag{2-3-54}$$

We call Eq.(2-3-52) the mixing junction equation which is a simultaneous equation of order $2l_{q+1}$, i.e., twice as many as the number of mixing junctions. Matrix $(B_{d_k})^{-1}B_{R_k}$ and vector $(B_{d_k})^{-1}\tilde{F}_k$ are obtained in subroutines REINV and IVBAND, while matrix C and vector G are obtained in subroutine REDUCM. Equation (2-3-52) is solved in subroutine GAUSS.

By tracing back the discussions, we can obtain Δx in Eq.(2-3-22). First of all, we solve Eq.(2-3-52) to obtain the mixing junction vector $\Delta\tilde{x}_{q+1}$. Secondly, substituting $\Delta\tilde{x}_{q+1}$ into Eq.(2-3-51), we obtain chain vectors $\Delta\tilde{x}_k$ (k=1,2,...,q). Thus, we have obtained junction vector Δx_{N+1} corresponding to Eq.(2-3-45). Thirdly, substituting Δx_{N+1} into Eq.(2-3-26), we obtain normal node vector Δx_n (n=1,2,...,N). Thus, we have obtained the state vector of the system Δx. This procedure will be repeated following the scheme in Fig.2-3-3 until the solution converges.

2.4 Hydraulic Machine, Accumulator and Moisture Separator

In this chapter, we discuss the hydraulic machine model, the accumulator model and the moisture separator model. The discussions in this section correspond to a part of step 1 of Fig.2-3-2. We note that

accumulators are excluded from the implicit scheme discussed in the preceding section and that they are linked to our hydraulic network via boundary junctions.

2.4.1 Hydraulic Machine

It should be noted that both the head and torque of a machine are proportional to density. In THYDE-W, L_{head} is defined without density (see Eq.(2-2-66)), whereas $\mathcal{T}$, $\mathcal{T}_h$ and $\mathcal{T}^r$ are defined with density.

The equation of angular momentum of the machine shaft is given by[20]

$$\frac{da}{dt} = \lambda [\tau_e(t) - b(t) \quad - k_1 a|a| - k_2 sign(a)|a|^{1/2}] \qquad (2\text{-}4\text{-}1)$$

where

$$a = \frac{\Omega(t)}{\Omega^r}$$

$$b = \frac{\sum_{k=1}^{M} (\mathcal{T}_h)_k(t)}{\mathcal{T}^r}$$

$$\tau_e = \frac{\mathcal{T}_e(t)}{\mathcal{T}^r}$$

and

$$\lambda = \frac{30\mathcal{T}^r}{(\pi I_m \Omega_r)} \quad .$$

M is the number of machines on this shaft and k_1 and k_2 are constants and subscript "r" referes to the rated values not to be confused with the initial or steady state values.

Heat loss in a turbine node (see Eq.(2-2-65) or (2-3-8)) may be given as

$$q''' = -\frac{G\Delta h^r a^3}{L} \quad ,$$

where the rated enthalpy losses Δh^r are inputs (see BB15).

Eq.(2-4-1) is integrated with respect to time to find the shaft speed. For each turbine and pump, we have to evaluate the hydraulic torque T_h in Eq.(2-4-1) and the machine head L_{head} in Eq.(2-2-66). This is performed by using the sigle phase homologous pump curves[21] (see Figs.2-4-1 and 2-4-2) with modifications for two-phase mixture or cavitation as follows.

First, we discuss how to obtain the hydraulic machine head L_{head} and torque T_h for a non-cavitating subcooled water flow when the flow rate and the machine speed are given. We set

$$p_{head}=\frac{L_{head}}{L^r_{head}} \tag{2-4-2}$$

and

$$\omega=\frac{W}{W^r} \tag{2-4-3}$$

The head-discharge curve may be represented by two plots H^F_Q and H^R_Q which give h_{head}/a^2 versus w/a for all speeds in the forward and reverse directions, respectively. Then, $\tilde{p}_{head}$ can be given as

$$\tilde{p}_{head} = a^2 H^F_Q(\omega/a) \quad (a \geqq 0) \tag{2-4-4}$$

and

$$\tilde{p}_{head} = a^2 H^R_Q(\omega/a) \quad (a < 0) \tag{2-4-5}$$

where the tilde means the non-cavitating subcooled case to be modified later with the corrections for cavitation or saturated two-phase mixture. The similar homologous relations apply to the hydraulic torque :

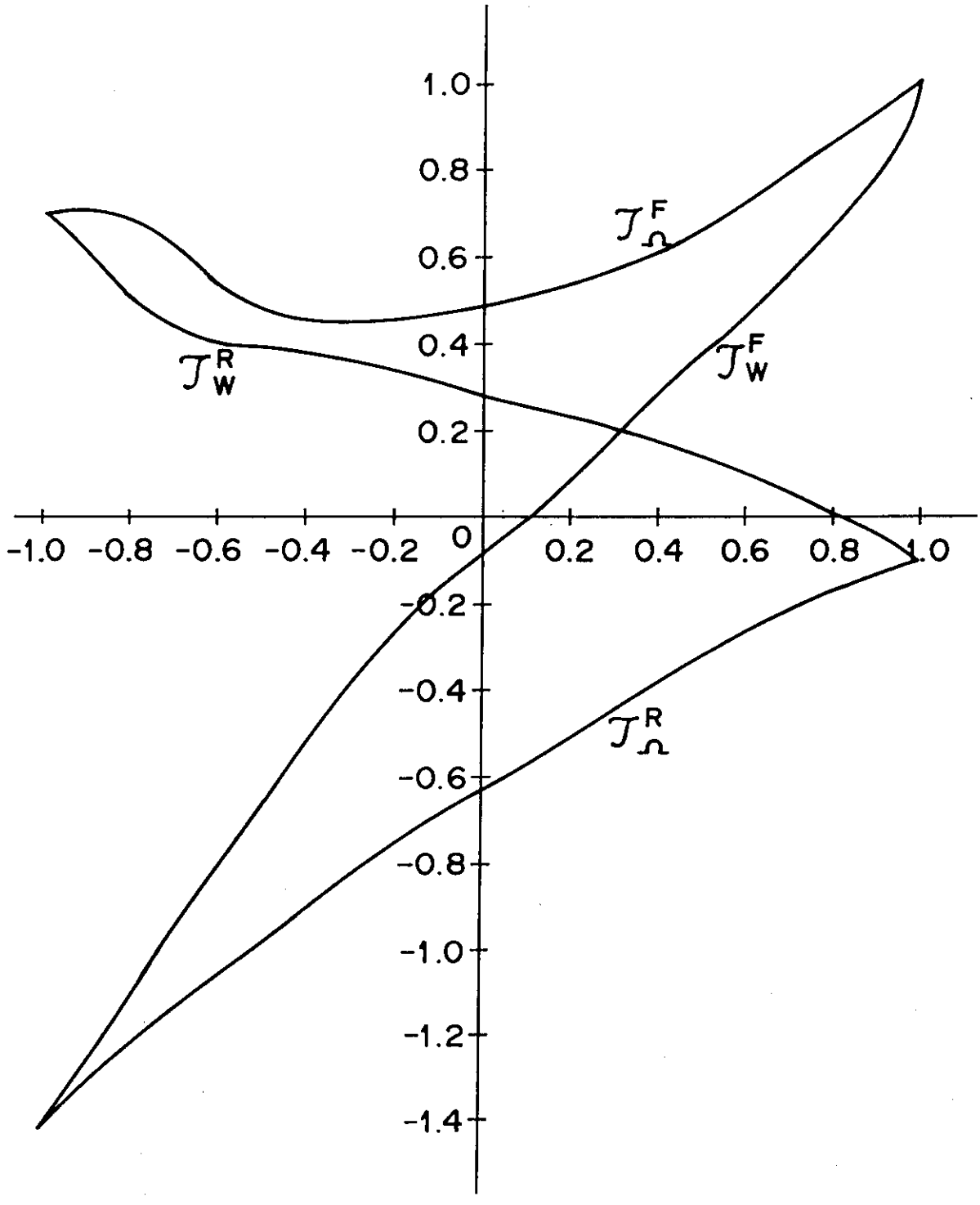

Fig. 2-4-1 Example of Homologous Torque Curve

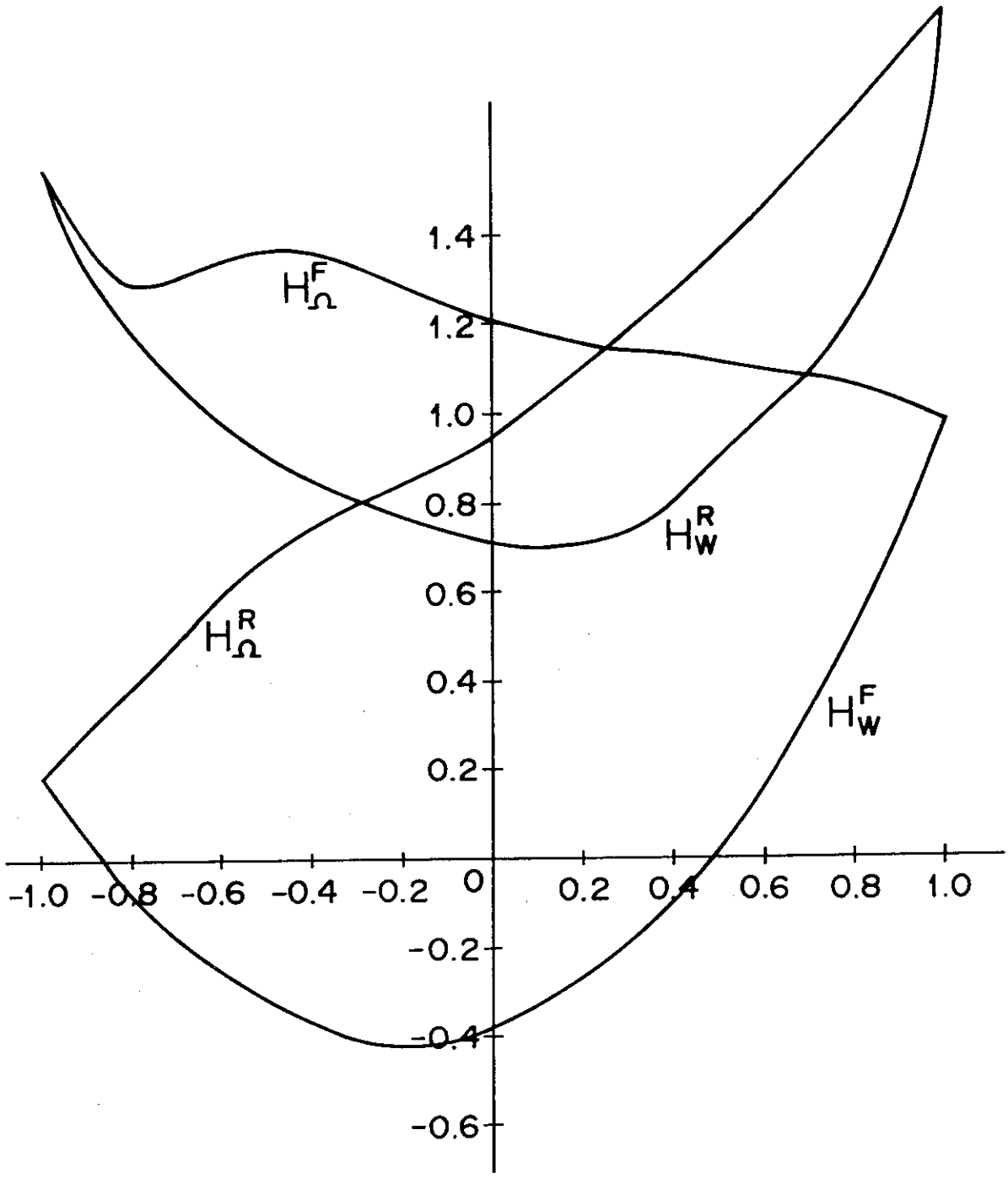

Fig. 2-4-2 Example of Homologous Head Curve

$$\tilde{b} = a^2 \mathcal{T}_{\omega}^{F}(\omega/a) \quad (a \geqq 0) \tag{2-4-6}$$

and

$$\tilde{b} = a^2 \mathcal{T}_{\omega}^{R}(\omega/a) \quad (a < 0) \quad . \tag{2-4-7}$$

For small $|a|$, the above relationships may become unsatisfactory so that the second set of homologous relations is utilized, although the two sets of relationships may be equivalent in principle. The THYDE-W code selects the applicable set of homologous relations according to the relative magnitudes of $|\omega|$ and $|a|$: If $|\omega| < |a|$, then the relationships (2-4-4) through (2-4-7) are selected. Otherwise, for $\omega \geqq 0$, we have

$$\tilde{p}_{head} = \omega^2 \mathcal{K}_{\omega}^{F}(a/\omega) \tag{2-4-8}$$

and

$$\tilde{b} = \omega^2 \mathcal{T}_{\omega}^{F}(a/\omega) \quad , \tag{2-4-9}$$

whereas for $\omega < 0$ we have

$$\tilde{p}_{head} = \omega^2 \mathcal{K}_{\omega}^{R}(a/\omega) \tag{2-4-10}$$

and

$$\tilde{b} = \omega^2 \mathcal{T}_{\omega}^{R}(a/\omega) \quad . \tag{2-4-11}$$

In the THYDE-W code, the correction of the above homologous relationships due to cavitation or two-phase mixture is performed as follows. First, we define the pressure and specific enthalpy at the impeller eye as

$$p_{eye} = p_{inlet}^{A} - (NPSH_R) g \frac{\rho_{inlet} + \rho_{outlet}}{2} \tag{2-4-12}$$

and

$$h_{eye} = \frac{h_{inlet} + h_{outlet}}{2}$$

where subscripts inlet and outlet refers to the inlet and outlet nodes of

the machine, respectively. In Eq.(2-4-12), the required net positive suction head $NPSH_R$ will be given as a function of a and ω. The cavitation is assumed to occur if the quality at the impeller eye x_{eye} obtained from p_{eye} and h_{eye} is caluclated to be positive. We assume that for each machine on the shaft the torque and head under cavitation can be expressed as

$$T_h = \frac{\rho_{eye}}{\rho^r}\tilde{T}_h - M_T(\tilde{T}_h - T_h) = \frac{\rho_{eye}}{\rho^r}\tilde{T}_h - M_T \Delta T_h \qquad (2\text{-}4\text{-}13)$$

and

$$L_{head} = \tilde{L}_{head} - M_h(\tilde{L}_{head} - L_{head}) = \tilde{L}_{head} - M_h \Delta L_{head} \qquad (2\text{-}4\text{-}14)$$

where M_T and M_h are the torque and head multipliers as functions of void fraction. Thus, we have

$$b = \frac{\rho_{eye}}{\rho^r}\tilde{b} - M_T \Delta b_{hyd} \qquad (2\text{-}4\text{-}15)$$

and

$$p_{head} = \tilde{p}_{head} - M_h \Delta l_{head} \qquad (2\text{-}4\text{-}16)$$

where $\Delta b_{hyd} = \Delta T_h / T^r$ and $\Delta l_{head} = \Delta L_{head} / L^r_{head}$ are input functions of shaft speed. It should be noted that the factor ρ_{eye}/ρ^r in Eq.(2-4-15) can be traced back to the definition of torque in THYDE-W. Therefore, a care must be taken for the inputs Δb_{hyd} and Δl_{head} .

2.4.2 *Accumulator*

The accumulator (ACC) system is one of the safety injection subsystems. It consists of a large volume reservoir of borated water maintained under gas pressure with a check valve in the accumulator piping to isolate the accumulator water from the primary coolant flow during a normal operation. The accumulator model can also be used to simulate a reactor containment vessel, for example. The ACC piping is not included

in the THYDE-W accumulator nodel, but is to be simulated by a linkage duct possibly with valves. The schematic figure of an accumulator is presented in Fig.2-4-3.

We have

$$\frac{d}{dt}(\rho hV)_L = -m_{inj}h_{inj} \tag{2-4-17}$$

and

$$\frac{d}{dt}(\rho V)_L = -m_{inj} \quad . \tag{2-4-18}$$

From Eqs.(2-4-17) and (2-4-18), we obtain

$$\frac{d}{dt}h_L = \frac{h_{inj}-h_L}{\tau} \quad , \tag{2-4-19}$$

where

$$\tau = \frac{-(\rho V)_L}{m_{inj}} \qquad if\ m_{inj} > 0 \quad (inflow)$$

$$= (a\ very\ large\ constant) \qquad otherwise \quad (outflow) \quad .$$

Applying the ideal gas law to the gas, we obtain the gas pressure p_G such that

$$p_G = p_G^0\left(\frac{V_G^0}{V_G}\right)^\gamma = p_G^0\left(\frac{V_T-V_L^0}{V_T-V_L}\right)^\gamma \tag{2-4-20}$$

where the water volume V_L is obtained from Eq.(2-4-18). In terms of V_L, h_L and p_G obtained from Eqs. (2-4-18), (2-4-19) and (2-4-20), respectively, the accumulator bottom pressure p_x can be given as

$$p_x = p_G + g\rho\left(\frac{p_G+p_x}{2}, h_L\right)(L_H)_L \quad , \tag{2-4-21}$$

where the height of the water volume $(L_H)_L$ is given in terms of the ACC cross section A_{ACC} as

$$(L_H)_L = \frac{V_L}{A_{ACC}} \quad .$$

In a transient calculation, we set $p_x = p_x^{old}$ on the right hand side of Eq.(2-4-21). The solutions p_x and h_L to Eqs.(2-4-19) and (2-4-21), respectively, give a p-source boundary condition of the thermal-hydraulic

network described in section 2.4.

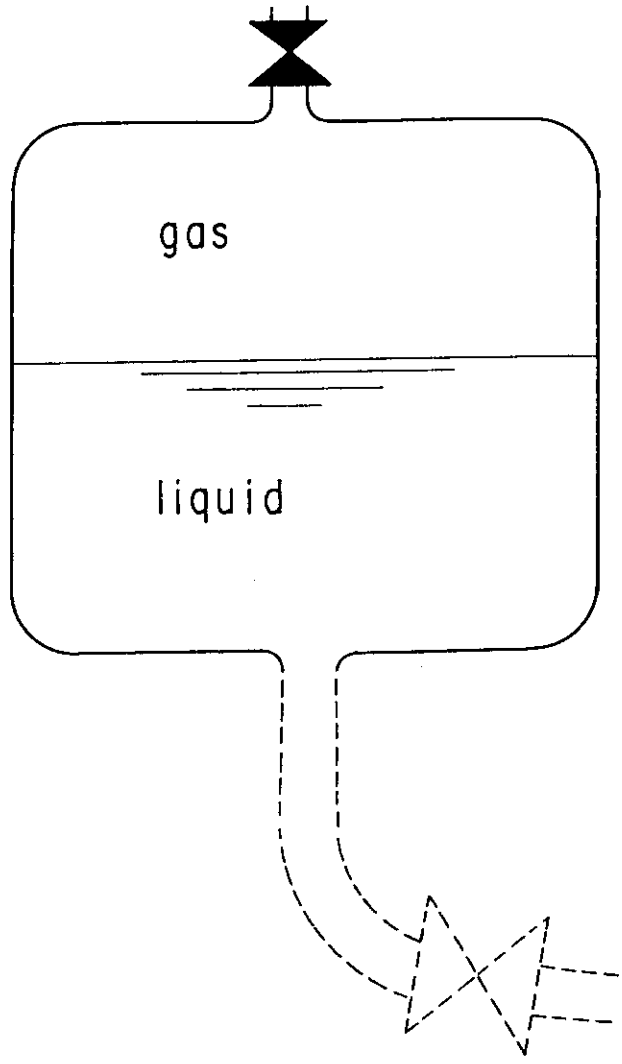

Fig. 2-4-3 Schematic Figure of Accumulator

2.4.3 Moisture Separator

A moisture separator is simulated by a special kind of mixing junction as shown in Fig.2-4-4 where flows W_1, W_2 and W_{in} are the flow to the SG downcomer, the flow to the turbine and the flow from the SG riser, respectively. We assume that entire steam goes to the SG outlet , while water goes patially to the the SG outlet and mostly to the downcomer. Let β_{sep} be the separation efficiency such that

$$W_1=\beta_{sep}(1-x^+)W_{in} \quad . \tag{2-4-22}$$

Therefore, separation efficiency β_{sep} is the fraction of the recirculated liquid mass to the total liquid mass in the separator. Thus, the flow rate W_2 to the turbine is composed of the vapor flow rate x^+W_{in} and the liquid flow rate $(1-\beta_{sep})(1-x^+)W_{in}$. Thus, we obtain W_2 and its quality $(x_2)^+_{eff}$ as follows :

$$\begin{aligned} W_2 &= x^+W_{in}+(1-\beta_{sep})(1-x^+)W_{in} \\ &= [\,1-\beta_{sep}(1-x^+)\,]W_{in} \quad , \end{aligned} \tag{2-4-23}$$

and

$$\begin{aligned} (x_2)^+_{eff} &= \frac{x^+W_{in}}{W_2} \\ &= \frac{x^+}{1-\beta_{sep}(1-x^+)} \quad . \end{aligned} \tag{2-4-24}$$

Thus, the specific enthalpy h* for the main steam flow to be used for h^+_{from} in Eq.(2-2-69) may be expressed as

$$h^* = h^+_{gs}(x_2)^+_{eff} + h^+_{fs}(\,1-(x_2)^+_{eff}\,) \quad . \tag{2-4-25}$$

In a transient, separation efficiency β_{sep} may be deteriorated so that the recirculation flow W_1 may contain vapor. Thus, the specific enthalpy h* of the recirculation flow to be used for h^+_{from} in Eq.(2-2-69) may be expressed as

$$h^* = h_{fs}^+ \frac{\beta_{sep}}{\beta_{sep}^0} + h^+ \left(1 - \frac{\beta_{sep}}{\beta_{sep}^0}\right)$$

$$= h_{fs}^+ \frac{\beta_{sep}}{\beta_{sep}^0} + \left(1 - \frac{\beta_{sep}}{\beta_{sep}^0}\right) \left[h_{gs}^+ x^+ + (1 - x^+) h_{fs}^+ \right] \quad , \qquad (2\text{-}4\text{-}26)$$

where β_{sep}^0 is given by Eq.(6-4-1). Define $(x_1)_{eff}^+$ such that

$$h^* = h_{gs}^+ (x_1)_{eff}^+ + h_{fs}^+ \left(1 - (x_1)_{eff}^+\right) \quad . \qquad (2\text{-}4\text{-}27)$$

Then, equating Eqs.(2-4-26) and (2-4-27), we obtain

$$(x_1)_{eff}^+ = x^+ \left(1 - \frac{\beta_{sep}}{\beta_{sep}^0}\right) \quad . \qquad (2\text{-}4\text{-}28)$$

In the present version of THYDE-W, the separation efficiency β_{sep} is assumed to vanish if $W_1 < 0$ or $W_2 < 0$ or $G_{in} < 50$ kg/(m^{2}sec) or $x^+ < 0.1$ or $x^+ > 0.995$.

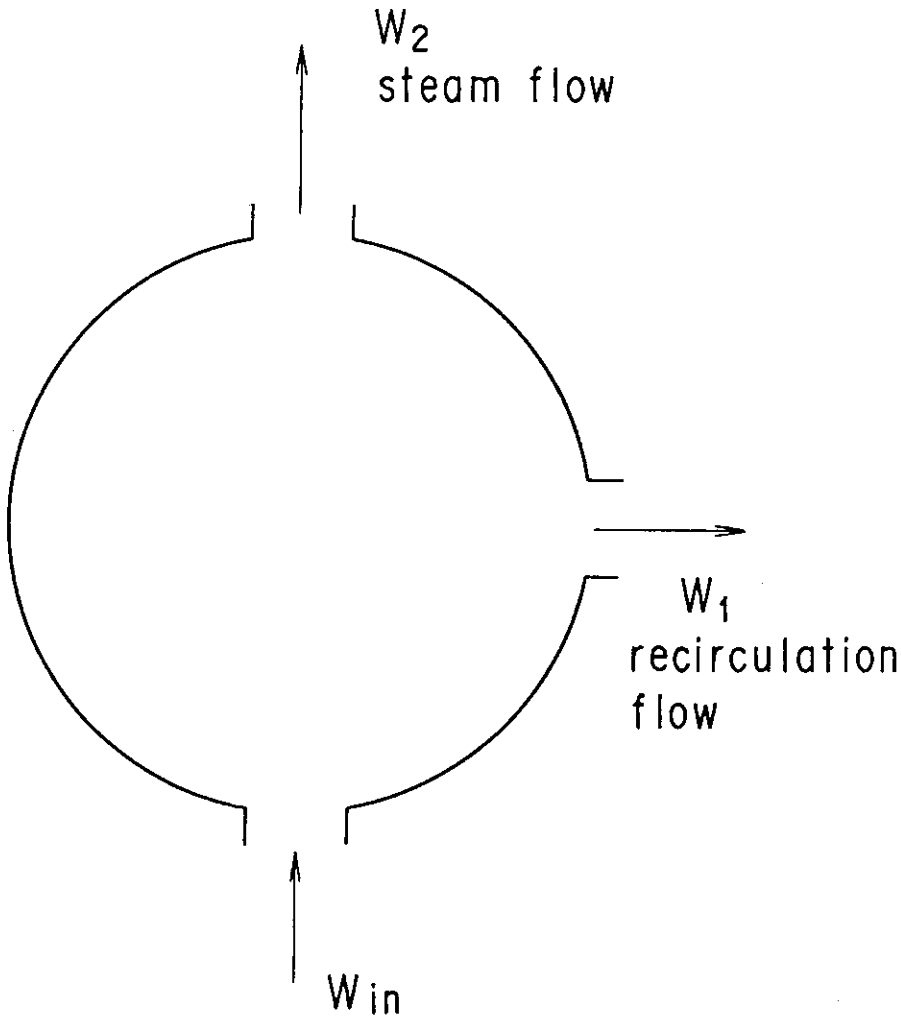

Fig. 2-4-4 Moisture Separator Mixing Junction

2.5 Form Loss Coefficient, Valve and Critical Flow

2.5.1 Junction Area

For each normal node, we define in this subsection

$$A^A = A\varepsilon^A \tag{2-5-1}$$

and

$$A^E = A\varepsilon^E \ , \tag{2-5-2}$$

where constriction factors ε^A and ε^E are inputs (BB10). In this subsection, only for the sake of clarity, we assume a single parallel node and a single normal junction. For each normal or boundary junction, we define the junction area A_j^+ such that

$$A_j^+(t) = (A_j^+)_{opn}\xi_{to}^A(t) \tag{2-5-3}$$

and

$$= (A_j^+)_{opn}\xi_{from}^E(t) \tag{2-5-4}$$

where we note that $\xi_{to}^A = \xi_{from}^E$ (refer to Eq.(2-5-12)) and $(A_j^+)_{opn}$ is obtained as follows.

If junction j is normal,

$$\begin{aligned}(A_j)_{opn}^+ &= min(A_{from}^E, A_{to}^A, A_{input}^+) \quad for\ A_{input}^+ \neq 0 \\ &= min(A_{from}^E, A_{to}^A) \qquad\quad for\ A_{input}^+ = 0 \ ,\end{aligned} \tag{2-5-5}$$

where A^A and A^E have been defined in Eqs.(2-5-1) and (2-5-2). If junction j is a boundary junction,

$$\begin{aligned}(A_j)_{opn}^+ &= A_{from}^E \qquad\quad for\ A_{input}^+ = 0 \\ &= min(A_{from}^E, A_{input}^+) \quad for\ A_{input}^+ \neq 0 \ .\end{aligned} \tag{2-5-6}$$

Given Eqs.(2-5-5) and (2-5-6), we define effective constriction factors γ^A and γ^E for each normal node such that

$$\gamma_n^A = \varepsilon_n^A \ (an\ input)\ if\ from\text{-}junc\ is\ a\ mixing\ junction$$

$$= \frac{(A^{\dagger}_{from})_{opn}}{A_n} \qquad otherwise \quad , \tag{2-5-7}$$

and

$$\gamma^E_n = \varepsilon^E_n \ (an\ input)\ if\ to\text{-}junc\ is\ a\ mixing\ junction$$

$$= \frac{(A^{\dagger}_{to})_{opn}}{A_n} \qquad otherwise \quad . \tag{2-5-8}$$

For a normal junction j, substituting Eqs.(2-5-7) into Eq.(2-5-3), we obtain

$$A^{\dagger}_j = \xi^A_{to}(A_j)_{opn} = \xi^A_{to}\gamma^A_{to}A_{to} \quad . \tag{2-5-9}$$

Similarly for a normal or boundary junction j, substituting Eqs.(2-5-8) into Eq.(2-5-4), we obtain the other expression for $A^{\dagger}_j$;

$$A^{\dagger}_j = \xi^E_{from}(A_j)_{opn} = \xi^E_{from}\gamma^E_{from}A_{from} \quad . \tag{2-5-10}$$

Owing to Eq.(2-5-12), we obtain from Eqs.(2-5-9) and (2-5-10)

$$\gamma^A_{to}A_{to} = \gamma^E_{from}A_{from} \quad ,$$

for a normal junction.

2.5.2 Form Loss Coefficient

Loss coefficients to be inputted are those for reverse flow at initially flowing nodes, those at initially stagnant nodes and those at a break point after its break. Loss coefficients at node average points k^{av} will be obtained by the steady state adjustment for initially non-stagnant nodes. Junction loss coefficients k^A and k^E are inputted or calculated in the code.

The option to calculate junction loss coefficients is as follows.

if $A_{from} < A_{to}$, then

$$(k^F_A)_{to} = (k^R_A)_{to} = 0$$

$$(k^F_E)_{from} = (1 - A^{\dagger}/A_{to})^2 = (1-\gamma^A_{to})^2$$

and

$$(k_E^R)_{from} = 0.45(1-A^+/A_{to}) = 0.45(1-\gamma_{to}^A) \quad .$$

If $A_{from}>A_{to}$, then

$$(k_E^F)_{from} = (k_E^R)_{from} = 0$$

$$(k_A^R)_{to} = (1-A^+/A_{from})^2 = (1-\gamma_{from}^E)^2$$

and

$$(k_A^F)_{to} = 0.45(1-A^+/A_{from}) = 0.45(1-\gamma_{from}^E) \quad .$$

2.5.3 *Valve*

The valve behavior can be simulated by

$$\frac{d\xi}{dt}=\frac{\xi_c-\xi}{\tau} \qquad (2-5-11)$$

where ξ_c is the valve opening such that

$\xi_c = 1$ when it is completely open

$= 0$ when it is completely closed .

The time constant τ (an input) and the logic to determine ξ_c depend on the type of the valve.

In addition to the valves specified by the inputs, there are pseudo valves presumed in the code which include :

(1) dead end valves ; always closed

(2) open valves at ordinary normal nodes ; always open
(except at nodes with actual valves)

(3) valves to imperatively cut off accumulators ; to be closed when residual water is less than 5 %.

All valves including the pseudo valves can be placed only on the E point of a normal node. For the sake of clarity, we allocate variables ξ^A and ξ^E to all nodes. Thy are unity, if the corresponding place does

not have a valve. Then, for a normal junction,

$$\xi^{A}_{to} = \xi^{E}_{from} \quad . \tag{2-5-12}$$

If the from-junction is a mixing junction, the point A can not have a valve so that

$$\xi^{A} = 1 \quad .$$

2.5.4 Critical Flows

Given the specific enthalpy h and the pressure p at the discharge point, the critical flow G_M can be given by the following set of equations.

a) If the coolant is subcooled, the critical flow is given by

$$G_M = c_1 \sqrt{2\rho(p,h)(p - C_2 p_s)} \tag{2-5-13}$$

where

$$\rho = \rho_{fs}\ (\mathrm{p}) \qquad x \geqq 0$$

$$= \rho_f\ (\mathrm{p,h}) \qquad x < 0$$

and c_1 is a function of enthalpy h such that

$$c_1 = C_d G_M(p_s,h) / \sqrt{2\rho_{fs}(h)(1 - C_2 p_s)} \quad .$$

b) If $0.02 < x < 1$, then

$$G_M = C_X C_D g_M(p,h) \tag{2-5-14}$$

where $g_M(p,h)$ is given by Moody Table[17] and C_X is the factor to ensure continuity of G_M at x=0.02.

c) If $x > 1$, then

$$G_M = C_2 \sqrt{\gamma (2/(\gamma+1))^{((\gamma+1)/(\gamma-1))} \rho_g(p,h) p} \tag{2-5-15}$$

where

$$C_2(p) = C_X C_D g_M(p, h_{gs}(p)) / \sqrt{\gamma (2/(\gamma+1))^{((\gamma+1)/(\gamma-1))} \rho_{gs}(p) p} \quad .$$

3. Heat Transfer

In this chapter, we will discuss heat transfer aspects of THYDE-W. In section 3.1, various heat sources in a fuel rod including metal-water reaction are discussed. In section 3.2, given a heat transfer coefficient, we will give the method to calculate heat transfer rate to a coolant flow. In section 3.4, rod-to-rod radiative heat transfer is discussed, using the 3 x 3 rod cluster model. In section 3.5, the heat transfer and critical heat flux correlations are cited.

3.1 Heat Generation inside Fuel

Heat sources inside fuel Ξ to be used in Eq.(3-3-1) are (i) fission power, (ii) decay heat of fission products, (iii) decay heat of actinides and (iv) metal-water reaction heat. In the following, we will discuss them, separately. Items (i), (ii), and (iii) are not accounted for in a non-nuclear calculation option.

3.1.1 Fission Power

The nuclear reactor kinetics equation in the THYDE-W code is based on the point kinetics model with 6 groups of delayed neutron precursors.

$$\frac{dn}{dt}=\frac{\beta}{l}(\Gamma_{tot}-1)n+\sum_{i=1}^{6}\lambda_i C_i \qquad (3\text{-}1\text{-}1)$$

$$\frac{dC_i}{dt}=-\lambda_i C_i+\frac{\beta_i}{l}n \qquad (i=1,2,.....6) \qquad (3\text{-}1\text{-}2)$$

where

$$\beta=\sum_{i=1}^{6}\beta_i$$

3. Heat Transfer

In this chapter, we will discuss heat transfer aspects of THYDE-W. In section 3.1, various heat sources in a fuel rod including metal-water reaction are discussed. In section 3.2, given a heat transfer coefficient, we will give the method to calculate heat transfer rate to a coolant flow. In section 3.4, rod-to-rod radiative heat transfer is discussed, using the 3 x 3 rod cluster model. In section 3.5, the heat transfer and critical heat flux correlations are cited.

3.1 Heat Generation inside Fuel

Heat sources inside fuel Ξ to be used in Eq.(3-3-1) are (i) fission power, (ii) decay heat of fission products, (iii) decay heat of actinides and (iv) metal-water reaction heat. In the following, we will discuss them, separately. Items (i), (ii), and (iii) are not accounted for in a non-nuclear calculation option.

3.1.1 Fission Power

The nuclear reactor kinetics equation in the THYDE-W code is based on the point kinetics model with 6 groups of delayed neutron precursors.

$$\frac{dn}{dt}=\frac{\beta}{l}(\Gamma_{tot}-1)n+\sum_{i=1}^{6}\lambda_i C_i \qquad (3-1-1)$$

$$\frac{dC_i}{dt}=-\lambda_i C_i+\frac{\beta_i}{l}n \qquad (i=1,2,.....6\ ) \qquad (3-1-2)$$

where

$$\beta=\sum_{i=1}^{6}\beta_i$$

and

$$n(0)=1 \quad .$$

Total reactivity $\Gamma_{tot}(t)$ in Eq.(3-1-1) is calculated as the sum of five reactivity components, i.e.,

$$\Gamma_{tot}(t) = \Gamma_{ex}(t) + \Gamma_{T_F} + \Gamma_{T_C} + \Gamma_{\rho} + \Gamma_B \quad . \tag{3-1-3}$$

In Eq.(3-1-3), the first term $\Gamma_{ex}(t)$ represents the external reactivity contributions such as control rod insertion, whereas the second, third, fourth and fifth terms are the feedback effects due to a fuel temperature change, a coolant temperature change and a coolant density change (a void fraction change) and a boron concentration change, respectively, such that

$$\Gamma_{T_F}=\gamma_{T_F}(T_F(t)-T_F(0)) \quad ,$$

$$\Gamma_{T_C}=\gamma_{T_C}(T_C(t)-T_C(0)) \quad ,$$

$$\Gamma_{\rho}=\Gamma_{\rho}(\rho) \quad ,$$

and

$$\Gamma_B = -\frac{\sigma_B(N_B-N_B^0)}{\Sigma_a} \quad , \tag{3-1-3a}$$

where T_F, T_C, ρ and N_B are the averages over the entire core. In Eq.(3-1-3a), absorption cross section of natural boron σ_B is 755 b, while atomic number density of natural boron N_B (cm^{-3}) is given by boron concentration c_B (ppm) as

$$N_B = C_{cv}\frac{[\rho_f(1-\alpha)c_B]_{core}A_v}{M_B} = C_{cv}\frac{(\rho\tilde{c})_{core}A_v}{M_B} \quad , \tag{3-1-3b}$$

where $C_{cv}=10^{-9}$, M_B = 10.8 g/mole, and $\tilde{c}$ = $(1-x)c_B$. In Eq.(3-1-3b), $(\rho\tilde{c})_{core}$ is the average of $\rho\tilde{c}$ over the core, where $\tilde{c}$ is the solutions to Eqs.(5-1-2) and (5-1-5).

3.1.2 Fission Products Decay Heat

The decay heat due to FP (fission products) except actinides is calculated[7] such that

$$R_{FP}=\varepsilon\sum_{i=1}^{11}x_i \tag{3-1-4}$$

where

$$\frac{d}{dt}x_i=\lambda_i(nE_i-x_i) \qquad (1\leqq i\leqq 11) \tag{3-1-5}$$

$$\varepsilon = 1.0 \text{ for a BE calculation}$$
$$= 1.2 \text{ for an EM calculation} \tag{3-1-6}$$

and

$$x_i(0)= E_i \qquad (1\leqq i\leqq 11)\ .$$

For the BE and EM calculations, see chap 7. Parameters E_i and λ_i are given in Ref.(7).

3.1.3 Actinides Decay Heat

The heat contribution from actinides decay is calculated as follows. We consider only ^{239}U and ^{239}Np .

$$^{238}_{92}U(n,\gamma)^{239}_{92}U\xrightarrow{\beta^-}{}^{239}_{93}Np\xrightarrow{\beta^-}{}^{239}_{94}Pu$$

Then

$$\frac{d}{dt}N_{29}=-\lambda_{29}N_{29}+C_c\Sigma_a\varphi(0)n(t) \tag{3-1-7}$$

and

$$\frac{d}{dt}N_{39}=-\lambda_{39}N_{39}+\lambda_{29}N_{29}. \tag{3-1-8}$$

where

$$\lambda_{29}=4.91\times10^{-4}\ sec^{-1}$$

and

$$\lambda_{39}=3.41\times10^{-4}\ sec^{-1} \quad .$$

If the chain is at a steady state, then

$$N_i(0)=C_c\Sigma_a\varphi(0)/\lambda_i \qquad (i=29\ and\ 39) \quad .$$

Relative power R_{ACT} produced by actinides decay is given by

$$R_{ACT}=\frac{(y\lambda N)_{29}+(y\lambda N)_{39}}{Y\Sigma_f\varphi(0)} \qquad (3-1-9)$$

where

Y = 207.3 MeV/fission

y_{29} = 0.456 MeV/decay

and

y_{39} = 0.434 MeV/decay .

If we set

$$N_i=C_c\Sigma_a\frac{\varphi(0)x_i}{\lambda_i} \qquad (i=29,39) \quad ,$$

then Eq.(3-1-9) will be transformed to the following equation.

$$R_{ACT}=C_c\frac{\Sigma_a}{\Sigma_f}\frac{(yx)_{29}+(yx)_{39}}{Y} \qquad (3-1-10)$$

where

$$\frac{d}{dt}x_{29}=\lambda_{29}(n-x_{29}) \qquad (3-1-11)$$

and

$$\frac{d}{dt}x_{39}=\lambda_{39}(x_{29}-x_{39}) \qquad (3-1-12)$$

with the initial condition

$$x_i(0)=1 \qquad (i=29\ and\ 39) \quad .$$

3.1.4 Metal-Water Reaction

Heat generation in the cladding due to the metal-water reaction

is calculated based on the equation of Baker and Just[26] with no limitations for steam availability as required by Ref.(1). When a burst is calculated to occur, the Zircaloy cladding is assumed to react on the inside as well as on the outside for a length of the burst node. The equation of Baker and Just is

$$\frac{d\Theta}{dt}=K_1\frac{e^{-K_2/(T+273)}}{\Theta} \qquad (3-1-13)$$

where

$$K_1=0.775\times10^{-4} \quad m^2/sec$$

and

$$K_2=2.29\times10^{-4} \quad {}^\circ K \quad .$$

In the THYDE-W code, it is assumed that the heat generation is uniformly distributed in the clad node where the boundary of the reacted zircaloy is present. The volumetric heat source of the node with thickness Δr is given by

$$\Xi_{MW}=\rho_{zr}\Delta h_{reac}\frac{d\Theta}{dt}/\Delta r \qquad (3-1-14)$$

where

$$\rho_{zr}=6.568\times10^{-3} \quad kg/m^2 \quad .$$

Following assumption (b) in subsection 4.1.2, oxide thinning resulting from clad burst will be taken into consideration in Eq.(3-1-13).

3.2 Heat Transfer from Fuel to Coolant

A distinction is made for two kinds of heat transfer coefficients , i.e., the one which is the coefficient of heat transfer to the coolant and the other which is the heat transfer coefficient for the calculation of the wall surface temperature. The difference arises when rod-to-rod radiation becomes effective, for example, after clad

burst. In section 3.3, heat conduction is discussed.

3.2.1 Before burst (Elevation without Burst)

In the following discussion, we will drop the subscript indicating the core node in question. The heat source to the core coolant q''' in Eq.(2-3-8) is given by

$$q''' = \frac{2\pi r_R \varphi_R}{A} \qquad (3\text{-}2\text{-}1)$$

with

$$\varphi_R = h_{tr}^{c}(T_R - T_b) \qquad (3\text{-}2\text{-}2)$$

where h_{tr}^{c} is the coefficient of heat transfer to the coolant which is not to be confused with h_{tr}^{cs}, i.e., the heat transfer coefficient for the calculation of the clad surface temperature (see section 3.5). The heat transfer coefficient h_{tr}^{c} can be divided into two components such that

$$h_{tr}^{c} = h_{tr}^{w-c} + h_{tr}^{cvn} \quad , \qquad (3\text{-}2\text{-}3)$$

where h_{tr}^{w-c} is the rod-to-coolant radiative heat transfer coefficient, whereas h_{tr}^{cvn} is the rest due to convective or boiling or condensation heat transfer. The readers can refer to subsections 3.5.1 and 3.5.3 for the latter and the former, respectively.

3.2.2 After burst (Elevation with Burst)

The core will be divided into several regions, each of which will be regarded as a collection of identical coolant channels. Suppose that the fuel rod in a certain region was calculated to burst at a certain elevation. Then, it will be interpreted that bursts have occurred at that elevation with a certain pattern in the entire region. With the calculated occurence of a burst, the two fuel rod calculation will be

started for the region to include rod-to-rod radiative heat transfer on the basis of the 3 x 3 rod matrix to be described in section 3.4.

Among the parameters in Eqs.(3-2-1) and (3-2-2), not only the heat transfer coefficient, but also the wetted perimeter and the cross-sectional flow area will be influenced. The former will be explained in section 3.4, while the latter two in the following.

Averaging the latter two over the 3 x 3 matrix , the heat input from the burst axial node of the matrix to the average core flow is obtained as follows:

First we obtain the change in the wetted perimeter. If the center rod is burst, then the wetted perimeter in the matrix changes from

$$l_w = 8\pi r_R$$

to

$$l_w^* = \pi r_R^*(8 - M_b - \frac{N_b}{2}) + \pi r_R(M_b + \frac{N_b}{2}) \quad . \qquad (3\text{-}2\text{-}4a)$$

And if the center rod is not burst, then the wetted perimeter changes to

$$l_w^* = \pi r_R^*(6 - M_n - \frac{N_n}{2}) + \pi r_R(2 + M_n + \frac{N_n}{2}) \quad . \qquad (3\text{-}2\text{-}4b)$$

Thus the heat input from the axial matrix node with clad burst to the average core flow is given by

$$q''' = \frac{\omega_1(2\pi r_R)\varphi_R + \omega_2(2\pi r_R^*)\varphi_R^*}{A_9^*} \qquad (3\text{-}2\text{-}5)$$

with

$$\omega_1 + \omega_2 = 4$$

$$\omega_1 = M_b/2 + N_b/4 \qquad \textit{if center rod is burst}$$

$$\omega_1 = 1 + M_b/2 + N_b/4 \qquad \textit{if center rod is non-burst}$$

$$\varphi_R^* = h_{tr}^{cs^*}(T_R^b - T_b) = (h_{tr}^{c^*} + h_{tr}^b)(T_R^b - T_b)$$

and

$$\varphi_R = h_{tr}^{cs}(T_R^n - T_b) = (h_{tr}^c + h_{tr}^n)(T_R^n - T_b) \quad ,$$

where h_{tr}^{cs} is defined in Eqs.(3-5-3) and (3-5-4). The flow area A_9^* in Eq.(3-2-5) is given by Eq.(4-1-20) or (4-1-22). The heat transfer coefficient h_{tr}^{c} is given by Eq.(3-2-3), and h_{tr}^{c*} is the coefficient of heat transfer to coolant for the burst node. For the meaning of N_b and M_b or N_n and M_n, reference should be made to section 3.4.

3.3 Heat Conduction

3.3.1 Heat Conductor Configuration

Heat conduction in heat conductors is assumed one-dimensional so that direct heat transfer (heat conduction) between adjacent two conductors are not taken into cosideration.

Depending on the type of boundary condition at the left (or inner) and right (or outer) surfaces of a conductor, there are 5 cases as shown in Fig.3-3-1. The case of a constant wall temperature can be simulated by case 4 or 5 by inputting a sink temparature equal to the desired wall temperature along with a very large convective heat transfer coefficient.

3.3.2 Temperature Distribution

The heat conduction in a heat conductor is given by

$$\rho C_p \frac{\partial T}{\partial t} = \frac{1}{r^\alpha} \frac{\partial}{\partial r} (\lambda r^\alpha \frac{\partial T}{\partial r}) + \Xi \qquad (3-3-1)$$

where

α = 0 for cartesian coordinate system

= 1 for cylindrical coordinate system

= 2 for spherical coordinate system .

We define the noding convention in a heat conductor as shown in Fig.3-3-2. For a solid cylinder, we let $r_0 = 0$.

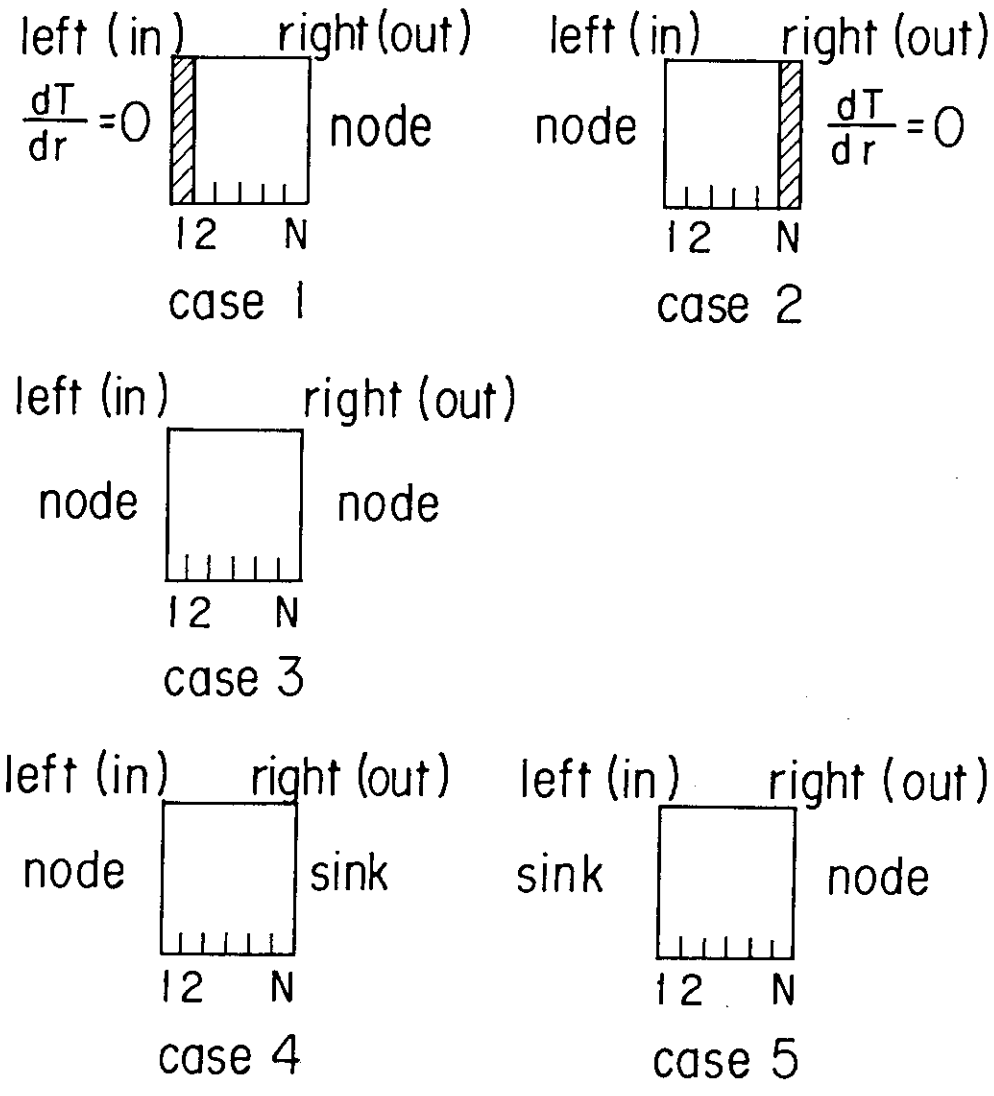

Fig. 3-3-1 Heat Conductor Configurations

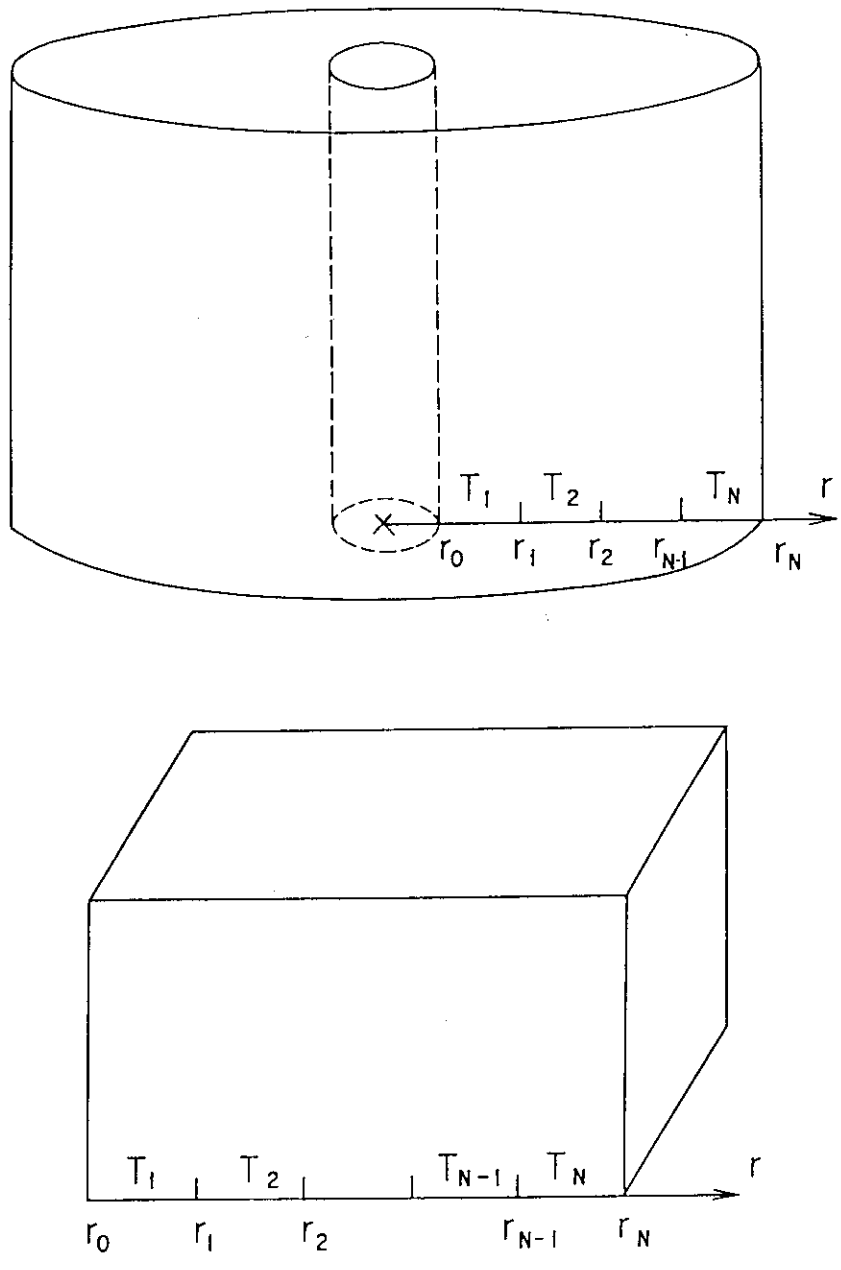

Fig. 3-3-2 Noding Convention of Heat Conductor

For rod type fuel, the heat production rate $\Xi(r,t)$ may be represented by

$$\Xi = \frac{2}{r_F}\varphi_F(z,0)\Pi(t) \quad ,0<r<r_F \tag{3-3-2}$$

$$= \Xi_{MW} \quad ,r_{CL}^{IN}<r<r_R \tag{3-3-3}$$

where heat production is assumed uniform in the fuel pellet, whereas Ξ_{MW} is given by Eq.(3-1-14) such that it does not vanish in the clad nodes where the boundary of the reacted zirconium is present. The temporal behavior of the heat generation in nuclear fuel $\Pi(t)$ is given by

$$\Pi = \frac{[\,n+R_{FP}+R_{ACT}\,]}{(1+R_{FP}(0)+R_{ACT}(0))} \tag{3-3-4}$$

where R_{FP} and R_{ACT} are given by Eqs.(3-1-4) and (3-1-10), respectively. It should be noted in Eq.(3-3-4) that the condition $\Pi(0)=1.0$ is satisfied.

Integrating Eq.(3-3-1) from r = r_{i-1} to r = r_i, we obtain

$$\gamma_i V_i(\frac{\partial T_i}{\partial t}) = \delta_i T_{i+1} - (\delta_i+\delta_{i-1})T_i + \delta_{i-1}T_{i-1} + \Xi_i V_i \quad ,$$

which can be transformed to

$$\frac{\partial T_i}{\partial t} = G_i = \frac{\delta_i T_{i+1} - (\delta_i+\delta_{i-1})T_i + \delta_{i-1}T_{i-1}}{\gamma_i V_i} + (\frac{\Xi}{\gamma})_i \quad . \tag{3-3-5}$$

In Eq.(3-3-5), the parameters are defined as follows ;

$$V_i = L(r_i - r_{i-1})\delta z \qquad \alpha = 0$$

$$= \pi(r_i^2 - r_{i-1}^2)\delta z \qquad \alpha = 1$$

$$= \frac{2\pi}{3}(1-\cos\theta)(r_i^3 - r_{i-1}^3) \qquad \alpha = 2$$

$$S_i = L\delta z \qquad \alpha = 0$$

$$= 2\pi r_i \delta z \qquad \alpha = 1$$

$$= 2\pi(1-\cos\theta)r_i^2 \qquad \alpha = 2$$

$$\delta_i = 2S_i\frac{\lambda_{i+1}(r_i - r_{i-1}) + \lambda_i(r_{i+1} - r_i)}{(r_{i+1} - r_{i-1})^2}$$

and

$$\gamma_i = (\rho c_p)_i \quad .$$

Especially, for δ_0, δ_N, T_0 and T_{N+1}, we have

$$\delta_0 = 0 \qquad for\ IC = 1$$

$$= S_0 h_{tr} \qquad for\ IC = 2,3,4$$

$$= \frac{S_0 h_{rad}((T_0^{old}+273)^3-(T_1^{old}+273)^3)}{(T_0^{old}-T_1^{old})} \qquad for\ IC = 5$$

$$\delta_N = S_N h_{tr} \qquad for\ IC = 1,3,5$$

$$= 0 \qquad for\ IC = 2$$

$$= \frac{S_N h_{rad}((T_{N+1}^{old}+273)^3-(T_N^{old}+273)^3)}{(T_{N+1}^{old}-T_N^{old})} \qquad for\ IC = 4$$

$$T_0 = T_b \qquad for\ IC = 2,3,4$$

$$= T_{sink} \qquad for\ IC = 5$$

(not defined for IC = 1)

and

$$T_{N+1} = T_b \qquad for\ IC = 1,3,5$$

$$= T_{sink} \qquad for\ IC = 4$$

(not defined for IC = 2)

We now solve Eq.(3-3-5) by the Crank-Nicolson method, i.e.,

$$\frac{T_i^{new}-T_i^{old}}{\Delta t} = \tilde{\theta} G_i^{new} + (1-\tilde{\theta}) G_i^{old} \qquad (0 < \tilde{\theta} \leqq 1) \qquad (3-3-6)$$

which can be transformed to be

$$(-A_i T_{i+1} + B_i T_i - C_i T_{i-1})^{new} = D_i \qquad (3-3-7)$$

where

$$A_i = \tilde{\theta}\,\delta_i$$

$$B_i = \frac{V_i \gamma_i}{\Delta t} + \tilde{\theta}\,(\delta_i + \delta_{i-1})$$

$$C_i = \tilde{\theta}\,\delta_{i-1}$$

$$D_i = \frac{V_i\gamma_i T_i^{old}}{\Delta t} + (1-\tilde{\theta})V_i\gamma_i G_i^{old} + V_i\,\tilde{\theta}\,\Xi_i^{new}$$

Especially,

$$D_N = \frac{V_N\gamma_N T_N^{old}}{\Delta t} + (1-\tilde{\theta})V_N\gamma_N G_N^{old} + \tilde{\theta}\,(\Xi V)_N^{new} + \frac{V_N\gamma_N A_N T_b}{\Delta t} \qquad for\ IC=3$$

$$D_N = \frac{V_N\gamma_N T_N^{old}}{\Delta t} + (1-\tilde{\theta})V_N\gamma_N G_N^{old} + \tilde{\theta}\,(\Xi V)_N^{new} + \frac{V_N\gamma_N A_N T_{sink}}{\Delta t} \qquad for\ IC=4$$

and

$$D_1 = \frac{V_1\gamma_1 T_1^{old}}{\Delta t} + (1-\tilde{\theta})V_1\gamma_1 G_1^{old} + \tilde{\theta}\,(\Xi V)_1^{new} + \frac{V_1\gamma_1 C_1 T_{sink}}{\Delta t} \qquad for\ IC=5\ .$$

In the linear implicit scheme, the coefficient A_i, B_i, C_i and D_i in Eq.(3-3-7) are the old values so that it becomes a tri-diagonal matrix equation to which Thomas algorithm can be applied as follows.

Cases 1 and 5 :

Set

$$T_{i-1} = E_{i-1}T_i + F_{i-1} \qquad (i=1,2,.....N) \quad . \qquad (3\text{-}3\text{-}8)$$

Substituting Eq.(3-3-8) into Eq.(3-3-7) and solving the resultant equation for T_i, we can identify

$$E_i = \frac{A_i}{B_i - C_i E_{i-1}} \quad , \qquad (3\text{-}3\text{-}9)$$

and

$$F_i = \frac{D_i + C_i F_{i-1}}{B_i - C_i E_{i-1}} \quad . \qquad (3\text{-}3\text{-}9a)$$

Equation (3-3-8) with Eqs.(3-3-9) and (3-3-9a) gives T_i successively from i=N to i=1, since $E_0 = F_0 = 0$ and $T_{N+1} = T_{bulk}$.

Cases 2, 3 and 4 :

Set

$$T_i = E_i T_{i-1} + F_i \qquad (i=1,2,.....N) \quad . \qquad (3\text{-}3\text{-}10)$$

Substituting it into Eq.(3-3-7) and solving the resultant equation for T_i, we can identify

$$E_i = \frac{C_i}{B_i - A_i E_{i+1}} \quad , \tag{3-3-10a}$$

and

$$F_i = \frac{D_i + A_i F_{i+1}}{B_i - A_i E_{i+1}} \quad . \tag{3-3-10b}$$

Equation (3-3-10) with Eqs.(3-3-10a) and (3-3-10b) gives T_i successively from i=1 to i=N, since $E_{N+1} = F_{N+1} = 0$ and $T_0 = T_{bulk}$.

3.3.3 Gap Conductivity[27),(28)]

Special treatments are needed for a fuel rod with a gap. We assume the following relationship to hold

$$\varphi_{CL}^{in}(r_F + r_{gap}) = \varphi_F^{out} r_F \tag{3-3-11}$$

which means that the total heat flux at the clad inner surface coincides with that at the pellet outer surface. In THYDE-W, the gap conductivity h_{gap}^t is defined in terms of φ_{CL}^{in} such that

$$\varphi_{CL}^{in} = h_{gap}^t (T_F^{out} - T_{CL}^{in}) \quad . \tag{3-3-12}$$

Substituting Eq.(3-3-12) into Eq.(3-3-11), we obtain

$$\varphi_F^{out} = \frac{r_F + r_{gap}}{r_F} h_{gap}^t (T_F^{out} - T_{CL}^{in}) \quad . \tag{3-3-12a}$$

Gap conductivity h_{gap}^t is composed of two components ; (1) heat conduction and (2) radiation. We first discuss heat conduction. If $r_{gap} > 0$, then

$$h_{gap} = \frac{\lambda_{gap}}{r_{gap} + 4.39 \times 10^{-6}} \tag{3-3-13}$$

and if $r_{gap} = 0$, then

$$h_{gap} = 1.16 \times 10^{-6} p_{gc} + \frac{\lambda_{gap}}{4.39 \times 10^{-6}} \tag{3-3-14}$$

where p_{gc} is the contact pressure between fuel pellet and cladding. The conductivity of the gas mixture λ_{gap} in Eqs.(3-3-13) and (3-3-14) is calculated from a formula based on the work of Brokaw[29], that is,

$$\lambda_{gap}=\sum_{i=1}\lambda_i/(1+\sum_{j=1,j\neq i}\Psi_{ij}y_j/y_i) \tag{3-3-15}$$

where

$$\Psi_{ij}=\frac{\Phi_{ij}[1+(\lambda_i/\lambda_j)^{1/2}(M_i/M_j)^{1/4}]^2}{2^{1.5}(1+M_i/M_j)^{1/2}} \tag{3-3-16}$$

$$\Phi_{ij}=1+2.41\frac{(M_i-M_j)(M_i-0.142M_j)}{(M_i+M_j)^2} \tag{3-3-17}$$

and :

M = molecular weight of a component gas

y = molecular fraction of the gas

λ = the thermal conductivity of the pure gas.

In Eq.(3-3-15), the summations extend over all the component gases. The following expressions are used for the thermal conductivities of He, Xe, Kr, air, N_2 and H_2 :

If r_{gap} is less than the mean free path of a helium molecule, then

$$\lambda_{He}=\lambda^o_{He}f_1(p_{gap},T_{gap}) \tag{3-3-18}$$

and otherwise

$$\lambda_{He}=\lambda^o_{He} \tag{3-3-19}$$

where

$$\lambda^o_{He}=5.43\times10^{-7}[1.8(T_{gap}+273)]^{0.668} \tag{3-3-20}$$

The others are[5]

$$\lambda_{Xe}=5.75\times10^{-9}[1.8(T'_{gap}+273)]^{0.872} \tag{3-3-21}$$

$$\lambda_{Kr}=6.56\times10^{-9}[1.8(T_{gap}+273)]^{0.923} \tag{3-3-22}$$

$$\lambda_{Air}=3.03\times10^{-8}[1.8(T_{gap}+273)]^{0.846} \tag{3-3-23}$$

$$\lambda_{N_2}=3.03\times10^{-8}[1.8(T_{gap}+273)]^{0.846} \tag{3-3-24}$$

$$\lambda_{H_2}=2.41\times10^{-7}[1.8(T_{gap}+273)]^{0.821} \tag{3-3-25}$$

and

$$\lambda_{H_2O}=f_2(p_{gap},T_{gap}) \tag{3-3-26}$$

In the above, f_1 and f_2 are input functions of p_{gap} and T_{gap}.

The second component of h^t_{gap}, i.e., the gap conductivity due to thermal radiation is given by [30]

$$h_{rad}=\frac{1.369\times10^{-11}\left[(T_F^{out}+273)^4-(T_{CL}^{in}+273)^4\right]}{(2r_F+r_{gap})/2r_F\left[1/\varepsilon_F+r_F/(r_F+r_{gap})(1/\varepsilon_{CL}-1)\right](T_F^{out}-T_{CL}^{in})} . \quad (3-3-27)$$

Thus, the total gap conductivity h^t_{gap} is given by

$$h^t_{gap}=h_{gap}+h_{rad} , \quad (3-3-28)$$

where h_{gap} and h_{rad} are given by Eq.(3-3-13) or (3-3-14) and Eq.(3-3-27), respectively. In summary, the parameters influencing the gap conductivity are (1) the temperatures of the surrounding surfaces, (2) the gas temperature, (3) the gas composition, (4) the gas pressure (p_{gap}) and (5) the gap width (r_{gap}) . The temperatures of the surrounding surfaces can be calculated by the method discussed in subsection 3.3.2, while the gas temperature is set equal to the arithmetic average of the pellet surface temperature and the clad inner surface temperature (see Eq.(3-3-31) or (4-2-10)). The temperature of the upper and lower plenums are assumed to be given as

$$T_{upl}=T_b^{top}+C_T \quad (3-3-29)$$

and

$$T_{lpl}=T_b^{bottom} , \quad (3-3-30)$$

where T_b^{top} and T_b^{bottom} are the bulk temperatures at the top and bottom nodes of the core channel flow, respectively. The gap gas composition is an input to the THYDE-W code and is assumed to remain constant throughout the transient except that, if burst is calculated to occur, the gas composition in the burst node is assumed to be steam. For the calculation of the gap width r_{gap} and the mixture gas pressure p_{gap}, the

readers can refer to section 4.2.

Thus, we have the following set of equations :

$$T_{gap}=\frac{T_F^{out}+T_{CL}^{in}}{2} \qquad from\ Eq.(4\text{-}2\text{-}10) \qquad (3\text{-}3\text{-}31)$$

$$p_{gap}=p_{gap}(T_{gap},r_{gap}) \qquad from\ Eq.(4\text{-}2\text{-}9) \qquad (3\text{-}3\text{-}32)$$

and

$$r_{gap}=r_{gap}(p_{gap},temp\ distribution) \qquad from\ Eq.(4\text{-}2\text{-}3a) \qquad (3\text{-}3\text{-}33)$$

Suppose that the temperature distribution in fuel is known. Then, we can obtain p_{gap} and r_{gap} by solving Eqs.(3-3-32) and (3-3-33) simutaneously. Thus, having obtained p_{gap} and r_{gap}, we can obtain λ_{gap}, h_{gap} and h_{rad} from the following equations.

$$\lambda_{gap}=\lambda_{gap}(p_{gap},T_{gap}) \qquad from\ Eq.(3\text{-}3\text{-}15) \qquad (3\text{-}3\text{-}34)$$

$$h_{gap}=h_{gap}(\lambda_{gap},r_{gap}) \qquad from\ Eq.(3\text{-}3\text{-}13) \qquad (3\text{-}3\text{-}35)$$

and

$$h_{rad}=h_{rad}(T_F^{out},T_{CL}^{in},r_{gap}) \qquad from\ Eq.(3\text{-}3\text{-}27). \qquad (3\text{-}3\text{-}36)$$

3.4 Rod-to-Rod Radiative Heat Transfer

In this section, we will obtain the radiative heat transfer coefficients for burst and non-burst rods, h_n and h_b, which are to be used for Eqs.(3-5-3) and (3-5-4) to give φ_R and φ_R^* in Eq.(3-2-5), repsectively. To this end, we will consider a 3 x 3 rod matrix[5] as shown in Fig. 3-4-1, in which some of the rods are burst.

In THYDE-W, rod-to-rod radiative heat transfer will be accounted for in the following way only after a clad burst. The core will be divided into several regions, each of which will be regarded as a collection of identical coolant channels. Suppose that a fuel rod in a region was calculated to burst at a certain elevation. Then, it will be interpreted that bursts have occurred at that elevation with a certain

pattern in the entire region. With the calculated occurence of a burst, the two fuel rod calculation will be started for the region to include rod-to-rod radiative heat transfer on the basis of the 3 x 3 rod matrix.

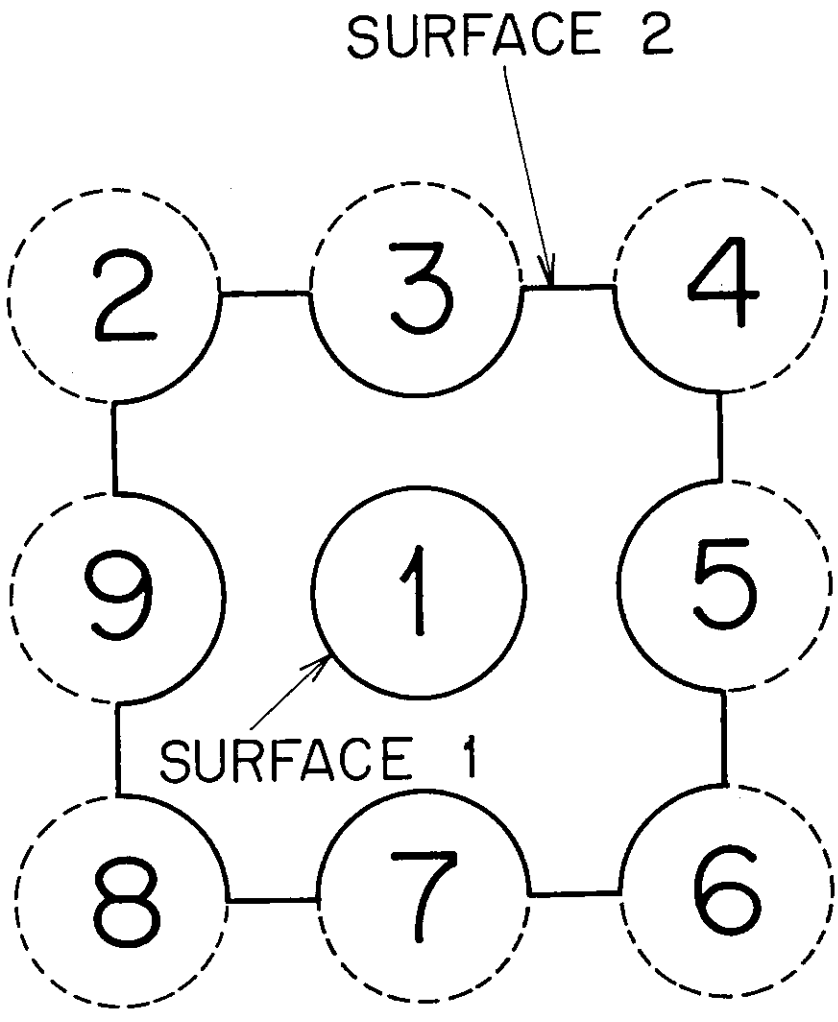

Fig. 3-4-1 3×3 Rod Cluster Model

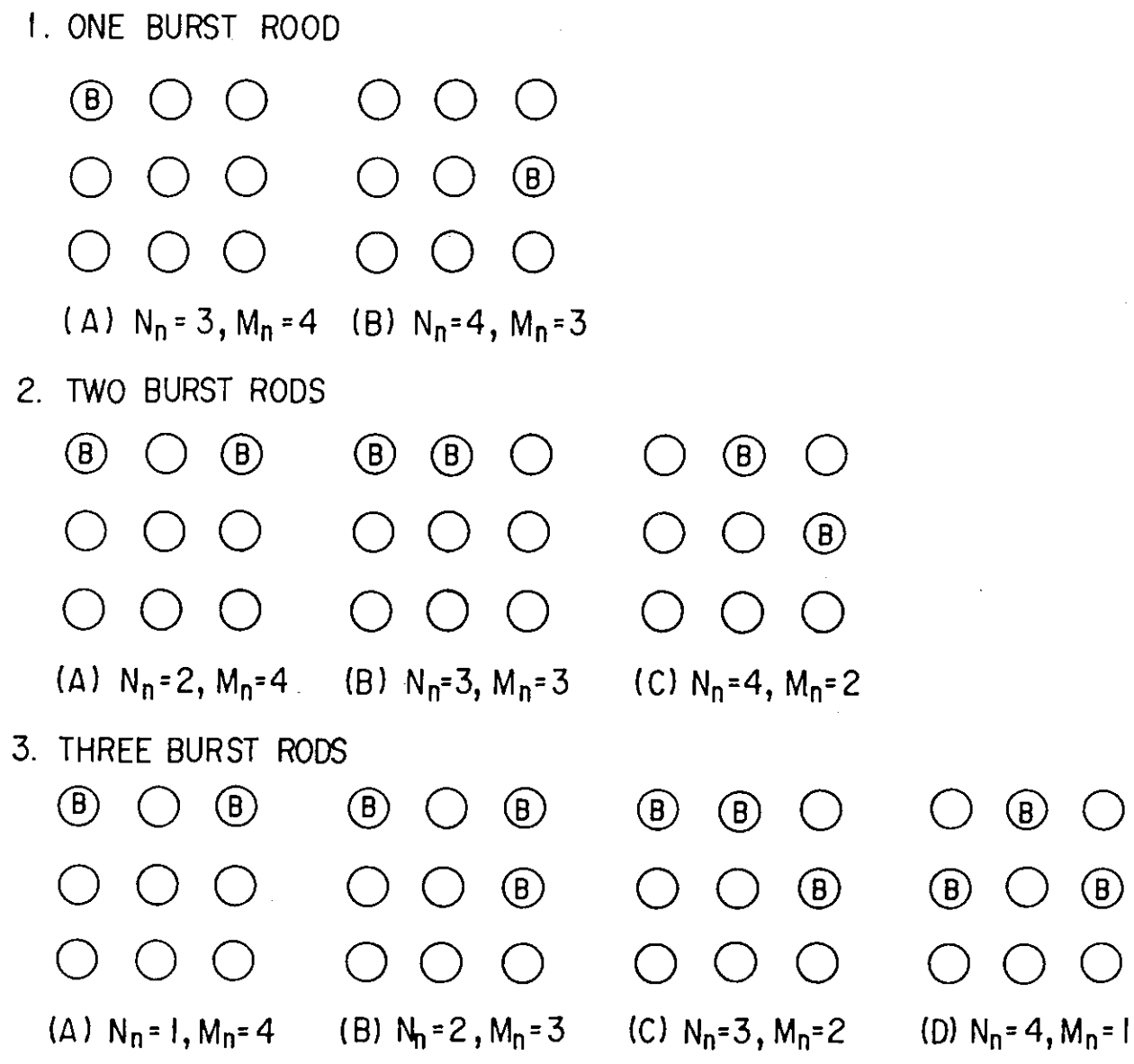

Fig. 3-4-2 Burst Patterns (Non-burst center rod)

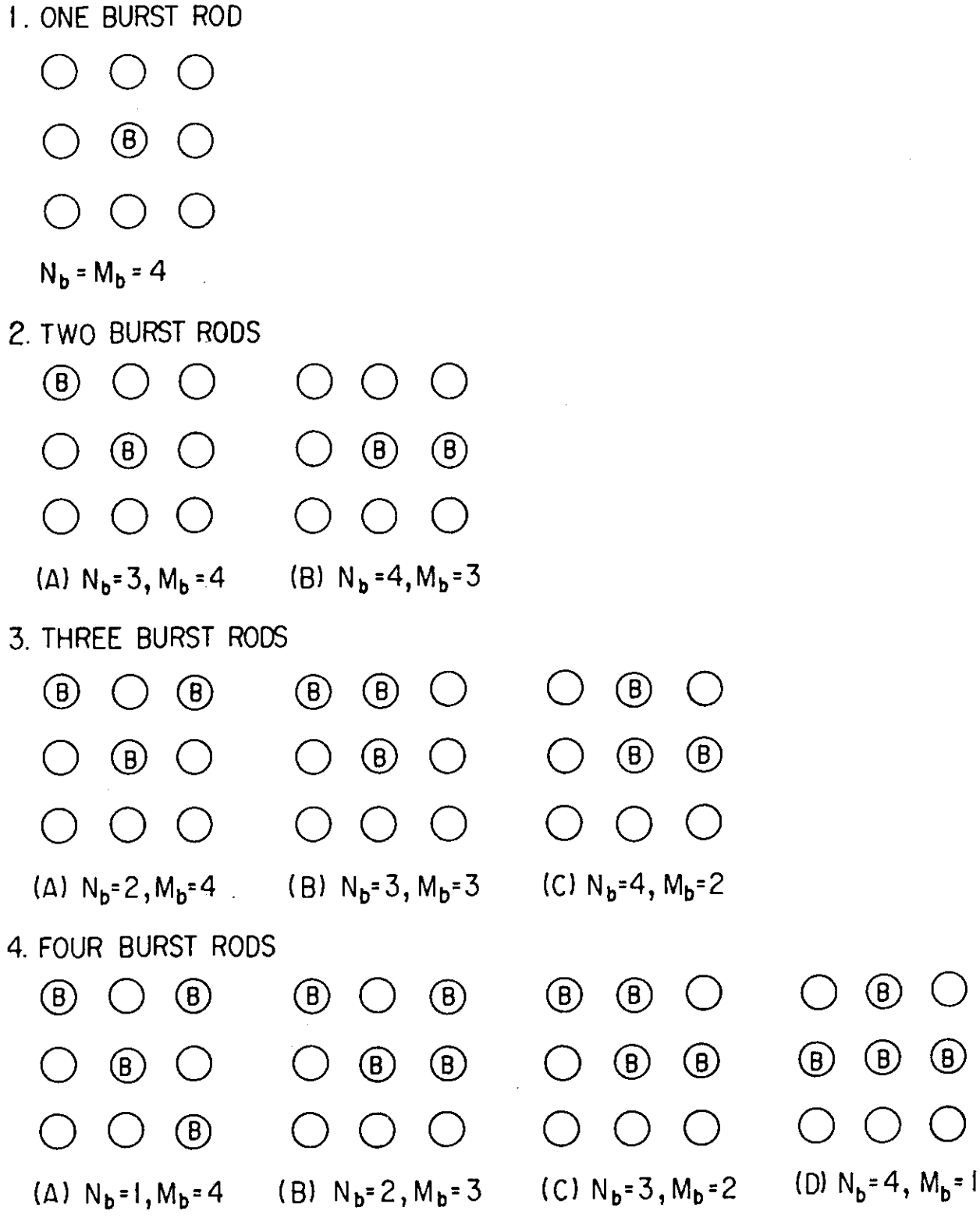

Fig. 3-4-3 Burst Patterns (Burst center rod)

The burst pattern must be specified as inputs by choosing it from Figs. 3-4-2 or 3-4-3. We also assume that the matrices with the prescribed burst pattern are isolated from each other with respect to rod-to-rod radiation.

The conceivable rods burst patterns are shown in Figs. 3-4-2 and 3-4-3, where the definitions of M_n, N_n, M_b and M_b are shown in Nomenclature. The diagonal rod refers to rod 2, 4, 6 and 8, and the off-diagonal rod to rod 3, 5, 7 and 9. Let n_b be the number of burst rods in the matrix. Then we have a relationship

$$M_n + N_n = 8 - n_b$$

if the center rod is non-burst, while

$$M_b + N_b = 9 - n_b$$

if the center rod is burst.

According to Hottel[30], the radiative heat flux from the center rod may be given by

$$\varphi^i = F_{12}\sigma\left[(T_R^i + 273)^4 - (T_2 + 273)^4\right] \quad (i = n \text{ or } b) \qquad (3\text{-}4\text{-}1)$$

where

$$F_{12} = \frac{1}{\overline{F}_{12} + (1/\varepsilon_1 - 1) + A_1/A_2\ (1/\varepsilon_2 - 1)}$$

$\overline{F}_{12}$= modified geometrical factor,

A_1= area of surface 1 ,

A_2= area of surface 2 ,

T_2= average temperature of surface 2,

ε_1= emissivity of surface 1 ,

and

ε_2= average emissivity of surface 1 .

Since surface 1 does not see itself, but only surface 2, we can set

$$\overline{F}_{12} = 1$$

whence

$$F_{12}=\frac{1}{1/\varepsilon_1+A_1/A_2\ (1/\varepsilon_2-1)} \quad . \tag{3-4-2}$$

The emissivity ε_1 is that of zircaloy ε_{zr}, i.e.,

$$\varepsilon_1=\varepsilon_{zr}(T_R^i) \quad (\ i\ =\ n\ \ or\ \ b\ ) \tag{3-4-3}$$

as a function of temperature.

The ratio A_1/A_2 can be obtained in terms of the radii of the burst and non-burst rods

$$d_n=2r_R$$

and

$$d_b=2r_R^*$$

as

$$\frac{A_1}{A_2}=\frac{d_i}{3d_b+((M_i+M_i)/\pi-N_i/4-M_i/4)(d_b-d_n)+8/\pi(l_p-d_b)}$$

$$(\ i\ =\ n\ \ or\ \ b\ ) \quad .$$

In calculating the avarage values of T_2 and ε_2 over surface 2, we will neglect the values at the coolant portion of surface 2 and obtain them, for example, as area-weighed averages, i.e.,

$$\varepsilon_2=\frac{3d_b\varepsilon_{zr}(T_R^b)-(N_i/4+M_i/2)\,[\,d_b\varepsilon_{zr}(T_R^b)-d_n(T_R^n)\,]}{3d_b-(d_b-d_m)(N_i/4+M_i/2)} \tag{3-4-4}$$

and

$$T_2=\frac{3d_bT_R^b-(N_i/4+M_i/2)\,[\,d_bT_R^b-d_nT_R^n\,]}{3d_b-(d_b-d_m)(N_i/4+M_i/2)} \quad . \tag{3-4-5}$$

Thus, the rod-to-rod radiative heat transfer coefficient to be used for the calculation of clad surface temperature (see section 3.5) is given by

$$h_i=\frac{\varphi^i}{T_R^i-T_2} \quad (\ i\ =\ n\ \ or\ \ b\ ) \quad . \tag{3-4-6}$$

The outer rod diameter of the burst rod $d_b=2r_R^*$ can be obtained from

Eq.(4-1-5).

3.5 Heat Transfer and CHF Correlations

First of all, it is important to make the following distinction between two kinds of heat transfer coefficients, h_{tr}^{c} and h_{tr}^{cs}. The heat transfer coefficient h_{tr}^{c} will be used in Eq.(3-2-2) to obtain a heat transfer rate from the wall to the coolant, whereas the heat transfer coefficient h_{tr}^{cs} will be used in Eq.(3-3-12) to obtain the wall surface temperature. These two heat transfer coefficients are identical if rod-to-rod radiation is absent.

The heat transfer coefficient from the wall to the coolant h_{tr}^{c} is composed of two components; the one is the convective or boiling or condensation heat transfer coefficient, while the other is the wall-to-coolant radiative heat transfer coefficient. We will refer to the former as h_{tr}^{cvn} and the latter as h_{tr}^{w-c}. Thus, the coefficient of heat transfer from a fuel rod to a coolant flow can be represented by Eq.(3-2-3), which we reproduce here again,

$$h_{tr}^{c}=h_{tr}^{w-c}+h_{tr}^{cvn} \quad . \tag{3-5-1}$$

The heat transfer coefficient h_{tr}^{cs} to be used for the calculation of the wall surface temperature is given as follows :

$$h_{tr}^{cs}=h_{tr}^{c} \qquad \textit{before burst} \tag{3-5-2}$$

$$h_{tr}^{cs}=h_{tr}^{c}+h_{tr}^{b} \quad (\textit{burst rod}) \qquad \textit{after burst} \tag{3-5-3}$$

and

$$h_{tr}^{cs}=h_{tr}^{c}+h_{tr}^{n} \quad (\textit{non-burst rod}) \quad \textit{after burst} \ . \tag{3-5-4}$$

The radiative heat transfer coefficients h_b and h_n are given by Eq.(3-4-6).

In the following subsections 3.5.1 to 3.5.3, we will show the heat

transfer correlations used in THYDE-W.

Table 3-1 Heat Transfer Coefficients

mode	Condition	Correlation
11-13	$T_b, T_w < T_s$, Re < 2,000 (natural convection)	Fishinden and Saunders
10	$T_b, T_w < T_s$, Re > 2,000 (subcooled forced convection with wall parallel to flow)	Dittus-Boelter
19	$T_b, T_w < T_s$, Re > 2,000 (subcooled forced convection with tube rows perpendicular to flow)	Fishinden and Saunders
20/21	$T_b < T_s < T_w$	Interpolation between modes 10/11 and 31
20/22	$T_b < T_s < T_w$	Interpolation between modes 10/11 and 32
31/32	$T_b = T_s$, $T_s < T_w$ (nucleate boiling)	Jens-Lottes (31) or Thom(32)
41-45	$T_b = T_s$, $T_s < T_w$ (film boiling)	(see Table 3-2)
60	$T_b = T_s$, $T_s > T_w$ (condensation)	Nusselt[36]
51	$T_b > T_s$, Re < 3,000 (laminar steam flow cooling)	
52	$T_b > T_s$, 3,000 < Re < 5,000	Interpolation between modes 51 and 53
53	$T_b > T_s$, Re < 5,000 (turbulent steam flow cooling)	McEligot

Table 3−2 Post−CHF Heat Transfer Coefficients

[G_t = 271.2 kg/(m^2s)]

mode	Condition		Correlation	
41	x > 0.5	G > G_t	Groeneveld	
	p > 30 ata			
42	x > 0.5	G > G_t	Dougall and Rohsenow	
	p < 30 ata			
43	x < 0.5	G > G_t	Interpolation between h_{tr}^{41} or h_{tr}^{42}(x=0.5) and h_{tr}^{CHF}(x=0)	
44		G < G_t		
			Berenson	IHTROP(2) = 1
			Modified Bromley	IHTROP(2) = 2
			Bromley−Pomeranz	IHTROP(2) = 3

3.5.1 Correlations of Heat Transfer Coefficients

(a) Subcooled Forced Convection

The heat transfer coefficient at a wall parallel to a subcooled forced convection flow is given by Dittus and Boelter[31] as

$$h_{tr}=0.023\frac{\lambda}{D}\left(\frac{|G|D}{\mu}\right)^{0.8}Pr^{0.4} \quad . \tag{3-5-5}$$

When a coolant is flowing perpendicular to tube rows, then the heat transfer coefficient is given[37] as

$$h_{tr}=0.33\ \frac{\lambda}{D}C_H\Phi\left(\frac{\rho_f u_{max}D}{\mu}\right)^{0.6}Pr^{0.3} \quad .$$

(b) Nucleate Boiling

Jens and Lottes[32] gave the heat transfer coefficient for nucleate boiling as

$$h_{tr}=7.92\times10^3\frac{(T_w-T_s)^4(e^{p/17.3})}{(T_w-T_b)} \quad , \tag{3-5-6}$$

where T, p and h_{tr} are in ^{0}C, ata and kcal/(m^{2}sec^{0}C), respectively. Thom[40] gave a different correlation ;

$$h_{tr}=\frac{(T_w-T_s)^2(e^{p/1260}/4.32)^2}{(T_w-T_b)}$$

where T, p and h_{tr} are in ^{0}F, psia and BTU/(ft^{2}sec^{0}F), respectively.

(c) Subcooled Boiling under Natural and Forced Convection

When a coolant is subcooled, but the wall temperature is higher than the saturation temperature, then an intermediate process is assumed to take place with a heat transfer coefficient

$$h_{tr}=h_{tr}^1+c_{eff}h_{tr}^2 \quad , \tag{3-5-7}$$

where h_{tr}^1 and h_{tr}^2 are subcooled heat transfer coefficient (mode 10 or 11) and saturated heat transfer coefficient (mode 31/32), respectively.

In the present version, c_{eff} is set to be 0.1 in Eq.(3-5-7).

(d) Stable Film Boiling

The stable film boiling heat transfer correlation by Groeneveld[34] is used to calculate heat transfer after DNB.

$$h_{tr}=0.052\frac{\lambda_g}{D}\left[\frac{|G|D}{\mu_g}\left(x+\frac{\rho_g}{\rho_f}(1-x)\right)\right]^{0.688}Pr_g\&^{1.26}Y^{-1.06} \qquad (3-5-8)$$

where

$$Y=\max[0.1,1-0.1(\rho_g/\rho_f-1)^{0.4}(1-x)^{0.4}]$$

and Pr_g is the Prantle number of superheated steam whose temperature is equal to the caldding surface temperature.

(e) Steam Cooling

The following correlations are used for steam cooling. For a laminar flow (Re < 3000)[5], we use

$$h_{tr}=C_1\frac{\lambda_g}{D}\left(\frac{T_b+273}{T_w+273}\right)^{C_2} \qquad (3-5-9)$$

where C_1 and C_2 are constants. For a turbulent flow (Re<5,000), we use

$$h_{tr}=0.02\left(\frac{\lambda_g}{D}\right)Re^{0.5}Pr^{0.4}\left(\frac{T_b+273}{T_w+273}\right)^{0.5} \qquad (3-5-10)$$

given by McEligot[35].

(f) Condensation

When wall temperature is lower than bulk temperature of saturated fluid, condensation may occur. Define a Reynolds number Re_d such that

$$Re_d=4\Gamma_c/\mu_f=\frac{4h_{tr}(T_s-T_b)L_x}{\mu_f h_{fg}} \qquad (3-5-11)$$

where L_x is the distance from the wall top. For a laminar flow (Re_d < 1,800), Nusselt[36] gave

$$h_{tr}=1.28\left(\frac{\lambda_f^3\rho_f^2 g}{\mu_f^2}\right)^{1/4}\left(\frac{4L_x(T_s-T_b)}{\mu_f h_{gf}}\right)^{-1/4}$$

For a turbulent flow (Re_d > 1,800), the following heat transfer correlation is used for condensation.

$$h_{tr}=0.0077\left(\frac{\lambda_f^3\rho_f^2 g}{\mu_f^2}\right)^{1/3}Re_d^{0.4} \quad . \tag{3-5-12}$$

For Re_d > 1,800, substituting Eq.(3-5-11) into Eq.(3-5-12) and solving the resultant equation for h_{tr}, we obtain

$$h_{tr}=0.0077^{5/3}\left(\frac{\lambda_f^3\rho_f^2 g}{\mu_f^2}\right)^{5/9}\left(\frac{4L_x(T_s-T_b)}{\mu_f h_{gf}}\right)^{2/3} \quad .$$

(g) Natural Convection

For a single phase flow , the following natural convection heat transfer correlation is available.[37]

$$h_{tr}=0.47\frac{\lambda}{D}(Gr_F Pr_F)^{1/4} \qquad (Gr_F Pr_F<1.0\times10^8)$$

$$=0.17\frac{\lambda}{D}(Gr_F Pr_F)^{0.33} \qquad (Gr_F Pr_F>2.0\times10^9)$$

where subscript F refers to qauntities evaluated at average film temperature and

$$Gr=(3\eta)\frac{D^3\rho_f^2 g\,|T_w-T_b|}{\mu_f^2} \quad .$$

3.5.2 CHF Correlations

The following CHF correlations are implemented in the THYDE-W code.

G > G_t

(1) Biasi[46]

(2) GE[33]

$$\varphi_{CHF}=7.54\times10^2(0.84-x) \qquad |G|<0.678\times10^3$$

$$\varphi_{CHF}=7.54\times10^2(0.80-x) \qquad 0.678\times10^3<|G|<1.02\times10^3 \tag{3-5-13}$$

(3) RELAP[7]

$G \leq G_t$

(1) Interpolation between $\varphi_{CHF}(G=G_t)$ for $G > G_t$ and 0.9×10^5 Btu/ft^2

(2) Modified Zuber[47]

(3) Zuber[47]

3.5.3 *Rod-to-Coolant Radiative Heat Transfer Coefficient*

The following additional heat transfer coefficient due to thermal radiation should be added in each mode of the previous subsection before clad burst (see Eq.(3-5-1)).

$$h_{tr}=\eta_a \frac{(T_w+273)^4-(T_b+273)^4}{T_w-T_b} \tag{3-5-14}$$

where η_a is a function of a to be determined experimentally, e.g.[5],

$$\eta_a=\frac{1-0.6a}{1.25-0.15a}$$

3.5.4 *Pool Quenching Model*

Suppose that a heat conductor with volume V, length Δz is placed in a coolant, which is at saturated pool condition and that the conductor surface is at post-CHF.

First, we heuristically derive a necessary condition for pool quenching. Integrating Eq.(3-3-1) over the material regions in the conductor, we obtain

$$\frac{d}{dt}\sum_i(\rho c_p TV)_i=\sum_i (\Xi V)_i - l_w \Delta z \varphi . \tag{3-5-15}$$

where subscript i stands for a material region. Dividing this equation by V, we obtain

$$\frac{d}{dt}<\rho c_p T> = <\Xi> - \frac{l_w \Delta z \varphi}{V}$$

$$= \frac{l_w \Delta z}{V}(\varphi^* - \varphi) \qquad (3-5-16)$$

where

$$\varphi^* = \frac{V}{l_w \Delta z}<\Xi>$$

and the bracket means averaging over fuel.

In order for the temperature not only at the surface, but also in its interior to be quenched, Eq.(3-5-16) requires [49] that

$$\varphi^* < \varphi \qquad (3-5-17)$$

at saturated post-CHF condition.

In THYDE-W, we use the modified form of Eq.(3-5-17) such that

$$\varphi^* < c\varphi \qquad (3-5-18)$$

where

$$c = 1.5 \ .$$

Factor c obviously depends upon the correlation of heat transfer coefficient for pool film boiling. The quenching heat flux, when the quenching criterion (3-5-18) is satisfied, will be assumed to be

$$\varphi_q = 200 \ kcal/(m^2 sec) \quad 80 < |G| < G_t \qquad (3-5-19)$$

$$= 100 \ kcal/(m^2 sec) \quad Otherwise.$$

In summary, it is assumed that if condition (3-5-18) is satisfied under saturated post-CHF pool condition, quenching will take place with the heat flux given by Eq.(3-5-19).

4. *Mechanical Behavior of Clad and Fuel*

Mechanical behaviors of a clad and a fuel rod influence the gap width, the gap pressure, the flow area, the rod-to-rod radiation and the oxide thinning. Among them, the last three are assumed in THYDE-W to be effective only after a clad burst.

The geometrical dimensions of a fuel rod at an initial operating condition must be determined by calculating, for example, deformations due to pressure and temperature changes from a room to an operating condition. Such complicated calculations, however, are outside the scope of this work so that all the geometric dimensions of a fuel rod at an intial operating condition are assumed to be given as inputs. Throughout this report, we will neglect an axial deformation of a clad and a fuel.

4.1 Clad Deformation

Prior to a burst, a clad expands due to thermal- and pressure-induced elastic strains and a plastic hoop strain. In THYDE-W, as long as a clad burst does not occur, only their effects on the gap width is taken into consideration. If a clad continues to strain plastically, it will eventually burst. When a burst is predicted, we, for the first time, take into account the contribution of clad deformation to flow area reduction, rod-to-rod radiation and oxide thinning.

Before we discuss clad deformation, we will present the expressions Eqs.(4-1-1) and (4-1-5) for clad inner and outer radii, r_{cl}^{in} and r_R, respectively.

First, we express clad inner radius r_{CL}^{in} as

$$r_{CL}^{in} = r_{CL}^{in0} + \Delta r_{CL}^{in} = r_{CL}^{in0}(1+s_p+s_t+s_{in}) \qquad (4\text{-}1\text{-}1)$$

where s_p, s_t and s_{in} are the strains of the clad inner radius due to a pressure change, a temperature change and a hoop stress, respectively. Hoop strain s_{in} of the clad inner radius will be given in Eq.(4-1-9), whereas $s_p^{(4)}$ and s_t are given by

$$s_p=\frac{[\{1+\mu_p+e^2(1-2\mu_p)\}(p_{gap}-p_{gap}^0)-(2-\mu_p)(p_{CLNT}-p_{CLNT}^0)]}{[E_y(1-e^2)]} \quad (4-1-2)$$

where

$$e=[\frac{r_{CL}^{in0}}{r_R^0}] \quad (4-1-3)$$

and

$$s_t=\eta_{CL}(T_{CL}^{in})(T_{CL}^{in}-T_{CL}^{ino}) \quad . \quad (4-1-4)$$

As stated above, s_p and s_t are so small that they need be accounted for only in the calculation of a gap with. Otherwise, they will be neglected.

Next, we express the clad outer radius r_R as

$$r_R=r_R^o(1+s_{out}) \quad (4-1-5)$$

where the elastic strains are neglected. Equation (4-1-5) will be used in Eq.(4-1-15).

We now try to express s_{in} in Eq.(4-1-1) and s_{out} in Eq.(4-1-5) in terms of s and e, where s is the hoop strain at the initial radius, $(r_{CL}^{in0}+r_R^0)/2$. Assuming a constant cross-sectional area under plastic or burst hoop strain, we obtain,

$$r_m\theta=r_m^o\theta^o \quad (4-1-6)$$

where r_m is the radius which was initially equal to $(r_R^o+r_{CL}^{ino})/2$ and θ is the clad thickness. Since

$$r_m=r_m^o(1+s) \quad (4-1-7)$$

Eq. (4-1-6) gives

$$\theta = \frac{\theta^o}{(1+s)} \quad . \tag{4-1-8}$$

Then, the plastic or burst radial strains at the inner and outer surfaces, s_{in} and s_{out} can be given in terms of s and e as

$$s_{in} = \left[r_m - \frac{\theta}{2} - \left(r_m^o - \frac{\theta^o}{2} \right) \right] / r_{CL}^{ino} = \frac{s}{2e}\left(1+e+\frac{1-e}{1+s}\right) \tag{4-1-9}$$

and

$$s_{out} = \left[r_m + \frac{\theta}{2} - \left(r_m^o + \frac{\theta^o}{2} \right) \right] / r_R^o = \frac{s}{2}\left(1+e-\frac{1-e}{1+s}\right) \quad . \tag{4-1-10}$$

Therefore, once hoop strain s is given, we can obtain s_{in} and s_{out} from Eqs.(4-1-9) and (4-1-10), respectively. The plastic and burst hoop strains s in Eqs.(4-1-9) and (4-1-10) are discussed in subsections 4.1.1 and 4.1.3, respectively.

4.1.1 Clad Deformation prior to Burst

Hardy[41] performed a series of tests in which rods with constant internal pressure were ramped to a series of temperatures at various ramp rates. Analyzing his data, the following form of equation for plastic hoop strain s may be obtained.

$$\frac{ds}{dt} = f_1\left(s, \sigma_h, T_{CL}, \frac{dT_{CL}}{dt}\right) \tag{4-1-11}$$

where

$$\sigma_h = \frac{r_m}{r_c}\left(p_{gap} - p_{CLNT}\right) \tag{4-1-12}$$

and f_1 is an input function.

Substituting the solution s of Eq.(4-1-11) into Eqs.(4-1-9) and (4-1-10), we obtain s_{in} and s_{out}. Then substituting s_{in} and s_{out} into Eqs.(4-1-1) and (4-1-5), we obtain r_{CL}^{in} and r_R.

4.1.2 Clad Burst

Clad is assumed to burst if the hoop strain s calculated by Eq.(4-1-11) reaches a certain value (an input) or if the clad temperature reaches the burst temperature. The burst temperature is calculated from a correlation of σ_h versus cladding temperature with the following form from various sources, notably ORNL[42]

$$T_{burst} = f_2(\sigma_h) \qquad (4\text{-}1\text{-}13)$$

where f_2 is an input function.

If burst is predicted, the following assumptions are used to calculate the rupture rod conditions:

(a) The rod internal pressure is reduced in one time step to that in the corresponding coolant node and is set equal to it for the remainder of the calculation.

(b) The metal-water reaction is continued on the surface with the oxide layer being thinned in accordance with the calculated swelling.

(c) The local hoop strain and the flow blockage after burst are calculated according to the method described in the next section. The axial length of the swollen zone is that of the burst node.

(d) The metal-water reaction is started on the inside of the burst clad node. The reaction inside the cladding is assumed not to be steam limited, i.e., the gas composition of the burst node is set to be steam for the rest of the calculation.

4.1.3 Local Hoop Strain and Flow Blockage after Burst

It is assumed that at the time of clad burst the localized diametral swelling occurs very rapidly and changes the hydraulic diameter of the corresponding core flow node discontinuously. The diameteral swelling is calculated from a correlation of the form,

$$s=f_3(\sigma_h) \tag{4-1-14}$$

where f_3 is an input function of σ_h, which is the hoop stress at the time of burst. Substituting s obtained from Eq.(4-1-14) into Eqs.(4-1-9) and (4-1-10), we obtain s_{in} and s_{out}, respectively. Then, substituting resultant s_{in} and s_{out} into Eqs.(4-1-1) and (4-1-5), we obtain

$$r_R^*=r_R^o(1+s_{out}(s)) \tag{4-1-15}$$

and

$$r_{CL}^{in*}=r_{CL}^{ino}(1+s_{in}(s)) \tag{4-1-16}$$

where elastic strains have been ignored.

The outer radius after burst r_R^*, however, is limited such that

$$r_R^* \leq r_{Rmax}$$

and hence

$$r_R^o(1+s_{out}(s)) \leq r_{Rmax} \tag{4-1-17}$$

where r_{Rmax} is an input. Hence, s also is limited by s_{max}, which can be obtained from from Eq.(4-1-17) such that

$$s_{max}=a+\sqrt{a^2+4b}\ /2 \tag{4-1-18}$$

where

$$a=(2/(1+\sqrt{R}))(\frac{r_{Rmax}}{r_R^o}-1-e)$$

and

$$b=\frac{2}{1+e}\ (\frac{r_{Rmax}}{r_R^o}-1).$$

In the THYDE-W code, the flow area after burst A^* is not simply set

equal to $l_p^2-\pi r_R^{*2}$, but is obtained in the following way by utilizing the 3 x 3 rod matrix model introduced in section 2.4.

If the center rod is burst, then the flow area in the 3 x 3 matrix changes from

$$A_9=4(l_p^2-\pi r_R^2) \tag{4-1-19}$$

to

$$A_9^*=4l_p^2-(\frac{M_b}{2}+\frac{N_b}{4})\pi r_R^2-(4-\frac{M_b}{2}-\frac{N_b}{2})\pi r_R^{*2} \tag{4-1-20}$$

Thus the flow blockage is given by

$$BL=100(1-\frac{A_9^*}{A_9})=\frac{(4-M_b/2-N_b/4)\pi(r_R^{*2}-r_R^2)}{4(l_p^2-\pi r_R^2)}\times 100 \tag{4-1-21}$$

If the center rod is not burst, then the flow area at the burst elevation of the matrix change's to

$$A_9^*=4l_p^2-\pi r_R^2(\frac{M_n}{2}+\frac{N_n}{4}+1)-\pi r_R^{*2}(3-\frac{M_n}{2}-\frac{N_n}{4}) \tag{4-1-22}$$

so that the flow blockage in this case is given by

$$BL=\frac{(3-M_n/2-N_n/4)\pi(r_R^{*2}-r_R^2)}{4(l_p^2-\pi r_R^2)}\times 100 \tag{4-1-23}$$

Since we consider two elevations with clad burst in the 3 x 3 rod bundle, we have two values for BL. We choose the larger of the two as the effective values for BL. We also assume that BL is bounded from below so that BL > BLM (an input value; see BB24).

When clad burst occurs, it is assumed that the flow area of the corresponding flow node change from A to

$$A^*=0.25A_9^* \tag{4-1-24}$$

which, in turn, changes the hydraulic diameter and the Reynolds number of the burst node to

$$D^*=2\frac{A^*}{(\pi r_R^*)} \tag{4-1-25}$$

and

$$Re = |G| \frac{D^*}{\mu} \qquad (4-1-26)$$

It should be noted in view of the discussions in subsection 2.1.5, that the effect of sudden contraction and expansion of the flow area brought about by clad burst are automatically incorporated in the formulation.

4.2 Mechanical Behavior of Fuel and Gap

In section 3.3.3, it was assumed that the gap gas pressure and the gap width were given as shown in Eqs.(3-3-32) and (3-3-33), respectively. In this section, we will obtain their explicit expressions. To this end, we have to investigate the deformation of the bounding surfaces of the gap, i.e., the clad inner surface and the fuel pellet surface. The former has already been discussed in section 4.1.

4.2.1 Gap Width

Radial thermal expansion of the pellet is calculated by

$$r_F = r_F^o + \Delta r_F \qquad (4-2-1)$$

where the increment due to temperature rise Δr_F is given by

$$\Delta r_F = \sum_{n=0}^{N_F-1} (r_{n+1}^o - r_n^o) \eta_F(T_{n+1})(T_{n+1} - T_{n+1}^o) \quad . \qquad (4-2-2)$$

Then, with the help of Eqs.(4-1-1) and (4-2-1), we obtain

$$r_{gap} = r_{CL}^{in} - r_F = r_{gap}^0 + r_{CL}^{in0}(s_t + s_p + s_{in}) - \Delta r_F \quad . \qquad (4-2-3)$$

Substituting Eqs.(4-1-4) and (4-2-2) into Eq.(4-2-3), we obtain the gap width for each axial node as

$$r_{gap} = r_{gap}^o + r_{CL}^{in0} [\, \eta_{CL}(T_{CL}^{in})(T_{CL}^{in} - T_{CL}^{ino}) + s_p + s_{in}(s) \,] - \sum_{n=0}^{N_F-1} (r_{n+1}^o - r_n^o) \eta_F(T_{n+1})(T_{n+1} - T_{n+1}^o) \quad , \qquad (4-2-3a)$$

where s_p and $s_{in}(s)$ are given by Eqs.(4-1-2) and (4-1-9), respectively. The hoop strain s, in turn, is given by Eqs.(4-1-11) and (4-1-14) before and after burst, respectively.

4.2.2 Gap Gas Pressure

The gas volume inside a fuel rod may be composed of the following volumes in addition to the clad-pellet gap: plenum volume , crack and dish volume, open porosity volume and chip and roughness volume. We note the difference between the fuel envelope volume and the net fuel volume is composed of the crack and dish volume, the open porosity volume and the chip and roughness volume. In THYDE-W, we neglect the open porosity volume and the chip and roghness volume.

The pellet envelope volume in an axial node is given by

$$V_{en}(t)=\pi r_F^2(t)\Delta z \quad . \tag{4-2-4}$$

The initial net fuel pellet volume is given by

$$V_F^0 = V_{en}^o - V_{cd}^o = \pi (r_F^o)^2 \Delta z - V_{cd}^o \tag{4-2-5}$$

where the initial dish and crack volume is an input to the THYDE-W code. Utilizing the initial net fuel volume obtained by Eq.(4-2-5), we can obtain the thermally expanded net pellet volume at any time during the transient as

$$V_F(t) = V_F^0 [\, 1+3\eta_F(<T_F>)(<T_F>-<T_F^o>)\,] \quad . \tag{4-2-6}$$

With the help of Eqs.(4-2-4) and (4-2-6), the crack and dish volume at any time during the transient can be obtained as

$$\begin{aligned} V_{cd}(t) &= V_{en}(t) - V_F(t) \\ &= \pi r_F^2(t)\Delta z - V_F^0 [\, 1+3\eta_F(<T_F>)(<T_F>-<T_F^o>)\,] \quad . \end{aligned} \tag{4-2-7}$$

Substituting Eq.(4-2-1) into Eq.(4-2-7), we obtain

$$V_{cd}(t) = V_{cd}^0 + 2\pi r_F^0 \Delta r_F \Delta z - 3V_F^0 \eta_F(<T_F>)(<T_F>-<T_F^0>),$$

where Δr_F is given by Eq.(4-2-2). The gap gas volume of the axial node is given by

$$V_{gap}(t)=\pi\Delta z\,[\,r_{CL}^{in}(t)^2-r_F^2\,]=\pi\Delta z\,[\,2r_F(t)+r_{gap}(t)\,]\,r_{gap}(t) \qquad (4-2-8)$$

where the fuel pellet radius r_F and the gap width r_{gap} are given by Eqs.(4-2-1) and (4-2-3), respectively.

The upper and lower plenum volumes are assumed to remain constant throughout the transient.

Thus the gas pressure inside a fuel rod is given by

$$p_{gap}=R_g N_{gap}/\,[\,V_{upl}/T_{upl}\;+\;V_{lpl}/T_{lpl}+\sum_j (V_{gap,j}/T_{gap,j} + V_{cd,j}/T_{cd,j})\,] \qquad (4-2-9)$$

where the summation extends over all the axial nodes of a fuel rod and the number of mols of gap gas N_{gap} is an input. The plenum temperatures T_{upl} and T_{lpl} are given by Eqs.(3-3-29) and (3-3-30), respectively, in subsection 3.3.3, while the temperatures T_{gap} is given by

$$T_{gap}=\frac{T_F^{out}+T_{CL}^{in}}{2} \qquad (4-2-10)$$

for each axial node. The crack and dish temperature T_{cd} may be set equal to the volume-averaged temperature of the fuel, but then the steady state adjustment will become unnecessarily complicated. Since T_{cd} appears only in Eq.(4-2-9), we set the crack and dish temperature T_{cd} be equal to the arithmetic average of the fuel center and fuel surface temperatures.

5. *Boron Transport*

Behaviors of boron transported by a coolant flow can be simulated by considering only mass consevation in the following way.

We assume that boron is dissolved uniformly in the liquid phase. Thus, the boron concentration c_B obeys the following equation.

$$\frac{d}{dt}c_B(1-\alpha)\rho_f = \frac{[c_B(1-\alpha)\rho_f u_f]_A - [c_B(1-\alpha)\rho_f u_f]_E}{L} \quad . \qquad (5-1-1)$$

Obtaining from Eq.(2-2-3)

$$(1-\alpha)\rho_f = (1-x)\rho \quad ,$$

letting

$$\tilde{c} = (1-x)c_B$$

and neglecting u_{rel}, we obatain from Eq.(5-1-1)

$$\frac{d}{dt}\rho\tilde{c} = \frac{\tilde{c}_A G_A - \tilde{c}_E G_E}{L} \quad . \qquad (5-1-2)$$

Then, $\tilde{c}_A$ and $\tilde{c}_E$ can be defined such that

$$\tilde{c}_A = \tilde{c}^{old}_A \qquad if\ point\ A\ is\ closed.$$

$$= \frac{\tilde{c}^{old}_A \tau + \tilde{c}_{from}\Delta t}{\Delta t+\tau} \qquad if\ G_A > 0.$$

$$= \frac{\tilde{c}^{old}_A \tau + \tilde{c}\,\Delta t}{\Delta t+\tau} \qquad if\ G_A \leqq 0. \qquad (5-1-3)$$

and

$$\tilde{c}_E = \tilde{c}^{old}_E \qquad if\ point\ E\ is\ closed.$$

$$= \frac{\tilde{c}^{old}_E \tau + \tilde{c}_{to}\Delta t}{\Delta t+\tau} \qquad if\ G_E < 0.$$

$$= \frac{\tilde{c}^{old}_E \tau + \tilde{c}\,\Delta t}{\Delta t + \tau} \qquad if\ G_E \geq 0. \tag{5-1-4}$$

The equation for a mixing junction is given by

$$V^+ \frac{d}{dt}\rho_j^+ \tilde{c}_j^+ = \sum_{from} [\,(AG\tilde{c})_n\,]_E - \sum_{to} [\,(AG\tilde{c})_n\,]_A \tag{5-1-5}$$

where $\sum_{to}$ and $\sum_{from}$ are the summations over the to- and from-nodes of junction j, respectively. Boron concentration at a normal junction is given as

$$\tilde{c}^+ = h_{from} \ . \tag{5-1-6}$$

Equation (5-1-2) is implicitly solved for $\tilde{c}$ as follows. First, substitute Eqs.(5-1-3) and (5-1-4) into the time-differenced form of Eq.(5-1-2) and then solve the resulting equation for $\tilde{c}$. Similarly, Eq. (5-1-5) can be solved for $\tilde{c}_j^+$ implicitly. Looking over the above discussions as well as Eq.(3-1-3b), it should be realized that the programming of boron transport can be made in terms of $\tilde{c}$ without using boron concentration in the liquid phase c_B. It should be noted that an injected borated water is usually subcooled.

In order to obtain a steady state distribution of $\tilde{c}$, we let either time derivatives vanish or Δt infinitely large in Eqs.(5-1-2) to (5-1-6) as well as Eq.(2-3-4). Then, we can show that at a steady state a distribution of $\tilde{c}$ is uniform along a continuous stream line without an boron source. It should be noted that, usually at a steady state, boron is used in a subcooled water for which $\tilde{c} = c_B$.

6. *Steady State Adjustment*

6.1 Overall Procedure

For an initial value problem to be well posed, the initial steady state should be an exact solution to the transient equations without external disturbances. Thus, when we wish to solve an initial value problem described by a set of equations, we first must obtain the steady state solution of the equations with their time derivatives vanishing. In other words, we must be able to produce a solution to the null transient problem. Therefore, any transient model should contain a steady state analysis capability so that it can be applied to thermal-hydraulic design. We will call the procedure to set up the initial state the steady state adjustment.

The overall procedure to obtain a steady state of a thermal-hydraulic network is shown in Fig.6-1-1, where step 2 is explained in sections 6.2, 6.3 and 6.4, while step 3 is in sections 6.5 and 6.6. The part of step 6 regarding loss coefficients is given in section 6.7. In the following, we may drop the subscript "o" referring to a steady state whenever confusions can be avoided.

A steady state distribution of boron concentration has already been discussed at the end of chapter 5.

(1) Give initial guess values for heat fluxes from heat fluxes to coolant. (Subroutine STHINT)

(2) Obtain thermal−hydraulic quantities such as densities. (Subroutines STFLOW, STHTBL, STENT, STPRHO, STSHFT and STHYM)

(3) Obtain temperature distributions inside heat slabs and renew their heat fluxes (Subroutines STSLGP & STSLAB). Obtain steady states of accumulators (Subroutine STACMC).

(4) Check convergence of T_b of coolant nodes (Subroutine STPYCK). If not converged, repeat steps(2) and (3), until both converge. (This is controlled by Subroutine STEADY).

(5) After convergence, print out calculated steady state information such as distributions of mass, specific enthalpy and pressure as well as loss coefficients. (Subroutine STCHK)

(6) If printed out information is not satisfactory, the code user can try a new set of input data based on information in step 5.

Fig.6−1−1 Overall Procedure to Obtain Steady State

6.2 Thermal-Hydraulic Quantities

This section corresponds with step 2 in Fig.6-1-1, which can further be subdivided as shown in Fig.6-2-1. Main inputs to THYDE-W in conjunction with steady state thermal-hydraulics include p_n^A's for all nodes and G_{IVOL}^A and h_{IVOL}^A for certain nodes IVOL's and the ratios γ of the outflow rates at each mixing junction as well as heat flows Qout's out of each loop.

In the following, the tilde is used to refer to chains. Let q^* be the number of the branches in the network. We note $q \leqq q^*$ where q stands for the number of the branches with at least one normal junction.

(1) Determination of mass velocity G of all normal nodes (STFLOW)

We have a simple linear simultaneous equation for mass flow rates $\tilde{m}_i$ describing mass balance and branching at each mixing junction. It should be noted that for certain node(s) IVOL, G^A is given as an input. Therefore, the mass flow rate $\tilde{m}_i$ of the corresponding chain(s) has already been specified. The linear simultaneous equation can iteratively be solved for $\tilde{m}_i$ and hence for $G_n^A = G_n^A = \tilde{m}_i / A_n$ at all the nodes in each chain i. In order to obtain fast convergence of the iteration, it is important to choose suitable node number(s) for IVOL.

(2) Calculation of Loop-wise Heat Balance and Heat Input to Each Node (STHTBL)

Since heat fluxes through heat conductors have already been given, (see Fig. 6-1-1), heat inputs to flowing nodes can be obtained. Then, for each loop, the heat input and output through heat exchangers are

(1) Determination of G of All Flow Nodes (subroutine STFLOW)

(2) Detrermination of Loop-wise Heat Balance and Node-wise Heat Input (subroutine STHTBL)

(3) Determination of Specific Enthalpies h_n^{Λ}, h_n^E and h_j^+ (subroutine STENT)

(4) Determination of ρ_n^{Λ}, ρ_n^E, p_n^E and p_j^+ for nodes (subroutine STPRHO)

(5) Determination of k_n of non-stagnant nodes (subroutine STAJDW)

Fig.6-2-1 Procedure to Obtain Thermal-Hydraulic Quantities (Step 2 in Fig.6-1-1)

obtained. If they do not coincide, either h_{IVOL}^{A} or the heat transfer area of the "out" heat exchanger conductors will be changed to balance the heat output and input of each loop (refer to section 7.2).

(3) Determination of specific enthalpies at inlet and outlet of each chain and at mixing junctions. (STENT)

Let us use superscripts A and E for the inlet and outlet of a chain as well, respectively. Then, we obtain

$$\tilde{h}_i^E = \tilde{h}_i^A + \sum_{chain\ i} [\, q_n''' L_n + (I_n^A - I_n^E)\,] A_n / \tilde{m}_i \qquad (1 \leqq i \leqq q^*)$$

$$\tilde{h}_j^+ \sum_{j-out} \tilde{m}_i = \sum_{j-in} \tilde{m}_i \tilde{h}_i^E + \sum_{j-in} A_n \tilde{I}_n^E - \sum_{j-out} A_n \tilde{I}_n^A \qquad (1 \leqq j \leqq l_{q+1})$$

and

$$h_i^A = h_j^+ \qquad for\ all\ chain\ flows\ out\ of\ mixing\ junction\ j\ ,$$

where $\sum_{chain\ i}$, $\sum_{j-out}$ and $\sum_{j-in}$ mean the summations over all nodes in chain i, all chain flows out of mixing junction j and all chain flows into mixing junction j, respectively. There are q^* equations of the last type in the above so that we have $2q^* + l_{q+1}$ equations whereas there are the same number of unknowns, i.e., $\tilde{h}_i^A$ and $\tilde{h}_i^E$ for inlets and outlets of chains i = 1,2,.....,q^* and specific enthalpies of mixing junctions whose number is l_{q+1}.

(4) Determination of h_n^A and h_n^E of flowing normal nodes (STENT)

Suppose that all nodes in a chain are labelled successively from upstream to downstream. For any node n in the chain, we have

$$h_n^E = h_n^A + \frac{I_n^A - I_n^E + L_n q_n'''}{G_n}$$

which gives $h_n^E = h_{n+1}^A$ successively from the inlet node to the outlet node

of the chain, since h_n^A of the inlet node, which is equal to the specific enthalpy of the from-mixing junction equation, has already been decided in step 3.

In subroutine STENT, $\beta_{sep}^0 = \omega /(1-x^+)$ (see Eq.(6-3-1)) is obtained for a moisture separator mixing junction.

(5) Determination of ρ_n^A, ρ_n^E, p_n^E and p_j^+ for non-stagnant node (STPRHO)

(a) First, we obtain

$$\rho_n^A = \rho(p_n^A, h_n^A) \quad .$$

(b) Next, we determine junction pressures as

$$p_j^+ = \frac{1}{j_{out}} \sum_{j-out} \left(p_n^A + \frac{K_n^A}{2\rho_n^A}\right) \quad , \qquad (6-2-1)$$

where $\sum_{j-out}$ means the summation over all the flows out of junction j.

(c) Obtain density of mixing junctions such that

$$\rho_j^+ = \rho(p_j^+, h_j^+) \quad .$$

(d) For a node n whose from-junction is a mixing junction, update inputted p_n^A by the solution to the following equations,

$$p_n^A + \frac{K_n^A}{2\rho(p_n^A, h_n^A)} = p_{from}^+ \quad .$$

(e) Solve the following equations to obtain p_n^E for all the normal nodes,

$$p_n^E - \frac{K_n^E}{2\rho(p_n^E, h_n^E)} = p_{to}^+ \quad .$$

(6) Determination of ρ_n^A, ρ_n^E, p_n^A and p_n^E for stagnant nodes (STPRHO)

(a) a stagnant normal chain with a closed valve :

From the valve to the A-node of the chain, solve for p_E

$$0 = p^A - p^E - \rho\left(\frac{p^A+p^E}{2}, h^{av}\right) g L_H \quad , \qquad (6-2-2)$$

succesively, starting with p_A equal to the from-mixing junction pressure and ending with p_E of the valve node. We note in Eq.(6-2-2) that h_{av} = (h^E + $h^E_{to-node}$)/2 , whose right hand side can be decided from inputs (BB19). Similarly, we solve the above equation backwards for p_A, starting with p_E equal to the to-mixing junction pressure and ending with p_A of the to-node of the valve.

(b) a stagnant normal chain without a closed valve :

For each chain, solve Eq.(6-2-2). Then, for comparison, print out the calculated pressures and the inputted pressures for the to- and from-mixing junctions. If the difference is found too large, the code user must change the input data or redesign the system in question. This is part of step 6 in Fig.6-1-1.

(7) Determination of k_n for non-stagnant nodes (STAJDW)

For a turbulent flow, we obtain loss coefficients k_n such that

$$k_n = \frac{2\rho_n}{G_n^{A^2}}\left(p_n^A - p_n^E + \frac{G_n^{A^2}}{\rho_n^A} - \frac{G_n^{E^2}}{\rho_n^E} - \rho_n g L_{Hn}\right) - \frac{f_n}{D_n} L_n \quad . \tag{6-2-3}$$

For a laminar flow, similarly, we can obtain k_n. If the loss coefficient thus obtained turns out to be negative or unrealistically large, then, its adjustment will be necessary. For this, refer to section 6.7.

6.3 Moisture Separator

Letting $\omega = W_1 / W_{in}$ in Eq.(2-4-22), we obtain

$$\beta^0_{sep} = \frac{\omega}{1-(x^+)^0} \quad , \tag{6-3-1}$$

where branching ratio ω at the separator junction is an input in BB12.

6.4 Hydraulic Machine Shaft

Since $\Omega(0)$ is an input, we have

$$a(0) = \frac{\Omega(0)}{\Omega^r} \quad . \tag{6-4-1}$$

Assuming that W(0) has already been known, we have

$$w(0) = \frac{W(0)}{W^r} \quad . \tag{6-4-2}$$

Given a(0) and w(0) by Eqs.(6-4-1) and (6-4-2), respectively, the homologous law gives $p_{head}(0)$ and b(0), which in turn give

$$L_{head}(0) = p_{head}(0) L^r_{head}$$

and

$$T_e(0) = T^r \tau_e(0)$$

where $\tau_e(0)$ is given by Eq.(2-4-1) as

$$\tau_e(0) = b(0) + k_1 a(0)^2 + k_2 a(0)^{1/2} \quad .$$

6.5 Heat Conductors

First of all, we note that some of the equations do not have a steady state, e,g., Eq.(3-1-13) for metal-water reaction of Zircaloy cladding and Eq.(4-1-11) for plastic hoop strain of Zircaloy cladding. Since $d\Theta/dt$ and dS/dt are very small at a steady state, they are neglected in the steady state adjustment.

Since THYDE-W is intended primarily to analyze transient phenomena, we will, if possible, try to keep unnecessary complications from being involved in the steady state calculation. For example, the calculation of hot geometrical dimensions of a fuel element at the initial operating condition is outside the scope of this work, since it is a complicated steady state problem itself, involving various

calculations such as the deformations due to pressure and temperature changes from room to operating condition. Thus, in THYDE-W, all the hot geometrical dimensions of a fuel rod are assumed to be given as inputs and we consider only the deviations from the hot dimensions, e.g., Eqs.(4-1-2), (4-1-4) and (4-2-3a).

Moreover, we note if we defined the crack and dish temperature T_{cd} in Eq.(4-2-9) to be the volume-averaged temperature of the fuel, then the steady state adjustment would become unnecessarily complicated. Since T_{cd} appears only in Eq.(4-2-9), we have simply defined T_{cd} to be the arithmetic average of the fuel center temperature and the fuel surface temperature.

The equation to govern a steady state temperature distribution in a heat conductor is given by letting the time derivative in Eq.(3-3-5) vanish. Thus, we have

$$\delta_i T_{i+1} - (\delta_i+\delta_{i-1})T_i + \delta_{i-1}T_{i-1} + V_i\Xi_i = 0 \quad . \qquad (6-5-1)$$

Equation (6-5-1) has the same form as Eq.(3-3-7) with $\tilde{\theta}=1$ and $\Delta t = \infty$. Thus, a steady state temperature distribution in a heat conductor can be obtained in exactly the same manner as a transient distribution discussed in subsection 3.3.2.

For heat conductors simulating a fuel rod with a gap, a steady state similarly can be obtained, by solving Eq.(3-3-1) successively from the outer surface mesh to the center node. But, the procedure is different due to the existence of the gap, since relationships Eqs.(3-3-31) to (3-3-36) along with Eq.(3-3-11) must be satisfied. We note that Eq.(3-3-33) or (4-2-3a) is automatically satisfied at a steady state. Figure 6-5-1 shows the procedure to obtain gap quantities, when the clad surface heat flux φ_R and the inner surface temperature of the clad T_{CL}^{in} are known. It should be reminded that dimensions such as r_{gap}^{0}

are inputs.

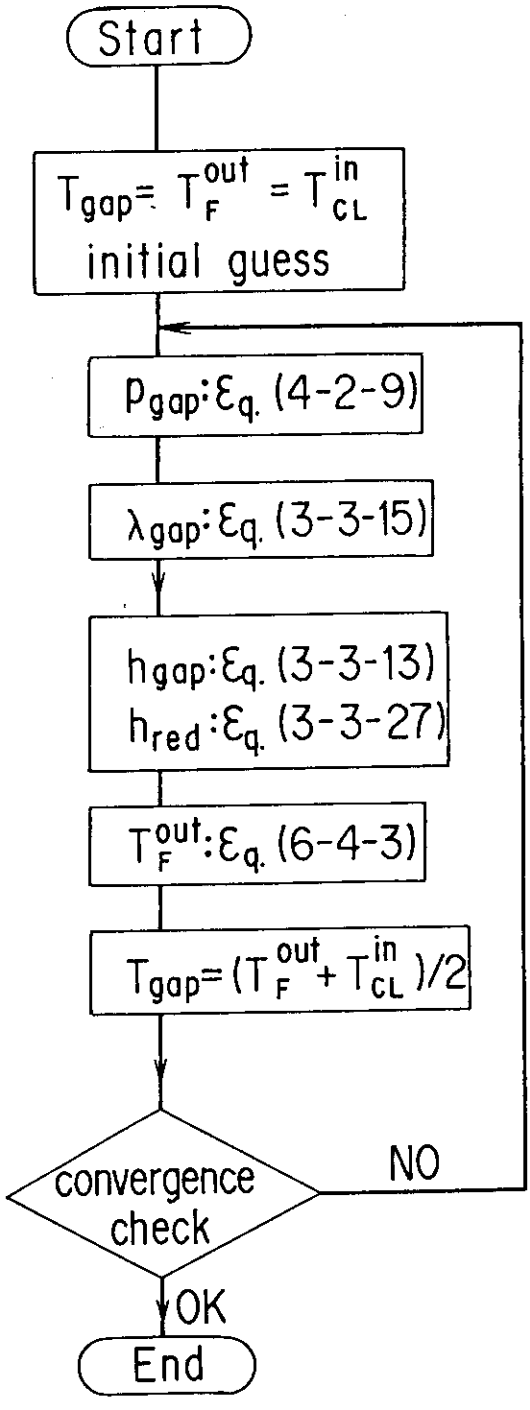

Fig. 6-5-1 Procedure to Obtain Gap Quantities at Steady State

In Fig. 6-5-1, T_F^{out} is obtained as follows. At a steady state, we have

$$\varphi_{CL}^{in}(r_F+r_{gap})=\varphi_R r_R \quad . \tag{6-5-2}$$

Eliminating φ_{CL}^{in} from Eqs.(3-3-12) and (6-5-2) and solving the resltant equation for T_F^{out}, we obtain

$$T_F^{out}=T_{CL}^{in}+\frac{r_R}{r_F+r_{gap}}\frac{\varphi_R}{h_{gap}^t(T_{gap},T_F^{out},T_{CL}^{in})} \quad . \tag{6-5-3}$$

6.6 *Accumulator*

Equation (2-4-21) must be satisfied. The height of water volume $(L_H)_L^0$ can be determined by inputs (BB17) as

$$(L_H)_L^0 = \frac{V_{ACC}-V_G^0}{A_{ACC}} \quad .$$

Suppose that an ACC junction is closed so that it is isolated from the network. Then, since $p_G(0)$ and $h_L(0)$ are inputs (see BB17), ACC bottom pressure p_x can be obtained by iteratively solving Eq.(2-4-21).

On the other hand, suppose that an ACC junction is open so that ACC is connected with the main network. Then, we solve Eq.(2-4-21) iteratively to obtain p_G, assuming that $(p_x,h_L) = (p^+,h^+)$ at the ACC junction, whose state has already been obtained by the steady state calculation for the main network.

6.7 *Adjustment of Form Loss Coefficients*

The loss coefficient k given by Eq.(6-2-3) often turns out to be unrealistic or negative. In the following, a recipie to obtain realistic loss coefficients, by changing inputted pressures (or sometimes hydraulic diameters) will be shown. This is part of step 6 in Fig.6-1-1.

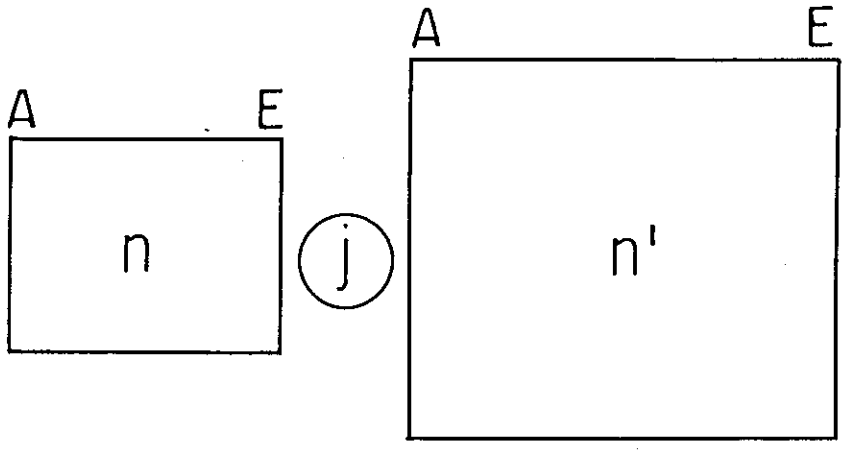

Fig. 6-7-1 Node-Node Coupling

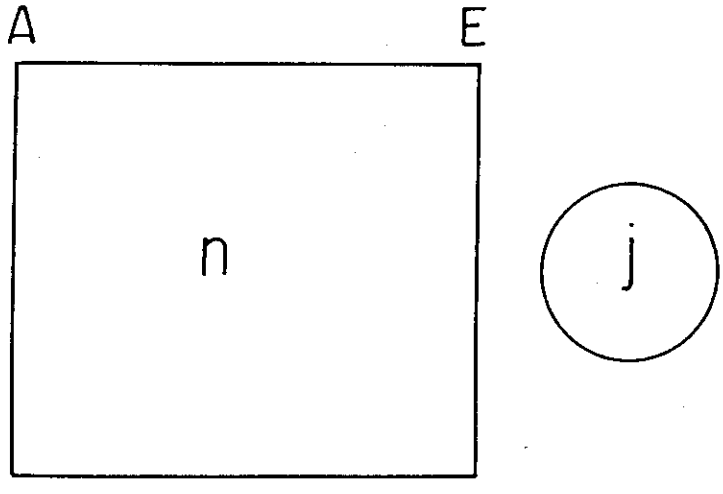

Fig. 6-7-2 Node-Mixing Junction Coupling

6.7.1 Relationship between Form Loss Coefficient and Neighboring Pressures

We make use of the relationship which exists between the loss coefficient and the neighboring pressures , depending on node-node coupling (Fig.6-7-1) or node-mixing junction coupling (Fig.6-7-2). In the following, only for clarity, we assume a turbulent flow.

(a) Node-Node Coupling

We consider Fig. 6-7-1. For the sake of clarity, we assume

$$(k^A)_{n'} = 0 \quad .$$

Then, Eq.(2-3-6) for node n and Eq.(2-3-5) for node n' give

$$p_n^E + \frac{k_n^E G_n^2}{2 \rho_n^E} = (p^A)_{n'} \quad , \tag{6-7-1}$$

while Eq.(2-3-7) for node n gives

$$p_n^A + \frac{G_n^2}{\rho_n^A} - p_n^E - \frac{G_n^2}{\rho_n^E} - \frac{1}{2}\left(k_n + \frac{f_n L_n}{D_n}\right)\frac{G_n^2}{\rho_n} - \rho_n g L_{Hn} = 0 \quad . \tag{6-7-2}$$

Eliminating p_n^E from Eqs.(6-7-1) and (6-7-2) and solving the resulting equation for k_n, we obtain

$$k_n = \frac{2\rho_n}{G_n^2}\left\{ p_n^A - p_{n'}^A - \frac{k_n^E G_n^2}{2\rho_n^E} - \rho_n g (L_H)_n - \left(\frac{G^2}{2\rho^A}\right)_{n'} \right\} - \frac{f_n L_n}{D_n} \tag{6-7-3}$$

(b) Node-Mixing Junction Coupling

We consider Fig. 6-7-2. Suppose that junction friction factor k^E at E-point of node n has been inputted (see Fig.6-7-2). Then, equation f_3 for node n is

$$p_n^E - k_n^E \frac{G_n^2}{2\rho_n^E} = p_j^+ \quad , \tag{6-7-4}$$

for a turbulent flow. Eliminating p_n^E from Eqs.(6-7-2) and (6-7-4) and

solving the resulting equation for k_n, we obtain

$$k_n=\frac{2\rho_n}{G_n^2}\left\{p_n^A-p_j^+-\frac{k_n^E G_n^2}{2\rho_n^E}-\rho_n g(L_H)_n\right\}-\frac{f_n L_n}{D_n} \qquad (6\text{-}7\text{-}5)$$

We note that mixing junction pressure p_j^+ is given by Eq.(6-2-1).

We cast Eqs.(6-7-3) and (6-7-5) into the following forms, respectively,

$$(p^A)_n'=p_n^A+x_1k_n+x_2 \qquad (6\text{-}7\text{-}6)$$

and

$$p_j^+=p_n^A+x_1k_n+x_2 \qquad (6\text{-}7\text{-}7)$$

It can also be shown that the same expression holds for a laminar flow. In Eqs.(6-7-6) and (6-7-7), it shoud be noted that x_1 and x_2 are insensitive to p or k. Therefore, the values x_1 and x_2 of each node will be printed out as a guide to estimate new pressure distribution to yield realistic loss coefficients (refer to the next subsection).

6.7.2 Adjustment Procedure

Consider a sample calculation for Fig. 2-3-1. First, input system pressures 150 ata and 60 ata, for example, for p^A's uniformly in the primary and secondary nodes, respectively (BB10). Then, on the basis of the printed out information discussed in the previous subsection, the pressure of each node will be decided one by one.

Suppose that the information for node 10 is printed out such that

p_{10}^A = 152.0644 (ata)

p_{11}^A = 151.9945 (ata)

x_1 = -0.013973 (ata)

x_2 = -0.070156 (ata)

and

k_{10} = -0.021

The result is not satisfactory, since k_{10} = -0.021. If k_{10} is desired to be, say, 0.01, then, p_{11}^A to be inputted can be obtained as follows. Substituting the above information along with k_{10} = 0.01 instead of -0.021 into Eq.(6-7-6), we obtain

$$p_{11}^A = p_{10}^A - 0.01 \times 0.013973 - 0.070156 = 151.994 \ (ata) \ ,$$

which is the pressure to be inputted for p_{11}^A .

Usually, the procedure will start with a pump inlet and end up with the pump outlet or in the opposite way, thus finally deciding the pump head. Or, it can start with the core outlet and end up with the core inlet or in the opposite way, thus eventually deciding the core pressure drop or the number of grids.

6.8 Check of Thermal-Hydraulic Design

There are a number of variables which may have to be changed to ensure consistency among the input data. These variables include (a) the pressure distribution (refer to section 6.7), (b) especially pressures associated with stagnant mixing junctions (refer to item 6-b in section 6.2), (c) heat transfer areas of heat exchanger conductors, (d) external heat inputs and (e) specific enthalpies of hydraulic sources. For items (c), (d) and (e), refer to item 2 in section 6.2. THYDE-W will print out the originally inputted and adjusted values of these variables for comparison so that the user can check the design of the system to be analyzed.

7. *Program Control*

In this chapter, we will briefly present the main program controls of the THYDE-W code.

7.1 Null Transient Calculation

The system simulated by THYDE-W is a very complicated non-linear system whose exact transient solution is in general impossible to obtain. But, there is one exception for which we know the exact solution, i.e., the null transient problem. In the null transient problem, as time goes by, the solution must not deviate from the initial steady state obtained by the procedure described in chapter 6, provided that the system is stable. In the course of the THYDE-W development, the null transient calculation capability has been confirmed whenever a new modification was made to the code. A null transient calculation can be made with NPERT=1 in BB01 (see subsection 8.4.2) and without external disturbances such as a trip action.

7.2 EM and BE Calculations

For a calculation of a PWR LB-LOCA, a special option is provided in the THYDE-W code, i.e., the evaluation model (EM) calculation based on the conservative assumptions. The ordinary calculation not based on these assumptions is called the best estimate (BE) option as opposed to the EM option. The BE option includes all the up-to-date knowledge or realistic assumptions so that it can be applied to all the transients including an LB-LOCA.

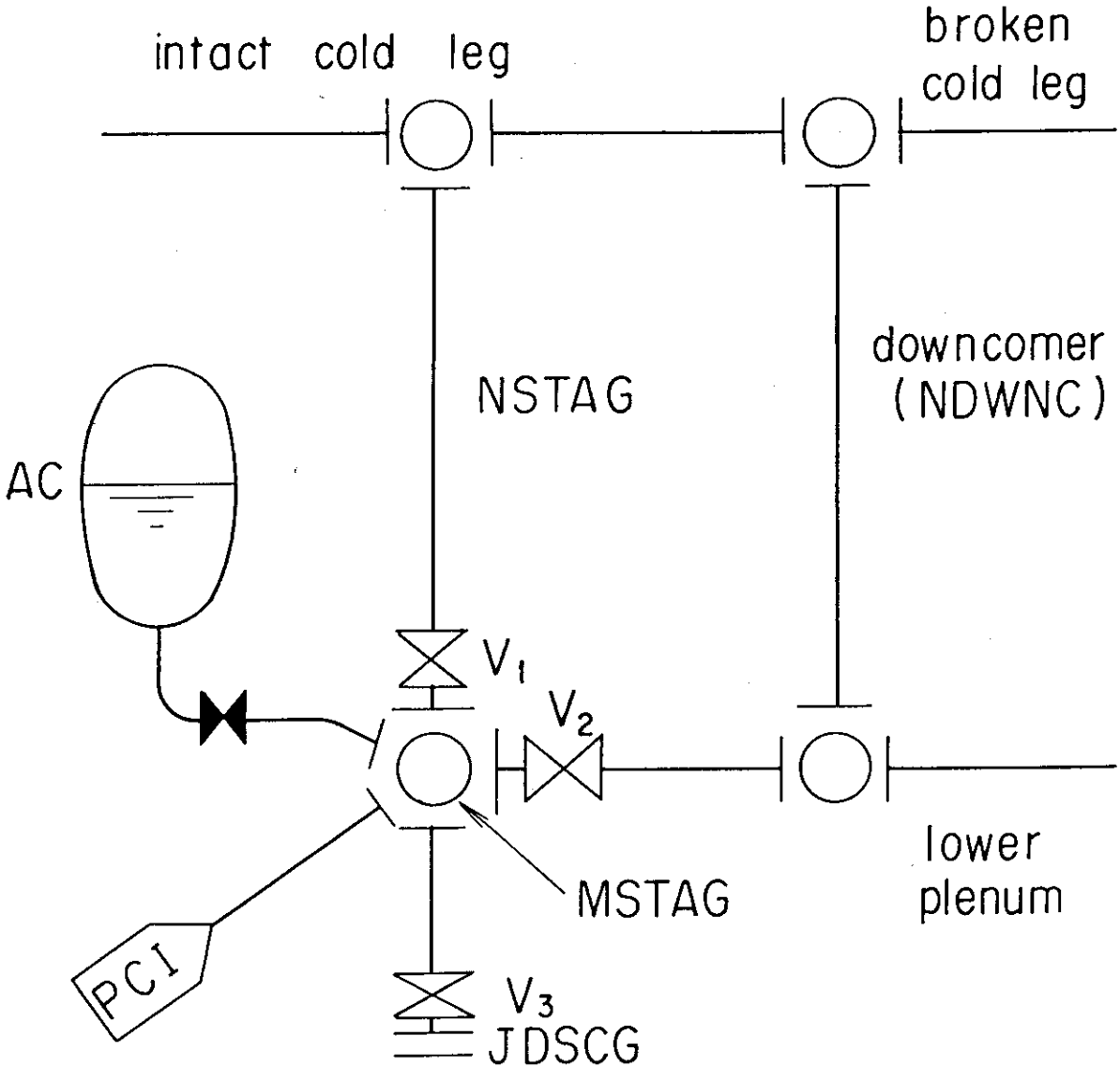

Fig. 7-2-1 PWR LB-LOCA EM Noding

Table 7-1 PWR LB-LOCA EM Calculation Scheme

Time		T_{EOBP}		T_{LPINJ}	T_{BOCREC}
phase		blowdown	fictitious heatup of sub-cooled and saturated nodes	refill	reflood
ECC injection mode		cold leg injection	discharging out of system	lower plenum injection	
fictitious valve aperations	V_1	open	closed	closed	
	V_2	closed	closed	open	
	V_3	closed	open	closed	
core heat transfer		no return to nucleate boiling	adiabatic heatup (h_{tr} = 0)		(1) h_{tr} = 50 + 950 (1-x) for quenched and quenching nodes (2) FLECHT correlation for other nodes

The EM option is composed from the following items ;

(1) the special noding, for example, a single downcomer (see Fig.7-2-1),

(2) the FLECHT correlation so that the core is assumed to be 12 ft long,

(3) factor 1.2 fqr FP decay (see Eq. 3-1-6),

(4) a series of closings and openings of the fictitious valves V_1, V_2 and V_3 after blowdown (see Fig.7-2-1),

(5) a special form of equation f_2 for the downcomer node,

(6) no return to nucleate boiling during blowdown,

(7) hypothetical heating of subcooled and saturated nodes from the end of bypass to the beginning of lower plenum injection,

and

(8) saturated enthalpy for ECC water after the end of blowdown.

In the EM calculation, the scenario of the transient (see Table 7-1) must be specified in advance by means of the input data in BB06 in subsection 8.4.7 and the input data for valves V_1, V_2 and V_3 (BB29 in subsection 8.4.30) in addition to the corresponding valve trip data (BB04 in subsection 8.4.5). The time of the end of bypass T_{EOBP} should be determined by the plotter output or the major edit of a tentative run with a very large input value for it. The time of bottom of core recovery T_{BOCREC} should likewise be obtained. We note that lower plenum injection is assumed to start as soon as the hypothetical heatup of subcooled and saturated nodes (see BB06 in subsection 8.4.7) ends.

On the other hand, in the BE calculation, the program determines the scenario by itself in response to the "scenario" of the boundary conditions and the external disturbances.

The EM assumptions may conform to Ref.(1). Therefore, if this code should be used as part of a licencing application, the calculation may be performed using the EM option. Judgment of the overall adequacy of each engineered ECCS features may be made in the light of the criteria stated in Ref.(1), which, for example, requires that the calculated maximum fuel cladding temperature shall not exceed 1,200°C.

7.3 Time Step Width Control

The time step width control (TSWC) of THYDE-W has been made possible as a result of the efforts made to ensure continuity of all the parameters in the conservation equations. Such efforts have been indispensable for the THYDE-W nonlinear implicit method.

TSWC with respect to the number of the iterations in the thermal-hydraulic network calculation is performed according to the criteria shown in Table 7-2. For TSWC with respect to the rates of change of the following variables, the two TSWC options are available (see next two subsections) ;

(a) normal node variables p, G, h and E,

(b) accumulator variables M_L , h_L , V_G and,

(c) all center and surface temperatures of heat conductors.

If a steam table error takes place, the calculation will be done all over again with the halved time step width. TSWC for the reactor power is not explicitly performed, since it is effectively done by means of the heat conductor temperatures.

7.3.1 2-and-1/2 TSWC

This TSWC is based on the relative increments of the above-mentioned variables. At each time step, the value

$$\frac{|x^{new}-x^{old}|}{(|x^{old}|+e_3)} \qquad (e_3: \textit{an input})$$

will be calculated. Let the maximum of these values be REL. If REL is greater than e_1 (an input value), the time step width will be halved and the calculation is to be done over again. If REL is less than e_1e_2 (e_2 ; an input value), then the calculation proceeds to the next time step which has twice as large a width as the last. If REL is in between e_1 and e_1e_2, then the next time step calculation is to be done with the same time step width as the last. The parameters e_1, e_2 *and* e_3 are given in Table 7-3 or to be inputted by BB03 (see subsection 8.4.4).

7.3.2 Table-Controlled TSWC

In this option, the time step width control with respect to the rates of change of the above-mentioned variables (a) to (c) will be done as shown in Fig.7-3-1, on the basis of dx/dt/x versus Δt table to be inputted by input data block BB03 (see subsection 8.4.4). In this method, efficiency of the time step width control is dependent on how the TSWC table is chosen. Generally speaking, however, it is very difficult to obtain a table with a wide range of applicability. The table can easily be changed by giving input data subblock SB0301, whose default is shown in Table 7-4.

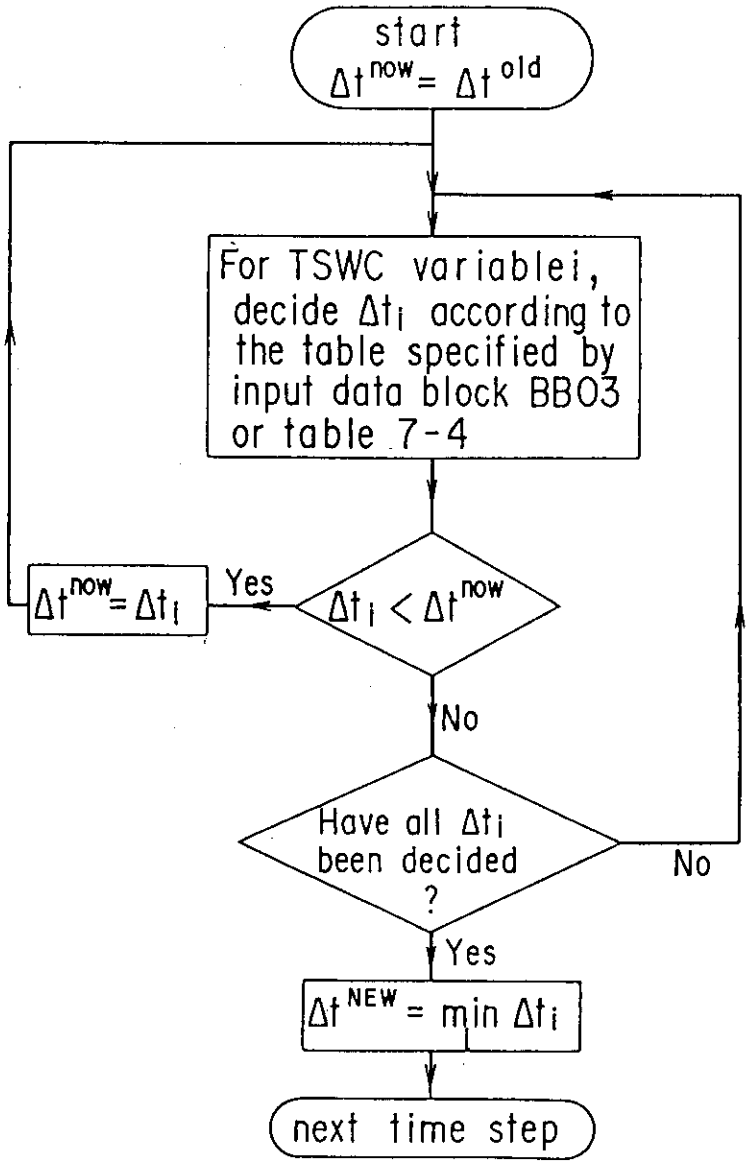

Δt^{now} : present TSW (time step width)

Δt^{new} : TSW to be used in next time step

Fig. 7-3-1 Table-Controlled TSWC

Table 7-2 TSWC w.r.t Thermal-Hydraulic Iteration

Condition	TSWC
$N > N_1$	Recalculate with $0.5\Delta t$.
$N_1 > N > N_2$	Go to next time step width $0.5\Delta t$.
$N_2 > N > N_3$	Go to next time step width Δt.
$N_3 > N$	Go to next time step width $2\Delta t$.

If ITSTYP < 0 is inputted, then the default values (N_1,N_2,N_3) = (20,13,9) will be used. Otherwise, (N_1,N_2,N_3) must be inputted (see subsection 8.4.4).

Table 7-3 2-and-1/2 TSWC Parameters

Variables	e_1	e_2	e_3
p	0.1*	0.2	0.001
G	0.2*	0.2*	100.*
h	0.1*	0.2	0.001
T	0.01*	0.2	0.001
E	0.1*	0.2	0.001

The parameters shown above are those for use in ITSTYP = -1. For ITSTYP = 1, the data with * must be inputted (see subsection 8.4.4).

Table 7-4 Default for Table-Controlled TSWC Parameters

Δt (ms)	dp/dt/p	dG/dt/G	dh/dt/h	dE/dt/E	dX/dt/X
128.	0.1 <	2.0<	0.4<	1.0<	1.0<
64.	0.2	4.0	0.8	2.	2.
32.	0.4	8.0	1.6	4.	4.
16.	0.8	16.	3.2	8.	8.
8.	1.6	32.	6.4	16.	16.
4.	3.2	64.	12.8	32.	32.
2.	6.4	128.	25.6	64.	64.
1.	12.8	256.	51.2	128.	128.
0.5	25.6	512.	102.4	256.	256.
0.25	51.2	1024.	>102.4	512.	512.
0.125	> 51.2	>1024.		>512.	>512.

X stands for variables other than node variables p, G, h and E.

7.4 Loop-Wise Initial Heat Balance

Whether a solution for an initial steady state can be obtained or not depends sometimes on input data in BB09, namely, QOUT1, QOUT2, QOUT3, QOUT4, G_A and h_A so that they should be inputted by try-and-error. With regard to adjustment of heat transfer areas of heat exchangers which transfer heat from net INET to other nets NETT1, NETT2, NETT3, NETT4, the following two options are available.

If INET is inputted with a positive sign, then fixing h^A_{IVOL}'s for net INET as inputted, the heat conductor areas of the out-SG's will be changed to obtain heat balance of net INET, that is , to make its heat output equal to its input. On the other hand, if INET is inputted with a negative sign, then fixing the heat conductor areas of the out-SG's as inputted, h^A_{IVOL}'s for net INET will be changed to attain heat balance of net INET. It is recommended to try first INET with a positive sign.

8. *Input Requirements*

In the following, the requirements for noding, data deck organization, input data cards and problem restart are presented.

8.1 Noding Conventions for Thermal-Hydraulic Network

When we intend to use THYDE-W, first of all we have to reticulate the coolant system by means of nodes and junctions according to the THYDE-W network model:

(a) The network has at least one mixing junction.

(b) A normal node without heat source must be placed both at the most downsteam and most upstream ends of a core channel.

(c) Normal nodes should be numbered loop after loop in numeric order chain-wise from one mixing junction to another according to the direction of the steady state chain flow. But, normal nodes in a linkage flow should be numbered from the mixing junction to the boundary junction regardless of the direction of the flow. Points A and E should be named likewise.

(d) Accumulator nodes should be numbered after all normal nodes.

(e) Among junctions, first, normal (and guillotine break) junctions should be numbered loop after loop in numeric order chain-wise from upstream to downstream. Then, the mixing junctions should numbered loop after loop according to the direction of the steady state flow. After them, the injection junctions and finally the dead-end junctions should be numbered loop after loop.

(f) For PWR EM calculation, special noding is required (see section 7.2).

(g) A pump should be represented by a single node, while a turbine should be represented by at most 7 nodes.

(h) A plural number of core channels can be simulated. But, the axial noding of the channels must be identical.

An example of thermal-hydraulic noding is shown in Fig. 2-3-1. In the figure, junctions 1-47, 48-70 and 71-89 are normal junctions, mixing junctions and boundary junctions, respectively. Nodes 1-99 are normal nodes, whereas nodes 100 and 101 are the accumulators. In Fig. 2-3-1, we note that there are 37 heat conductors and 22 valves. Nodes 57 and 68 are PSSS's[54], which should be dummy nodes in usual calculations.

8.2 Numbering and Noding Convention for Heat Conductors

An example of heat conductors numbering is shown in Fig. 8-2-1. In Fig. 2-3-1, there are 37 heat conductors. The symbol (48) in the rectangle for heat conductor 37 means that node 48 is the other node to which it is connected. Depending on the type of boundary condition at the left (or inner) and right (or outer) surfaces of the conductor, there are 5 cases as shown in Fig.3-3-1. We define the noding convention in the heat conductor as shown in Fig.3-3-2. For a solid cylinder, we let $r_0 = 0$.

In the following, the requirements for numbering and noding of heat conductors are listed in order.

(a) At least, one heat conductor is required.

(b) First, fuel conductors with a gap and then fuel conductors

without a gap and finally other conductors should be numbered.

(c) Heat conductors must be either rectangular or cylindrical or spherical. Fuel with a gap must be cylindrical.

(d) The first inputted fuel is regarded as the average fuel rod (or plate) with IDROD = 1.

(e) More than one heat conductor can be associated with one normal coolant node. But, it is not allowed that one surface of a conductor is associated with plural coolant nodes.

(f) For a given fuel rod or plate, numbering of heat conductors must be in numeric order.

(g) For a given core coolant channel, it is possible to define more than one kind of fuel.

(h) A heat conductor is radially composed of one or more regions, each of which has the same heat conductivity, the same specific specific heat under constant pressure, the same density and the same heat production rate. Each region is made from one or more meshes. Numbering of meshes in a region should be made from the left to the right for a rectangular conductor and from the inside to the outside for a cylindrical or spherical conductor.

(i) Numbering of meshes must be made not region-wise, but conductor-wise.

(j) For a given fuel rod or plate, the most upstream and most downstream conductors must be without heat sources.

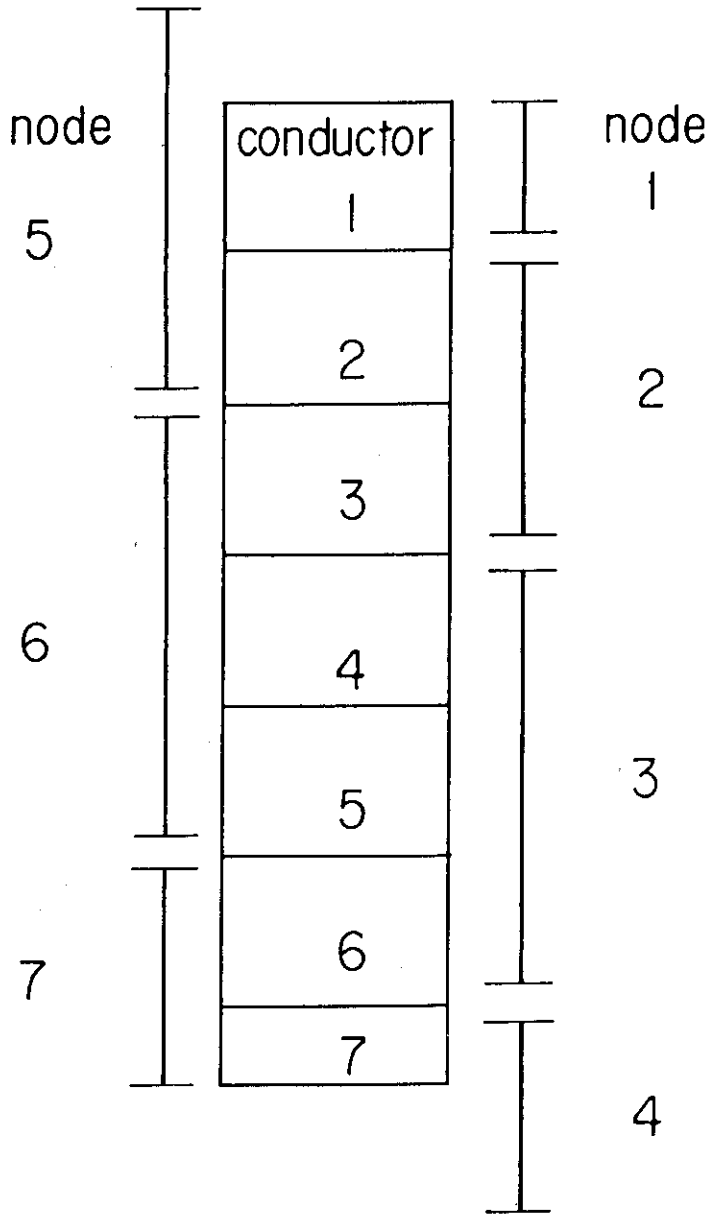

Fig. 8－2－1 Example of Heat Conductor Numbering

8.3 Data Deck Organization

A THYDE-W data deck, ending with the terminator BEND card, could contain more than one problem, each of which consists of a title card, data cards and the subterminator card. The terminator is a card whose first 4 columns are punched as BEND, while the subterminator is the identification card for dummy data block 99. The listings of the inputted and compiled data sets are printed at the beginning and end of each THYDE-W job, respectively.

A block identification card is placed for the top of each data block and is punched in the first 4 columns as BBXX, where XX indicates the data block number. If the block XX has more than one sub-block, a sub-block identification card must be placed at the top of each data sub-block and will be punched in the first 6 columns as SBXXYY where YY indicates the sub-block number starting with 01.

8.4 Input Data Summary

In the following description of the data cards, the data block number is given along with a descriptive title of the data block and the number of the sub-blocks. Then, the order of the data (1,2,.....), the format (I,R,A or table), the variable name and the input data description are given where applicable. The formats of the field, i.e., integer, real (floating), alphanumeric and table is indicated by I, R, A, and T, respectively. Table data for an independent variable should be given as follows. First, the number of points must be given. Then as many sets of the independent and dependent variables as the number of points must

be inputted.

A card whose first column is "/" is regarded as a comment card which must not be placed before the title card. Some limitations exist in placing a comment card in BB05, BB06 and BB00. Reading input cards is performed soley by the free-format input routine REAG[52].

(1) Problem Title (No block numbers)

1-A ITITLE Problem title

The problem title must be punched in columns 1 to 72 on an IBM card

(2) Problem Control Data BB01

TSWC stands for time step width control. Variable ranges such as NTRIP$ are given by the include statement RANGE in the program.

1-I LDMP Restart file control
0 = no restart file used
N = Restart at restart number N using the file on FORTRAN Unit 3.

2-I NEDI Number of minor edit variables desired
(0≦NEDI≦9)

3-I NTC Number of time step width controls
(1≦NTC ≦20)

4-I NTRP Number of trip controls to be inputted in BB04
(1≦NTRP ≦NTRIP$)

5-I MTRP Number of logical conditions to be inputted in BB30
(1≦MTRP ≦NTRPC$)

6-I IOUT Output option for edited input
0 = no output
1 = output

7-I NPERT Flag for the following conditions :
(1) no metal-water reaction in cladding
(2) TEOBP = + infinite for IEM = 0
(3) TBOCREC = + infinite for IEM = 0
etc.
0 = The conditions are not satisfied.
(To be used for a normal transient calculation)
1 = The conditions are satisfied.
(To be used for a null transient calculation)

Note: For a null transient calculation, NPERT=1 is not sufficient, but also no trip is needed.

8-I	ICLASS	T.? in JCL card (1≦ICLASS ≦12)
9-I	LSEC	CPU time (sec) to end calculation (0 = no limitation)
10-I	IDPSTP	Time step to end calculation (0 = no limitation)
11-R	DMPTM	Physical time to end calculation (sec) (0.0 = no limitation)
12-I	NOCK	Number of nodes to which TSWC for G is not applied. (1≦NOCK ≦50)
13-I	ND_1 ND_2 : : ND_{NOCK}	Number of node free from TSWC for G : :

(3) Minor Edit Variable Data BB02

Data block BB02 is required if NEDI is greater than zero. This data block specifies the variables to be edited in the minor edits. NEDI specifications must be inputted. Each specification consists of an alphanumeric entry and an integer entry such that

1 - A4	XXX-YY
.	.
.	.
NEDI - A4	XXX'-YY'

where

XXX~XXX' ; are the variable symbols to be edited,

and

YY ~YY' ; are the position indexes.

The symbols of available minor edit variables are shown below. In

the present version ,however, minor edit is not possible for fuel variables. See Table 8-1 for the convention of the position index.

Table 8-1 Position Index Convention for Minor Edit

	position index
node variables	node number
junction variables	junction number
hydraulic machine shaft speed	shaft number
other hydraulic machine variables	machine number
accumulator variables	accumulator number
core variables	rod ID number
fuel(with gap) variables	heat conductor number
heat conductor variables	heat conductor number

Symbol	Variable (with reference to normal node)
PRA	Pressure as point A
PRE	Pressure as point E
GLA	Mass velocity at point A
GLE	Mass velocity at point E
HLA	Specific enthalpy at point A
HLE	Specific enthalpy at point E
RHA	Density at point A
RHE	Density at point E
XLA	Quality at point A
XLE	Quality at point E
ALA	Void fraction at point A
ALE	Void fraction at point E
QQQ	Power density
TMP	Temperature
KLX	Form Loss Coefficient
REA	Reynolds number at point A
REE	Reynolds number at point E
(CBA	Boron concentration at point A)
(CBE	Boron concentration at point E)

Symbol	Variable (With reference to hydraulic source)
JMI	Injection flow rate

Symbol	Variable (with reference to hydraulic machine shaft)
AAA	Relative shaft speed
(TRQ	Relative external torque)

Symbol	Variable (with reference to hydraulic machine)

HDP	Head
BBB	Relative torque
WWW	Relative volumetric flow rate

Symbol	Variable (with reference to accumulator)
PAC	Nitrogen pressure
GAJ	Mass flow rate
HAC	Water specific enthalpy
VAG	Nitrogen volume
MAL	Water mass

Symbol	Variable (with reference to core)
QCR	Relative power
RCR	External reactivity
RRH	Void (density) reactivity
RTM	Fuel temperature feedback reactivity plus Coolant temperature feedback reactivity
RBR	Boron reactivity
RXN	Xenon reactivity
RTT	Total reactivity

Symbol	Variable (with reference to fuel with gap)
PG1	Gap pressure of rod 1
PG2	Gap pressure of rod 2
HC1	Heat transfer coefficient of rod 1
HC2	Heat transfer coefficient of rod 2
HG1	Gap conductivity of rod 1
HG2	Gap conductivity of rod 2
LI1	Thickness of zircaloy reacted at the clad inner surface of rod 1
LI2	Thickness of zircaloy reacted at the clad inner surface of rod 2
L01	Thickness of zircaloy reacted at the clad outer surface of rod 1
L02	Thickness of zircaloy reacted at the clad outer surface of rod 2
QM1	Metal-water heat production rate of rod 1
QM2	Metal-water heat production rate of rod 2
TS1	Fuel rod surface temperature of rod 1
TS2	Fuel rod surface temperature of rod 2
TC1	Fuel rod center temperature of rod 1
TC2	Fuel rod center temperature of rod 2

Symbol	Variable (with reference to heat conductor)
BSL	Temperature at left/inner surface
BSR	Temperature at right/outer surface
BCL	Heat transfer coefficient at left/inner surface
BCR	Heat transfer coefficient at right/outer surface

(4) Time Step Width Control (TSWC) Data BB03

Number of subblocks = 1+NTC

The time step width control is made according to the method described in section 7.3.

The following data form the first subblock SB0301, which includes the option-dependent data. Data 2 to 4 are the parameters to be used for TSWC with regard to the thermal-hydraulic network iteration.

1-I	ITSTYP	1 = 2-and-1/2 TSWC (Data 2 to 12 must be inputted. Data 13 to 17 are not needed.) -1 = 2-and-1/2 TSWC (Use the default values, i.e., Table 3-3 and (N_1,N_2,N_3) =(20,13,9). Data 2 to 17 are not needed.) 2 = table-controlled TSWC (Data 2 to 4 and data 13 to 17 must be inputted with data 14 to 17 repeated ITBLN times. Data 5 to 12 are not needed.) -2 = table-controlled TSWC (Use the default values i.e., Table 3-4 and (N_1,N_2,N_3) =(20,13,9). Data 2 to 17 are not needed.)
2-I	N_1	
3-I	N_2	(see Table 7-2.)
4-I	N_3	
5-R	P-E_1	e_1 for node pressure p
6-R	H-E_1	e_1 for node enthalpy h
7-R	T-E_1	e_1 for heat conductor temperature T
8-R	AC-E_1	e_1 for AC variables
9-R	E-E_1	e_1 for node energy E
10-R	G-E_1	e_1 for node mass flux G
11-R	G-E_2	e_2 for node mass flux G
12-R	G-E_3	e_3 for node mass flux G
13-I	ITBLN	Number of variables whose TSWC are to be changed from the default method.
14-I	ICOMP	ID of variable x for which the input specified table-controlled TSWC is to be applied 1 = node pressure 2 = node mass flux 3 = node enthalpy 4 = heat conductor temperature 6 = AC variables 7 = node energy
15-I	NTBN	Number of points in TSWC table for x
16-R	$\Delta T(1)$	Value of Δt

	ΔT(NTBN)	
17−R	ΔX(1)	Value of $\Delta x/\Delta t/x$
	ΔX(NTBN)	

In ITSTYP =2 or −2, the time step width Δt will be chosen such that

$\Delta t = \Delta T(i+1)$ if $\Delta X(i) < x < \Delta X(i+1)$.

NTC sets of the following data must be inputted as subblock SB0302, SB0303,....., SB030(NTC+1).

1−I	NMIN	Number of DTMAX's per minor edit (1≦NMIN≦1000) Note: Minor edit frequency is the same for output to plotter file FT50F001.
2−I	NMAJ	Number of minor edits per major edit (1≦NMAJ≦1000)
3−I	NDMP	Number of major edits per restart file edit (1≦NDMP≦100)
4−R	DTMAX	Maximum time step width (sec)
5−R	DTMIN	Minimum time step width (sec) : If time step width Note:If the time step width becomes less than DTMIN, then the calculation stops.
6−R	TLAST	End of control by this subblock (sec)

(5) Trip Control Data BB04

Number of subblocks = NTRP

Note: (1) There must be only one subblock with IDTRP=7.
(2) For IDTRP=2, 4 and 5, if a CSSM is simultaneously inputted then the TRIP overrides the CSSM.
(3) A trip can be used to define its TRTM (see BB31) to be used in CSSM.

1−I	IDNUM	Trip control ID number (0≦*IDNUM*≦32767)
2−I	IDTRP	Trip action index 1 = end of problem 2 = hydraulic machine shaft trip 3 = external reactivity insertion such as scram (The reactivity must be inputted as IDC1 in BB21.) 4 = valve on/off (Time constants are to be inputted in BB27.) 5 = heat source in heat conductor 6 = control block output 7 = guillotine or split break as specified by BB18 8 = break of accumulator top
3−I	IZ1	Index for trip action location (1)

(0≦IZ1≦100)
=0 for IDTRP=1,3 or 6
=shaft number for IDTRP=2
=valve number for IDTRP=4
=heat conductor number for IDTRP=5
=junction number for IDTRP=7
=accumulator number for IDTRP=8

4-I IZ2 Index for trip action location (2)
(0≦IZ2≦6)
=0 for IDTRP=1,2,3,4,6,7 and 8
=region number for IDTRP=5

5-I ION Number of on-action specified in BB30
(0≦ION≦32767).
0 = no on-action
For an initially closed valve, on-action means opening.
For an initially open valve, on-action means closing.

6-I IOFF Number of off-action specified in BB30
(0≦IOFF≦32767).
0 = no off-action
For an initially closed valve, off-action means closing.
For an initially open valve, off-action means opening.

7-I IOCS Selection index for ON/OFF conflict
0 = Continue the old action.
1 = Take the new action.

8-R DELAY Delay time for initiation of action after reaching setpoint (sec)

(6) Delay Constant Data BB05

(Not required when NOPTD = 2 or 4 (see BB07))

1-I NTAUD Number of nodes whose delay constants are to be changed
(0≦NTAUD≦50)

2-R DTAUD Default value (sec)

In the following, first 10 ITAUD's and corresponding 10 TAUD's shoud be inputted. Then, next 10 ITAUD's and corresponding 10 TAUD's should be inputted, and so on.

3-I ITAUD1 Number of node whose delay constant is set to be TAUD1
(≠ DTAUD)
ITAUD2 Number of node whose delay constant is set to be TAUD2
(≠ DTAUD)

4-R TAUD1 Delay constant to be set for node ITAUD1 (sec)
TAUD2 Delay constant to be set for node ITAUD2 (sec)

5-I NTAUDJ Number of junction whose delay constant are to be changed
(0≦NTAUDJ≦50)

6-R DTAUDJ Default value for TAUDJ (sec)

In the following, first 10 ITAUDJ's and corresponding 10 TAUDJ's shoud be inputted. Then, next 10 ITAUDJ's and corresponding 10 TAUDJ's should be inputted, and so on.

7-I ITAUDJ1 Number of junction whose delay constant is set to be TAUDJ1 (≠ DTAUDJ)
ITAUDJ2 Number of junction whose delay constant is set to be TAUDJ2 (≠ DTAUDJ)

.
.

8-R TAUDJ1 Delay constant to be set for node ITAUDJ1 (sec)
TAUDJ2 Delay constant to be set for node ITAUDJ2 (sec)

.
.

(7) PWR LB-LOCA EM Option Data BB06
(Not required for IEM = 1 (see BB07).)
(Refer to section 6.2 for the detail of this data block.)

1-I MSTAG
2-I NSTAG (See Fig.7-2-1)
3-I JDSG
4-I JCOLD
5-I NDWNC Downcomer node number
6-R RCOLD Height of downcomer top mixing junction (m)
7-R TEOBP EOBP time (sec)
8-R TBOCREC BOCREC time (sec)
9-R TQDELT Hypothetical heating time (sec)
(TEOBP + TQDELT = TLPINJ)
10-I NQ Number of nodes for which hypothetical heating is assu

In the following, first, 10 NQNODE's and corresponding 10 QNODE' shoud be inputted. Then, next 10 NQNODE's and corresponding 10 QNODE's should be inputted, and so on.

11-I ND_1 Number of node for which hypothetical heating is assumed
ND_2

.
.

ND_{NQ}
12-I Q_1 Hypothetical heating for node ND_1 (kcal/sec)
Q_2 Hypothetical heating for node ND_2 (kcal/sec)

.
.

Q_{NDNQ} Hypothetical heating for node ND_{NQ} (kcal/sec)

(8) Problem Option Data (BB07)

1-I NMODEL Option flag for steady state calculation model
0= For each flowing node, input pressure p_A and obtain a loss coefficient.
1= Input loss coefficinet k for flowing nodes and p^+ for mixing junctions and obtain pressure distribution.

2-I IEM BE/EM option flag
0= EM calculation for PWR LB-LOCA
1= BE calculation

3-I NOPTF Fuel heating mode flag
0= nuclear heating (reactor kinetics and decay heat)
1= non-nuclear heating

4-I NOPTD Relaxation model index
1= relaxation of void fraction ,r input (BB05)
2= relaxation of void fraction ,r internal calculation
3= relaxation of density ,r input (BB05)
4= relaxation of density ,r internal calculation

5-I ICHFOP1 CHF correlation index for flow condition
1= Biasi's correlation
2= GE correlation
3= RELAP type correlation (combination of B&W2, Barnet and modified Barnett)

6-I ICHFOP2 CHF correlation index for pool condition
1= Interpolation by G between CHF of ICHFOP(1) at $G = G_t$ (= 271.2 $kg/m^2/s$) and 66.9 $kcal/m^2/sec$.
2= Modified Zuber's correlation
3= Zuber's correlation

7-I IHTROP1 Index for heat transfer correlation for nucleate boiling
1= Jens - Lottes
2= Thom

8-I IHTROP2 Index for heat transfer correlation for film boiling at pool condition
1= Berenson
2= Bromley and Pomerantz
3= Modified Bromley

9-I ISTM Option flag for steam table of light water
1= table for high pressure
2= table for low pressure

10-I EPSRD Convergence judgement parameter for calculation of steady state temperature distribution in conductors

(9) Problem Dimensions Data BB08

CSSM stands for the control system simulation model desribed in in Appendix D.

1-I NNET Number of disjoint hydraulic nets
(1≦NNET≦NNET$)

2-I NVOL Number of normal and accumulator nodes
(1≦NVOL≦NVOL$)

3-I NJUNC Number of junctions including boundary junctions
(1≦NJUNC≦NJUNC$)

4-I NMIX Number of mixing junctions
(1≦NMIX≦NMIX$)
5-I NHYDS Number of hydraulic sources including dead-end ducts, i.e number of all boundary junctions except ACC junctions
(0≦NHYDS≦NPINJ$)
6-I NPUMP Number of hydraulic machines
(0≦NPUMP≦NPUMP$)
7-I NSHFT Number of hydraulic machine shafts
(0≦NSHFT≦NSHFT$)
8-I NACCUM Number of accumulators
(0≦NACCUM≦NACCUM$)
9-I KROD Number of nuclear fuel types
(0≦KROD ≦NKROD$)
10-I NCTOT Total number of nuclear fuel slabs ($\sum_{i=1}^{KROD} N_i$ where N_i is number of heat conductors of fuel type i)
(1≦NCTOT ≦NCTOT$)
= 0 when KROD = 0
11-I NCORE Maximum number of axial coolant nodes per core channel
(3≦NCORE ≦NCORE$)
= 0 when KROD = 0
12-I NSLB Number of heat conductors
(1≦NSLB ≦NSLB$)
13-I NRGN Maximum number of material regions in conductors
(Gap of fuel rod should not be counted.)
(1≦NRGN ≦NRGN$)
14-I NMESH Maximum number of radial meshes in conductors
(3<NMESH ≦NMESH$)
15-I NVLV Number of valves
(Exclude valves attached to ACC gas volumes.)
(0≦NVLV ≦NVLV$)
16-I NSEP Number of moisture separators
(0≦NSEP ≦NSEP$)
17-I NIMP =1 when boron transport is simulated
=0 otherwise
18-I NMAT Number of material property tables
(0≦NMAT ≦NMAT$)
19-I NHSTG Number of stagnant nodes
(0≦NHSTG ≦NHSTG$)
20-I NCI Number of control inputs to be used by CSSM (See BB31.)
(0≦NCI ≦NCI$)
21-I NCB Number of control blocks to be used by CSSM (See BB31.)
(0<NCB ≦NCB$)
22-I NCTBL Number of tables to be used in CSSM (See BB32.)
(0≦NCTBL ≦NCTBL$)

(10) Initial Loop-wise Thermal-Hydraulics Data BB09

Number of subblocks = NNET

Whether a solution for the initial staedy state can be obtained or not depends on inputs QOUT1, QOUT2, QOUT3, QOUT4 as well as G_A and h_A so that they should be inputted by try-and-error.

1-I INET Net number
(1≦ | *INET* | ≦NNET)

With regard to adjustment of heat transfer areas of heat exchangers which transfer heat from net INET to other nets NETT1, NETT2, NETT3, NETT4, the following two options are available.
positive sign =Adjust heat exchanger areas, but fix h^A_{IVOL}.
negative sign =Adjust h^A_{IVOL}, but fix heat exchanger areas.

2-I ICLNT Coolant identification flag
0 = light water
1 = heavy water

3-I NETF Number of incoming net-net heat flows at steady state
(1≦NQIN≦4)

4-I NETF1 From-net number (1)
(0≦NETF1≦NNET)

5-I NETF2 From-net number (2)
(0≦NETF2≦NNET)

6-I NETF3 From-net number (3)
(0≦NETF3≦NNET)

7-I NETF4 From-net number (4)
(0≦NHQIN4≦NNET)

8-I NETT Number of outgoing net-net heat flows at steady state
(1≦NETT≦4)

9-I NETT1 To-net number (1)
(0≦NETT1≦NNET)

10-I NETT2 To-net number (2)
(0≦NETT2≦NNET)

11-I NETT3 To-net number (3)
(0≦NETT3≦NNET)

12-I NETT4 To-net number (4)
(0≦NHQOUT4≦NNET)

13-I NADJ Number of sets of initial data 18 to 21

14-R QOUT1 Guess value for heat flow from net INET to INETT1 (kcal/sec)

15-R QOUT2 Guess value for heat flow from net INET to INETT2 (kcal/sec)

16-R QOUT3 Guess value for heat flow from net INET to INETT3 (kcal/sec)

17-R QOUT4 Guess value for heat flow from net INET to INETT4 (kcal/sec)

NADJ sets of the following data must be inputted. For NIMP=0, datum 21 must not be inputted.

18-I IVOL Number of the node from which iteration of steady state calculation for (G,h) ditribution starts
(Node IVOL must be an outlet node of a mixing junction.)

19-R G_A G at point A of node IVOL ($kg/m^2/sec$)

20-R h_A h at point A of node IVOL (kcal/kg).

21-R $\tilde{c}^0$ Initial value of $\tilde{c}^0 = c_B(1-x)$ at point A of node IVOL (ppm)
(Note that, at a steady state, boron is usually used in a subcooled water for which $\tilde{c}$ is identical with c_B.)

(11) Normal or Linkage Node Data BB10

Number of subblocks = NLOOP

1-I	INO	Node number (1≦NOV≦NLOOP)
2-I	FJN	From-junction number (1≦IW1≦NJUNC)
3-I	TJN	To-junction number (1≦IW2≦NJUNC)
4-I	INU	Number of parallel nodes (1≦INU≦ 99999)
5-I	INET	Loop number (1≦INET≦NNET)
6-I	IXCV	CSSM Control ID number for a calculation of relative external heat input per node (1) positive sign : initial value = 1.0 reference value = QEXO (datum 18) or updated value (2) negative sign : initial value = 0.0 reference value = QEXO (datum 18) (3) 0 : no control for external heat input
7-R	p^A/k	= initial pressure (ata) for flowing node (NMODEL=0) = loss coefficient (-) for flowing node (NMODL=1) = loss coefficient (-) for stagnant node (NMODL=0,1) with minus sign
8-R	A^{av}	Cross section at average point (m^2)
9-R	ε^A	A^A/A^{av} (to be updated if $A^+_{from} < A^A$.)
10-R	ε^E	A^E/A^{av} (to be updated if $A^+_{to} < A^E$.)
11-R	D	(1) Hydraulic diameter (m) $= (4A^{av}/\pi)^{1/2}$ if zero is inputted (2) Tube outer diameter if the flow is perpendicular to a group of tubes (Input with a negative sign.) (m)
12-R	L	Node length (m)
13-R	L_H	Node height (height of the to-junction center with reference to the from-junction center)
14-R	k^f_A	Junction loss coefficient at point A for a forward flow
15-R	k^r_A	Junction loss coefficient at point A for a reverse flow
16-R	k^f_E	Junction loss coefficient at point E for a forward flow
17-R	k^r_E	Junction loss coefficient at point E for a reverse flow
18-R	*QEXO*	Heat input/node other than those from heat conductors (kcal/sec) : If IXCV ≧0, it is to be used for initial value as as well as for reference value. For IXCV > 0, it will possibly be updated. : For IXCV < 0, this is to be used only for reference value.

If D < 0, then input the following data.

19-I		Number of tube rows perpendicular to flow (-)
20-R	A_{min}	Minimum cross sectional flow area (m^2)

(1) For a core flow associated with a fuel rod ,for example, whose pitch and outer radius are l_p and r_R, respectively , A and D to be inputted may be given as follows.

$$A = l_p^2 - \pi r_R^2$$

and

$$D=\frac{2A}{\pi r_R}$$.

(2) If one wants to input a loss coeffcient for a forward/reverse flow at normal junction j, then one can do it by inputting either k_A^f/k_n^r of the to-node or k_E^f/k_E^r of the from-node, respectively. Moreover, the built-in formula can be used for a normal junction, if - 1.0 is inputted for either A or E point adjacent to the junction. No built-in formula, however, is available for the junction loss coefficients around a mixing junction (see subsection 2.5.1).

(3) A^A and A^E are used only in resistance calculation.

(4) L_H should be the height between the centers of the two adjacent junctions.

(12) Junction Data BB11

For data 5 to 7, input 0.0 if junction JNO is initially non-stagnant. For NIMP=0, datum 8 must not be imputted.

1-I JNO Junction number
(1≦JNO≦NJUNC)

2-I JTP Junction type
1 = normal junction
2 = mixing junction (upper plenum)
3 = mixing junction (downcomer top)
4 = other mixing junction
5 = ACC injection junction
7 = hydraulic source junction or dead end junction

3-I INET Loop number
(1≦INET≦NNET)

4-I IJU Number of parallel junctions

5-R $(V^+/A^+)_{unit}$
Junction volume/unit for mixing junction (m^3) or
Junction area/unit for volumeless junction (m^2)
Note: (1) If A^+_{unit} = 0.0 is inputted for a volumeless junction, the minimum of $(A^{av}\xi^E)_{from}$ and $(A^{av}\xi^A)_{to}$ will be set for A^+_{unit} by the code.
Otherwise, the minimum of $(A^{av}\xi^E)_{from}$, $(A^{av}\xi^A)_{to}$ and inputted A^+_{unit} will be set by the code (refer to section 2.5.2).
(2) A^+_{unit} is used only in resistance calculation.

6-R PJO For NMODEL = 0 :
(a) initial pressure for stagnant mixing junction (ata)
(b) initial pressure for flowing boundary junction (ata)
(c) initial pressure for stagnant boundary junction of a chain with a closed valve (ata)
(d) 0.0 otherwise.
For NMODEL = 1 :
(a) initial pressure for stagnant mixing junction (ata)
(b) initial pressure for flowing mixing junction (ata)
Note: For each net, the following must be satisfied
(1) For at least one flowing mixing junction, its initial pressure must be inputted.
(2) For other flowing mixing junctions whose initial pressures are to be specified, their

values should be inputted with a negative sign.
(3) It is recommended to input a pressure for a mixing junction with a plural number of merging flowing flows.
(4) For a flowing branch immediately upstream of a mixing junction whose pressure is inputted, the pressure balance will be taken by adjusting the form loss coefficints of the nodes.

(c) initial pressure for stagnant boundary junction of a boundary chain with a closed valve (ata)
(d) 0.0 otherwise.

7-R HJO Initial enthalpy of stagnant junction (kcal/kg)
(dummy for JTP > 4)

8-R BCJO Initial concentration of boron in liquid phase for initially stagnant junction (ppm)
(dummy for flowing junction)
(For NIMP=0, this must not be imputted.)

(13) Mixing Junction Data BB12

Number of subblocks = NMIX

(a) Data 5 are the ratios of mass flow rates in (kg/s).
(b) Subblocks must be inputted netwise.
(c) For each subblock, the first line must have data 1 and 2 only.

1-I JNO Junction number
($1 \leqq JNO \leqq NJUNC$)

2-I IDC Contrl ID number for calculation of relative external heat input (Reference value is the initial value calculated by the code.) ($0 \leqq IDC$)

3-I NOUT Number of outgoing flows at steady state
($1 \leqq NOUT \leqq NOUT\$$)

4-I ND_1 To-node (1)
($0 \leqq ND_1 \leqq NVOL$)

:
:

ND_{NOUT} To-node (NOUT)
($0 \leqq ND_{NOUT} \leqq NVOL$)

5-R ω_1 Fraction of outgoing flow (kg/sec) through node ND_1 at steady state

:
:

ω_{NOUT} Fraction of outgoing flow (kg/sec) through node ND_{NOUT} at steady state

(14) Hydraulic Source Data BB13

Number of subblocks = NHYDS

If IFPT = 0, then data 4 to 8 are arbitrary.

1-I IH Hydraulic source number
($1 \leqq NOPINJ \leqq NHYDS$)

2-I IJ Boundary junction number
($1 \leqq IJ \leqq NJUNC$)

3-I	IFPT	Option flag 0 = dead end 1 = G-source (G(t) or G(p)) 2 = p-source (p(t) or p(G))
4-I	IHFLG	Initial steady state flag 1 = inflow -1 = outflow 0 = stagnant (closed)
5-I	IDC	CSSM ID number for control of flow rate or pressure (a) Control of flow rate relative to the initial (IHFLG ≠0) or reference (IHFLG=0) value for IFPT= (b) Control of pressure (ata) for IFPT=2 0 = no control for flow rate or pressure
6-I	IDB	CSSM ID number for control of boron concentration (ppm) in liquid phase 0 = no control
7-I	IDH	CSSM ID number for control of specific enthalpy of flowing-in coolant (reference value = h_{HS}) 0 = no control
	Note :	This control is effective only during inflow.
8-I	JPARA	Number of parallel units
9-R	h_{HS}	Reference specific enthalpy of water injected at junction IJ (kcal/kg) ; dummy for IHFLG = -1
10-R	m^r_{HS}	Reference flow rate per unit for flow rate control (kg/sec) (When either IHFLG ≠0 or IFPT ≠1, this input is a dummy, and the calculated initial flow rate will be used as the reference value for a flow rate control.) > 0 if reference flow enters the network. < 0 otherwise

(15) Hydraulic Machine Shaft Data BB14

Number of subblocks = NSHFT

If IDT=0 is inputted, data 4 to 9 and 11 are dummy.

1-I	IDM	Shaft number ($1 \leqq IDM \leqq NSHFT$)
2-I	IDT	Trip mode index 0 = locking of shaft (speed trip) 1 = disconnection of motor or generator (electric torque trip)
3-I	IDC	CSSM ID number 0 = no contrl (usual calculation) positive sign = speed control negative sign = electric torque control
4-R	Ω^r	Rated shaft speed (rpm) ($0 \leqq \Omega^r$)
5-R	$\Omega(0)$	Initial shaft speed (rpm) ($0 \leqq \Omega(0)$)
6-R	Ω_s	Steady state speed (rcm) $=\Omega(0)$ if 0.0 is inputted.
7-R	I_m	Moment of inertia (kgm^2/rad^2)
8-R	k_1	Coefficient of angular momentum equation ($0 \leqq k_1$) (See Eq.(2-4-51).)
9-R	k_2	Coefficient of angular momentum equation ($0 \leqq k_2$) (See Eq.(2-4-51).)

10-R	τ	Trip decay constant (sec) (decay constant for speed when ID=0) (decay constant for electric torque when ID=1) =0.01 (default)
11-R	T^r	Rated torque (J/rad)

(16) Hydraulic Machine Data BB15

Number of subblocks = NPUMP

Data 4 to 10 should be in order of initial steady flow. For each subblock, the first line should consist of data 1,2 and 3 only. The number of parallel units is specified by INU in BB10 to be inputted for nodes N_1, N_2, .., N_{NNM}.

1-I	NM	Machine number ($1 \leqq NM \leqq NPUMP$)
2-I	IDM	Shaft number ($1 \leqq IDM \leqq NSHFT$)
3-I	NNM	Number of nodes in machine NM ($1 \leqq NPNODE \leqq 7$)
4-I	N_1	Node number ($1 \leqq N_1 \leqq NLOOP$)
.	.	.
.	.	.
.	.	.
.	.	.
5-I	N_{NNM}	Node number ($0 \leqq N_{NNM} \leqq NLOOP$)
6-I	ITAP	Number of table group to be used (see BB16) ($1 \leqq ITAP \leqq NPTB$)
7-R	W^r	Rated volumetric flow rate per unit (m^3/sec) positive : pump negative : turbine
8-R	L^r_{head}	Rated head (m)
9-R	Δh_1	Rated enthalpy loss in node N_1 (kcal/kg)
.	.	.
.	.	.
.	.	.
10-R	Δh_{NNM}	Rated enthalpy loss in node N_{NNM} (kcal/kg)
11-R	ρ^r	Rated density (kg/m^3)

(17) Hydraulic Machine Characteristic Curves Data BB16
Number of subblocks ≦NPUMP

0-I NPTB Table group number
(1≦NPTB≦NPUMP)

The following 18 tables should be inputted according to THYDE-W table input specification. In the data from 9 to 16, Δb_{hyd} and Δl_{head} mean $((\mathcal{T}_h)_{2\varphi}-(\mathcal{T}_h)_{1\varphi})/(\mathcal{T}_h)^r$ and $((L_{head})_{2\varphi}-(L_{head})_{1\varphi})/L^r_{head}$, respectively, with 1φ = single phase and 2φ = two pahse.

1 (Head-flow curve for positive speed : $\mathcal{K}^F_Q$)
1a-I IP1 Number of points
1b-T IP1 pairs of (w/a, $\tilde{p}_{head}/a^2$)
2 (Head-flow curve for negative speed : $\mathcal{K}^R_Q$)
2a-I IP2 Number of points
2b-T IP2 pairs of (w/a, $\tilde{p}_{head}/a^2$)
3 (Head-speed curve for positive flow : $\mathcal{K}^F_W$)
3a-I IP3 Number of points
3b-T IP3 pairs of (a/w, $\tilde{p}_{head}/w^2$)
4 (Head-speed curve for negative flow : $\mathcal{K}^R_W$)
4a-I IP4 Number of points
4b-T IP4 pairs of (a/w, $\tilde{p}_{head}/w^2$)
5 (Torque-flow curve for positive speed : $\mathcal{T}^F_Q$)
5a-I IP5 Number of points
5b-T IP5 pairs of (w/a, $\tilde{b}/a^2$)
6 (Torque-flow curve for negative speed : $\mathcal{T}^R_Q$)
6a-I IP6 Number of points
6b-T IP6 pairs of (w/a, $\tilde{b}/a^2$)
7 (Torque-speed curve for positive flow : $\mathcal{T}^F_W$)
7a-I IP7 Number of points
7b-T IP7 pairs of (a/w, $\tilde{b}/w^2$)
8 (Torque-speed cuver for negative flow : $\mathcal{T}^R_W$)
8a-I IP8 Number of points
8b-T IP8 pairs of (a/w, $\tilde{b}/w^2$)
9 (Δl_{head}-flow curve for positive speed)
9a-I IP9 Number of points
9b-T IP9 pairs of (w/a, Δl_{head})
10 (Δl_{head}-flow curve for negative speed)
10a-I IP10 Number of points
10b-T IP10 pairs of (w/a, Δl_{head})
11 (Δl_{head}-speed curve for positive flow)
11a-I IP11 Number of points
11b-T IP11 pairs of (a/w, Δl_{head})
12 (Δl_{head}-speed curve for negative flow)
12a-I IP12 Number of points
12b-T IP12 pairs of (a/w, Δl_{head})
13 (Δb_{hyd}-flow curve for positive speed)
13a-I IP13 Number of points
13b-T IP13 pairs of (w/a, $\Delta \tau_{hyd}$)
14 (Δb_{hyd}-flow curve for negative speed)
14a-I IP14 Number of points
14b-T IP14 pairs of (w/a, $\Delta \tau_{hyd}$)
15 (Δb_{hyd}-speed curve for positive flow)
15a-I IP15 Number of points

15b-T IP15 pairs of (a/w, $\Delta\tau_{hyd}$)
16 (Δb_{hyd}-speed curve for negative flow)
16a-I IP16 Number of points
16b-T IP16 pairs of (a/w, $\Delta\tau_{hyd}$)
17 (Head multiplier)
17a-I IP17 Number of points
17b-T IP17 pairs of (α, M_h)
18 (Torque multiplier)
18a-I IP18 Number of points
18b-T Ip18 pairs of (α, M_t)
19 ($NPSH_R$ table)
19a-I IP191 Number of points for a
19b-I IP192 Number of points for w
19c-T (Give as follows.)

(blank)	a_1	.....	a_{IP191}
w_1	$NPSH(w_1, a_1)$	.....	$NPSH(w_1, a_{IP191})$
w_2	$NPSH(w_2, a_1)$	.....	$NPSH(w_2, a_{IP191})$
.	.	.....	.
.	.	.....	.
w_{IP192}	$NPSH(w_{IP192}, a_1)$	.....	$NPSH(w_{IP192}, a_{IP191})$

(18) Accumulator Data BB17

Number of sub-blocks = NACCUM

An accumulator to be specified by this block is only its tank parts so that its duct part should be modelled by a chain of normal nodes. If the accumulator duct does not have an initially closed valve, data 7 and 8 are used to obtain $(pV/T)_G$ = (a constant) and, using this relationship, data 7 and 8 will be updated in the steady state calculation. Otherwise, they will not be updated.

1-I	NOV	Node number (NLOOP+1≦NOV≦NVOL)
2-I	IJUNC	Injection junction number (1≦IJUNC≦NJUNC)
3-I	NPARA	Number of parallel units
4-I	ISTCAL	Option flag for steady state calculation for ACC duct without a closed valve (Input a dummy for ACC duct with a closed valve.) 0 = Regard inputted p_G^0 as dummy, fix inputted V_G^0 and obtain p_G^0. 1 = update p_G^0 and V_G^0, using relationship $(pV)_G$ = (a constant obtained from inputted data 8 and 9).
5-R	$h_{H_2O}^0$	Initial specific enthalpy of water (kcal/kg)
6-R	A_{ACC}	Cross sectional area per unit (m^2)
7-R	V_{ACC}	ACC tank volume per unit (m^3)
8-R	V_G^0	Initial gas volume per unit (m^3)
9-R	p_G^0	Initial pressure (ata)
10-R	p_{set}	Set point for opening of cover gas relief valve (ata)
11-R	C_B^0	Boron concentration of ACC water (ppm)

(19) Break Point Data BB18

In case of a dead-end break, data 3, 4, 7, 8 and 11 are dummy.

1-I	JBRK	Junction (1≦JBREAK≦NJUNC)
2-I	IDCTB	Control ID number for back pressure table specification
3-R	C_2	See Eq.(2-5-13). (-) (to-node of break junction)
4-R	C_D	Discharge coefficient for critical flow (-) (to-node of break junction)
5-R	C_2	See Eq.(2-5-13). (-) (from-node of break junction)
6-R	C_D	Discharge coefficient for critical flow (-) (from-node of break junction)
7-R	k_D^D	Loss coefficient at break (-) (to-node of break junction, discharge)
8-R	k_D^S	Loss coefficient at break (-) (to-node of break junction, suction)
9-R	k_U^D	Loss coefficient at break (-) (from-node of break junction, discharge)
10-R	k_U^S	Loss coefficient at break (-) (from-node of break junction, suction)
11-R	DTAUB	Break time constant at to-node of break (sec)
12-R	UTAUB	Break time constant at from-node of break (sec)

(20) Initially Stagnant Node Enthalpy Data BB19

Number of subblocks = NHSTG

1-I	INO	Node number (NLOOP+1≦INO≦NVOL)
1-R	h^E	Initial specific enthalpy at point E (kcal/kg) (dummy if connected to a mixing junction)

(21) Core Control Data BB20

(Not required for KROD=0)

Number of subblocks = KROD

Fuel rods or fuel plates should be inputted first. Fuel rods with gap should be inputted earlier than fuel rods without gap. First inputted fuel is rergarded as the average rod or plate.

1-I	IDROD	Rod type identification number ($1 \leqq IDROD \leqq KROD$)
2-I	NROD	Number of fuel rods ($1 \leqq NROD \leqq 50,000$)
3-I	NBOT	Number of most upstream core node ($1 \leqq NBOT \leqq NLOOP$)
4-I	NTOP	Number of most downstream core node ($NBOT \leqq NTOP \leqq NLOOP$)
5-I	NSLBOT	Number of most upstream conductor ($1 \leqq NSLBOT \leqq NSLB$)
6-I	NSLTOP	Number of most downstream conductor ($NSLBOT \leqq NSLTOP \leqq NSLB$)
7-I	IGAP	GAP option 0 = fuel without gap

1 = fuel with gap
Note: For IGAP = 1, fuel must be cylindrical.

8-I IQMW Metal-water reaction option
0 = without reaction
1 = with reaction

(22) Nuclear Heating Data BB21
(Not required for KROD=0)

1-I IDC1 CSSM Control ID number to calculate external reactivity after IDTRP=3 in BB04 is satisfied.
0 = no external reactivity

2-I IREAC2 Option flag for density reactivity calculation
0 = Do not use CSSM, but input data 16 and 17.
1 = Calculate reactivity with control IDC2.
2 = Calculate reactivity coefficient with control IDC2.

3-I IDC2 Control ID number in CSSM for density (or void) reactivity calculation. Set 0 for IREAC2=0.

4-I IREAC3 Option flag for fuel temperature reactivity calculation
0 = Do not use CSSM, but input data 18 and 19.
1 = Calculate reactivity with control IDC3.
2 = Calculate reactivity coefficient with control IDC3.

5-I IDC3 Control ID number in CSSM for fuel temperature reactivity calculation. Set 0 for IREAC3=0.

6-I IREAC4 Option flag for coolant temperature reactivity calculation
0 = Do not use CSSM, but input data 20 and 21.
1 = Calculate reactivity with control IDC4.
2 = Calculate reactivity coefficient with control IDC4.

7-I IDC4 Control ID number in CSSM for coolant temperature reactivity calculation. Set 0 for IREAC4=0.

8-I IREAC5 Option flag for boron reactivity calculation
0 = usual calculation
1 = calculation with control IDC5

9-I IDC5 Control ID number in CSSM for external calculation of boron reactivity : Set 0 for IREAC5=0.

10-I NFLG 0 = 6 delayed neutron groups
1 = 15 delayed neutron groups

11-R l Neutron lifetime (sec)

12-R (λ_1, β_1) : : (λ_K, β_K) λ_i= Decay constant of delayed neutron precursor of i-th group (1/sec)
β_i= Delayed neutron fraction of i-th group (-)
K = 6 for NFLG = 0
K = 15 for NFLG = 1

13-R C_c Conversion ratio (-)

14-R Σ_a Macroscopic thermal absorption cross section (cm^{-1})

15-R Σ_f Macroscopic thermal fission cross section (cm^{-1})

16-R Φ_0 Initial thermal neutron flux ($1/sec/cm^2$)

Input data 15 and 16 only when IREAC2 = 0.

16-I	IP1	Number of points in void reactivity table
17-T		IP1 sets of $(\rho/\rho_0, \Gamma_\rho)$ ρ : coolant density ρ_0 : initial coolant density Γ_ρ : density reactivity ($)

Input data 17 and 18 only when IREAC3 = 0.

18-I	IP2	Number of points in fuel temperature coefficient table
19-T		IP2 sets of (T_f, γ_{T_f}) T_f : fuel temperature (°C) γ_{T_f} : fuel temperature coefficient ($/°C)

Input data 19 and 20 only when IREAC4 = 0.

20-I	IP3	Number of points in coolant temperature coefficient table
21-T		IP3 sets of (T_c, γ_{T_c}) T_c : coolant temperature (°C) γ_{T_c} : coolant temperature coefficient ($/°C)

(23) Metal-Water Reaction Data BB22

(Not required if KROD=0 or if IQMW=0)
Number of subblocks = number of rod type subgroups, each of which has the same values forthe following data ($\leqq KROD$)

1-I	NN	Number of IDROD's (Input by a single card.)
2-I		$IDROD_1$ (Input by a single card.) $IDROD_2$: : $IDROD_{NN}$
3-R	Δh_{reac}	Heat of metal-water reaction (kcal/kg)
4-R	k_1	Coefficient of Eq.(3-1-13) (m^2/sec)
5-R	k_2	Coefficient of Eq.(3-1-13) (°k)
6-R	$(l^{out}, l^{in})_1$	
	:	
	:	from upstream to downstream
	:	
	$(l^{out}, l^{in})_{NCORE}$	

Note ; l^{out}= initial thickness of zircaloy reacted at outer surface (m)
and
l^{in} = initial thickness of zircaloy reacted at inner surface (m) .

(24) Fuel Gap Data BB23

(Not required if KROD=0)

Number of subblocks = number of rod type subgroups, each of which has the same values for the following data (≦KROD)

1-I	NN	Number of IDROD's (Input by a single card.)
2-I		$IDROD_1$ (Input by a single card.)
		$IDROD_2$
		:
		:
		$IDROD_{NN}$
3-R	N	Mols of gas in pin
4-R	p_{gc}	Contact pressure (ata)
5-R	$r_{gap}(0)$	Initial gap width (m)
6-R	V_{pe}	Plenum gas volume (m^3)
7-R	V_{opr}	Open porosity volume (m^3)
8-R	V_{cr}	Chip and roughness volume (m^3)
9-R	$V_{cd}(0)$	Initial clad and dish volume (m^3)
10-R	C_T	Constant in Eq.(3-3-29) (°C)
11-R	ε_{NF}	Fuel pellet emissivity (-)
12-R	ε_{cl}	Fuel clad emissivity (-)
13-R	FRASM	Mean free path (m)
14-R	η_{He}	Mol fraction of H_e (-)
15-R	η_{Xe}	Mol fraction of X_e (-)
16-R	η_{Kr}	Mol Fraction of K_r (-)
17-R	η_{air}	Mol fraction of air (-)
18-R	η_{N_2}	Mol fraction of N_2 (-)
19-R	η_{H_2}	Mol fraction of H_2 (-)
20-R	η_{H_2O}	Mol fraction of H_2O (-)

(25) Clad Burst Description Data BB24

(Not required if KROD=0)

Number of subblocks = number of rod type subgroups, each of which has the same values for the following data (≦KROD)

1-I	NN	Number of IDROD's (Input by a single card.)
2-I		$IDROD_1$ (Input by a single card.)
		$IDROD_2$
		:
		:
		$IDROD_{NN}$
3-I	N_j	Number of non-burst digonal rods in 3 x 3 matrix
4-I	M_j	Number of non-burst off-diagonal rods in 3 x 3 matrix
5-I	A	
6-R	B	
7-R	C	Coefficient of Eq.(4-1-11)
8-R	D	Coefficient of Eq.(4-1-11)
9-R	E	Coefficient of Eq.(4-1-11)
10-R	A_0	

11-R	A_1	
12-R	A_2	Coefficients of Eq.(4-1-14)
13-R	A_3	
14-R	A_4	
15-R	A	Coefficients of Eq.(4-1-13)
16-R	B	
17-R	S_{burst}	Threshold strain for burst (-) $(0.0 < S_{burst} < 1.0)$
18-R	BLM	Minimum blockage ratio (-) due to rod burst

(26) Heat Conductor Data BB26

Group the heat conductors so that each group has the same input values fo data 3 to 16. For each group, NSB1 is the first conductor number, while NSB2 is the last.

1-I	NSB1	Conductor number $(1 \leqq NSB1 \leqq NSLB)$
2-I	NSB2	Conductor number (NSB2=0 or $NSB1 \leqq NSB2 \leqq NSLB$)
3-I	KGEO	Geometric type 1 = rectangular 2 = cylindrical 3 = spherical
4-I	KSLB	Conductor category 0 = ordinary 1 = fuel 2 = heat exchanger conductor to couple two different hydraulic nets or a net and a heat sink.
5-I	NSLB	Number of conductors
6-I	NRGN	Number of regions For a fuel slab with gap, NRGN=2 only is acceptable.
7-R	r_{in}	Inner radius or width (m)
8-R	r_{out}	Outer radius or thickness (m)
9-R	T_{sink}	Sink temperature (°C) Effective when N_L= -1 or N_R= -1. Otherwise, arbitrary.
10-R	ε	Emissivity (-) Effective when N_L= -1 or N_R= -1. Otherwise, arbitrary.
11-R	DEG1	Angle (°) : φ for KGEO=2 and θ_1 for KGEO=3 = 360° if 0.0 is inputted for KGEO =2.

Input region-wise NRGN sets for data 12 to 16.

12-I	IDRGN	Region number (Numbering of regions should be started from inside/left
13-I	IM	Material number >0 : Material number (see BB27) -1 = UO_2 (Use built-in table) -2 = Zircaloy (Use built-in table)
14-I	IMESH	Number of meshes
15-I	IPC	CSSM ID number for relative power calculation 0 = Do not use CSSM (internal calculation).
16-R	WDTH	Region thickness (m)

Input (NSB2-NSB1+1) sets for data 17 to 25.

17-I N_L Coolant node number at inner or left side of conductor
=0 : adiabatic at inner/left side of conductor
=-1 : constant sink temperature at inner/left side of conductor

18-I N_R Coolant node number at outer or right side of conductor
=0 : adiabatic at outer/right side of conductor
=-1 : constant sink temperure at outer/right side of conductor

19-I KPL Option flag for position of slab w.r.t flow
0 = parallel to flow at node N_L
1 = perpendicular to flow at node N_L

20-I KPR Option flag for position of slab w.r.t flow
0 = parallel to flow at node N_R
1 = perpendicular to flow at node N_R

21-R SLEN Conductor length parallel to flow (m) for KGEO ≠ 3
DEG2 Angle θ_2 (°) ($\theta_1 > \theta_2$) for KGEO=3

22-R HTRCV (1) Initial convective heat transfer coefficient at inner/left side for $N_L = -1$ (kcal/m^2/^{0}C/s)
(2) Initial convective heat transfer coefficient at outer/right side for $N_R = -1$ (kcal/m^2/^{0}C/s)
(3) A dummy otherwise

23-R XLX Elevation (>0) between conductor center and wall top where condensation film starts.
(to be used in the calculation of heat transfer coefficient for filmwise condensation)

NRGN sets of the following data must be inputted in order of the regions.

24-R RQ0 Initial power density (kcal/sec/m^3)
0.0 for the most-upstream or most-downstream fuel slab

25-R RQR Rated power density (kcal/sec/m^3)
(To be used as the reference power in case of IPC ≠0 with zero initial power density.)

(27) Heat Conductor Material Property Tables BB27
Number of subblocks = NMAT

1-I MAT Material ID number
2-A Material name (in less than 72 characters)
3-I IP1 Number of points
4-T IP1 sets of (T,ρ)
T : temperature (^{o}C)
ρ : density (kg/m^3)
5-I IP2 Number of points
6-T IP2 sets of (T,C_p)
T : temperature (^{o}C)
C_p : specific heat (kcal/kg/^{o}C)
7-I IP3 Number of points
8-T IP3 sets of (T,λ)
T : temperature (^{o}C)
λ : heat conductivity (kcal/m/sec/^{o}C)

(28) Moisture Separator Data BB28

Number of subblocks = NSEP

1-I	JSEP	Junction number (1≦JSEP≦NJUNC)
2-I	N_{MIX}	Number of to-node (saturated mixture) (1≦NMIX≦NLOOP)
3-I	N_{FS}	Number of to-node (saturated water) (1≦NFS≦NLOOP)
4-R	τ_B	Time constant for separation efficiency (sec)

(29) Valve Data BB29

Number of subblocks = NVLV

Note :(1) A valve can be placed only at E point of a normal node.
(2) Neither a trip input nor a control input is required for a check valve.
(3) For a G-source boundary junction(IFPT=1), placing a control valve (IVTYP= ±2) with TRIP (IDTRP=4) or control IDCV is equivalent to inputting the corresponding operator for IDC in BB13.

1-I	IVLV	Valve number (1≦*IVLV*≦*NVLV*)
2-I	IVTYP	Valve type 1 = check valve, initially opened and to be opened for a forward flow -1 = check valve, initially closed and to be opened for a reverse flow 2 = control valve, initially open -2 = control valve, initially closed
3-I	NDV	Number of node where the valve is located
4-I	IDCV	CSSM ID number for calculation of valve opening $A(t)/A_{opn}$ (<1) only for IVTYP = ± 2) 0 = no control (either complete opening or complete closing with time lag)
5-R	TAUOPN	Time constant of opening by TRIP (sec) = 0.1 when zero is inputted (dummy for IDCV ≠0)
6-R	TAUCLS	Time constant of closing by TRIP (sec) = 1.0 when zero is inputted (dummy for IDCV ≠0)

(30) Logical Condition Data BB30

Number of subblocks = MTRP

Logical condition is evaluated by

$$X \quad op \quad (Y + R) \qquad (8\text{-}4\text{-}1)$$

where X, Y, R are specified by (IX1,IX2), (IY1,IY2) and RR (or IRR), respectively, while the operator op is given such that

op = .GT. for $1 \leqq IDSIG \leqq 8$
.LT. for $-8 \leqq IDSIG \leqq -1$
.AND. for IDSIG = 9
.OR. for IDSIG =-9

But, for IDISG = 0, we consider instead of Eq.(8-4-1)

$$0 \quad op \quad R \qquad (8\text{-}4\text{-}2)$$

where

op = .GT. for IX1 = 0
.LT. for IX1 = 1 .

In other words, both X and Y must vanish for IDSIG = 0.

Note :

(1) For $|IDSIG| \neq 5, 6$, the minor edit symbol is available so that a logical condition (8-4-1) reduces to IDSIG=0 such that

$$0 \quad op \quad R' \qquad (8\text{-}4\text{-}3)$$

where

$R' = Y+R-X$.

(2) A logical condition inputted in this data block will be used to define an on- or off-condition in TRIP (BB04) or a condition of operator IF in CSSM (BB31).

1-I IDT — Logical condition ID number
($1 \leqq IDT \leqq 32767$)
Input with a minus sign if R is to be calculated. by CSSM.

2-I IDSIG — Identification of dimension of X, Y and R
($-9 \leqq IDSIG \leqq 9$)
= 0 : arbitrary (R calculated by CSSM)
=±1 : time (sec)
=±2 : coolant pressure (ata)
=±3 : coolant temperature(°C)
=±4 : normalized reactor power(-)
=±5 : rector period (sec)
=±6 : liquid level (m)
=±7 : heat conductor temperature (°C)
=±8 : coolant mass flux (kg/sec/m^2)
=±9 : logical trip

3-I IX1 — See Table 8-2.

4-I IX2 — =mesh number for IDSIG=±7
=0 otherwise

5-I IY1 — See Table 8-2.

6-I IY2 — =mesh number for IDSIG=±7
=0 otherwise

Input the following on a new line.

7-R RR — (1) Setpoint for signal IDSIG if positive IDT is inputted. (same unit as for IDSIG)

or — (2) Set 0.0 for IDSIG = ± 9 .

7-I IRR Control ID number to calculate setpoint when IDT < 0.

Table 8-2 IDSIG, IX1 and IY1

ABS(IDSIG)	IX1	IY1
0	1 if op = LT (R>0) 0 if op = GT (R<0)	0
1	0	0
2	node number	node number or 0
3	node number	node number or 0
4	0	0
5	0	0
6	accumulator number	accumulator number or 0
7	heat conductor number	heat conductor number or 0
8	node number	node number or 0
9	logical cond. number	logical cond. number

(31) CSSM Data BB31

Number of subblocks = NCI + NCB

Note :

(1) NCI sets of data 1 to 4 should be inputted to form control inputs subblocks SB3101 - SB(3100+NCI).

(2) For each series of control blocks, the corresponding control control block ID numbers must be strictly in order of the operations.

(3) For the detail of this data block, refer to Appendix D.

1-A4 CSYM Symbol of control input
= Minor edit symbol for minor edit variable
= TIME for time
= TRIP for trip
TRIP= (0.0, 1.0) for (trip-on, trip-off), respectively.
= TRTM for elapsed time after trip condition has been satisfied
TRTM=0.0 before trip initiation.
(Note: Delay time for trip actuation is ignored.)
= CONS for constant

2-I IDC Control input ID number (IDC≦0)
(Number must be unique in this block)

3-I IREG Region number
= 0 for TIME and CONS
= trip control ID number (BB04) for TRIP or TRTM
= node number for minor edit node data
(set 1 for reactor power)
= junction number for minor edit junction data
= machine number for minor edit hydraulic machine data
= machine shaft number for minor edit of hydraulic machine shaft speed
= accumulator number for minor edit accumulator data
= conductor number for minor edit heat conductor data

4-R Gain Input multiplier
For CONS, this value is treated as the input itself.
For TIME and TRTM, this value is ignored.

NCB sets of the following data must be inputted as subblocks SB (3101+NCI+NO), SB(3102+NCI+NO),....., and SB(3100+NCB+NCI+NO) without a jump, where NO is a positive interger. For each series of control blocks, they must be inputted strictly in order of the control operations.

1-A3 ITYPE Control block type
= MUL : Multiplier
= DIV : Divider
= SUM : Weighted summer
= XPO : Exponentiation
= LN : Natural logarithm
= ABS : Absolute value
= MAX : Maximum
= MIN : Minimum
= VLM : Velocity limiter
= DER : Differentiator
= INT : Integrator
= EXT : Extrapolator
= FNG : Function generator
= FGT : FNG by time table
= DLY : Time delay
= LAG : Lag conpensation
= LLG : Lead-lag compensation
= IF : Logical-if controller
= TIF : Trip-if controller
= OUT : Output

2-I IDC Control block ID number (0<IDC)
(Number must be unique in this block)

3-I INC1 Control block input (1)
=control input ID number or other control block ID number
=0 for ITYPE=FGT

4-I INC2 Control block input (2)
=control input ID number or other control block ID number for ITYPE=MUL,DIV,SUM,XPO,MAX,MIN,IF,TIF
=control table ID number (BB32) for ITYPE=FNG,FGT
=time step interval for print out for ITYPE=OUT
(=0 for same frequency as minor edit)
=0 for otherwise

5-I INC3 Control block input (3)
=number of samplings for ITYPE = DLY
=trip-on condition ID number (BB30) for ITYPE=IF
=trip control ID number (BB04) for ITYPE=TIF
=0 otherwise

6-I INC4 Control block input (4)
=ID number (IDC) of control input which decides initial value of control block output
=0 if specified by CIC
=0 if ITYPE = OUT

7-R Gain Control block output multiplier
= 0.0 for ITYPE = OUT

8-R CP1 Control block parameter (1)

=weighting factor g_1 for ITYPE=SUM
=maximum output velocity V_{up} for ITYPE=VLM
=sampling time T for ITYPE=DLY
=lead time constant τ_1 for ITYPE=LLG
=0.0 otherwise

9-R CP2 Control block parameter (2)
=weighting factor g_2 for ITYPE=SUM
=maximum output velocity V_{down} for ITYPE=VLM
=lead time constant τ_2 for ITYPE=LLG and LAG
=0.0 otherwise

10-R CIC Initial value of control block output
= 0.0 for ITYPE = OUT
(This input is ignored if INC4 ≠ 0 .)

11-R CMIN Minimum for control block output
= 0.0 for ITYPE = OUT

12-R CMAX Maximum for control block output
= 0.0 for ITYPE = OUT

(32) CSSM-related Table Data BB32

Number of subblocks = NCTBL

1-A40 CTBL Comment on table
2-I MTBL Table ID number
3-I NPI Number of points
4-T NPI sets of (X,Y)
X : independent variable
Y : dependent variable

(33) Dump Control Data BB00

This data block must be placed after the BEND card.

1-I NCLL Dumping index of flow network iteration
0 = no dumping
-1 = Dumping starts at time step NCSTEP.

2-I NCSTEP Time step number when dumping of network iteration star

3-I NXDMP Numer of groups of array dumping

8.5 Input Data for Restarting Job

An old restart data file to be used must be mounted on FORTRAN Unit 3 and a blank on Unit 2. A new plotter file will be generated on Unit 50. There are two methods to control creation of restart file, i.e., by specifying (1) one of ICLASS, LSEC, IDPSTP and DMPTM in BB01 or (2) NDMP in BB03. Input data specifications for a restarted run are given in the

following. The other data need not be inputted except the dump control data block BB00 and the BEND card.

Probelm Control Data BB01 :

LDMP = a positive integer

NTRP must be equal to be the value at the previous run.

The others can be changed.

Minor Edit variable Data BB02 :

The quantities being edited on the new run need not have any relation to those of the original run. The same rules apply as for the original problem.

Time Step Width Control Sequence Data BB03 :

TLAST must be greater than the time at which the present run satrts. The same rules as for the original problem apply to the rest of the variables.

Trip Control Data BB04 :

Data block BB04 must not be changed only with the following exception. For the sub-block corresponding to IDTRP = 1, the value for SETPT must be greater than that of the previous run.

Delay Constant Data BB05 :

Data block BB05 can be changed.

EM Option Data BB06 :

This data block is not required for a BE calculation.

9. *Execution of THYDE-W Job*

The following data sets are reguired to perform a THYDE-W calculation. The relationship among these data sets are shown in Fig.9-1-1.

input data sets
- FT30F001 : steam table of H_2O for high pressure
- FT31F001 : steam table of H_2O for low pressure
- FT32F001 : steam table of D_2O
- FT03F001 : restart data
- FT12F001 : input data

output data sets
- FT02F001 : data for next restart
- FT06F001 : data for ordinary FORTRAN output
- FT08F001 : data for compiled output
- FT09F001 : data for debugging output
- FT10F001 : data for restart at the latest major edit in case of abnormal ending
- FT20F001 : data for output of input data
- FT50F001 : data for plotter

When a THYDE-W calculation is started from an initial state, all the data described in section 8.4 are required with LDMP = 0 in BB01 (see subsection 8.4.2) and with a dummy data set FT03F001. When a THYDE-W calculation is restarted from a restart dump point in a previous run, all the data in section 8.4 is not required. Input data requirements for a restart are described in section 8.5.

Restart dump fequency can be controlled by NDMP in BB03 (see subsection 8.4.4). In addition, a restart dump is also made, when ICLASS or IDPSTP or DMPTM in problem control Data block BB01 (see subsection 8.4.2) is specified. The restart dump is made on FORTRAN Unit 2 in case of normal ending. To back up the cases when the run stops abnormally, the restart data at the latest major edit is stored in FORTRAN Unit 10 with LDMP = 1.

Control cards for execution is computer system dependent so that they will not be discussed in detail. Tables 9-1 to 9-3 show examples of control cards.

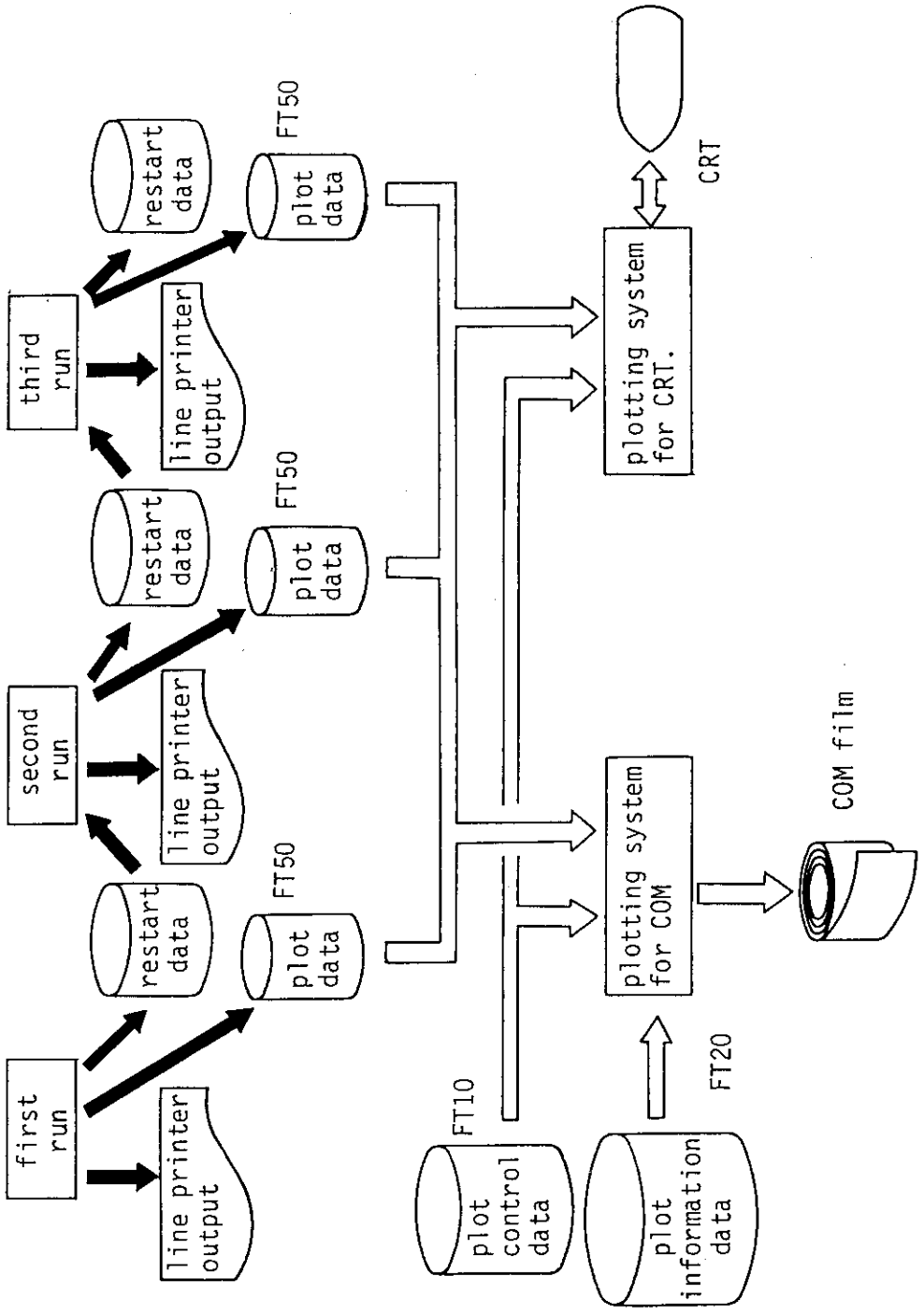

Fig. 9－1－1 Data Flow of THYDE-W Runs

Table 9-1 Control Cards for Compile of Source J2937.W.FORT77, Linkage with Load Module J2937.A.LOAD and Execution for a First Run

```
00010    //JCLG JOB
00020    //JCLG EXEC JCLG
00030    //SYSIN DD DATA,DLM='++'
00040    // JUSER   23282937,ASAHI.YOSHIR,0431.01,THYDE.W
00050     T.6W.4 I.4 C.5 E.0 SRP
00060     OPTP PASSWORD= ,CLASS=0,MSGLEVEL=(1,1,1)
00070    // EXEC FORT77VP,SO='J2937.W',Q='.FORT77',
00080    // A='NOSOURCE,NOVS,NOVMSG,ELM(*),ALIGNC',
00090    // OBJS='300,10',DISP=NEW
00100    //SYSINC    DD DSN=J2937.A.INC.FORT77,DISP=SHR
00110    // EXEC LKEDIT,LM='J2937.A'
00120    // EXEC GOA
00130    //FT06F001 DD SYSOUT=*,
00135    //            DCB=(RECFM=FBA,LRECL=137,BLKSIZE=19043)
00140    //SYSPRINT DD SYSOUT=*
00150    //SYSIN DD DUMMY
00160    // EXPAND DISKTO,DDN=FT12F001,DSN='J2937.RUNDATA',
00160    //        Q='.DATA(IRIS)'
00190    //  EXPAND DISKTO,DDN=FT30F001,
00195    //         DSN='J2937.NSK.J3149.ALMST4.CONVERT',Q='.DATA'
00210    //  EXPAND DISKTO,DDN=FT31F001,
00220    //         DSN='J2937.NSK.JR3N18.NEWSTEAM.CONVERT',Q='.DATA
00230    //  EXPAND DISKTO,DDN=FT32F001,
00240    //         DSN='J2937.NSK4.NEW2.STMD2O',Q='.DATA'
00250    //FT08F001 DD SYSOUT=*,DCB=(RECFM=FBA,LRECL=137,BLKSIZE=274)
00260    //FT20F001 DD SYSOUT=*,DCB=(RECFM=FBA,LRECL=137,BLKSIZE=274)
00270    //FT09F001 DD DUMMY
00280    //FT10F001 DD DUMMY
00290    //FT60F001 DD DUMMY
00300    //*
00310    //FT03F001 DD DUMMY
00320    //    EXPAND DISKTO,DDN=FT02F001,DSN='J2937.R1',Q='.DATA'
00330    //    EXPAND DISKTO,DDN=FT50F001,DSN='J2937.P1',Q='.DATA'
00340    //
00350      ++
00360    //
```

Table 9-2 Control Cards for Execution of a First Run by Load Load Module J2937.A.LOAD

```
0010  //JCLG JOB
0020  //JCLG EXEC JCLG
0030  //SYSIN DD DATA,DLM='++'
0040  // JUSER   23282937,ASAHI.YOSHIR,0431.01,THYDE.W
0050   T.7 W.4 I.5 C.5
0060   OPTP PASSWORD= ,CLASS=3,NOTIFY=J2937
0070  //VP EXEC SYSA.
0080  //GO EXEC LMGOA,PNM=TEMPNAME,LM=J2937.A
0090  //FT06F001 DD SYSOUT=*,DCB=(RECFM=FBA,LRECL=137,BLKSIZE=274)
0100  //SYSPRINT DD SYSOUT=*
0110  //SYSIN DD DUMMY
0130  //*
0140  //*************** INPUT DATA FILE *********************************
0130  //*
0160  //  EXPAND DISKTO,DDN=FT12F001,DSN='J2937.RUNDATA',
0170  //         Q='.DATA(JRR3)'
0190  //*
0200  //*************** STEAM TABL ***************************************
0190  //*
0230  //  EXPAND DISKTO,DDN=FT30F001,
0240  //         DSN='J2937.NSK.J3149.ALMST4.CONVERT',Q='.DATA'
0250  //  EXPAND DISKTO,DDN=FT31F001,
0260  //         DSN='J2937.NSK.JR3N18.NEWSTEAM.CONVERT',Q='.DATA'
0270  //  EXPAND DISKTO,DDN=FT32F001,
0280  //         DSN='J2937.NSK4.NEW2.STMD2O',Q='.DATA'
0290  //*
0300  //*************** DATA SET TO PRINT OUT INPUT DATA  ************
0310  //*
0320  //FT20F001 DD DUMMY
0330  //*FT20F001 DD SYSOUT=*,DCB=(RECFM=VBA,LRECL=137,BLKSIZE=3164)
0350  //*
0360  //*************** OUTPUT LIST **************************************
0370  //*
0390  //FT08F001 DD SYSOUT=*,DCB=(RECFM=VBA,LRECL=150,BLKSIZE=3164)
0400  //FT09F001 DD DUMMY
0410  //FT10F001 DD DUMMY
0420  //*
0430  //*************** DATA SET FOR RESTART *************************
0440  //*
0460  //FT03F001 DD DUMMY
0470  //*
0480  //*************** DATA SET FOR RESTART DUMP ********************
0490  //*
0500  //  EXPAND DISKTO,DDN=FT02F001,DSN='J2937.R1',Q='.DATA'
0520  //*
0530  //*************** DATA SET FOR PLOT DATA OUTPUT  ***************
0540  //*
0550  //  EXPAND DISKTO,DDN=FT50F001,DSN='J2937.P1',Q='.DATA'
0580  ++
0590  //
```

Table 9-3 Control Cards for Execution of a Restarted Run by Load Module J2937.A.LOAD

```
0010  //JCLG JOB
0020  //JCLG EXEC JCLG
0030  //SYSIN DD DATA,DLM='++'
0040  // JUSER   23282937,ASAHI.YOSHIR,0431.01,THYDE.W
0050   T.7 W.4 I.5 C.5
0060   OPTP PASSWORD= ,CLASS=3,NOTIFY=J2937
0070  //VP EXEC SYSA
0080  //GO EXEC LMGOA,PNM=TEMPNAME,LM=J2937.A
0090  //FT06F001 DD SYSOUT=*,DCB=(RECFM=FBA,LRECL=137,BLKSIZE=274)
0100  //SYSPRINT DD SYSOUT=*
0110  //SYSIN DD DUMMY
0130  //*
0140  //**************** INPUT DATA FILE *******************************
0150  //*
0160  //  EXPAND DISKTO,DDN=FT12F001,DSN='J2937.RUNDATA',
0170  //         Q='.DATA(JRR3R)'
0190  //*
0200  //**************** STEAM TABL ************************************
0210  //*
0230  //  EXPAND DISKTO,DDN=FT30F001,
0240  //         DSN='J2937.NSK.J3149.ALMST4.CONVERT',Q='.DATA'
0250  //  EXPAND DISKTO,DDN=FT31F001,
0260  //         DSN='J2937.NSK.JR3N18.NEWSTEAM.CONVERT',Q='.DATA'
0270  //  EXPAND DISKTO,DDN=FT32F001,
0280  //         DSN='J2937.NSK4.NEW2.STMD2O',Q='.DATA'
0290  //*
0300  //**************** DATA SET TO PRINT OUT INPUT DATA  ************
0310  //*
0320  //FT20F001 DD DUMMY
0330  //*FT20F001 DD SYSOUT=*,DCB=(RECFM=VBA,LRECL=137,BLKSIZE=3164)
0350  //*
0360  //**************** OUTPUT LIST ***********************************
0370  //*
0390  //FT08F001 DD SYSOUT=*,DCB=(RECFM=VBA,LRECL=150,BLKSIZE=3164)
0400  //FT09F001 DD DUMMY
0410  //FT10F001 DD DUMMY
0420  //*
0430  //**************** DATA SET FOR RESTART **************************
0440  //*
0450  //  EXPAND DISKTO,DDN=FT03F001,DSN='J2937.R1',Q='.DATA'
0470  //*
0480  //**************** DATA SET FOR RESTART DUMP *********************
0490  //*
0500  //  EXPAND DISKTO,DDN=FT02F001,DSN='J2937.R2',Q='.DATA'
0520  //*
0530  //**************** DATA SET FOR PLOT DATA OUTPUT  ****************
0540  //*
0550  //  EXPAND DISKTO,DDN=FT50F001,DSN='J2937.P2',Q='.DATA'
0580  ++
0590  //
```

10. Output Specifications

10.1 Output Listing

The format of the output listing of THYDE-W is shown in Fig.10-1-1. Figure 10-1-2 shows the message which will be printed out when a need for time step width control occurs . When the module where this need occurred is TRPGH, the number AYYY indicated by* in Fig.10-1-3 has the following meaning.

A = 3 : TSWC due to pressure change at node YYY

4 : TSWC due to mass flux change at node YYY

5 : TSWC due to low pressure (≦ 1 atm) at node YYY

first job	restarted job
JCL	JCL
FT06F001	FT06F001
system messages	system messages
FT08F001	FT08F001
(1) output of editted input data	(1) output of editted input data
(2) output of steady state calculation	(2) output of transient calculation
(3) output of transient calculation	
FT20F001	FT20F001
output of input data	output of input data

Fig.10-1-1 Format of Output Listing

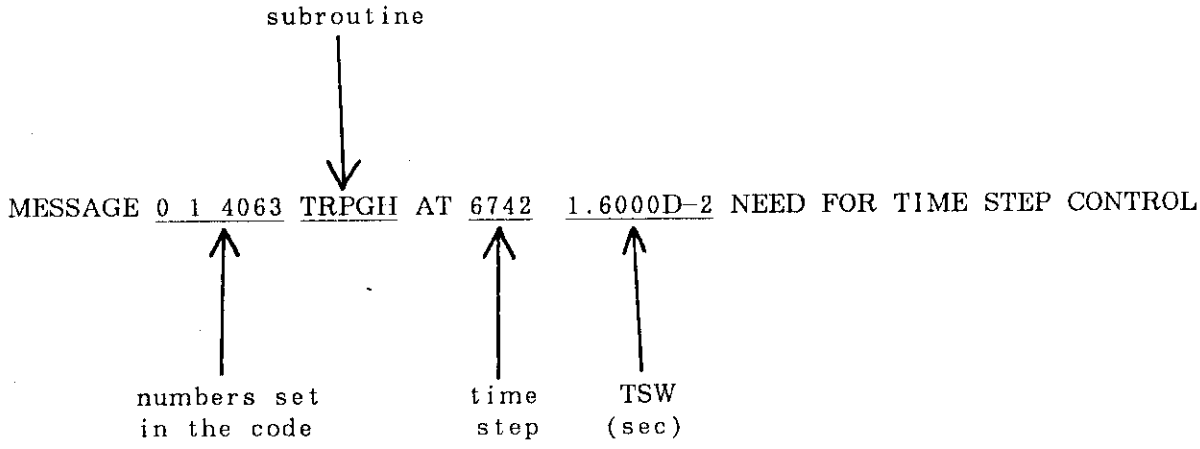

Fig. 10-1-2 Message of Time Step Width Control

10.2 THYDE-W Plotting System

The THYDE-W plotting system can depict results of THYDE-W by compiling data sets generated in a series of THYDE-W jobs. Data for the THYDE-W plotting system are stored in a data set defined by FT50F001 with the same frequency as for minor edits controlled by NMIN in BB03 (see subsection 8.4.4) during execution of a THYDE-W job. Figure 10-2-1 shows relationship between execution of THYDE-W jobs and generation of plot data.

Figure 10-2-2 shows relationship between the plotting system and the required input data sets. In the following, each of the data sets will be explained.

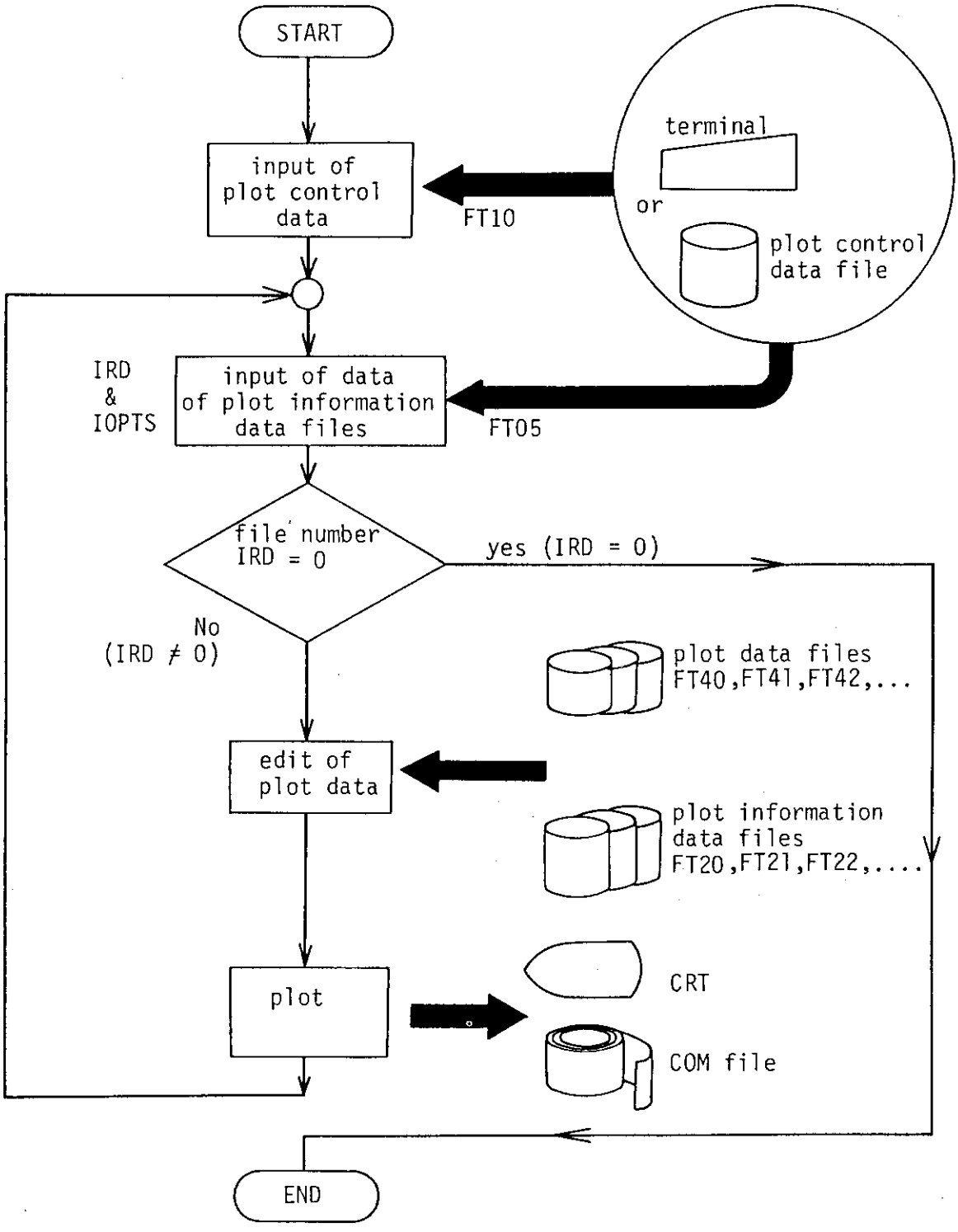

Fig. 10-2-1 Relationship between THYDE-W Execution and Plot Data

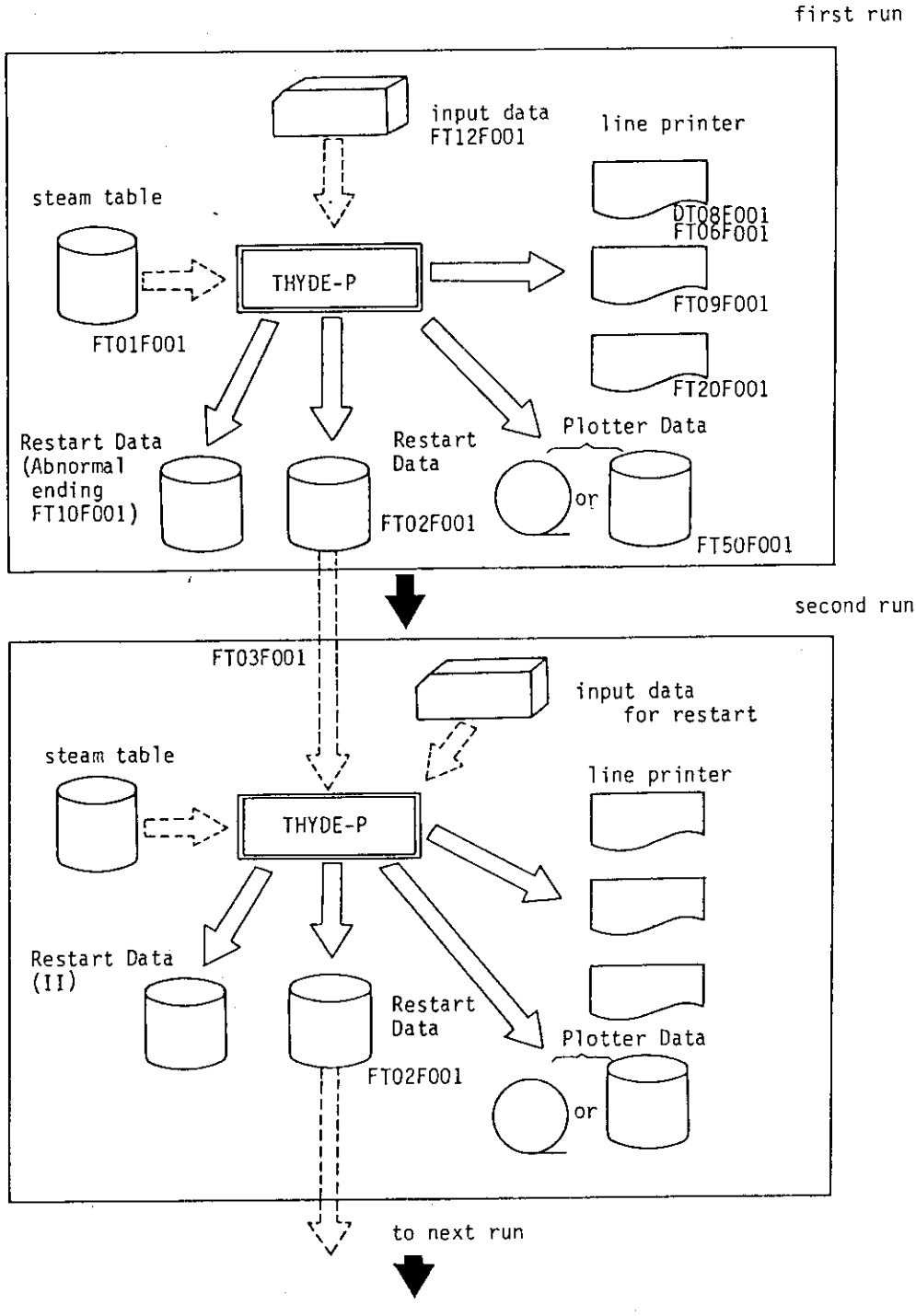

Fig. 10-2-2 Flow Chart of Plotting System

(1) Plot Control Data (to be inputted by FORTRAN Unit 10)

1-A	KTITLE	Title to be printed on top of each figure
2-(A,I)	(FEND, IXTIN)	
	FEND :	Number of plot data sets (1≦FEND)
	IXTIN :	Flag for editting plot data sets 0= When time spans of two data sets overlap, the data set for the earlier period overrides the other. 1= For each data set, the data in the period specified by additional inputs as indicated next are used.
2a-(R,R)	(TIMI, TIM2)	Not required for IXTIN=0. FEND pairs should be inputted. For each data set, the data in the period (TIMI, TIM2) are used.
3-(R,R)	(TIMES,TIMEE)	
	TIMES :	The smallest time of the abscissa(sec)
	TIMEE :	The largest time of the abscissa (sec)
4-I	IFLAG5	Flag for setting origin and scale (Not required for COM film outputting) 0= Use the default values shown in Appendix C : origin of abscissa = 0 for TYPE = 1 origin of ordinate = 0 for TYPE = 1 scale = 0.8 1= Origin of abscissa, origin of ordinate and scale should be inputted in order.

(2) Data of Plot Information Data Sets (to the inputted by FORTRAN Unit 5)

1-(I, I)	(IRD, IOPTS)	
	IRD	Number of the file unit which contains plot information data (20≦IRD) (Refer to next subsection.)
	IOPTS	Flag to classify plot information file 0= use index to select the valuables to be plotted. 1= mannual setting

(3) Plot Information Data (to be inputted by FORTRAN Unit 20, 21, 22 etc.)

The data specifies what is to be plotted among the variables contained in the plot data sets. In the following, only the case when IOPTS = 0 will be described. In this case, only the same kinds of variables can be plotted in a figure. Table 10-1 shows an example of plot information data.

1-I	IPLNO	Number of curves to be plotted in the figure ($1 \leqq IPLNO \leqq 20$)
2-I	IAXTY	1 = Give the minimum and maximum values of the oridnate. 0 = Use default values for each variable (see Appendix C)
2a - (R, R)	(YM1,YM2)	Give when IAXTY = 1. YM1 : Maximum value YM2 : Minimum value
3 - A	Title	Title of figure
4 - A	ITAX	Give within a single line IPLNO variables to be plotted with a blank between each pair. The variables must be represented by the symbols with an index as shown in Appendix C.

(4) Output to Cathod Ray Tube (T4014 or T4006)

Graphic display output of THYDE-W results can be made by source file TXPLOT.FORT. In the following, the method to use command procedure TXPLOT (see Table 10-2) will be described.

Before TXPLOT is actuated, plot data sets FT40F001, F41F001, ... and plot information data sets FT20F001, FT21F001, ... have to be allocated. When TXPLOT is actuated, FT05F001, and F10F001 are automatically allocated to the graphic display terminal. The former is to be used to give the data of the plot information data sets, while the latter the plot control data.

Table 10-1 Example of Plot Information Data

```
010   2    1
020   2.5E3   -2.5E3
030   CVCS FLOWS
040   GLE-037 GLE-038
050   1    1
060   1.       -1.
070   TOTAL REACTIVITY
080   RTT-001
090   1    1
100   1.2   0.
110   POWER
120   QCR-001
130   2    1
140   330.   280.
150   CORE INLET AND OUTLET TMPS
160   TMP-001   TMP-012
170   1    1
180   1.E3      0.
190   TURBINE BYPASS FLOW
200   GLE-071
210   2    1
220   3.E3   0.
230   FUEL TEMP (SLAB8)
240   TC1-008 TS1-008
250   1    1
260   1.01   0.99
270   MCP SPEED
280   AAA-001
290   2    1
300   1.6E7 4.E6
310   STEAM DOME AND MS PRESSURES
320   PRE-032   PRA-071
330   1    1
340   1.E5    0.
350   PRIMARY RELIEF FLOW
360   GLE-045
410   1    1
420   1.    -1.
430   CORE EXIT QUALITY
440   XLA-022
450   2    1
460   0.5      -0.5
470   BORON & DENSITY  REACTIVITIES
480   RBR-001   RRH-001
490   0  0
```

Numbers 2 and 1 in line 10 show that IPLNO and IAXTY are 2 and 1, respectively. Numbers 0 and 0 in line 490 indicate END of DATA.

Table 10-2 Command Procedure TXPLOT

```
00010  PROC 0
00020  CONTROL NOMSG FLUSH
00030  WRITE **** ENTER THYDEP PLOTTING SYSTEM (& SYSDATE & SYSTIME
00040  DELETE TEMP.OBJ
00050  FREE F(FT10F001)
00060  FREE F(FT06F001)
00070  FREE F(FT05F001)
00080  FREE AT(TY)
00220  LIB 'SYS9.PTS.LOAD'
00230  ATTR TY BLKSIZE(144) RECFM(UA)
00370  FREE AT(F10)
00380  ATTR F10 BLKSIZE(80) LRECL(80) RECFM(F)
00390  ALLOC DA(*) F(FT10F001) USING(F10)
00400  ALLOC DA(*) F(FT85F001)
00410  ALLOC DA(*) F(FT06F001) USING(TY)
00420  ALLOC DA(*) F(FT05F001)
00430  ALLOC DA(TEMP.OBJ) F(SYSLIN) NEW
00440  FORTHE TXPLOT.FORT TERM NOPRINT OBJ(TEMP.OBJ) ELM(*) BYNAME
00450  WRITE **** END OF FORTRAN COND CODE=&LASTCC ****
00460  WRITE **** ENTER LOADGO PROCESS ****
00470  LOADGO (TEMP.OBJ) LIB('SYS9.PTS.LOAD') FORTLIB NOLIBDD SIZE(5
00480  DELETE TEMP.OBJ
00490  FREE F(FT10F001)
00590   WRITE **** END OF PLOTTING SYSTEM (& SYSDATE & SYSTIME) ****
00600   EXIT
```

In this command procedure, FT05F001, FT06F001 and FT10 are allocated for the terminal.

11. Sample Input Data Set and Sample Problem

In section 11.1, we discuss a sample input data set for the NSSS of a typical 4-loop 1,000 MWe PWR. The input data set, corresponding to nodalization shown in Fig. 2-3-1, is listed in Appendix E. The list may be interpreted with the help of chapter 8. The input data set can be used for various transients such as a LB-LOCA. In section 11.2, the calculated steady state is described. In section 11.3, the results of a sample calculation for a LB-LOCA will be presented.

11.1 Description of Sample Input Data

In Fig. 2-3-1, the 2-loop nodalization is shown for the NSSS of a typical 4-loop 1,000 MWe PWR. The left and right of the primary loop in Fig. 2-3-1 are called loop A and B, respectively. Loop B represents a single loop, where an external disturbance may be introduced, whereas loop A represents the other three loops. The pressurizer is placed in loop A. Each of loop A and B has one LPIS and one HPIS. For a LOCA, the break point will be placed somewhere in loop B, which then can be called the broken loop, while loop A will be called the intact loop. The secondary loops are likewise represented in Fig. 2-3-1, where those corresponding to primary loop A and B will be referred to as secondary loop A and B, respectively. Nodes 57 and 68 are PSSS's[54]. In the present work, however, we ignore them by letting their node length very small (= 1.0×10^{-9} m) and always closing fictitious valves 11 and 12 (see Table 11-3). The core was divided radially into two regions , i.e. one collection of "average" channels and the other of "hot" channels. Nodes 33, 39, 40 and 46 are non-heated.

One of the features of Fig. 2-3-1 is split downcomer noding, that

is, the downcomer annulus is divided azimuthally into two, the one which is two thirds connected to loop A and the other which is one third connected to loop B.

There are several items over which the sample input data set should be improved. For example, (1) structures are not adequately taken into account as heat conductors, (2) a reactor control logic is not included, (3) a turbine-condensor system is not included.

In Tables 11-1 to 11-13, the sample input data are described. In the following, CVCS, FW, PZR, MSIV, LPIS, HPIS, LPCI, HPCI, DC and HC stand for chemical volume and control system, feewdwater, pressurizer, main steam isolation valve, low pressure injection system, high pressure injection system, low pressure coolant injection, high pressure coolant injection, downcomer and heat conductor, respectively.

Table 11-1 Geometrical Data of Nodes

node no.	description	flow area A (m^2)	length L (m)	no of nodes
1	hot leg (loop B)	0.43	2.50	1
2	hot leg (loop B)	0.43	2.750	1
3	SG inlet plenum (loop B)	2.898	1.664	1
4	SG U-tube	3.017D-04	4.539	3382
5	SG U-tube	3.017D-04	4.539	3382
6	SG U-tube	3.017D-04	1.413	3382
7	SG U-tube	3.017D-04	1.413	3382
8	SG U-tube	3.017D-04	4.539	3382
9	SG U-tube	3.017D-04	4.539	3382
10	SG outlet plenum	2.898	1.664	1
11	crossover leg (loop B)	0.487	7.327	1
12	MCP (loop B)	0.1920	12.39	1
13	cold leg (loop B)	0.3830	0.144	1
14	cold leg (loop B)	0.3830	3.000	1
15	cold leg (loop B)	0.3830	3.144	1
16	hot leg (loop A)	0.430	2.500	3
17	hot leg (loop A)	0.430	2.750	3
18	SG inlet plenum	2.898	1.664	3
19	SG U-tube	3.017D-04	4.539	10146
20	SG U-tube	3.017D-04	4.539	10146
21	SG U-tube	3.017D-04	1.413	10146
22	SG U-tube	3.017D-04	1.413	10146
23	SG U-tube	3.017D-04	4.539	10146
24	SG U-tube	3.017D-04	4.539	10146
25	SG outlet plenum	2.898	1.664	3
26	crossover leg (loop A)	0.4870	7.327	3
27	MCP (loop A)	0.1920	12.39	3
28	cold leg (loop A)	0.3830	3.144	3
29	cold leg (loop A)	0.3830	3.144	3
30	downcomer top	0.7000	6.090	2
31	downcomer	1.860	4.577	1
32	lower plenum	3.645	6.100	1
33	core (average channel)	8.788D-05	0.11	50752
34	core (average channel)	8.788D-05	0.7320	50752
35	core (average channel)	8.788D-05	0.7320	50752
36	core (average channel)	8.788D-05	0.7320	50752
37	core (average channel)	8.788D-05	0.7320	50752
38	core (average channel)	8.788D-05	0.7320	50752
39	core (average channel)	8.788D-05	0.1100	50752
40	core (hot channel)	8.788D-05	0.1100	200
41	core (hot channel)	8.788D-05	0.7320	200
42	core (hot channel)	8.788D-05	0.7320	200
43	core (hot channel)	8.788D-05	0.7320	200
44	core (hot channel)	8.788D-05	0.7320	200
45	core (hot channel)	8.788D-05	0.7320	200
46	core (hot channel)	8.788D-05	0.1100	200

Table 11-1 Geometrical Data of Nodes (Continued)

node no.	description	flow area A (m^2)	length L (m)	no of nodes
47	core cross flow	9.080D-04	0.1	200
48	core bypass flow	1.7203	3.880	1
49	upper plenum	9.290	4.454	1
50	downcomer	6.200D-01	4.577	1
51	lower plenum	1.215	6.100	1
52	pressurizer	4.750	3.430	1
53	pressurizer	4.750	3.430	1
54	pressurizer	4.750	3.430	1
55	pressurizer surge line	6.160D-02	14.66	1
56	pressurizer surge line	6.160D-02	14.66	1
57	PSSS (loop B)	1.150	1.D-09	1
58	pressurizer spray line	5.940D-03	44.90	1
59	pressurizer spray line	5.940D-03	44.9	1
60	accumulator duct (loop A)	3.880D-02	50.	3
61	injection duct (loop A)	4.700D-02	10.	3
62	LPIS duct (loop A)	4.700D-02	10.	1
63	HPIS duct (loop A)	4.700D-02	10.	1
64	accumulator duct (loop B)	3.880D-02	50.	1
65	injection duct (loop B)	4.700D-02	10.	1
66	HPIS duct (loop B)	4.700D-02	10.	1
67	LPIS duct (loop B)	4.700D-02	10.	1
68	PSSS (loop A)	1.150	1.D-09	3
69	PORV line	1.840D-02	0.1	1
70	safety valve line	1.840D-02	0.1	1
71	CVCS bleed line	4.700D-02	10.	3
72	upper head	3.855	3.658	1
73	SG downcomer (loop A)	ak	10.45	3
74	SG riser (loop A)	6.4242	3.450	3
75	SG riser (loop A)	6.4242	3.450	3
76	SG riser (loop A)	6.4242	3.450	3
77	separator inlet (loop A)	6.4242	0.1	3
78	recirculation flow (loop A)	7.853D-01	1.	3
79	steam dome (loop A)	8.7615	6.770	3
80	steam line (loop A)	4.560D-01	126.7	3
81	steam line (loop A)	1.3705	5.151	3
82	SG downcomer (loop B)	1.0568	10.45	1
83	SG riser (loop B)	6.4242	3.450	1
84	SG riser (loop B)	6.4242	3.450	1
85	SG riser (loop B)	6.4242	3.450	1
86	separator inlet (loop B)	6.4242	0.1	1
87	recirculation flow (loop B)	7.853D-01	1.	1
88	steam dome (loop B)	8.7615	6.770	1
89	steam line (loop B)	4.560D-01	126.7	1
90	steam line (loop B)	1.3705	5.151	1
91	main feedwater (loop B)	9.2903D-01	10.	1
92	main feedwater (loop A)	9.2903D-01	10.	3

Table 11-1 Geometrical Data of Nodes (Continued)

node no.	description	flow area A (m^2)	length L (m)	no of nodes
93	2ndry safety valve line	0.0184	0.1	3
94	2ndry relief valve line	0.0184	0.1	15
95	2ndry relief valve line	0.0184	0.1	5
96	2ndry safety valve line	0.0184	0.1	1
97	aux. FW line (loop B)	0.1	0.1	1
98	aux. FW line (loop A)	0.1	0.1	3
99	main steam line	1.3936	76.250	1

Table 11-2 Mixing Junction Data

Junc No.	description	to-node (1)	to-node (2)	to-node (3)	to-node (4)
48	upper plenum	1(0.25)	16(0.75)	72(0.0)	
49		2(1.0)	57(0.0)		
50		14(1.0)			
51		15(1.0)	58(0.0)	64(0.0)	
52		30(0.0)	50(1.0)		65(0.0)
53	core inlet	33(254.)	40(1.0)	48(10.0)	
54		36(1.0)	47(0.0)		
55		43(1.0)			
56	core outlet	49(1.0)			
57		17(1.0)	68(0.0)	71(0.0)	
58		28(1.0)			
59		29(1.0)	59(0.0)	60(0.0)	61(0.0)
60		52(1.0)	70(0.0)	69(0.0)	
61		31(1.0)			
62		66(0.0)	67(0.0)		
63		62(0.0)	63(0.0)		
64	moisture separator	78(0.75)	79(0.75)		
65		73(1.0)	92(-0.25)	98(0.0)	
66		81(1.0)	94(0.0)	93(0.0)	
67		82(1.0)	91(-0.25)	97(0.0)	
68	moisture separator	87(0.75)	88(0.25)		
69		90(1.0)	96(0.0)	95(0.0)	
70		99(1.0)			

In Table 11-2, the values in parentheses show relative branching flow rates.

Table 11-3 Valve Data

valve no.	description	node
1	PORV (PZR)	69
2	pressurizer safety valve	70
3	2ndry relief valve (loop A)	94
4	2ndry safety valve (loop A)	93
5	2ndry relief valve (loop B)	95
6	2ndry safety valve (loop B)	96
7	accumulator check valve (loop A)	60
8	HPIS control valve (loop A)	63
9	accumulator check valve (loop A)	64
10	HPIS control valve (loop B)	66
11	fictitious valve	68
12	fictitious valve	57
13	feedwater control valve (loop A)	92
14	feedwater control valve (loop B)	91
15	MSIV or governor valve	99
16	spray control valve	59
17	spray control valve	58
18	LPIS control vlave (loop A)	62
19	LPIS control vlave (loop B)	67
20	CVCS bleed contro valve	71
21	auxilliary FW control valve (loop A)	98
22	auxilliary FW control valve (loop B)	97

Table 11-4 Logical Condition Data

ID no.	description
3001	time > 0.01 sec
3002	p_{99} < 40 ata
3003	p_{52} > 159.91 ata
3004	p_{52} < 158.55 ata
3005	p_{52} > 170.11 ata
3006	p_{52} < 170.11 ata
3007	p_{80} > 74.85 ata
3008	p_{80} < 68.05 ata
3009	p_{89} > 74.85 ata
3010	p_{89} < 68.05 ata
3011	p_{80} > 66. ata
3012	p_{80} < 64. ata
3013	p_{89} > 66. ata
3014	p_{89} < 64. ata
3015	p_{52} < 123.8 ata
3016	p_{52} < 10. ata
3017	G_{14} < 0.85 x 10^4 kg/(secm^2)
3018	G_{28} < 0.85 x 10^4 kg/(secm^2)
3019	3017 or 3018
3020	3002 or 3015
3021	3019 or 3020
3022	normalized reactor power > 1.15
3023	3021 or 3022 (scram condition)

Logical conditions in Table 11-4 are to be used in TRIP (Table 11-5) or CSSM (Table 11-12). Condition 3023 is the scram condition, while condition 3020 is the MSIV closing condition.

Table 11-5 TRIP Data

TRIP no.	description	on condition	off condition	delay time (sec)
401	MCP (loop B) trip	3023	0	0.
402	MCP (loop A) trip	3023	0	0.
403	PORV on/off	3003	3004	0.
404	PZR safety valve on/off	3005	3006	0.
405	2ndry safety valve on/off	3007	3008	0.
406	2ndry safety valve on/off	3009	3010	0.
407	2ndry relief valve on/off	3011	3012	0.
408	2ndry relief valve on/off	3013	3014	0.
409	HPIS valve on (loop A)	3015	0	22.2
410	HPIS valve on (loop B)	3015	0	22.2
411	LPIS valve on (loop A)	3016	0	0.
412	LPIS valve on (loop B)	3016	0	0.
413	FW valve closes. (loop A)	3020	0	0.5
414	FW valve closes. (loop B)	3020	0	0.5
415	MSIV closes.	3020	0	0.5
416	aux. FW valve on (loop A)	3020	0	37.
417	aux. FW valve on (loop B)	3020	0	37.
418	reactor scram	3023	0	0.1
419	occurence of a piping break	3001	0	0.0

On- and off-conditions are given in Table 11-4. A trip defines its TRTM which is the elapsed time after the trip condition is satisfied.

Table 11-6 Hydraulic Source Data

HS no.	junc	description	h^r kcal/kg	W^r kg/sec	contrl ID
1	71	LPIS	50.	283.	3115
2	72	HPIS	50.	89.	3116
3	80	CVCS bleed	354.	-3.	0
4	73	HPIS	50.	89.	3117
5	74	LPIS	50.	283.	3118
6	85	feedwater (loop A)	225.	472.69	3109
7	84	feedwater (loop B)	225.	472.69	3109
8	86	turbine flow	655.	-1.890	3108
9	77	upper head dead-end	0.	0.	0
10	75	PORV	200.	0.	3112
11	76	pressurizer safety valve	200.	0.	3112
12	81	2ndry relief valve (V3)	200.	0.	3112
13	89	2ndry safety valve (V4)	200.	0.	3112
14	82	2ndry safety valve (V6)	200.	0.	3112
15	83	2ndry relief valve (V5)	200.	19.44	3112
16	87	auxilliary feedwater	30.	19.44	3113
17	88	auxilliary feedwater	30.		3114

Each control in Table 11-6 is described in Table 11-12.

Table 11-7 SG Data

U-tube pitch	3.0×10^{-2} m
number of U-tubes per unit	3,382
outer diameter of U-tube	1.112×10^{-2} m
inner diameter of U-tube	0.982×10^{-2} m
initial secondary system pressure	62 ata
initial specific enthalpy of feed water	224.8 kcal/kg
initial mass flow rate of feed water	472.7 kg/sec

Table 11-8 Initial Fuel Heat Flux

HC no.	heat flux kcal/(m^2sec)	mode
1	0.0	(non-heated)
2	94.4	10
3	179.4	10
4	180.4	10
5	180.0	10
6	94.6	10
7	0.0	(non-heated)
8	0.0	(non-heated)
9	123.4	10
10	234.1	10
11	233.9	22
12	234.8	22
13	123.0	22
14	0.	(non-heated)

Modes in Table 11-8 are calculated results.

Table 11-9 MCP Data

rated speed	1,190 (rpm)
initial speed	1,190 (rpm)
rated flow	5.58 (m^3 / sec)
rated torque	30,350 (J / rad)
rated head	84.0 (m)
rated density	755.0 (kg / m^3)
moment of inertia	30,350 (kgm^2/ rad^2)

The data of the single-phase head and torque homologous curves are shown in Figs. 11-1-1 and 11-1-2, respectively. And the head difference homologous curves are shown in Fig.11-1-3. The head and torque multipliers as functions of void fraction are shown in Figs.11-1-4 and 11-1-5, respectively.

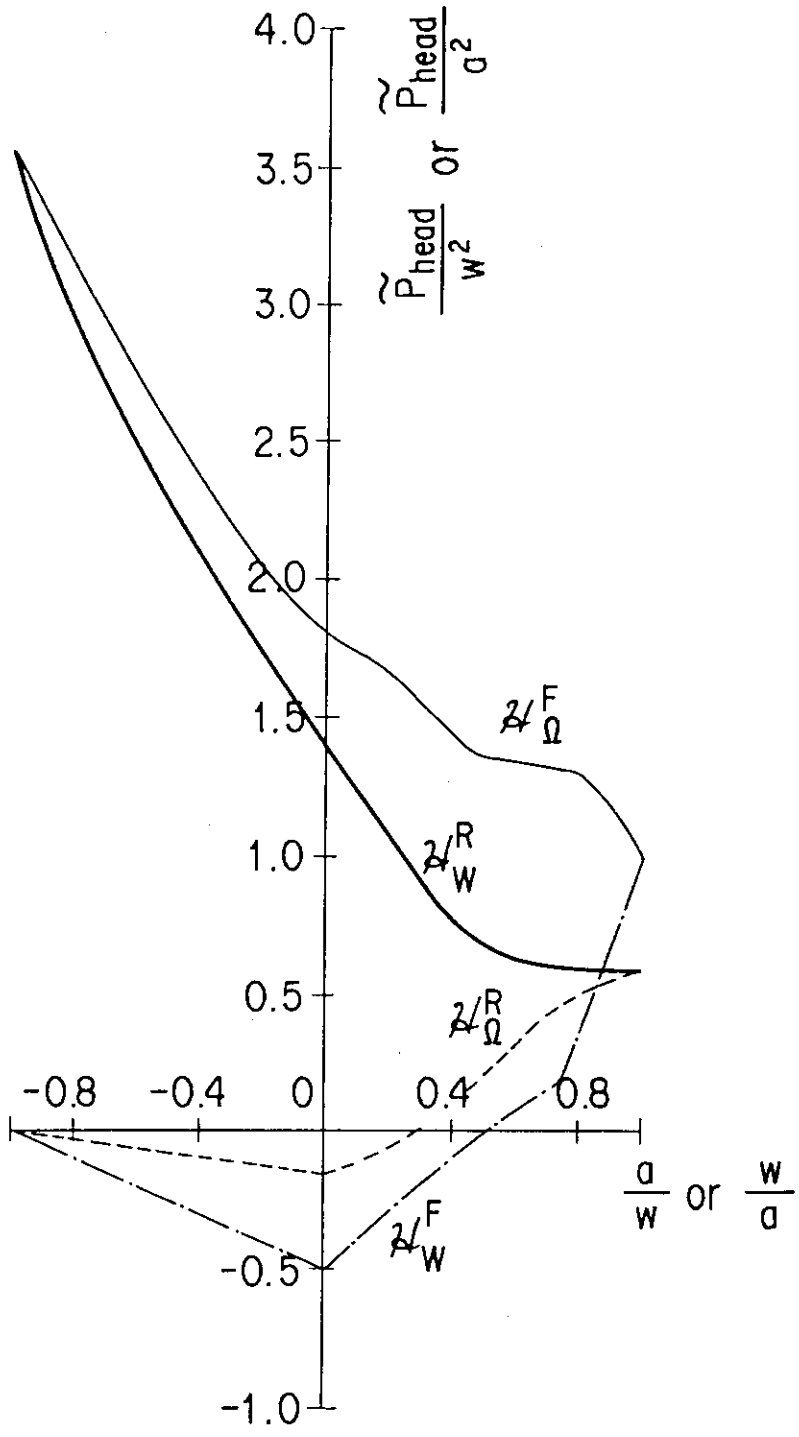

Fig.11-1-1 Single-phase Homologous Head Curves (Sample Problem)

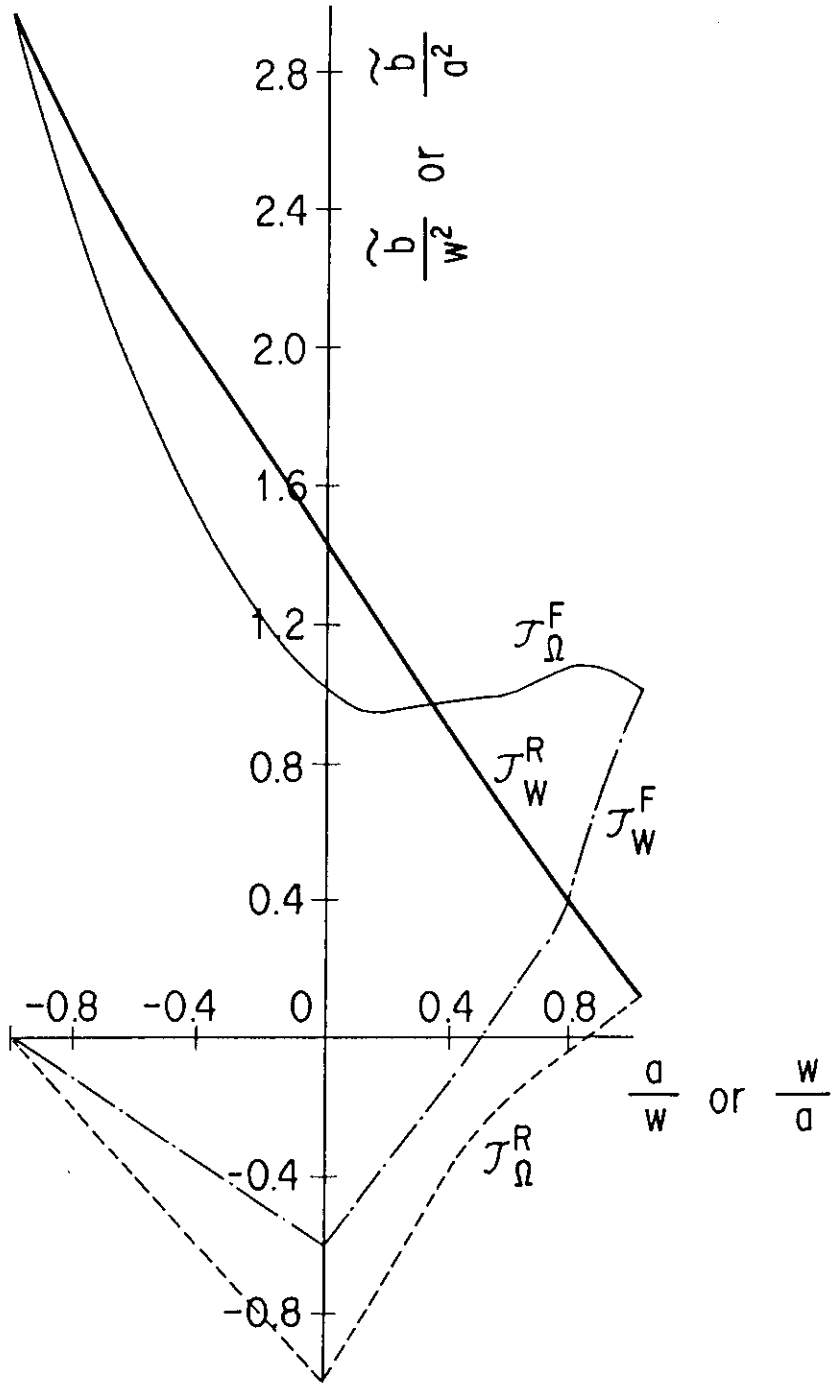

Fig.11-1-2 Single-phase Homologous Torque Curves

(Sample Problem)

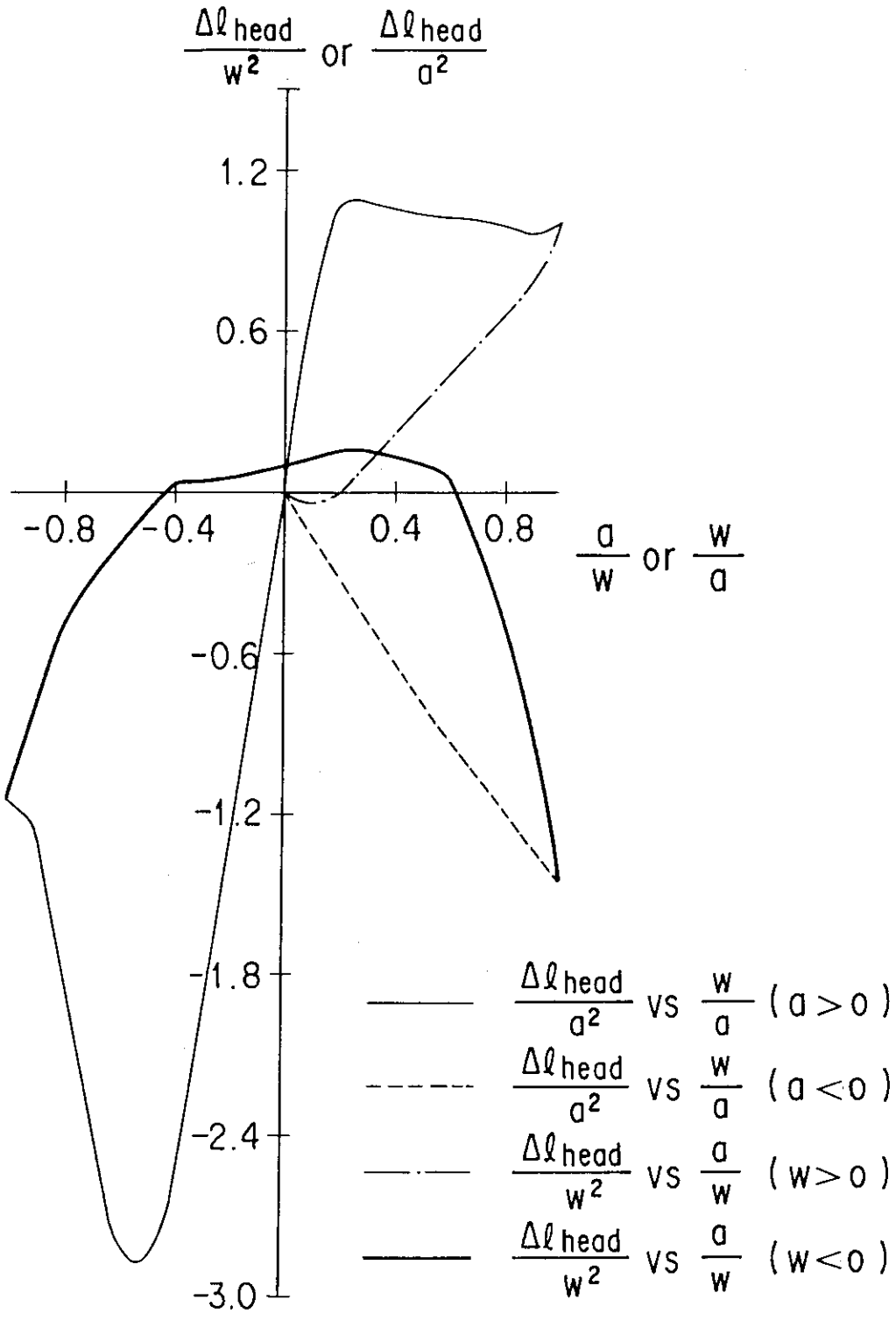

Fig. 11－1－3 Head Difference Homologous Curves

(Sample Problem)

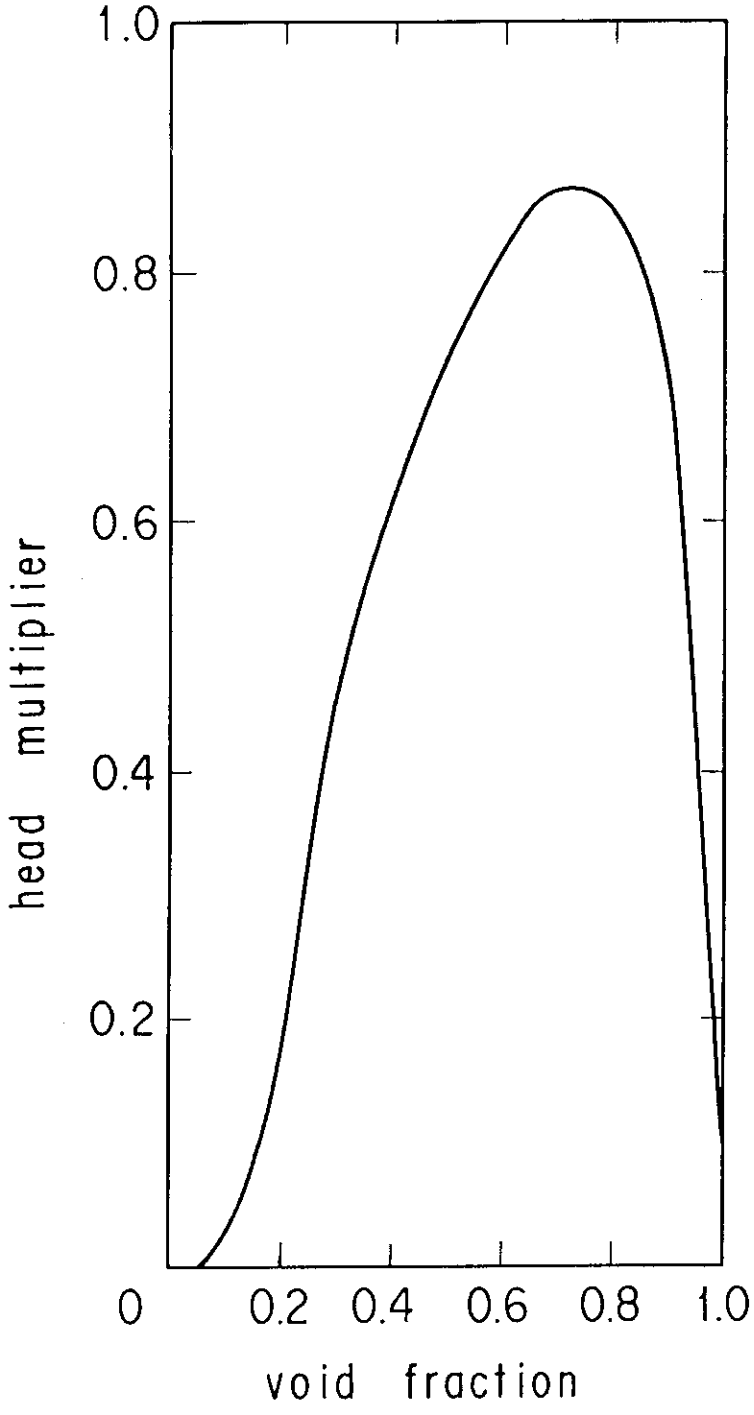

Fig.11-1-4 Head Multiplier Curve

(Sample Problem)

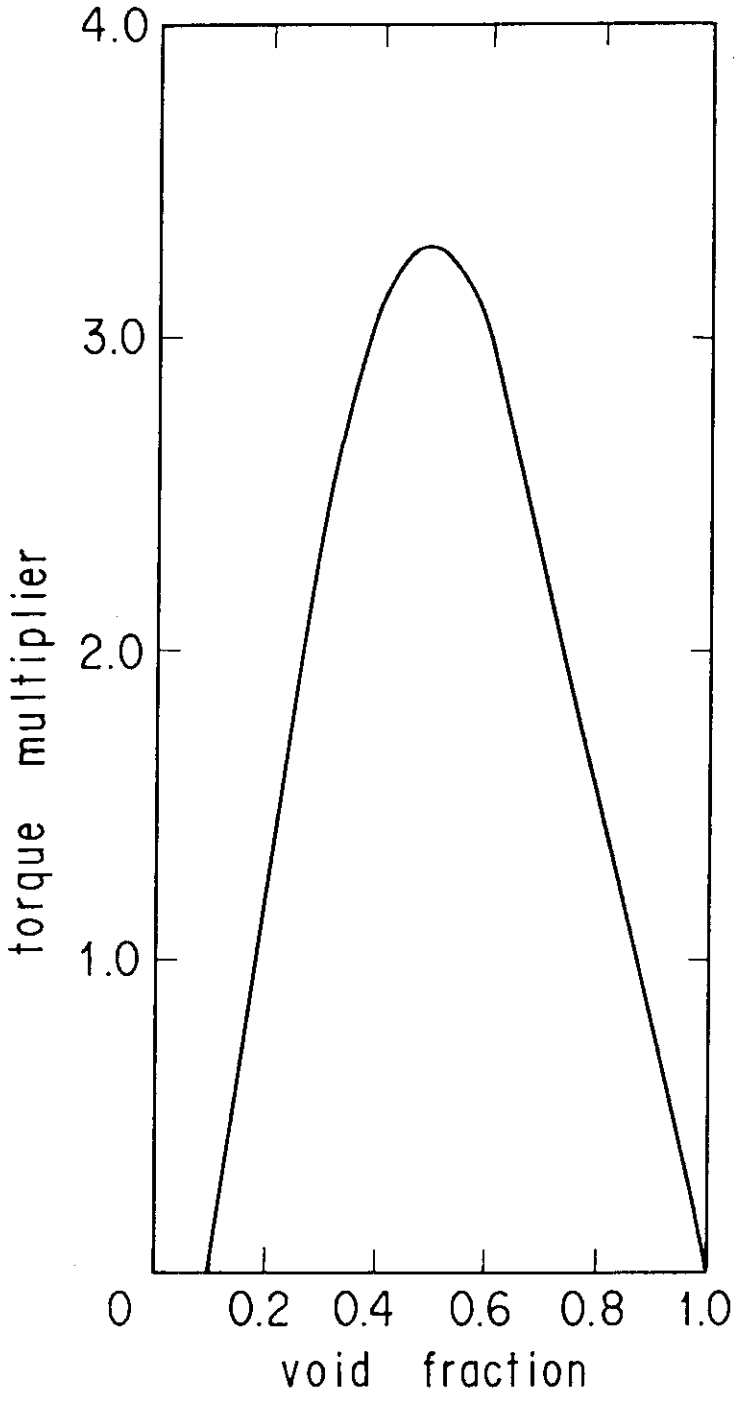

Fig.11－1－5 Torque Multiplier Curve

(Sample Problem)

Table 11-10 Core Data

reactor thermal power	3,409 MWt
active fuel length	3.66 m
plenum gas volume	5.493×10^{-6} m^3
clad outer diameter	9.50×10^{-3} m
clad thickness	0.64×10^{-3} m
pellet diameter	8.05×10^{-3} m
fuel rod pitch	1.26×10^{-2} m

In Table 11-10, the last four values are those at the full power operating condition.

Table 11-11 Accumulator Data

initial water volume/unit	23.3 m^3
initial nitrogen volume/unit	10.0 m^3
specific enthalpy of water	50. kcal/kg
initial pressure	46 ata
boron concentration	2,100 ppm

Table 11-12 CSSM Data

control ID no.	description
3108	m_{MS} = 0 if condition 3020 is satisfied = 1.0 otherwise
3109	$dm_{FW}/dt = (m_{MS} - m_{FW})/100$
3110	p_{RCV} = a function of time as given by SB3208.
3111	Γ_{SCRAM} = a function of time $(t - t_{SCRAM})$ as given by SB3207.
3112	p^+ = 1 ata
3113	m_{AFW} = 1.0 if TRIP 416 is on = 0.0 otherwise
3114	m_{AFW} = 1.0 if TRIP 417 is on. = 0.0 otherwise
3115	m_{LPCI} = 1.0 if TRIP 411 is on. = 0.0 otherwise .
3118	m_{LPCI} = 1.0 if TRIP 412 is on. = 0.0 otherwise .
3116	m_{HPCI} = 1.0 if TRIP 409 is on. = 0.0 otherwise .
3117	m_{HPCI} = 1.0 if TRIP 410 is on. = 0.0 otherwise .
3120	PZR heater trips if condition 3023 (scram condition) is satisfied.

It should be noted that the present input data set does not include a reactor control system.

11.2 Calculated Steady State

The data for steady state adjustment for the primary system are given in Table 11-13. The calculated results for the steady state are

shown in Tables 11-13 to 11-17. The heat transfer modes shown in Table 11-8 are calculated results.

Table 11-13 Initial Loop-wise Thermal-Hydraulics Data

primary loop	secondary loop
G_1^A = 9.804 x 10^3 kg/(m^2s) h_1^A = 354.4 kcal/kg C_B = 500 ppm	G_{91}^A = -508.8 kg/(m^2s) h_{91}^A = 224.8 kcal/kg G_{92}^A = -508.8 kg/(m^2s) h_{92}^A = 224.8 kcal/kg

Table 11-14 Center and Surface Temperatures of Fuel

HC no.	surface temperature	center temperature
2	305.6	749.3
3	325.1	1257.0
4	333.6	1265.9
5	341.7	1274.3
6	336.4	779.5
9	310.5	905.3
10	335.3	1636.8
11	346.3	1648.9
12	350.9	1654.0
13	347.8	942.5

Table 11－15 Loss Coefficients of Nodes

node no.	k	k_A^f	k_A^r	k_B^f	k_B^r
1	7.8400D－03	0.001	0.001	0.001	0.001
2	3.1761D－02	0.001	0.001	0.7253	0.7253
3	9.2229D－03	0.001	0.001	0.001	0.001
4	7.9070D－03	0.2916	0.4198	0.001	0.001
5	7.5159D－03	0.001	0.001	0.001	0.001
6	8.1567D－03	0.001	0.001	0.001	0.001
7	7.9599D－03	0.001	0.001	0.001	0.001
8	9.4543D－03	0.001	0.001	0.001	0.001
9	9.9808D－03	0.001	0.001	0.4198	0.4198
10	1.1736D－02	0.001	0.001	0.001	0.001
11	1.2628D－02	0.3744	0.6921	0.001	0.001
12	2.1390D－01	0.2726	10.	0.2487	10.
13	9.9409D－03	0.001	0.001	0.001	0.001
14	9.5391D－03	0.001	0.001	0.001	0.001
15	9.8438D－03	0.001	0.001	0.001	0.001
16	7.8400D－03	0.001	0.001	0.001	0.001
17	3.1761D－02	0.001	0.001	0.7253	0.7253
18	9.2229D－03	0.001	0.001	0.001	0.001
19	7.9070D－03	0.2916	0.4198	0.001	0.001
20	7.5159D－03	0.001	0.001	0.001	0.001
21	8.1567D－03	0.001	0.001	0.001	0.001
22	7.9599D－03	0.001	0.001	0.001	0.001
23	9.4543D－03	0.001	0.001	0.001	0.001
24	9.6260D－03	0.001	0.001	0.4198	0.4198
25	1.7462D－02	0.001	0.001	0.001	0.001
26	1.2547D－02	0.3744	0.6921	0.001	0.001
27	0.46492	0.2726	10.	0.001	10.
28	8.8506D－03	0.001	0.001	0.001	0.001
29	9.8438D－03	0.001	0.001	0.001	0.001
30	5.0000	0.001	0.001	0.001	0.001
31	1.3686D－03	0.001	0.001	0.2398	0.2398
32	1.0523D－02	0.001	0.001	0.001	0.001
33	0.99971	0.001	0.001	0.001	0.001
34	0.99907	0.001	0.001	0.001	0.001
35	1.0003	0.001	0.001	0.001	0.001
36	1.0053	0.001	0.001	0.001	0.001
37	1.0910	0.001	0.001	0.001	0.001
38	1.0942	0.001	0.001	0.001	0.001
39	1.1059	0.001	0.001	0.001	0.001
40	1.0018	0.001	0.001	0.001	0.001
41	0.99034	0.001	0.001	0.001	0.001
42	0.97100	0.001	0.001	0.001	0.001
43	1.0423	0.001	0.001	0.001	0.001
44	1.0419	0.001	0.001	0.001	0.001
45	1.0426	0.001	0.001	0.001	0.001
46	1.0416	0.001	0.001	0.001	0.001

Table 11－15 Loss Coefficients of Nodes (Continued)

node no.	k	k_A^f	k_A^r	k_E^f	k_E^r
47	1.0000D－02	0.001	0.001	0.001	0.001
48	1.1710D+03	0.001	0.001	0.001	0.001
49	9.2516D－03	0.001	0.001	0.001	0.001
50	1.3686D－03	0.001	0.001	0.2398	0.2398
51	1.0523D－02	0.001	0.001	0.001	0.001
52	1.0000D－02	0.001	0.001	0.001	0.001
53	1.0000D－02	0.001	0.001	0.001	0.001
54	1.0000D－02	0.001	0.001	0.001	0.001
55	20.	10.	0.9742	0.001	0.001
56	20.	0.001	0.001	1.	1.
57	10.	2.	2.	2.	2.
58	10.	10.	0.001	0.001	0.001
59	10.	10.	0.001	0.001	0.001
60	10.	0.001	0.001	10.	10.
61	1.	0.001	0.001	0.001	0.001
62	1.	0.001	0.001	0.001	0.001
63	1.	0.001	0.001	0.001	0.001
64	10.	0.001	0.001	10.	10.
65	1.	0.001	0.001	0.001	0.001
66	1.	0.001	0.001	0.001	0.001
67	1.	0.001	0.001	0.001	0.001
68	10.	2.	2.	2.	2.
69	1.	0.001	0.001	13.	13.
70	1.	0.001	0.001	53.3	53.3
71	1.	0.001	0.001	0.001	0.001
72	1.	0.001	0.001	0.001	0.001
73	7.3695D－03	0.001	0.001	0.6981	0.6981
74	4.3879	0.001	0.001	0.001	0.001
75	4.4113	0.001	0.001	0.001	0.001
76	4.4759	0.001	0.001	0.001	0.001
77	4.2813	0.001	0.001	100.	0.001
78	1.0179	0.001	0.001	0.001	0.001
79	5.0084D－01	0.001	0.001	0.001	0.001
80	4.9832D－02	0.4266	0.8986	0.001	0.001
81	3.5347D－02	0.001	0.001	0.001	0.001
82	7.3695D－03	0.001	0.001	0.6981	0.6981
83	4.3879	0.001	0.001	0.001	0.001
84	4.4113	0.001	0.001	0.001	0.001
85	4.4759	0.001	0.8986	0.001	0.001
86	4.2813	0.001	0.001	100.	0.001
87	1.0179	0.001	0.001	0.001	0.001
88	5.0084D－01	0.001	0.001	0.001	0.001
89	4.9832D－02	0.4266	0.001	0.001	0.001
90	3.5347D－02	0.001	0.001	0.001	0.001
91	1.6316	0.001	0.001	0.001	0.001
92	1.6316	0.001	0.001	0.001	0.001

Table 11-15 Loss Coefficients of Nodes (Continued)

node no.	k	k_A^f	k_A^r	k_E^f	k_E^r
93	1.0	0.001	0.001	74.45	74.45
94	1.0	0.001	0.001	18.6	18.6
95	1.0	0.001	0.001	18.6	18.6
96	1.0	0.001	0.001	74.45	74.45
97	1.0	0.001	0.001	0.001	0.001
98	1.0	0.001	0.001	0.001	0.001
99	0.048	0.001	0.001	0.001	0.001

In Table 11-15, loss coefficients k's at average points of flowing nodes only are determined in the manner described in section 6.6.

Table 11-16 Initial Heat Fluxes of Heat Conductors

HC no.	flux (L/IN) (kcal/(m^2sec)	mode (L/IN)	flux (R/OUT) (kcal/(m^2sec)	mode (R/OUT)
15	-100.4	10	88.7	32
16	-72.0	10	63.6	32
17	-59.8	10	52.8	32
18	-49.7	10	43.9	32
19	-35.1	10	31.0	32
20	-25.0	10	22.1	32
21	-100.4	10	88.7	32
22	-72.	10	63.6	32
23	-59.8	10	52.8	32
24	-49.7	10	43.9	32
25	-35.1	10	31.0	32
26	-25.0	10	22.1	32
27	3.5	10	-3.4	10
28	0.	10	0.	10
29	0.	0	0.	10
30	0.	0	0.	10
31	0.	0	0.	10
32	0.	0	0.	32
33	0.	0	0.	10
34	0.	0	0.	10
35	0.	0	0.	10
36	3.5	10	-3.4	10
37	0.	10	0.	10

For heat conductors 15 to 26, it was found necessary to multiply the inner and outer surfaces with factor 0.7078 in order to obtain a

system heat balance (refer to section 7.4).

Table 11-17 Calculated Heat Inputs to Pressurizer

	heat input (MW)
node 52	-1.986807D-02
node 53	-1.983249D-02
node 54	5.658184D+01
node 55	6.348951D-01
node 56	2.493490D-01
junction 60	-5.742638D+01

In the present calculation, spray valves 16 and 17 are closed so that nodes 52 to 56, which are saturated, are stagnant. Since the coolant is saturated, there is a heat transport in the PZR due to vapor drift, which must be canceled out by external heat addition or removal, if the system is to be at a steady state. Table 11-17 shows required heat inputs and outputs thus obtained. It should be noted that the total of them vanishes.

11.3 Sample Calculation : Analysis of PWR LB-LOCA

In this section, we will present the THYDE-W result calculated for an LB-LOCA of a typical 4-loop 1,000 MWe PWR with the input data sets listed in Appendices E.1 and E.2. The one shown in Appendix E.1 is for the first calculation starting from the initial steady state and the other shown in Appendix E.2 is for a caculation restarting from a restarting dump point 2 of the previous run. The input data listed in Appendices E.1 and E.2 could be interpreted in the light of Chap. 8.

The main assumptions for the calculation include ;

(1) a BE calculation

(2) a double-ended guillotine break at the outlet of an MCP, where a large change in cross section exists,

(3) a through calculation to the end of reflooding

(4) two (hot and average) channel representaion for the core with a single cross flow

(5) discharge coefficient 0.6

(6) coastdown of the centrifugal pumps

(7) ECC water enthalpy of 50 kcal/kg

(8) the same heat transfer correlations package in reflooding as in blowdown, and

(9) the time constant in the relaxation equation for void fraction was calculated according to the method described in subsection 2.2.3.

In conjunction with item (2), it should be noted that the break point is located upstream of the ECC water injection point of the broken loop (see Fig. 2-3-1). Therefore, it is expected that all ECC water injected into the broken loop will go out as part of the core side break flow.

No particular model for the reactor containment was provided except the temporal behavior of the containment pressure which was a function of time as given in Table 11-18.

Table 11-18 Containment Pressure during LOCA

Time (sec)	0.0	7.5	15.0	30.0	1000.0
Pressure(atm)	1.0	2.7	4.0	4.0	4.0

The maximum time step width allowed (BB04) in the present calculation is given in Table 11-19.

Table 11-19 Maximum Time Step Width Allowed

Δ_{max} = 0.001 sec	for		t < 0.5 sec
= 0.004 sec	for	0.5 <	t < 20.0 sec
= 0.064 sec	for	20.0 <	t < 40.0 sec
= 0.006 sec	for	40.0 <	t

The transient is assumed to start at 0.01 sec when the guillotine break takes place in the cold leg at junction 11. The chronology of events is summarized in Table 11-20.

The CPU time and memory required by a VP2600 FACOM computer are 31 minutes 40 seconds and 4,756 k bytes , respectively. The degrees of mass and energy imbalances are 4.20 $\times 10^{-8}$ % and 5.25 $\times 10^{-2}$ % , respectively, at the end of the calculation.

Table 11-20 Chronology of Events

Time(sec)	Events
0.01	The break occured.
0.08	Voiding started at the middle of the hot channel.
0.16	Voiding started at the intact loop hot leg.
0.24	Voiding started at the middle of the average channel.
4.2	Voiding started at the lower plenum.
4.2	Voiding started at the downcomer (intact loop).
8.	FWs were tripped off. (Fig. 11-3-6)
14.2	ACC injection started. (Fig. 11-3-2)
28.	Refill started.
30.	HPCI started. (Fig. 11-3-4)
32.	End of blowdown. (Fig.11-3-8)
40.	Reflooding started.
43.	The core bottom became subcooled. (BOCREC)
44.	Auxilliary FW started. (Fig.11-3-7)
55.	LPCI started. (Fig. 11-3-4)
74.	Reflooding of the average channnel ended. (Fig.11-3-27)
82.	ACC injection ended in the broken loop. (Fig. 11-3-3)
88.	ACC injection ended in the intact loop. (fig. 11-3-2)
115.	Reflooding of the hot channnel ended. (Fig.11-3-30)

It is also interesting to compare these results with the THYDE-P1 EM result[48] as well as LOFT results[53] . It is important to note that the decay heat level is sufficiently low so that the fuel can finally be quenched at the end of reflooding (see Figs. 11-3-19 to 11-3-22).

The detailed discussions on the calculated results will be made in the following subsections. It should be reminded that the positive

direction of a mass flux of a node is that from point A to point E of the node.

(1) Nuclear Power

As shown in Fig. 11-3-1, the nuclear power suddenly dropped to the level of the decay heat due to the scram as well as the negative feedback reactivity caused by voiding in the core.

(2) Pressure

The calculated pressure transients are shown in Figs. 11-3-8 and 11-3-9. The system pressure shown in Fig.11-3-8 decreased very quickly from 1.52×10^{7} Pa. (initial pressure) to 1.23×10^{7} Pa. in 0.16 sec. Then, the choking at the break points as well as in the pressurizer surge line and voiding in the core made the gradient smaller. By 5 sec, both break flows became saturated (see next subsection), making the gradient even less. At 32. sec, the system pressure is almost equal to that of the reactor containment (4 ata) (the end of blowdown).

The pressures in the primary system showed a very similar behavior except those of the pump-side break point and the pressurizer. The pressurizer pressure (Fig.11-3-8) showed a rather gradual transient because of the choking in the surge line. The pump-side break pressure (Fig.11-3-9) was substantially smaller during the blowdown, because the large break flow caused a large pressure drop across the pump.

The secondary system pressure gradually decreased (Fig. 11-3-8). Its tendency was augmented by auxilliary feedwaters, which started at 44 sec.

(3) Break Flows

The break flow rates and their qualities are shown in Figs. 11-3-10 to 11-3-12. Note that the negative flow means discharging at the core side of the break. With the occurence of the break, the break flows increased. As the flashing occurred in the core, the rate of depressurization decreased so that the break flow began decreasing.

At the core-side break, the quality continued to increase (Fig. 11-3-11) because of depressurization until 16. sec when it suddenly began decreasing due to the effect of the ACC injections, which had begun at 15. sec (Fig. 11-3-2 and 1-3-3). Moreover, the ACC injections as well as HPCIs stopped the decreasing tendency of the break flow and maintained it at a substantial level (Fig. 11-3-10). The HPCI, which started at 30. sec, helped the break flow to clear the threshold of zero quality (Fig. 11-3-11).

At the pump side of the break, voiding at the pump side break began at 4. sec. The quality tended to increase and remained superheated after 24 sec owing to heat addition from the SG secondary system. After 48 sec, the pump-side break flow practically vanished.

(4) Downcomer

Downcomer mass fluxes and qualities are shown in Figs. 11-3-13 to 11-3-16. Figure 11-3-11 shows that the intact loop DC flow was almost always positive (downwards), while the broken loop DC flow was almost always negative (upwards). Figure 11-3-14 shows that the

direction of the DC top flow was negative (from the intact to broken loop cold leg) until 64 sec, but after that it was opposite. The refill started at 28 sec, because after that at the inlet of the broken loop DC, (1) the coolant became subcooled (Fig.11-3-15) and (2) the flow not only became positive, but also tended to increase (Fig.11-3-13). Then, subcooled water kept on moving toward the core to finally reflood the core (Figs. 11-3-18, 11-3-22, 11-3-23 and 11-3-24). The DC qualities became positive after 80 sec due to the end of ACC injections (Figs. 11-3-15 and 11-3-16).

(5) Core Flow

The core flow in the hot channel and in the average channel showed quite a similar behavior. That is , (1) at first, just after the rupture, a reverse flow occurred and continued until 28 sec, (2) the reflooding started at 40 sec (Fig. 11-3-17), and (3) the coolant at the core bottom became subcooled at 43 sec (BOCREC) (Fig. 11-3-18).

(6) Intact Loop Flow

Comparing Figs. 11-3-17 and 11-3-19, it can be seen that the hot leg flow had almost the same tendency as the core flow. The SG inlet and outlet qualities are shown in Fig. 11-3-20, which implies that in the later period of the LB-LOCA, the SG secondary system acted as a heat source to the primary system.

(7) Broken Loop Flow

The mass flow rate in the broken loop was controlled by the pump-side break flow (Fig. 11-3-10). Comparing Figs. 11-3-12 and 11-3-21, it can be seen that the broken loop SG also behaved as a heat source to the primary system in the later period of the LB-LOCA.

(8) ECC Behavior

The ACC behaviors are shown in Figs. 11-3-2 and 11-3-3. As soon as the break took place, a premature ACC injection occurred in the broken loop. After 14.2 sec , persistent ACC injection continued in both loops, since the pressures of the boundary junction remained below the gas pressure minus the water head. In both loops, the HPCI and LPCI started at 30. and 57 sec, respetively. ACC water stopped voiding in the cold leg and increased the core-side break flow rate. Water in ACCs was exhausted by 81 and 88 sec, in the broken and intact loops, respectively.

(9) Fuel Temperatures and Qualities in Core

The qualities shown in Figs. 11-3-22 to 11-3-24 indicate how the ECC water penetrated through the hot channel. The fuel temperatures are shown in Figs. 11-3-25 to 11-3-29.

Looking over the calculated fuel temperatures shown in Figs. 11-3-25 to 11-3-30, we observe as follows. The temperatures at the centers of the fuel suddenly fell due to the scram. The cladding surface temperature rose quickly just after the rupture, because the decrease of the flow rate and the flashing due to depressurization in the core

caused a DNB (departure of nucleate boiling). The clad surfaces temporarily rewetted due to a negative core flow recovery from 10 to 20 sec (Fig.11-3-17) except at HCs 2 and 9 where qualities remained large during this period. But, prior to the start of core reflooding, the core flow became stagnant (Fig. 11-3-17) and again a DNB took place in HCs 3 to 6 and 10 to 13, followed by superheated steam cooling. Then, ECC water began to come into effect and the precursory cooling took place, evetually leading to quenching (Figs. 11-3-25 to 11-3-30).

(10) SG Secondary System Behavior

The FW flows were tripped off at 8 sec (Fig. 11-3-6). The auxilliary FWs were actuated at 44 sec (Fig. 11-3-7). The secondary relief valves were never opened, but the secondary system pressure gradually decreased (Fig. 11-3-8). In the later period of the accident, the secondary systems acted as heat sources to the primary system. In each of the SG secondary systems, a natural circulation continued, but it tended to vanish due to the injected ECC water and the auxilliary feedwaters.

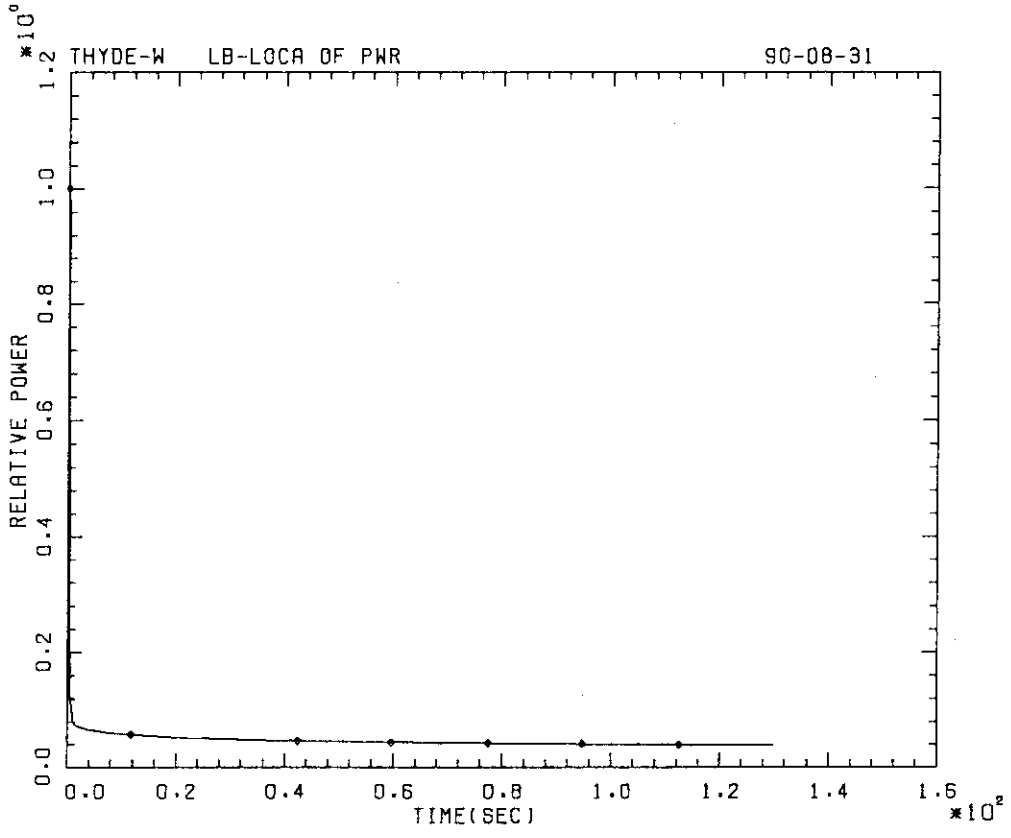

Fig. 11-3-1 Nuclear Power (Sample Problem)

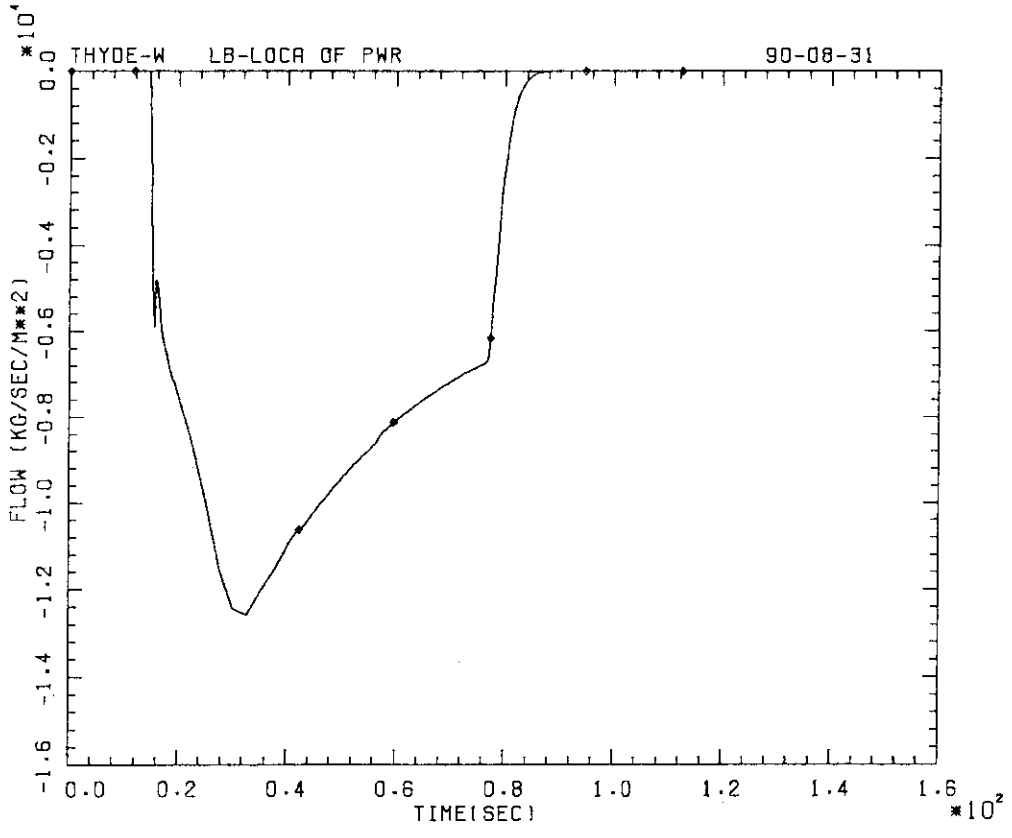

Fig. 11-3-2 ACC Injection Flow (Intact Loop) (Sample Problem)

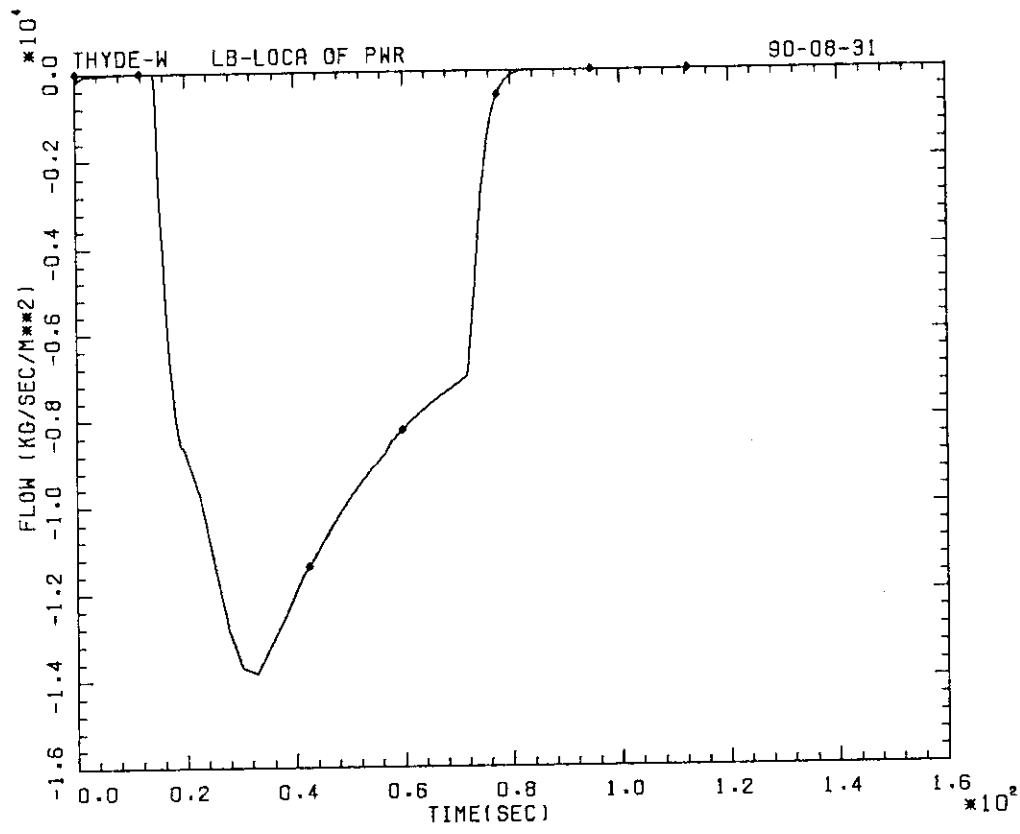

Fig. 11-3-3 ACC Injection Flow (Broken Loop) (Sample Problem)

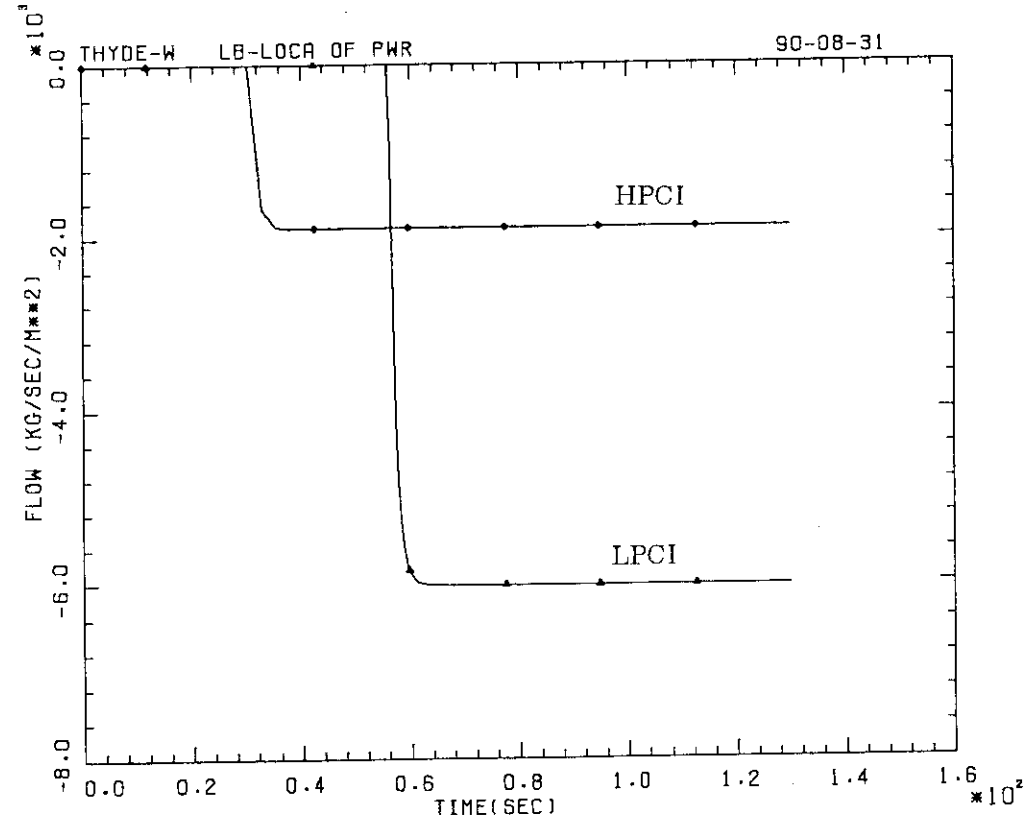

Fig. 11-3-4 HPCI and LPCI Flows (Sample Problem)

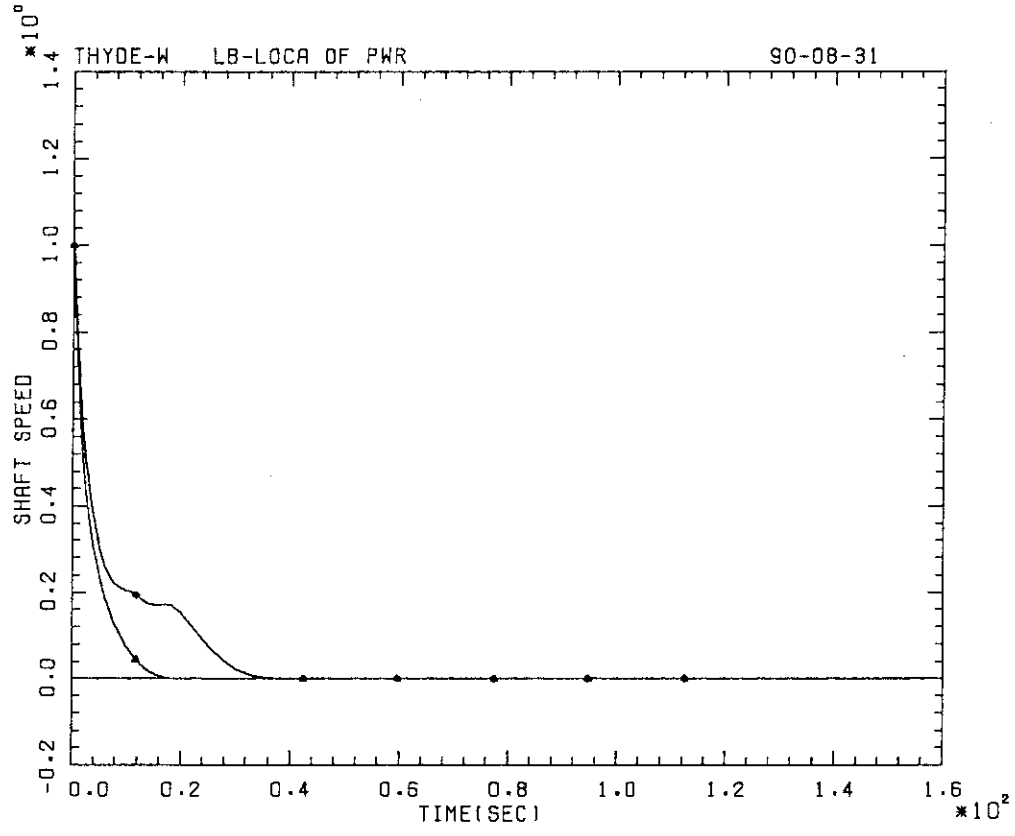

Fig. 11－3－5 MCP Speeds (Sample Problem)

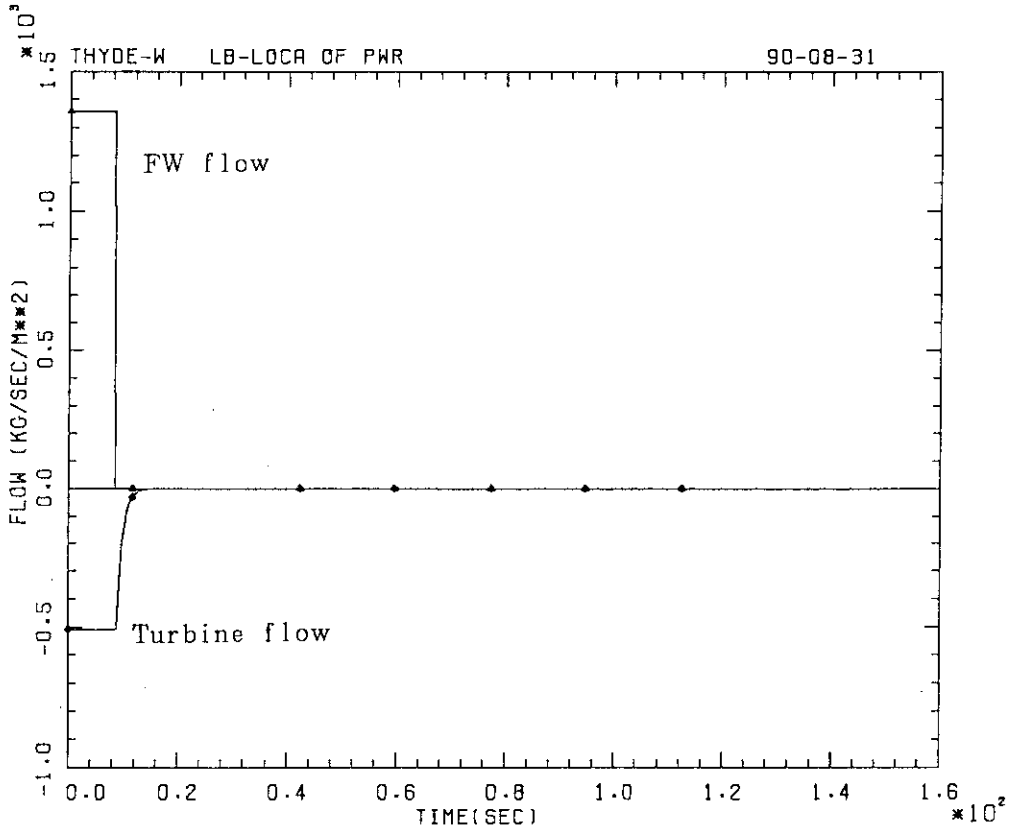

Fig. 11－3－6 FW and Turbine Flows (Sample Problem)

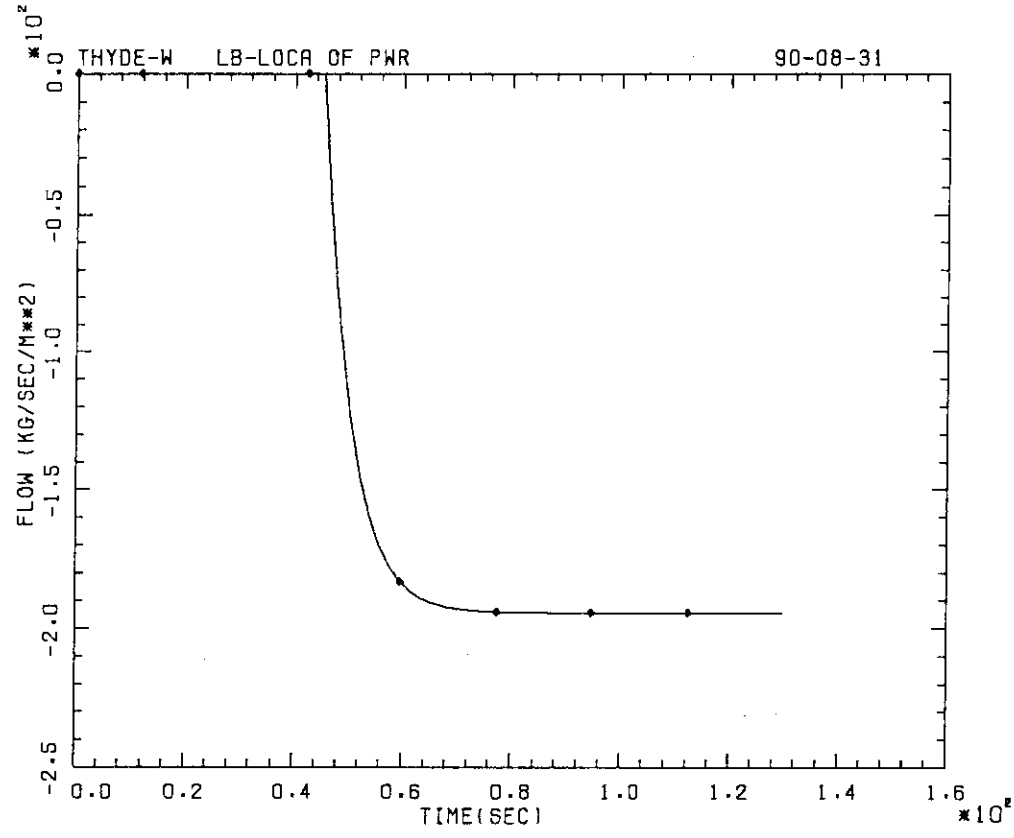

Fig. 11-3-7 Auxilliary FW Flows (Sample Problem)

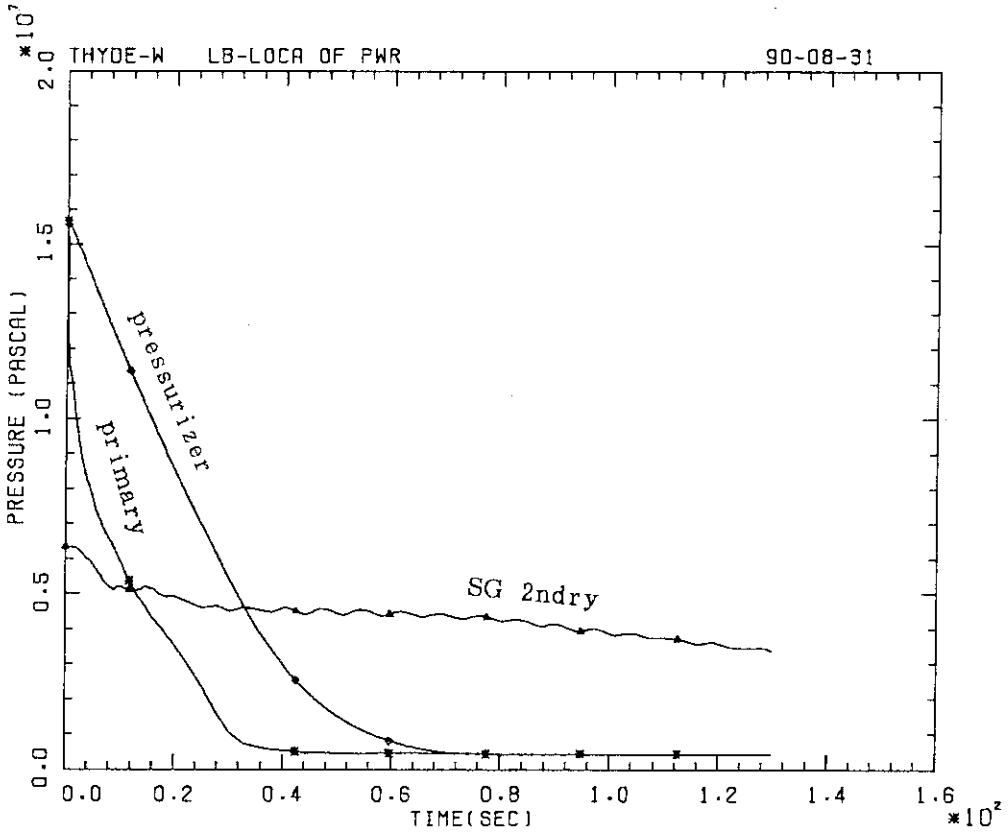

Fig. 11-3-8 Pressurizer and System Pressures (Sample Problem)

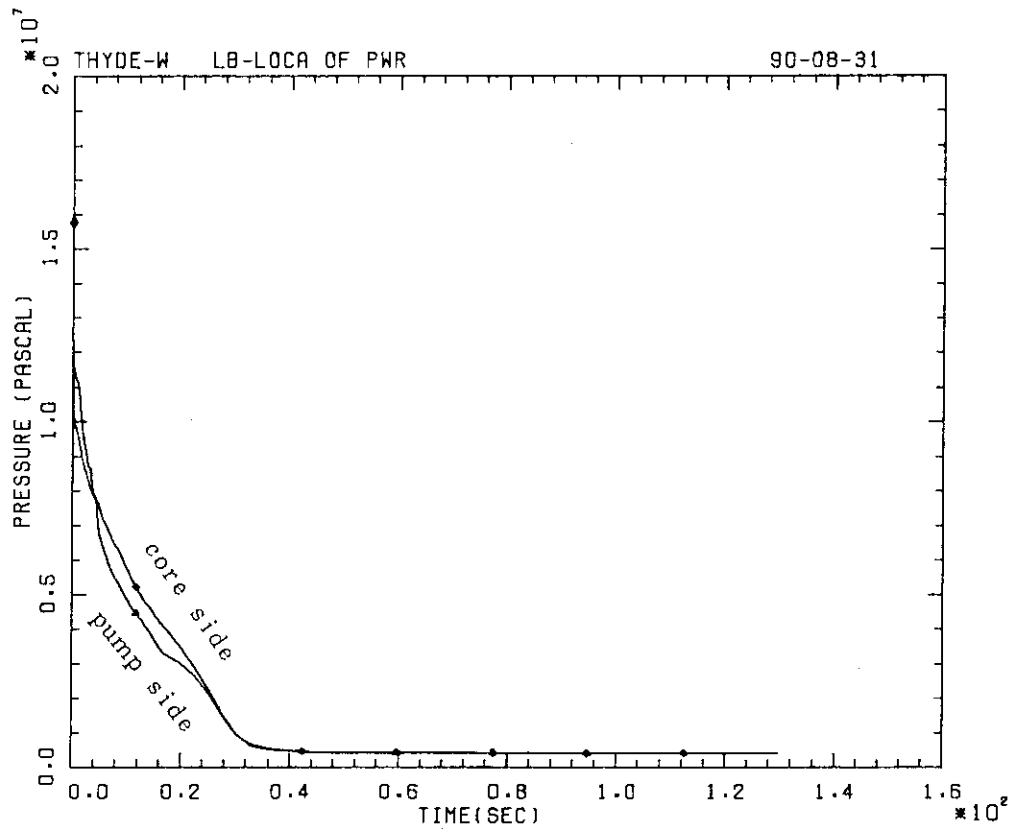

Fig. 11-3-9 Break Point Pressures (Sample Problem)

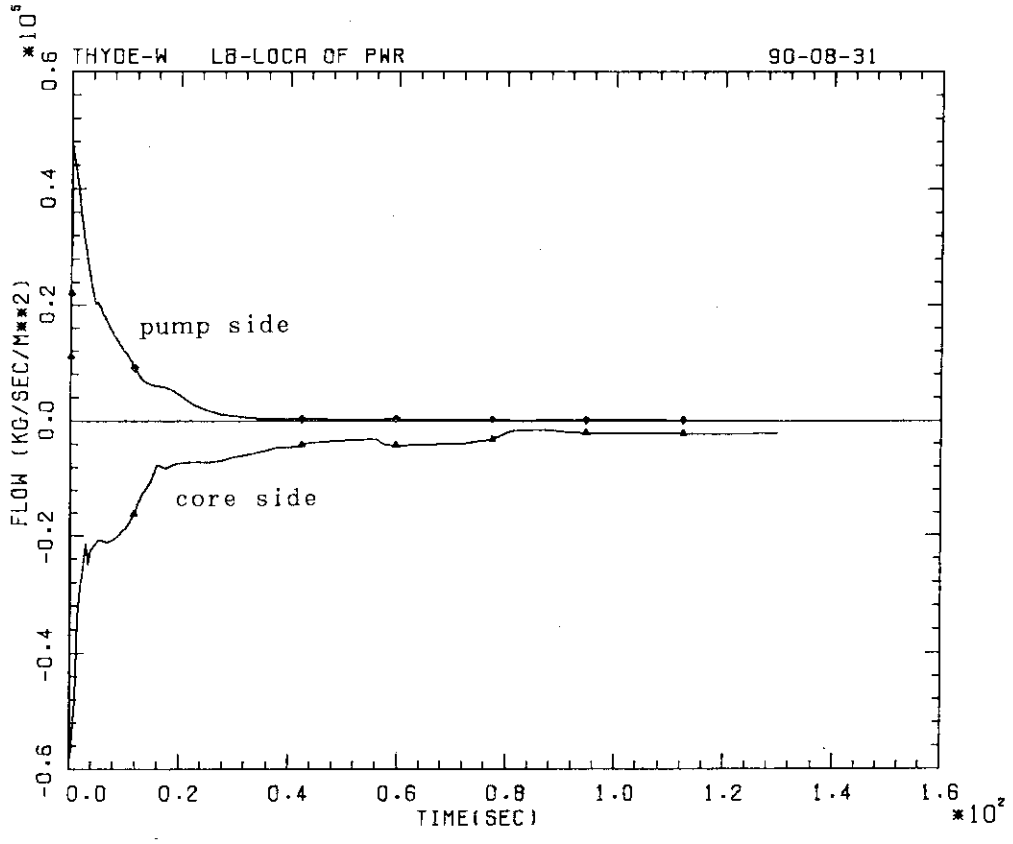

Fig. 11-3-10 Break Flows (Sample Problem)

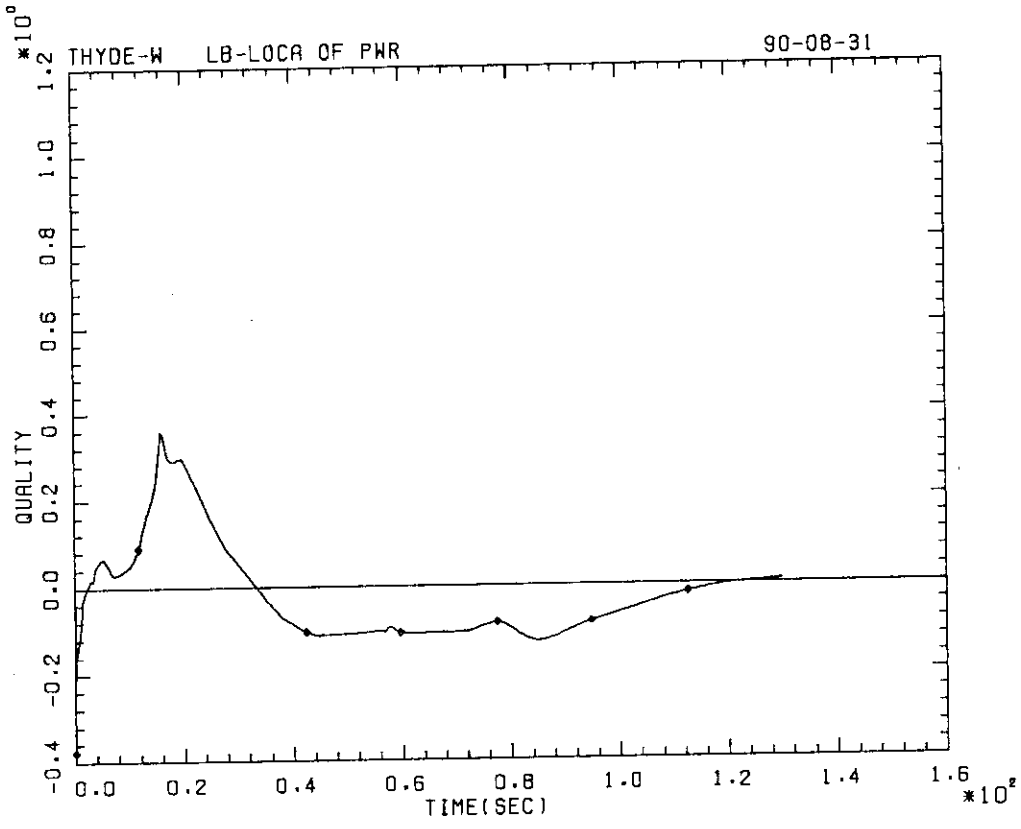

Fig. 11-3-11 Break Point Quality (Core Side) (Sample Problem)

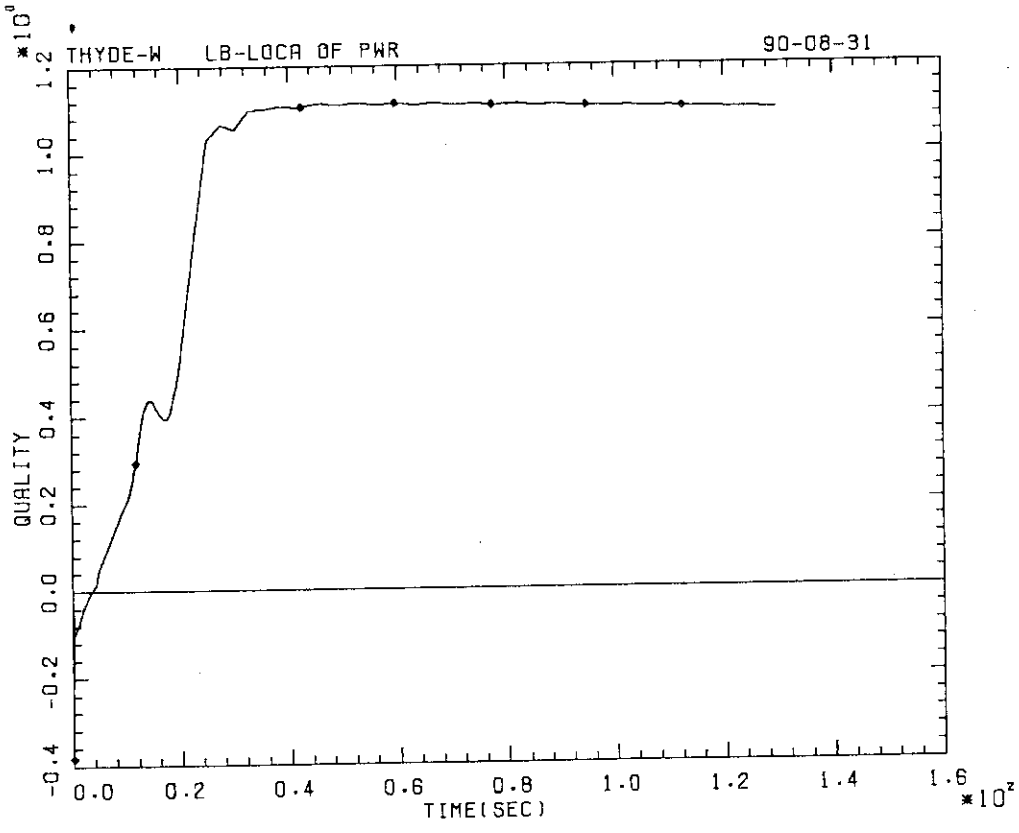

Fig. 11-3-12 Break Point Quality (Pump Side) (Sample Problem)

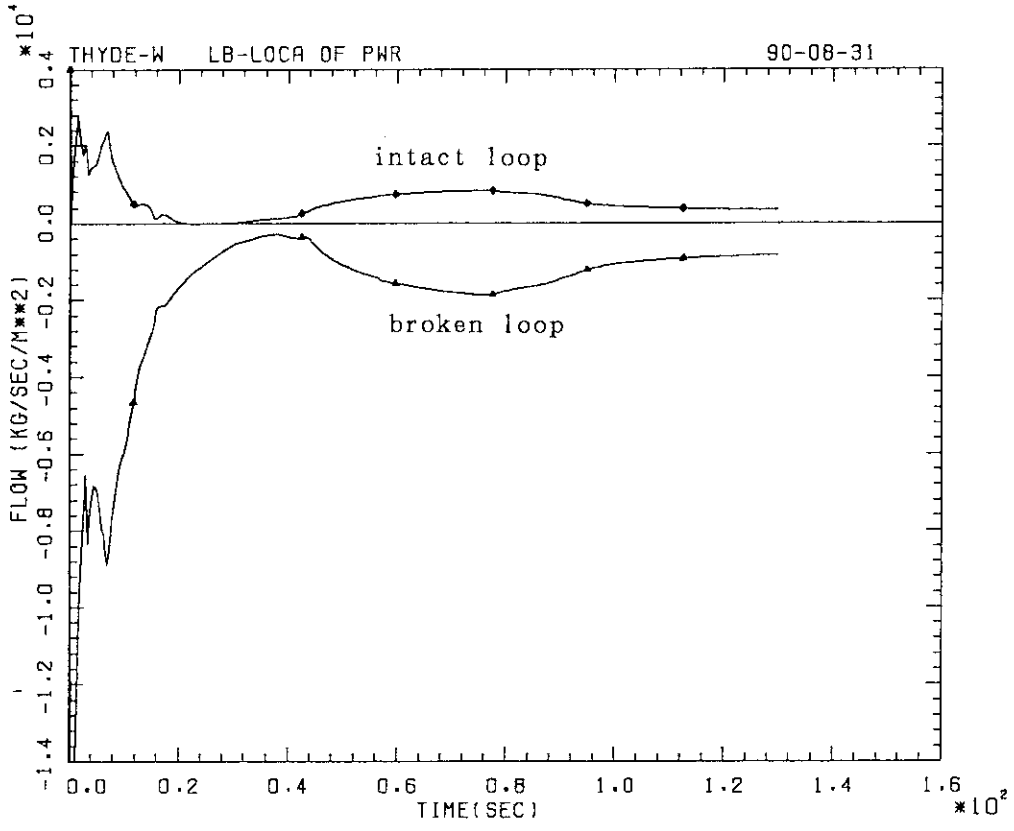

Fig. 11-3-13 Downcomer Flows (Sample Problem)

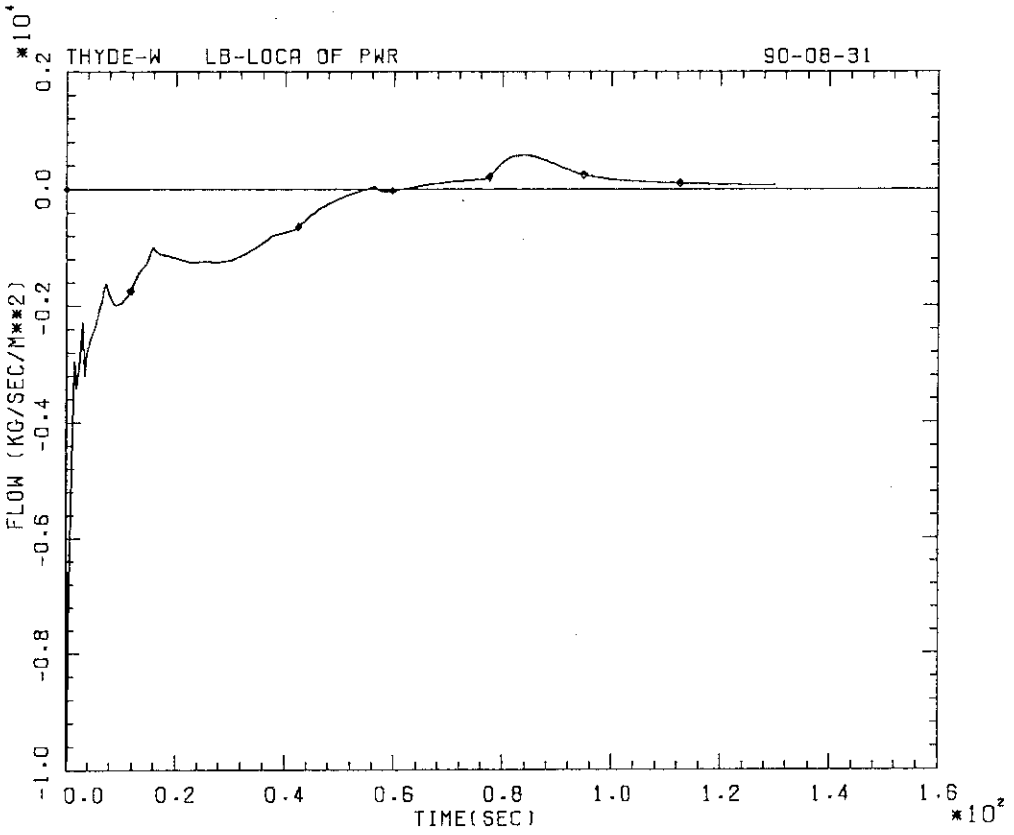

Fig. 11-3-14 Downcomer Top Flow (Sample Problem)

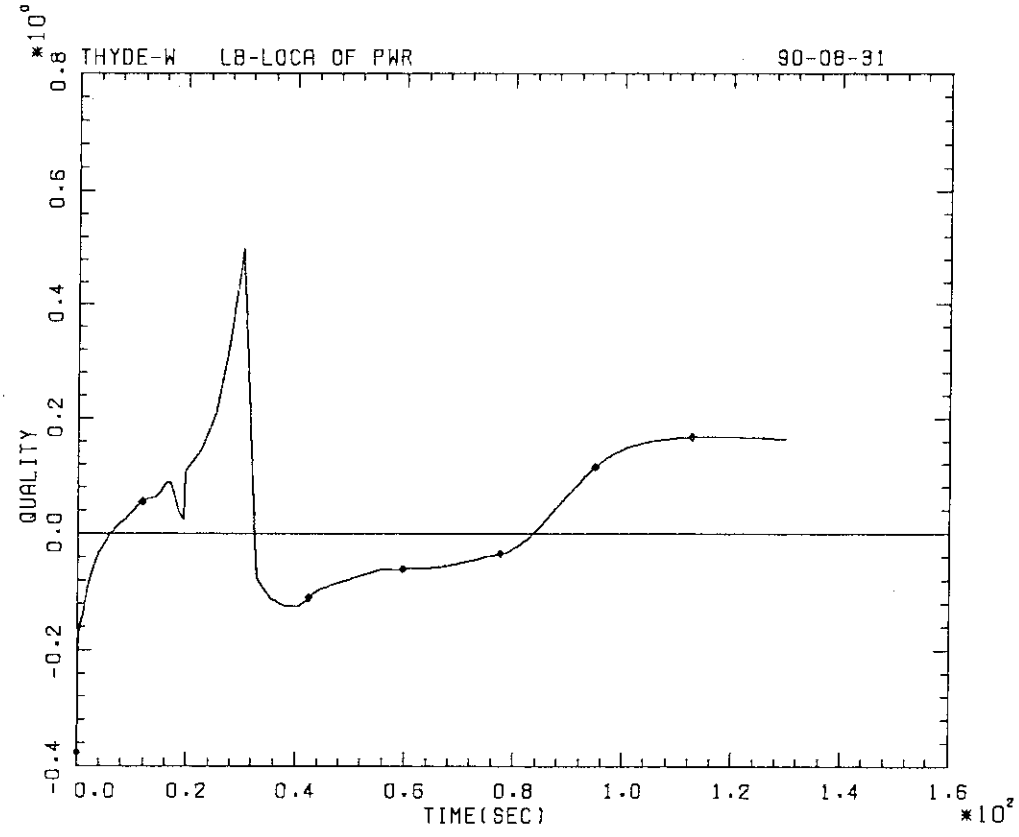

Fig. 11－3－15 Downcomer Inlet Quality (Intact Loop) (Sample Problem)

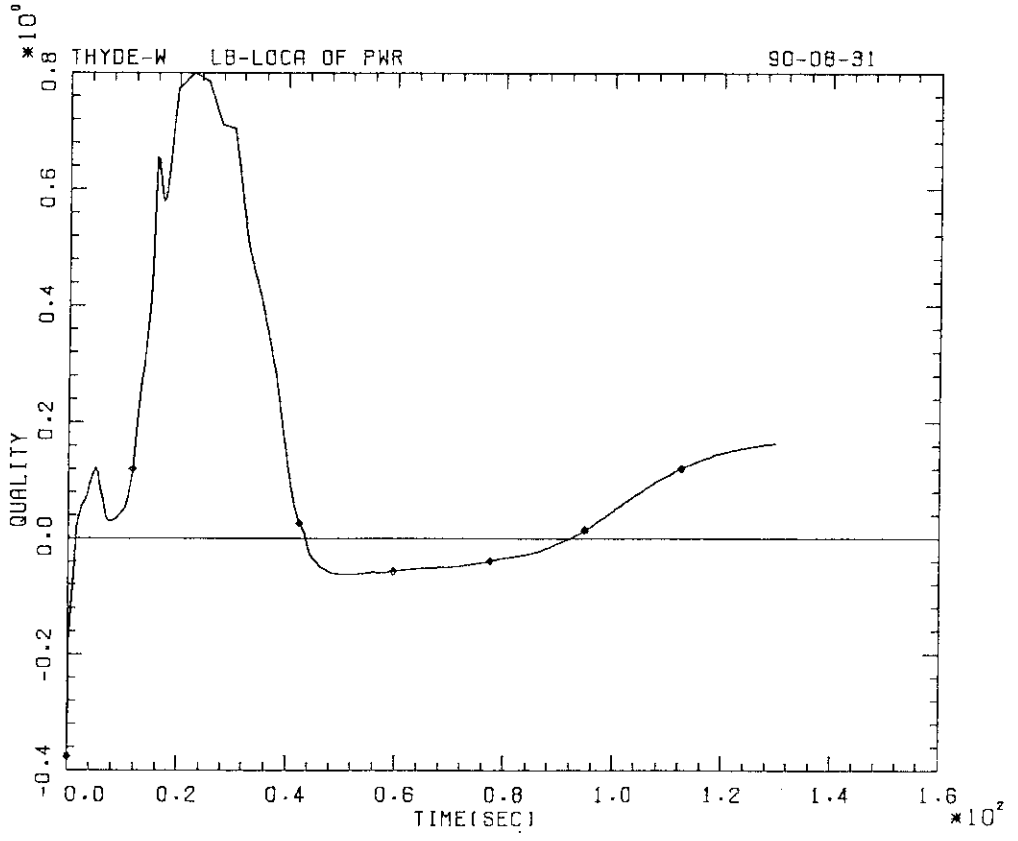

Fig. 11－3－16 Downcomer Inlet Quality (Broken Loop) (Sample Problem)

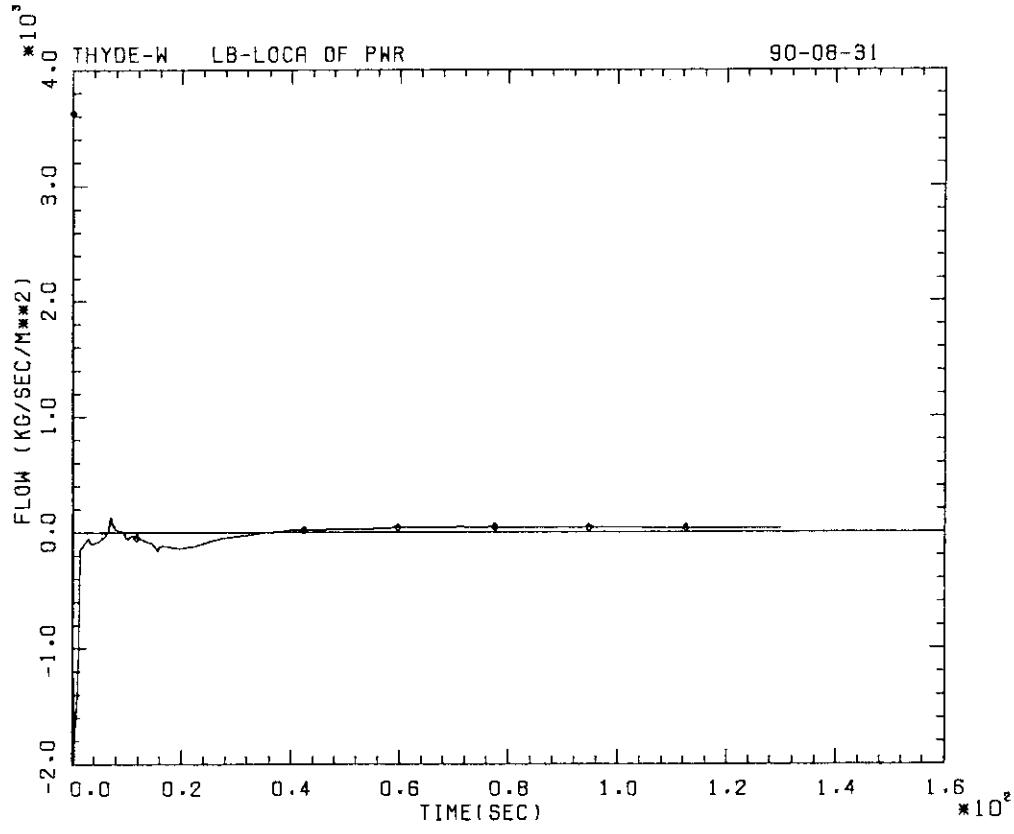

Fig. 11－3－17 Core Inlet Flow (Average Channel) (Sample Problem)

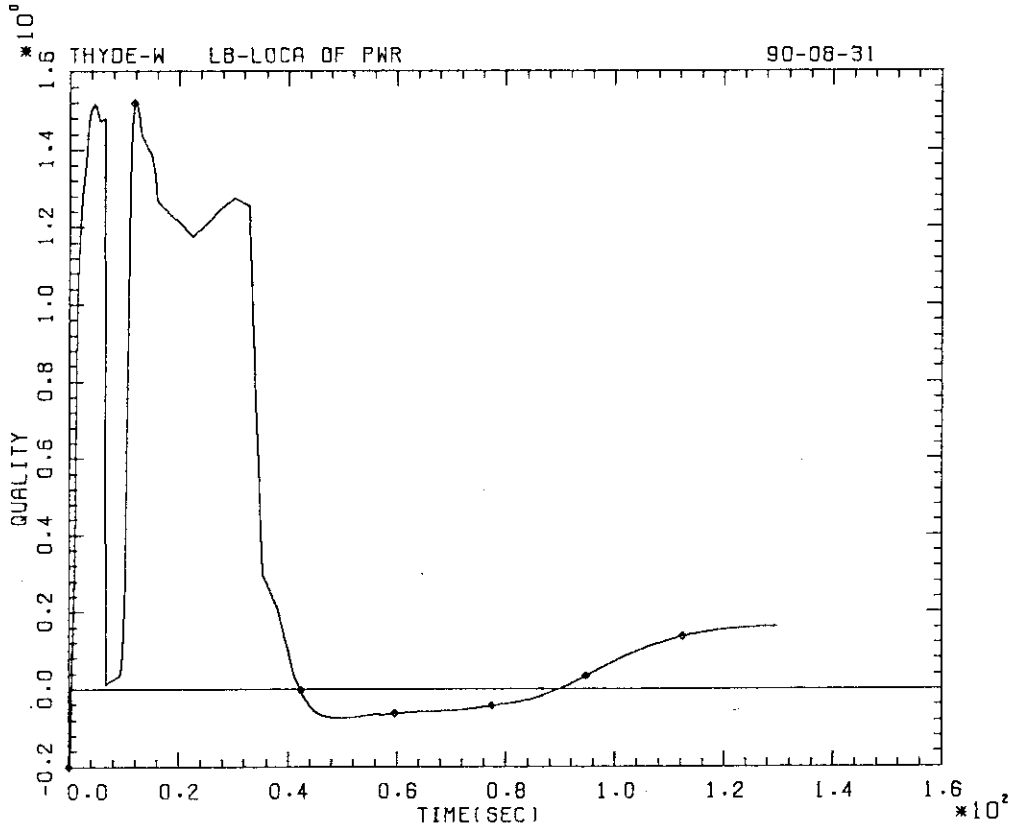

Fig. 11－3－18 Core Inlet Quality (Average Channel) (Sample Problem)

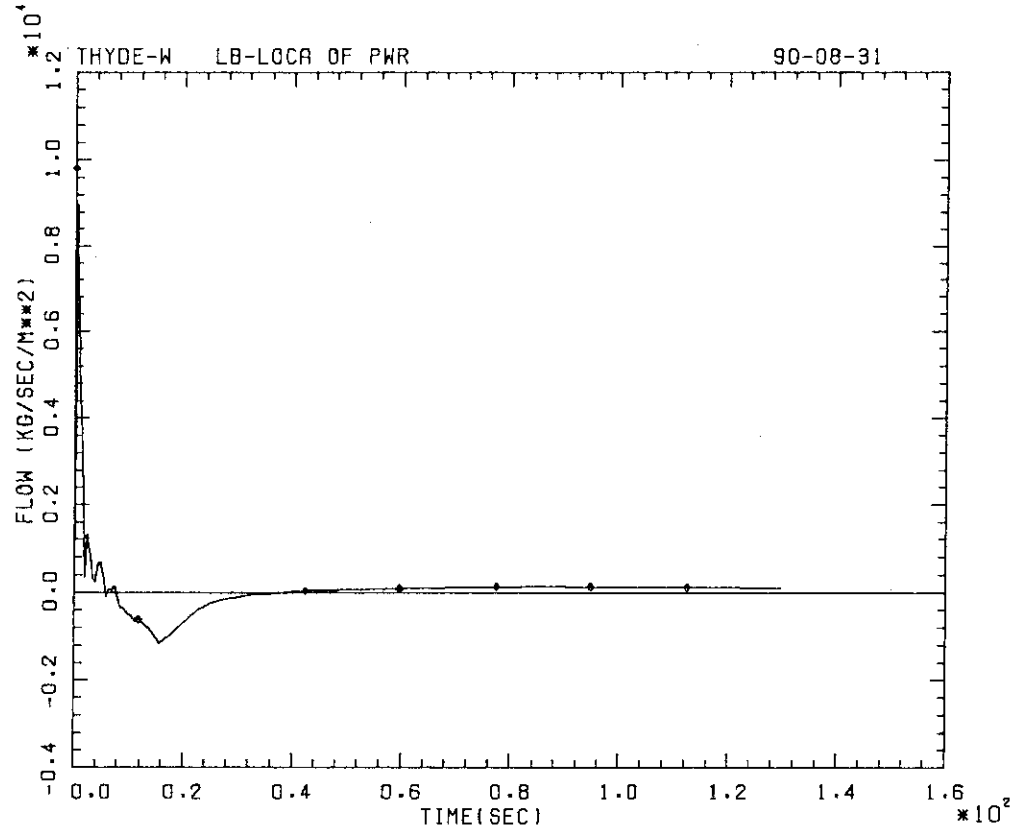

Fig. 11-3-19 Hot Leg Flow (Intact Loop) (Sample Problem)

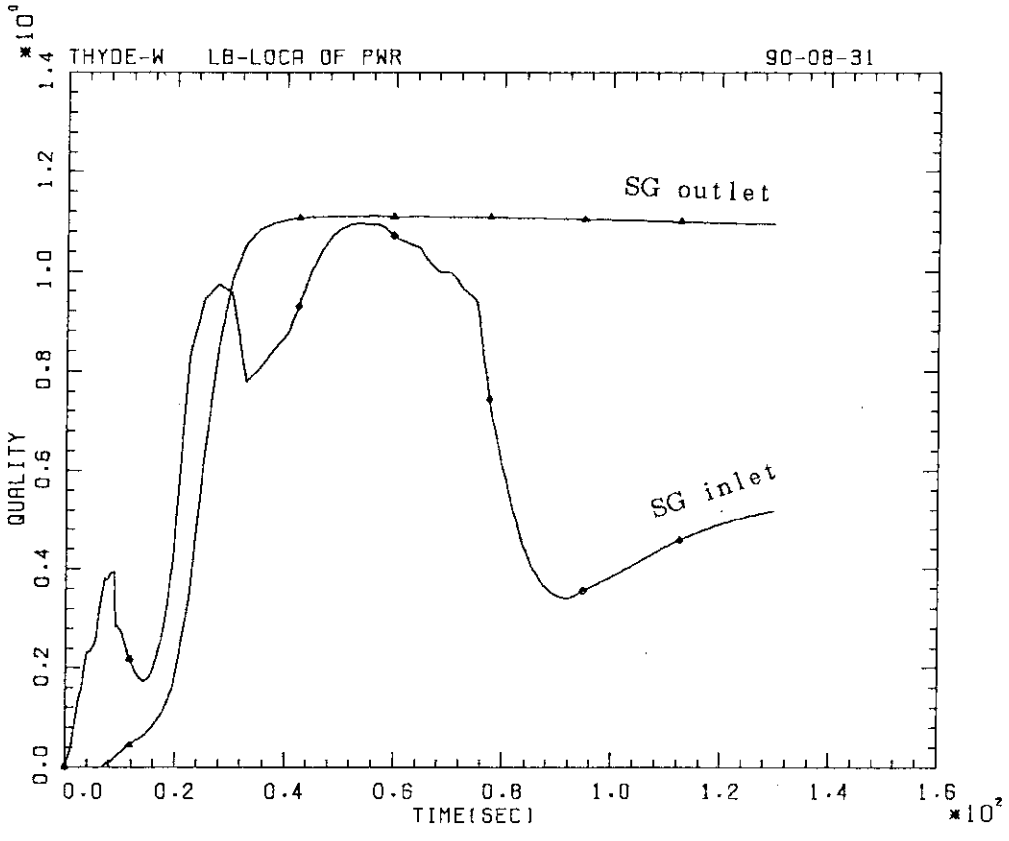

Fig. 11-3-20 SG Inlet and Outlet Qualities (Intact Loop) (Sample Problem)

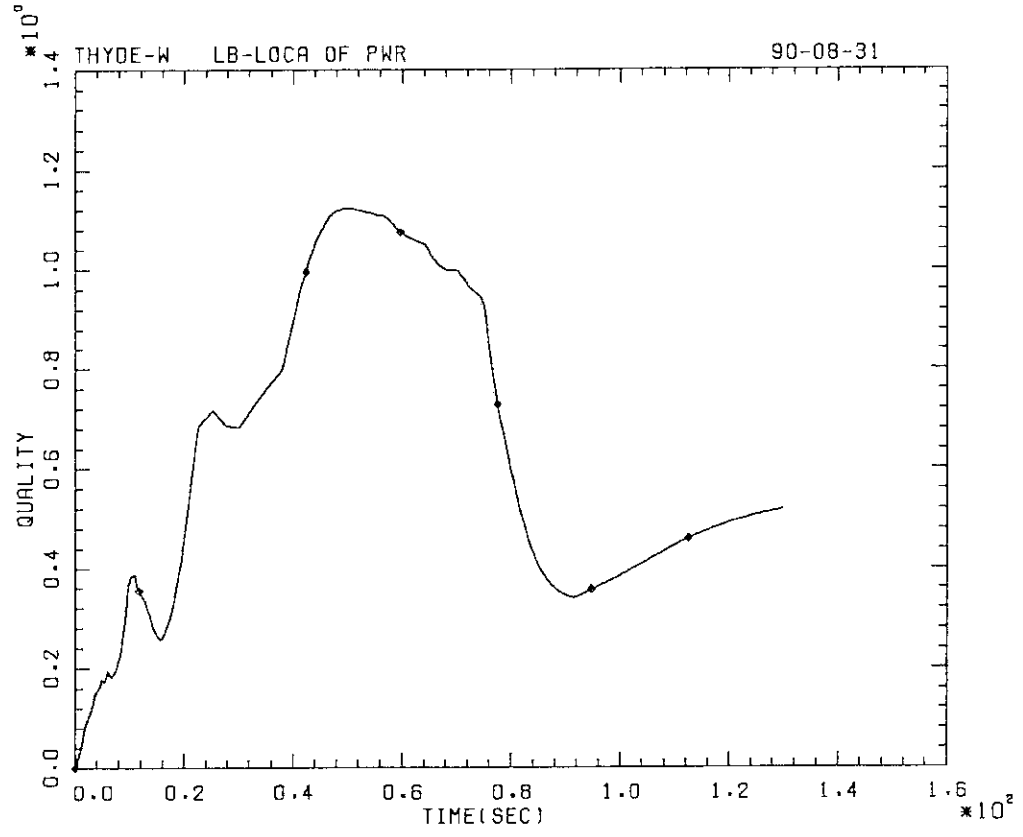

Fig. 11－3－21 Hot Leg Quality (Broken Loop) (Sample Problem)

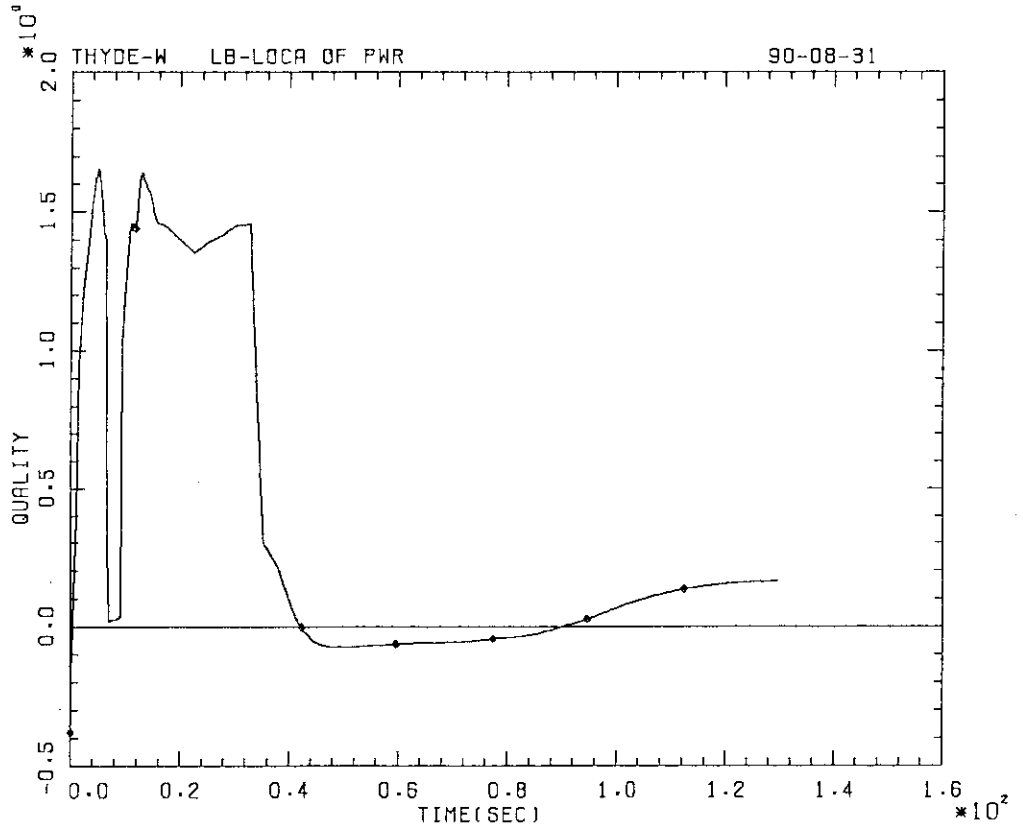

Fig. 11－3－22 Core Quality (node 41) (Sample Problem)

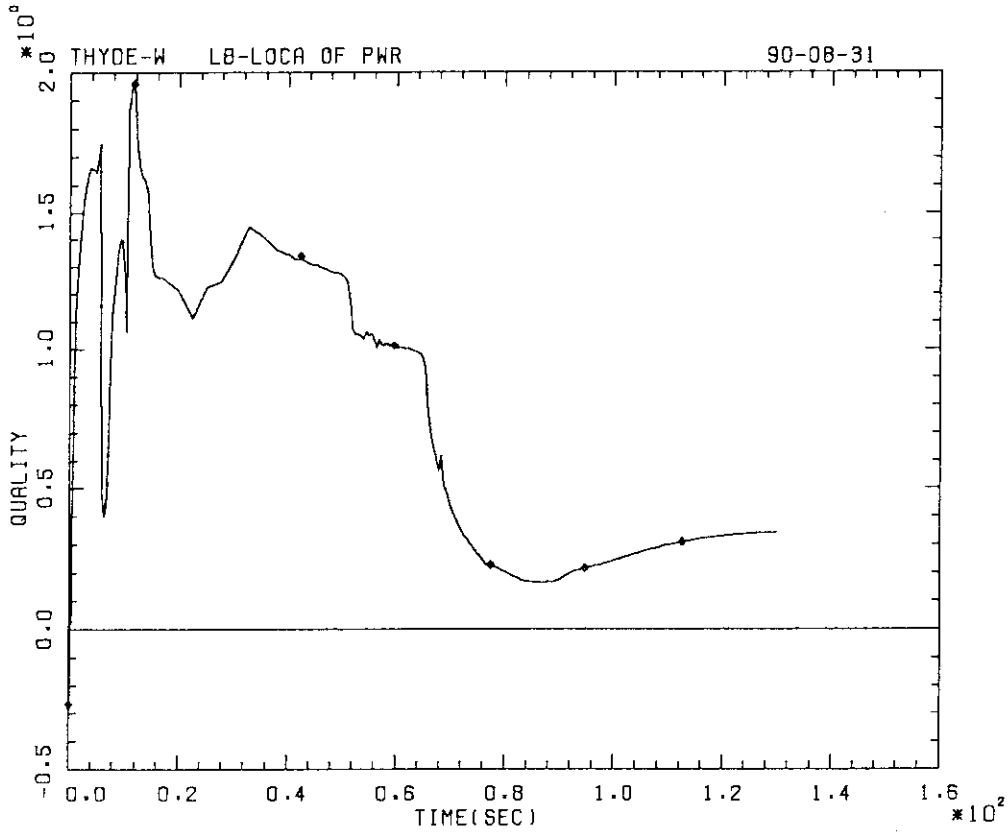

Fig. 11－3－23 Core Quality (node 43) (Sample Problem)

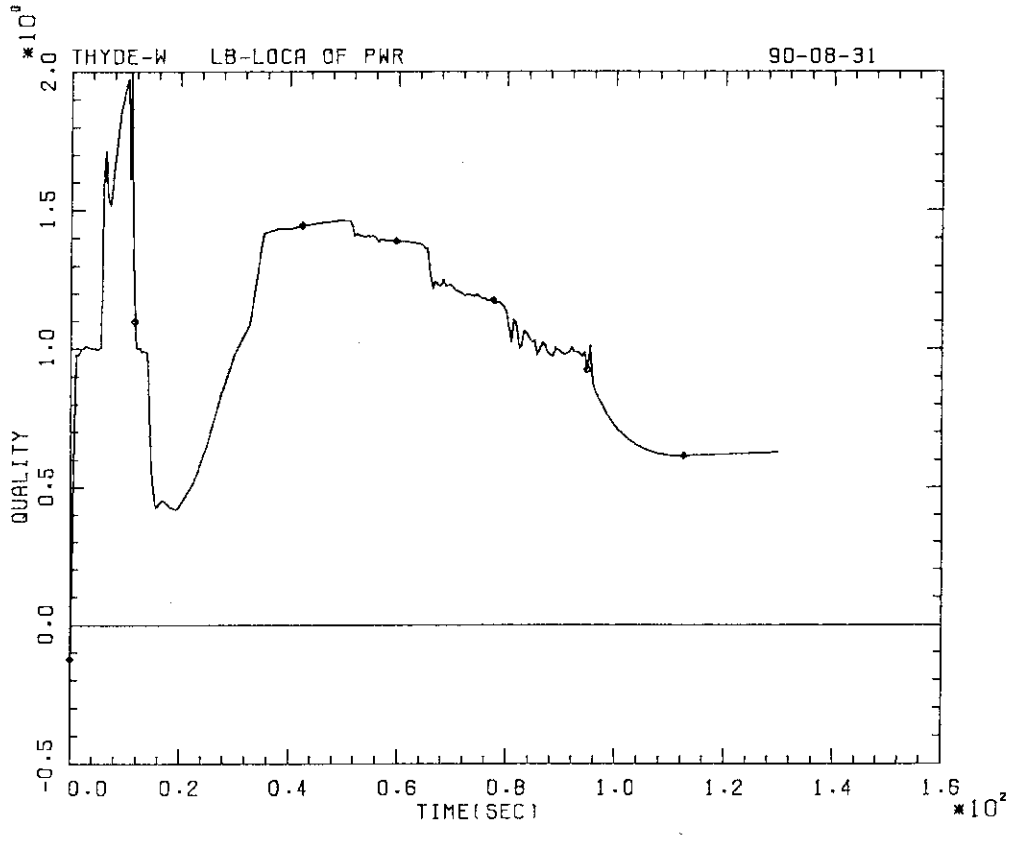

Fig. 11－3－24 Core Quality (node 45) (Sample Problem)

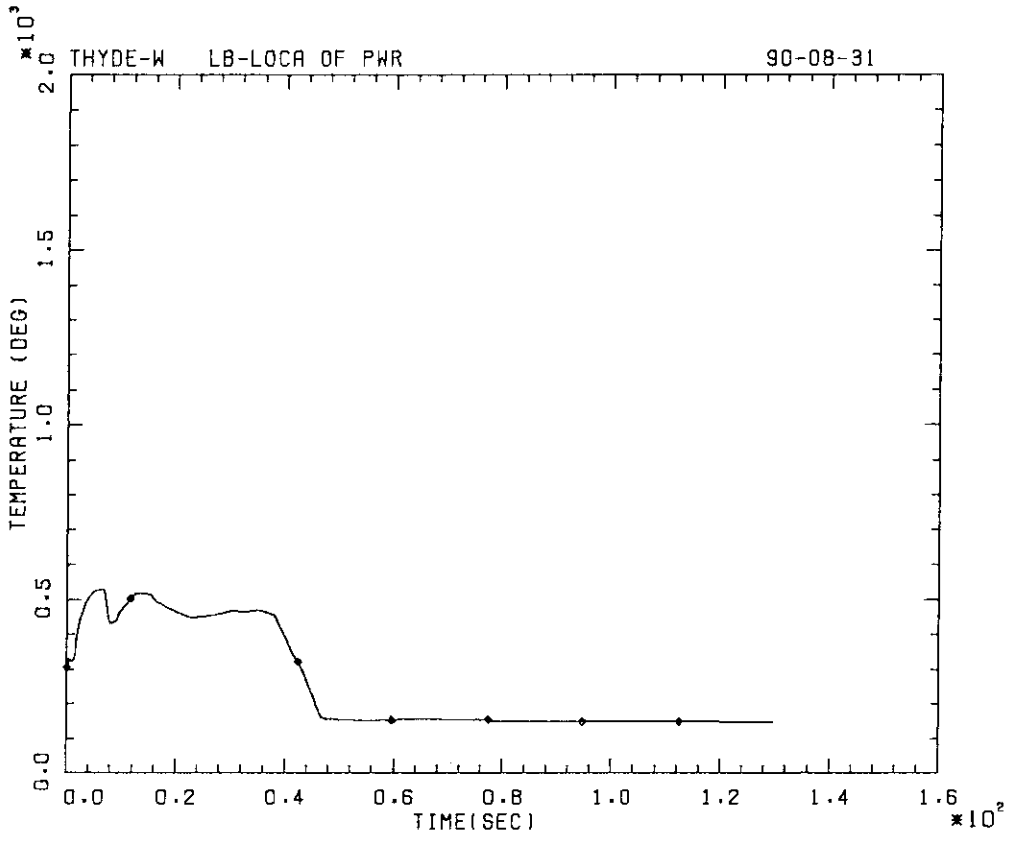

Fig. 11-3-25 Clad Surface Temperature (HC 2) (Sample Problem)

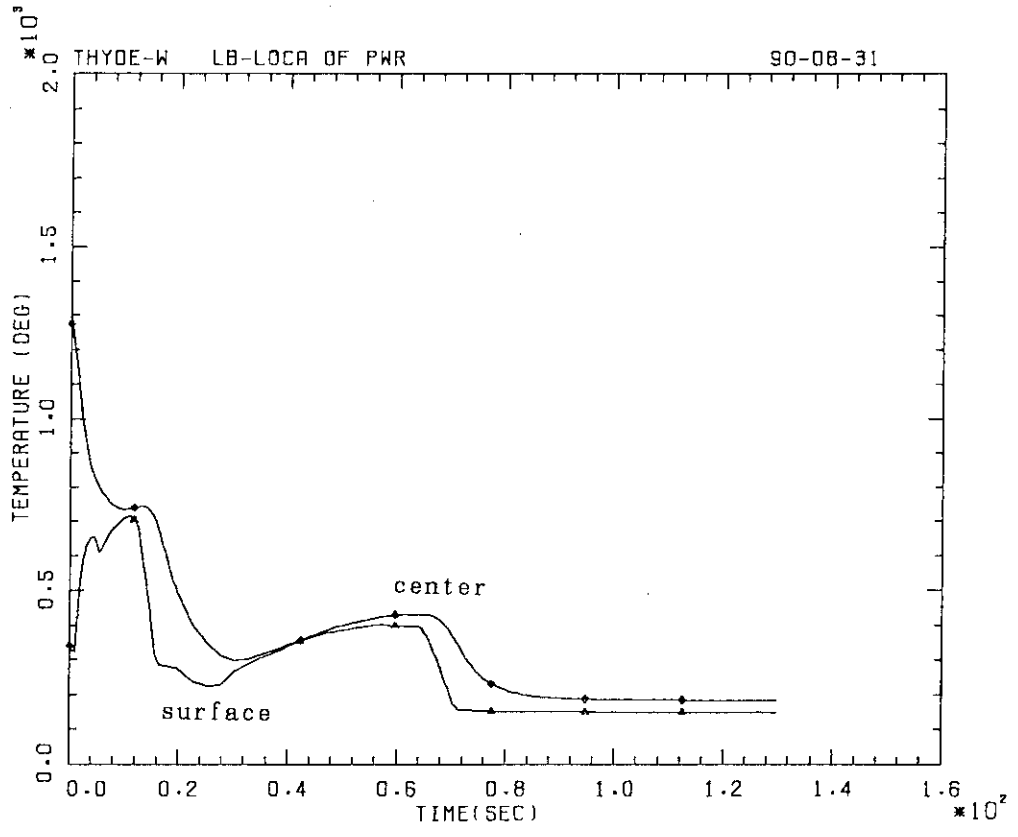

Fig. 11-3-26 Fuel Center and Clad Surface Temperatures (HC 5) (Sample Problem)

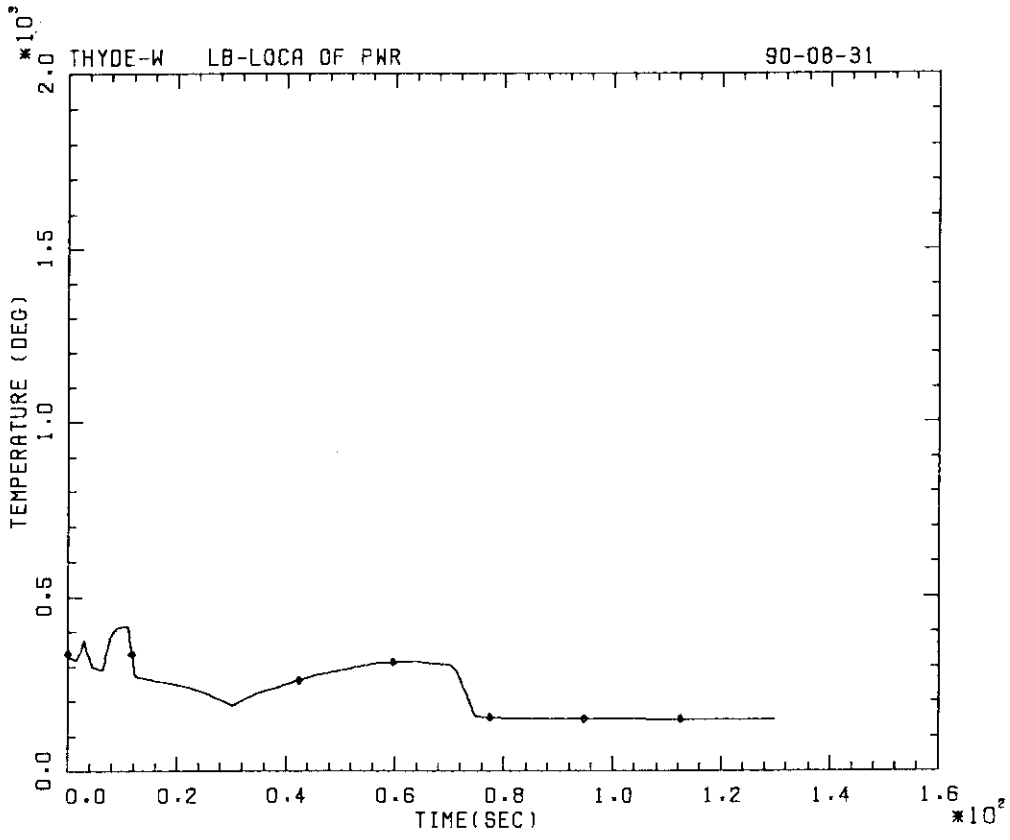

Fig. 11-3-27 Clad Surface Temperature (HC 6) (Sample Problem)

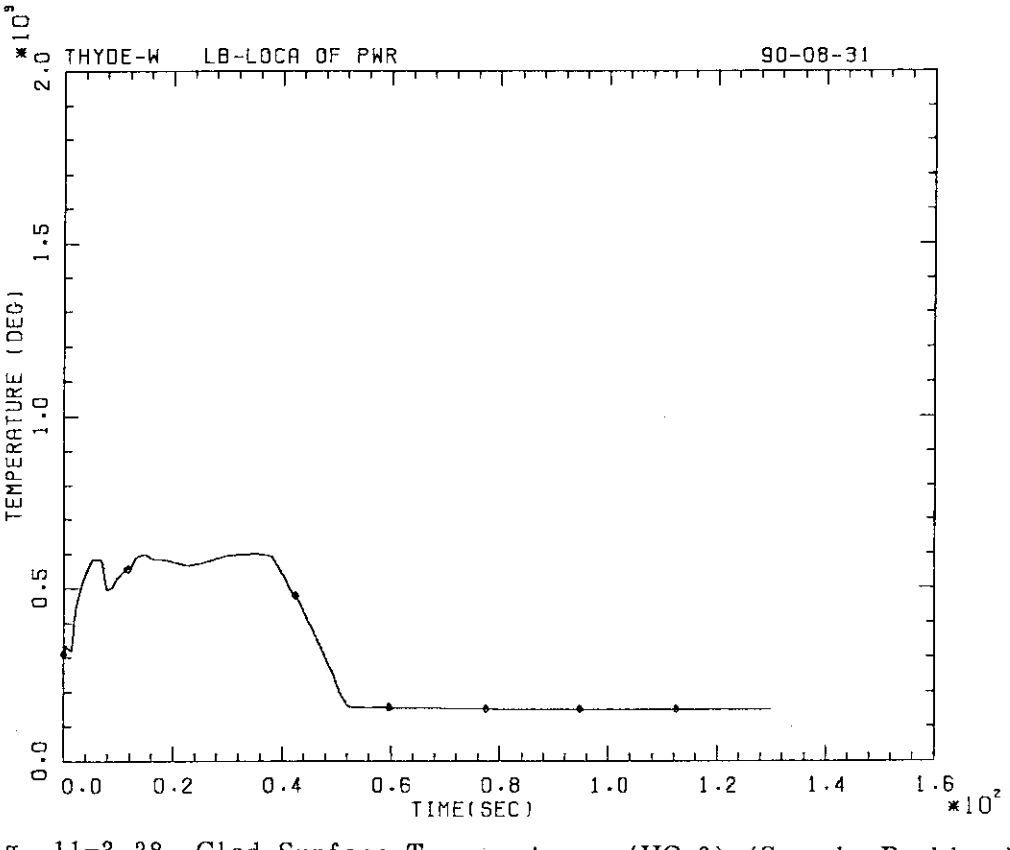

Fig. 11-3-28 Clad Surface Temperature (HC 9) (Sample Problem)

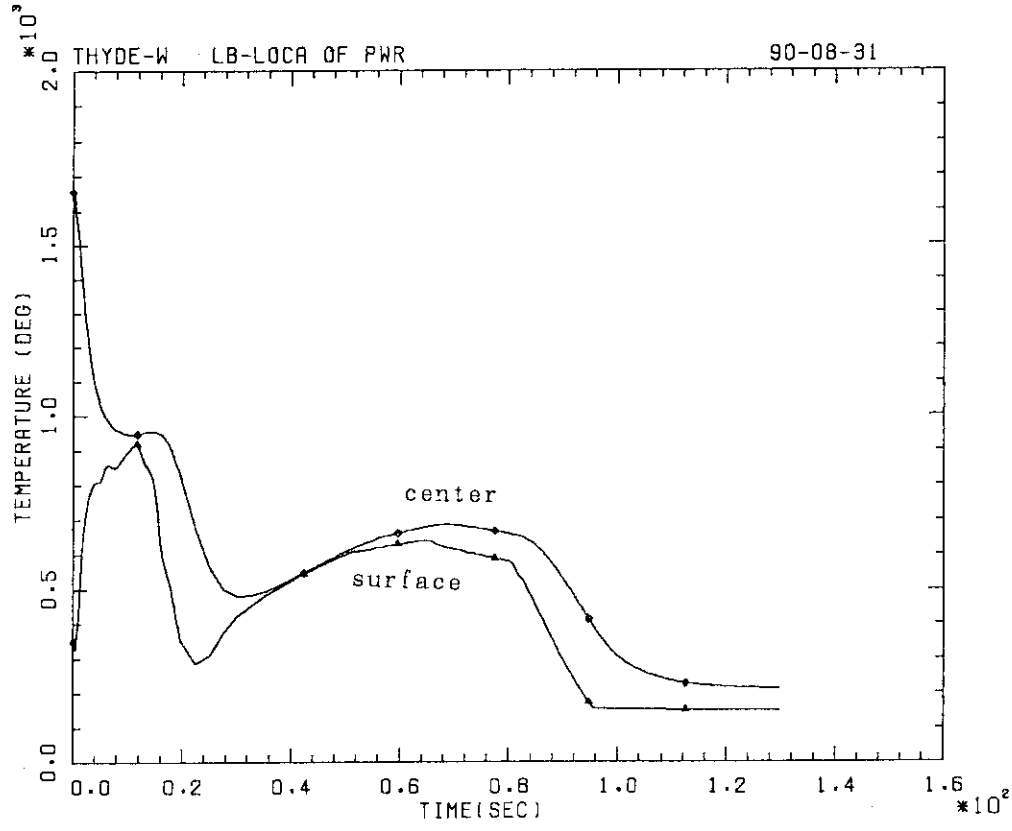

Fig. 11－3－29 Fuel Center and Clad Surface Temperatures (HC 12) (Sample Problem)

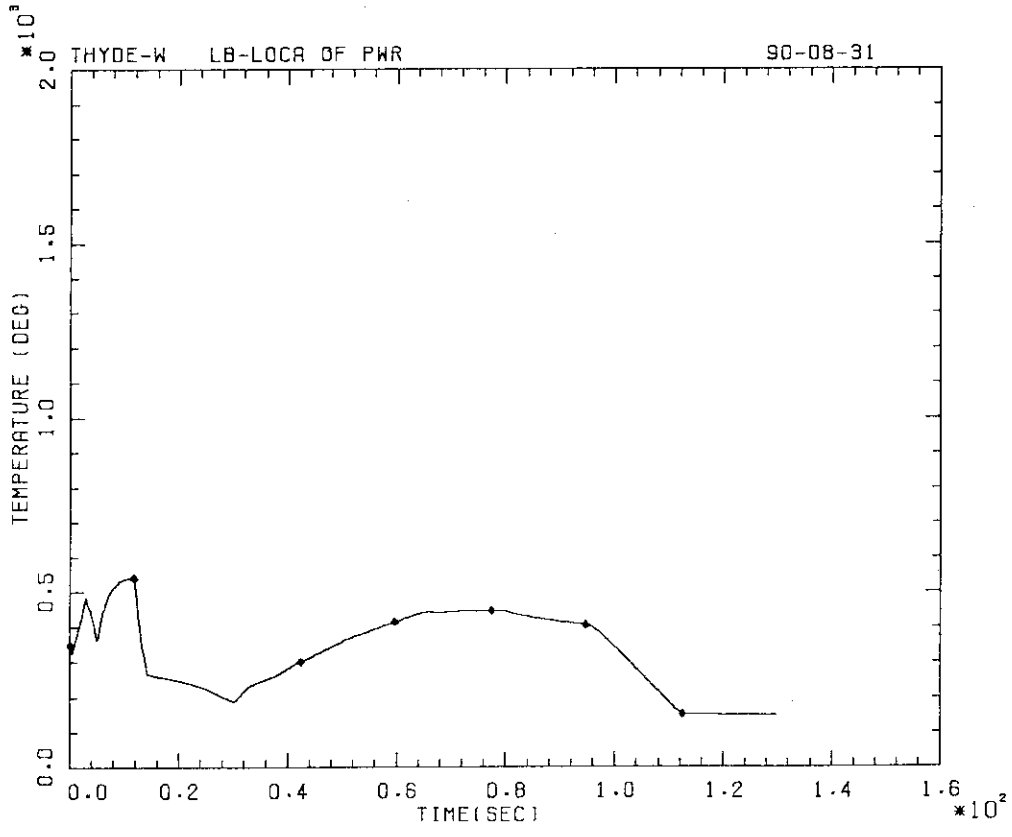

Fig. 11－3－30 Clad Surface Temperature (HC 13) (Sample Problem)

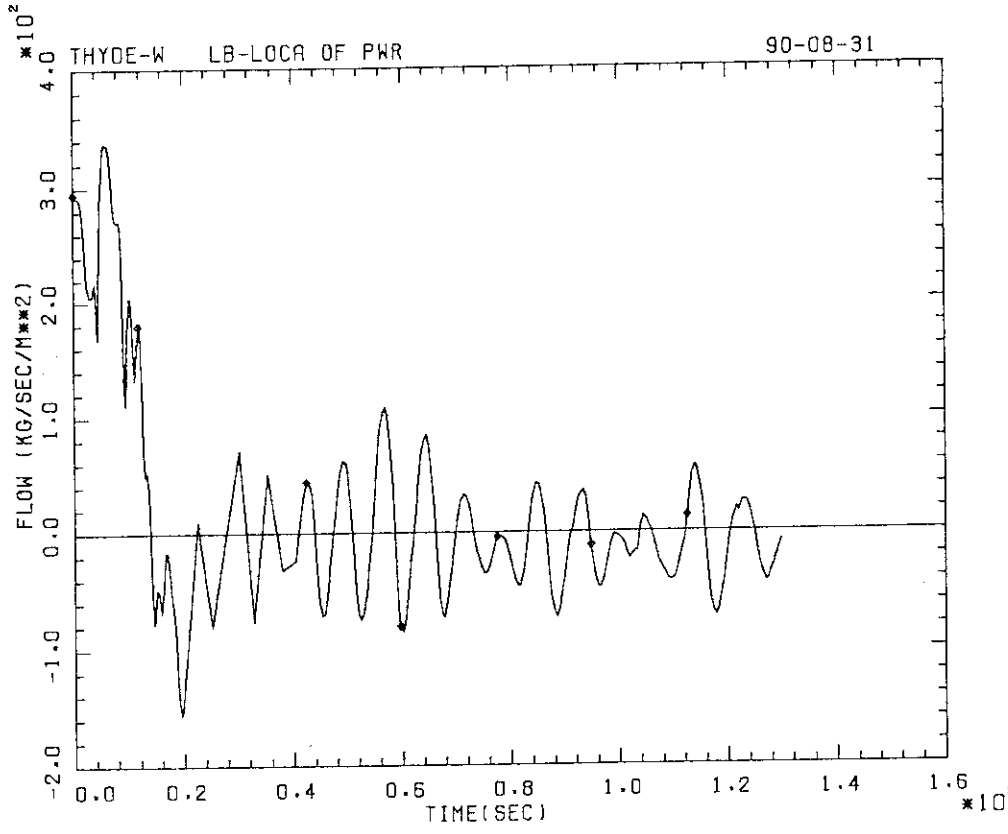

Fig. 11－3－31 SG Secondary Flow (Sample Problem)

12. Concluding Remarks

In RCS transients, the coolant can be regarded as the medium which combines various phenomena taking place in various parts of a RCS. Thus, in RCS transient analyses, we have to obtain coolant behaviors as correctly as possible. This means that since coolant behaviors are governed by the conservation laws, we have to solve the conservation equations as correctly as possible so that mass, energy and momentum conserve. To this end, two requirements must be satisfied , i.e., (1) the conservation equations are spatially differenced so that they retain conservative forms, and (2) the resulting equations are solved "exactly". In the course of the development of THYDW-W, it has been found that these rather mathematical requirements act as a guide to develop physical models.

The first requirement was satisfied by the new space differencing scheme. It is new in that the scheme leads to the new thermal-hydraulic network model, that is, the conservation equations are reduced by three steps, each corresponding to the geometrical features of the system. Especially, it should be noted that the rank of the finally reduced equation is determined solely by the geometrical feature of the network. Therefore, the programming of the three step reduction turned out to be rather straightforward regardless of the degree of network complexity.

The second requirement can be satisfied, only if a nonlinear implicit method with a strict convergence criterion is applied. The nonlinear implicit method of THYDE-W is based on the three step reduction procedure of the new thermal-hydraulic network model. To be practical, the nonlinear implicit scheme must converge as rapidly as possible under any realistically possible circumstances. Therefore, first of all, it was necessary to ensure continuity of all the parameters contained in the

conservation equations. Non-convergence of the nonlinear implicit scheme was solved not always by interpolating the parameter in question, but sometimes only by developing new physical models. For example, the relaxation model for void fraction was developed under certain assumptions concerning thermal non-equilibrium between the two phases. This model is vitally needed to overcome what is sometimes called the "water packing" problem.

There are several items which should be improved with THYDE-W. One of them is to refine the non-equilibrium model presented in section 2.2. In subsection 2.2.1, given h and p for a two-phase mixture, an equilibrium state was defined, but sometimes it is not a true equilibrium state, since the liquid or vapor phase is not necessarily at saturation temperature. Moreover, in deriving the relaxation model for void fraction α, several assumptions were made. They must be scrutinized.

The capabilities of THYDE-W is clearly shown in chapter 11, where the calculated results for a 1,100 MWe PWR LB-LOCA are presented. The BE calculation was made by a FACOM VP2600 computer untill 129.8 sec (physical time). It should be noted that a through calculation of the LB-LOCA was succesfully made without any artificial assumption, i.e., those cited in section 3.2. The overall tendency of the calculated result is very similar to that of LOFT L2-3[49,53] experiment, which was performed to simulate an LB-LOCA of a commercial PWR.

In view of the fact that THYDE-W is capable of a through calculation of an LB-LOCA, which is regarded as the most critical for testing methods and models for thermal-hydraulics, it is expected that there will be a great deal of possibilities[50,51,54,55] of THYDE-W applications to variuos RCS transient analyses.

Acknowledgment

The authors would like to express their sincere thanks to the other members of former Reactor Safety Evaluation Laboratory of JAERI, with whom they enjoyed fruitful discussions in the course of the work. The authors' thanks are also due to the members of NEDAC, who scrutinized the programming of THYDE-W in detail.

References

1) "Keisui-Gata Doryoku-ro no Hizyo-yo Roshin-Reikyaku-kei no Anzen-Hy Shishin" (translated title, "Safety Evaluation Guide Line for Emergency Core Cooling Systems of Light-Water-Cooled Nuclear Power Reactors") Committee on Reactor Safety Examination, Japanese Atomic Energy Commission, May 24, 1974, (revised in April 15, 1975)

2) Esposito, V. J., Kesavan, K. and Maul, B., "WFLASH - A FORTRAN-I Computer Program for Simulation of Transients in a Multi-Loop PWR" (Rev. 2), WCAP-8200, Westinghouse Electric Corporation (June, 1974).

3) Porsching, T. A., Murphy, J. H., Redfield, J. A., and Davis, V. C., "FLASH-4: A Fully Implicit FORTRAN-IV Program for the Digital Sim lation of Transients in a Reactor Plant", WAPD-TM-840, Bettis Atomic Power Laboratory (March, 1969).

4) Bordelon, F. M., et al, "SATAN-IV Program: Comprehensive Space-Ti Dependent Analysis of Loss-of-Coolant", WCAP-8302, (June, 1974).

5) Bordelon, F. M., et al, "LOCTA-IV Program: Loss-of-Coolant Tran- sient Analysis", WCAP-8305, (June, 1974).

6) Collier, G., et al, "Calculational Model for Core Reflooding after a Loss of Coolant accident (WREFLOOD Code)", WCAP-8170, (June,1974).

7) "TRAC-P1A : An advanced best estimate computer program for PWR LO analysis", Safety Code Develop. Group, Energy Div., Los Alamos Sci.

Lab., LA-7777-MS, NUREG/CF-0665,(1979)

8) Steinhoff,F., "DRUFAN-02 intrim program description", GRS-A685; GRS-A714,(1982)

9) "WREM : Water Reactor Evaluation Model (Rev. 1)", NUREG-75/056, USNRC, (May, 1975).

10) "General Electric Company Analytical Model for Loss-of-Coolant Analysis in Accordance with 10 CFR 50 Appendix K", NEDO-20566, (197

11) Zuber, N. and Staub, F. W., Ncl. Sci. and Eng., 30, 268 (1967).

12) Harmathy, T., AICHE Journal, 6, 281 (1960).

13) Peebles, F. N., and Garber, H. J., Chem, Eng. Sci., 49, 88 (1953).

14) Bordelon, F. M., Murphy, E. T., "Containment Pressure Analysis Code (COCO)", WCAP-8326, (June, 1974).

15) Zaloudek, F. R., "Steam-Water Critical Flow High Pressure Systems", HW-68936, Hanford Works (1964).

16) Zaloudek, F. R., "The Critical Flow of Hot Water through Short Tubes", HW-77594, Hanford Works (1963).

17) Moody, F. J., "Maximum Flow Rate of Single Component, Two-Phase Mixture", ASME, Paper No. 64-HT-35.

18) Porsching, T. A., Murphy, J. H., and Redfield, J. A., "Stable Numerical Integration of Conservation Equations for Hydraulic Networks", Ncl. Sci. and Eng., 43, 218-225 (1971).

19) Baron, R. C., "Digital Model Simulation of a Nuclear Pressurizer", Ncl. Sci. and Eng., 52, 283-291 (1973).

20) Boyd, G. M., Jr., Rosser, R. M., Cardwell, B. B., Jr., "Transient Flow Performance in a Multiloop Nuclear Reactor System", Ncl. Sci. and Eng., 9, 442-454, (1961).

21) Streeter, V. L., and Wylie, F. B., "Hydraulic Transients", McGraw-Hill, New York (1967).

22) Shure, K., "Fission Product Decay Energy", Report WAPD-BT-24, Westinghouse Atomic Power Division, (1961).

23) Proposed American Nuclear Society Standard - "Decay Energy Release Rates following Shutdown of Uranium-Fueled Thermal Reactors", approved by Subcommittee ANS-5, ANS Standard Committee, (October 1971, revised October 1973).

24) Perkins, J. F., King, R. W., "Energy Release from Decay of Fission Products", Ncl. Sci. and Eng. 3, 726-46, (1958).

25) Stehn, J. R., Clancy, E. F., "Fission Product Radioactivity and Heat Generation" in "Proceedings of the Second United Nations Internationa

Conference on the Peaceful Uses of Atomic Energy, Geneva 1958", vol. 13, PP. 49-54, United Nations, Geneva, (1958).

26) Baker, L., Just, L. C., "Studies of Metal Water Reactions at High Temperatures, iii. Experimental and Theoretical Studies of the Zirconium-Water Reaction", ANL-6548, (May, 1962).

27) Dean, R. A., "Thermal Contact Conductance Between UO_2 and Zircaloy-2", CVNA-127, (1962).

28) Ross, A. M., and Stoute, R. L., "Heat Transfer Coefficient Between UO_2 and Zircaloy-2", Report AECL-1552, (CRFD-1075), Chalk River, Ontario, (June, 1962).

29) Brokaw, R. S., "Alignment Charts for Transport Properties, Viscosity, Thermal Conductivity and Diffusion Coefficients for Nonpolar Gases and Gas Mixtures at Low Density", Report NASA TR R- (1961).

30) Hottel, H. C., "Radiation Heat Transmission", Chapter 4 or "Heat Transmission" by W. H. McAdams, McGraw-Hill, (1954).

31) Dittus, F. W., and Boelter, L. M. K., "Heat Transfer in Automobile Radiators of the Tubular Tube", 2, No. 13, P. 443-461. (1930).

32) Jens, W. H. and Lottes, "Analysis of Heat Transfer, Burnout, Pressur Drop and Density Data for High-Pressure Water", ANL-4627 (1951).

33) Slifer, B. C. and Hench, J. E., "Loss-of-Coolant Accident and

Emergency Core Cooling Models for General Electric Boiling Water" Reactors, NEDO-10329, General Electric Company, Equation C-32, (April, 1971).

34) Groeneveld, D. C., "An Investigation of Heat Transfer in the Liquid Deficient Regime", Report AECL-3281, Chalk Rever, Ontario, (Decemb 1968) (Revised December 1969 by E. O. Moeck).

35) McEligot, D. M., Ormand, L. W. and Perkins, H. C. Jr., Trans. Amer Soc. Mech. Engrs., 88, Series C, p. 239-245, (May, 1966).

36) McAdams, W. H., "Heat Transmission", 3rd Ed., P. 337, McGraw-Hill New York (1954).

37) Fishenden, M. and Saunders, O. A., "An Introduction to Heat Transfer ,p. 97, Oxford Univ. Press, London (1950).

38) Cadek, F. F., Dominicis, D. P., Leyse, R. H., "PWR FLECHT (Full Length Emergency Cooling Heat Transfer) Final Report", WCAP 7665,. (April 1971)..

39) Cadek, F. F., et al., "PWR FLECHT Final Report Supplement", WCAP-7931, (October, 1972).

40) Thom, J. R. S. et al., "Boiling in Subcooled Water During Flow Up Heated Tubes or Annuli", Proc. Instn. Mech. Engrs., Vol. 180, Part 3c, pp. 226-246, 1966.

41) Hardy, D. G., "High Temperature Expansion and Rupture Behavior of Zircaloy Tubing", National Topical Meeting on Water-Reactor Safety, Salt Lake City, Utah, (March, 1973).

42) Weir, J. R. Jr., et al, "Certain Aspects of LWR Fuel Pins During a LOCA", ORNL-CF-72-11-1.

43) Asahi,Y., Asaka,H., "New Non-equilibrium Thermal-Hydraulic Model, (2) : Application to LOFT L2-3", J. Nucl. Sci. Tech., 21(10),(1984)

44) Asahi,Y., "Description of THYDE-P Code (Preliminary Report of Meth and Models)",JAERI-M7751,(1978)

45) Taylor,G.I. : Proc. Roy. Soc. (London), A210, 192(1950)

46) Biasi,L., et al. "Studies on burnout", Part 3, Energ. Nucl. (Milan) 550-536 (1967).

47) Zuber,N., et al. "The Hydrodynamic Crisis in Pool Boiling of Saturated and Subcooled Liquids", International Developments in Heat Transfer, Part II, pp 230-236, 1961

48) Kanazawa,M. et al.,"A Through Calculation of 1,100 MWe PWR Large Break LOCA by THYDE-P1 EM Model", JAERI-M 84-132, 1984

49) Asahi.Y., et al.,"New Non-Equilibrium Thermal-Hydraulic Model ; (II) Application to LOFT L2-3", J. of Nucl. Sci. and Tech. 21(10), Oct. 1984

50) Harami.T., et al.,"A Safety Analysis of Research Reactor JRR-3", Int. Meeting on Reduced Enrichment for Research and Test Reactors (RERTER), Petten, The Netherlands, 14-16 Oct. 1985

51) Asahi.Y., and H. Wakabayashi, "Some Transient Characteristics of PIUS", Nuclear Technology, Vol. 72, pp.24-33, Jan. 1986

52) Asai,Y. and K.Tsuchihashi,"A Subroutine Reading Data in Free Format JAERI-M4458, May 1971

53) Prassions,P.G, "Experimental data report for LOFT power ascension test L2-3",NUREG/CR-0792, TREE-1326,(1979)

54) Asahi,Y., T. Watanabe and H. Wakabayashi, "Improvement of Pasive Safety of Reactors", Nucl. Sci. Eng., 96, 73-84(1987)

55) Asahi et al., "Conceptual Design of the Integrated Reactor with Inherent Safety", Nuclear Technology, Vol. 91, pp.28-50, July 1990

Appendix A Jacobian Elements

A.1 Partial Derivatives of h_n^A and h_n^E

(a) Partial Derivatives of h_n^A

Derivatives of h_n^A can be obtained from Eq.(2-2-69) as follows.

(1) if the from-junction is volumeless and open (but not a break), then

$$\frac{\partial h_n^A}{\partial h_n^{av}} = 0$$

$$\frac{\partial h_n^A}{\partial h_{from}^+} = 1$$

and

$$\frac{\partial h_n^A}{\partial h_{to}^+} = 0 \quad .$$

(2) If the from-junction is a break, then

$$\frac{\partial h_n^A}{\partial h_n^{av}} = 0 \qquad if\ (G_n^A)^{old} > 0,$$

$$= \frac{\Delta t}{\Delta t + \tau_h^A} \qquad otherwise.$$

$$\frac{\partial h_n^A}{\partial h_{from}^+} = 0$$

and

$$\frac{\partial h_n^A}{\partial h_{to}^+} = 0 \quad .$$

(3) If the from-junction is a mixing junction, then

$$\frac{\partial h_n^A}{\partial h_n^{av}} = 0 \qquad if\ (G_n^A)^{old} > 0,$$

$$= \frac{\Delta t}{\Delta t + \tau_h^A} \qquad otherwise.$$

$$\frac{\partial h_n^A}{\partial h_{from}^+} = \frac{\Delta t}{\Delta t + \tau_h^A} \qquad if\ (G_n^A)^{old} > 0,$$

$$= 0 \qquad otherwise.$$

and

$$\frac{\partial h_n^A}{\partial h_{to}^+} = 0 \quad .$$

(4) If the from-junction is closed, then

$$\frac{\partial h_n^A}{\partial h_n^{av}} = 0$$

$$\frac{\partial h_n^A}{\partial h_{from}^+} = 0$$

and

$$\frac{\partial h_n^A}{\partial h_{to}^+} = 0 \quad .$$

(b) Partial Derivatives of h_n^E

Derivatives of h_n^E can be obtained from Eq.(2-2-70) as follows.

(1) If the to-junction is volumeless and open (but not a break), then

$$\frac{\partial h_n^E}{\partial h_n^{av}} = 0$$

$$\frac{\partial h_n^E}{\partial h_{from}^+} = 0$$

and

$$\frac{\partial h_n^E}{\partial h_{to}^+} = 1 \quad .$$

(2) If the to-junction is a mxing junction or a boundary junction, then

$$\frac{\partial h_n^E}{\partial h_n^{av}} = 0 \qquad if\ (G_n^E)^{old} \leqq 0,$$

$$= \frac{\Delta t}{\Delta t + \tau_h^E} \qquad otherwise.$$

$$\frac{\partial h_n^E}{\partial h_{from}^+} = 0$$

and

$$\frac{\partial h_n^E}{\partial h_{to}^+} = \frac{\Delta t}{\Delta t + \tau_h^E} \qquad if\ (G_n^E)^{old} \leqq 0,$$

$$= 0 \qquad otherwise.$$

(3) If the to-junction is a break, then

$$\frac{\partial h_n^E}{\partial h_n^{av}} = 0 \qquad if\ (G_n^E)^{old} \leqq 0,$$

$$= \frac{\Delta t}{\Delta t + \tau_h^E} \qquad otherwise.$$

$$\frac{\partial h_n^E}{\partial h_{from}^+} = 0$$

and

$$\frac{\partial h_n^E}{\partial h_{to}^+} = 0 \quad .$$

(4) If the to-junction is closed, then always

$$\frac{\partial h_n^E}{\partial h_n^{av}} = 0$$

$$\frac{\partial h_n^E}{\partial h_{from}^+}=0$$

and

$$\frac{\partial h_n^E}{\partial h_{to}^+}=0 \quad .$$

A.2 Node Jacobian J_n

In this section, only for the sake of clarity, let a break mean a break under a critical mass flow condition.

(a) Derivatives of $(f_1)_n$

Differentiating Eq.(2-3-4), we obtain;

$$(j_{11})_n=1$$

$$(j_{12})_n=-\frac{L_n}{2\Delta t}\left(\frac{\partial \rho}{\partial p}\right)_n^{av}$$

$$(j_{13})_n=-1$$

$$(j_{14})_n=-\frac{L_n}{2\Delta t}\left(\frac{\partial \rho}{\partial p}\right)_n^{av}$$

and

$$(j_{15})_n=-\frac{L_n}{\Delta t}\left(\frac{\partial \rho}{\partial h}\right)_n^{av} \quad .$$

(b) Derivatives of $(f_2)_n$

If the to-junction is not a "break", then Eq.(2-3-5) gives ;

$$(j_{21})_n=-(\xi_n^A)^2\frac{G_n^A}{\rho_n^A}-\frac{1}{2}\left(\frac{\Phi^2}{\rho_f}\right)_n^A\frac{\partial}{\partial G_n^A}K_n^A$$

$$(j_{22})_n=(\xi_n^A)^2\left[-1+\frac{1}{2}\left(\frac{G_n^A}{\rho_n^A}\right)^2\left(\frac{\partial\rho}{\partial p}\right)_n^A-\frac{1}{2}\left(\frac{\partial B}{\partial p}\right)_n^A\right]-\frac{\kappa_n^A}{2}\left(\frac{\partial}{\partial p}\frac{\Phi^2}{\rho_f}\right)_n^A$$

$$(j_{23})_n=0$$

$$(j_{24})_n=0$$

and

$$(j_{25})_n=\frac{(\xi_n^A)^2}{2}\left[\left(\frac{G_n^A}{\rho_n^A}\right)^2\left(\frac{\partial\rho}{\partial h}\right)_n^A-\left(\frac{\partial B}{\partial h}\right)_n^A\right]\frac{\partial h_n^A}{\partial h_n^{av}}-\frac{\kappa_n^A}{2}\left(\frac{\partial}{\partial h}\frac{\Phi^2}{\rho_f}\right)_n^A\frac{\partial h_n^A}{\partial h_n^{av}}\quad .$$

If the to-junction is a "break", then Eq.(2-3-5a) gives ;

$$(j_{21})_n=\frac{f_B(p_n^A,G_n^A+\Delta G_n^A,h_n^A)-f_B(p_n^A,G_n^A,h_n^A)}{\Delta G_n^A}$$

$$(j_{22})_n=\frac{f_B(p_n^A+\Delta p_n^A,G_n^A,h_n^A)-f_B(p_n^A,G_n^A,h_n^A)}{\Delta p_n^A}$$

$$(j_{23})_n=0$$

$$(j_{24})_n=0$$

and

$$(j_{25})_n=\frac{\left[f_B(p_n^A,G_n^A,h_n^A+\Delta h_n^A)-f_B(p_n^A,G_n^A,h_n^A)\right]\partial h_n^A/\partial h_n^{av}}{\Delta h_n^A}\quad .$$

(c) Derivatives of $(f_3)_n$

There are three cases, depending on the type of the to-junction ; (1) a "break", (2) a G-source and (3) all others including p-sources.

Case 1 : The to-junction is neither a "break" nor a G-source.

Equation (2-3-6) gives ;

$$(j_{31})_n=0$$

$$(j_{32})_n=0$$

$$(j_{33})_n=(\xi_n^E)^2\left(\frac{G_n^E}{\rho_n^E}-\frac{\partial p_{to}^+}{\partial G_n^E}\right)-\frac{1}{2}\left(\frac{\Phi^2}{\rho_f}\right)_n^E\frac{\partial}{\partial G_n^E}\kappa_n^E$$

$$(j_{34})_n=(\xi_n^E)^2\left[1-\frac{1}{2}\left(\frac{G^2}{\rho}\right)_n^E\left(\frac{\partial \rho}{\partial p}\right)_n^E+\frac{1}{2}\left(\frac{\partial B}{\partial p}\right)_n^E-\frac{\partial p_{to}^+}{\partial p_n^E}\right]-\frac{\kappa_n^E}{2}\left(\frac{\partial}{\partial p}\frac{\Phi^2}{\rho_f}\right)_n^E$$

$$(j_{35})_n=(\xi_n^E)^2\left[-\frac{1}{2}\left(\frac{G_n^E}{\rho_n^E}\right)^2\left(\frac{\partial \rho}{\partial h}\right)_n^E+\frac{1}{2}\left(\frac{\partial B}{\partial p}\right)_n^E-\frac{\partial p_{to}^+}{\partial h_n^E}\right]\frac{\partial h_n^E}{\partial h_n^{av}}$$

$$-\frac{\kappa_n^E}{2}\left(\frac{\partial}{\partial h}\frac{\Phi^2}{\rho_f}\right)_n^E\frac{\partial h_n^E}{\partial h_n^{av}}$$

In THYDE-W, only p(G)- or p(t)-source is considered (see BB13) so that we can set in the above

$$\frac{\partial p_{to}^+}{\partial h_n^E}=0$$

and

$$\frac{\partial p_{to}^+}{\partial p_n^E}=0 \quad .$$

Case 2 : The to-junction is a "break".

Equation (2-3-6a) gives ;

$$(j_{31})_n=0$$

$$(j_{32})_n=0$$

$$(j_{33})_n=\frac{f_B(p_n^E,G_n^E+\Delta G_n^E,h_n^E)-f_B(p_n^E,G_n^E,h_n^E)}{\Delta G_n^E}$$

$$(j_{34})_n=\frac{f_B(p_n^E+\Delta p_n^E,G_n^E,h_n^E)-f_B(p_n^E,G_n^E,h_{nN}^E)}{\Delta p_n^E}$$

and

$$(j_{35})_n=\frac{\left[f_B(p_n^E,G_n^E,h_n^E+\Delta h_n^E)-f_B(p_n^E,G_n^E,h_n^E)\right]\partial h_n^E/\partial h_n^{av}}{\Delta h_n^E} \quad .$$

Case 3 : The to-junction is a G-source.

Equation (2-3-6b) gives ;

$$(j_{31})_n = 0$$

$$(j_{32})_n = 0$$

$$(j_{33})_n = 1$$

$$(j_{34})_n = -\frac{\partial G}{\partial p_n^E}$$

and

$$(j_{35})_n = -\frac{\partial G}{\partial h_n^E}\frac{\partial h_n^E}{\partial h_n^{av}} \quad .$$

In THYDE-W, we consider only G(t)- or G(p)-source (see BB13) so that we can set in the above

$$\frac{\partial G}{\partial h_n^E} = 0 \quad .$$

(d) Derivatives of $(f_4)_n$

Differentiating Eq.(2-3-7), we obtain ;

$$(j_{41})_n = \frac{2G_n^A}{\rho_n^A} - \frac{1}{4}\left(\frac{\Phi^2}{\rho_f}\right)_n^{av}\frac{\partial}{\partial G_n^{av}}\left[\ \kappa_n^{av} + \frac{f_n^{av}L_n}{D_n G_n^{av}}\,|\,G_n^{av}\,|\ \right] - \frac{L_n}{2\Delta t}$$

$$+ \frac{g}{2}\left(\frac{\partial}{\partial G}\rho L_{head}\right)_n^{av}$$

$$(j_{42})_n = 1 - \left(\frac{G_n^A}{\rho_n^A}\right)^2\left(\frac{\partial \rho}{\partial p}\right)_n^A + \left(\frac{\partial B}{\partial p}\right)_n^A - \frac{1}{4}\left(\kappa_n^{av} + \frac{f_n^{av}L_n}{D_n}\ G_n^{av}\,|\,G_n^{av}\,|\right)\left(\frac{\partial}{\partial p}\frac{\Phi^2}{\rho_f}\right)_n^{av}$$

$$+ \frac{g}{2}\left(\frac{\partial}{\partial p}\rho L_{head}\right)_n^{av}$$

$$(j_{43})_n = -\frac{2G_n^E}{\rho_n^E} - \frac{1}{4}\left(\frac{\Phi^2}{\rho_f}\right)_n^{av}\frac{\partial}{\partial G_n^{av}}\left(\kappa_n^{av} + \frac{f_n^{av}L_n}{D_n}\ G_n^{av}\,|\,G_n^{av}\,|\right) - \frac{L_n}{2\Delta t}$$

$$+ \frac{g}{2}\left(\frac{\partial}{\partial G}\rho L_{head}\right)_n^{av}$$

$$(j_{44})_n = -1 + \left(\frac{G_n^E}{\rho_n^E}\right)^2 \left(\frac{\partial \rho}{\partial p}\right)_n^E - \left(\frac{\partial B}{\partial p}\right)_n^E - \frac{1}{4}\left(\kappa_n^{av} + \frac{f_n^{av} L_n}{D_n} G_n^{av} \mid G_n^{av} \mid\right)\left(\frac{\partial}{\partial p}\frac{\Phi^2}{\rho_f}\right)_n^{av}$$

$$+ \frac{g}{2}\left(\frac{\partial}{\partial p}\rho L_{head}\right)_n^{av}$$

and

$$(j_{45})_n = \left[-\left(\frac{G_n^A}{\rho_n^A}\right)^2 \left(\frac{\partial \rho}{\partial h}\right)_n^A + \left(\frac{\partial B}{\partial h}\right)_n^A\right] \frac{\partial h_n^A}{\partial h_n^{av}} - \left[-\left(\frac{G_n^E}{\rho_n^E}\right)^2 \left(\frac{\partial \rho}{\partial h}\right)_n^E + \left(\frac{\partial B}{\partial h}\right)_n^E\right] \frac{\partial h_n^E}{\partial h_n^{av}}$$

$$- \frac{1}{2}\left(\kappa_n^{av} + \frac{f_n^{av} L_n}{D_n} G_n^{av} \mid G_n^{av} \mid\right)\left(\frac{\partial}{\partial h}\frac{\Phi^2}{\rho_f}\right)_n^{av} + g\left(\frac{\partial}{\partial h}\rho L_{head}\right)_n^{av} .$$

(e) Derivatives of $(f_5)_n$

Differentiating Eq.(2-3-8), we obtain ;

$$(j_{51})_n = \frac{h_n^A}{L_n}$$

$$(j_{52})_n = -\frac{h_n^{av}}{2\Delta t}\left(\frac{\partial \rho}{\partial h}\right)_n^{av}$$

$$(j_{53})_n = \frac{h_n^E}{L_n}$$

$$(j_{54})_n = -\frac{h_n^{av}}{2\Delta t}\left(\frac{\partial \rho}{\partial h}\right)_n^{av}$$

and

$$(j_{55})_n = \frac{G_n^A}{L_n}\frac{\partial h_n^A}{\partial h_n^{av}} - \frac{G_n^E}{L_n}\frac{\partial h_n^E}{\partial h_n^{av}} - \frac{\rho_n^{av} + h_n^{av}(\partial \rho / \partial h)_n^{av}}{\Delta t} .$$

A.3 Matrix $(b_{ij})_n$ *(i, j = to , from)*

To obtain matrix $(b_{ij})_n$ given by Eq.(2-3-4), we first have to obtain matrices

$$r_n = \begin{bmatrix} \partial f_n / \partial \chi_{from}^+ \\ \partial f_n / \partial \chi_{to}^+ \end{bmatrix}$$

and

$$l_n=\begin{bmatrix} \partial f^+_{from}/\partial x_n \\ \partial f^+_{to}/\partial x_n \end{bmatrix} .$$

(a) Matrix r_n

Let

$$\frac{\partial f_n}{\partial x^+_{from}}=\begin{bmatrix} \partial (f_1)_n/\partial p^+_{from} & \partial (f_1)_n/\partial h^+_{from} \\ \partial (f_2)_n/\partial p^+_{from} & \partial (f_2)_n/\partial h^+_{from} \\ \partial (f_3)_n/\partial p^+_{from} & \partial (f_3)_n/\partial h^+_{from} \\ \partial (f_4)_n/\partial p^+_{from} & \partial (f_4)_n/\partial h^+_{from} \\ \partial (f_5)_n/\partial p^+_{from} & \partial (f_5)_n/\partial h^+_{from} \end{bmatrix}$$

$$=\begin{bmatrix} (r_{11})_n & (r_{12})_n \\ (r_{21})_n & (r_{22})_n \\ (r_{31})_n & (r_{32})_n \\ (r_{41})_n & (r_{42})_n \\ (r_{51})_n & (r_{52})_n \end{bmatrix}$$

and

$$\frac{\partial f_n}{\partial x^+_{to}}=\begin{bmatrix} \partial (f_1)_n/\partial p^+_{to} & \partial (f_1)_n/\partial h^+_{to} \\ \partial (f_2)_n/\partial p^+_{to} & \partial (f_2)_n/\partial h^+_{to} \\ \partial (f_3)_n/\partial p^+_{to} & \partial (f_3)_n/\partial h^+_{to} \\ \partial (f_4)_n/\partial p^+_{to} & \partial (f_4)_n/\partial h^+_{to} \\ \partial (f_5)_n/\partial p^+_{to} & \partial (f_5)_n/\partial h^+_{to} \end{bmatrix}$$

$$=\begin{bmatrix} (r_{13})_n & (r_{14})_n \\ (r_{23})_n & (r_{24})_n \\ (r_{33})_n & (r_{34})_n \\ (r_{43})_n & (r_{44})_n \\ (r_{53})_n & (r_{54})_n \end{bmatrix} .$$

In the following, for the sake of clarity, subscript n for r_{ij} will be dropped. Then, differentiating Eqs.(2-3-4) to (2-3-8), we obtain ;

$$r_{11}=\frac{\partial (f_1)_n}{\partial p^+_{from}}=0$$

$$r_{12}=\frac{\partial (f_1)_n}{\partial h^+_{from}}=0$$

$$r_{13}=\frac{\partial (f_1)_n}{\partial p^+_{to}}=0$$

$$r_{14}=\frac{\partial (f_1)_n}{\partial h_{to}^+}=0$$

$$r_{21}=\frac{\partial (f_2)_n}{\partial p_{from}^+}=0 \qquad \textit{for a break}$$

$$=\frac{\partial (f_2)_n}{\partial p_{from}^+}=(\xi_n^A)_n^2 \qquad \textit{otherwise}$$

$$r_{22}=\frac{\partial (f_2)_n}{\partial h_{from}^+}=0 \qquad \textit{for a break}$$

$$=\frac{\partial (f_2)_n}{\partial p_{from}^+}=(\xi_n^A)^2\left[\left(\frac{G_n^A}{\rho_n^A}\right)^2\left(\frac{\partial \rho}{\partial h}\right)_n^A-\left(\frac{\partial B}{\partial h}\right)_n^A\right]\frac{\partial h_n^A}{\partial h_{from}^+}$$

$$-\frac{\kappa_n^A}{2}\left(\frac{\partial}{\partial h}\frac{\Phi^2}{\rho_f}\right)_n^A\frac{\partial h_n^A}{\partial h_{from}^+} \qquad \textit{otherwise}$$

$$r_{23}=\frac{\partial (f_2)_n}{\partial p_{to}^+}=0$$

$$r_{24}=\frac{\partial (f_2)_n}{\partial h_{to}^+}=0$$

$$r_{31}=\frac{\partial (f_3)_n}{\partial p_{from}^+}=0$$

$$r_{32}=\frac{\partial (f_3)_n}{\partial h_{from}^+}=0$$

$$r_{33}=\frac{\partial (f_3)_n}{\partial p_{to}^+}=0 \qquad \textit{for a break or a G-source}$$

$$=\frac{\partial (f_3)_n}{\partial p_{to}^+}=(\xi_n^E)^2 \qquad \textit{otherwise}$$

$$r_{34}=\frac{\partial (f_3)_n}{\partial h_{to}^+}=\frac{\partial (f_3)_n}{\partial h_n^E}\frac{\partial h_n^E}{\partial h_{to}^+}$$

with

$$\frac{\partial (f_3)_n}{\partial h_n^E} = \frac{f_B(p_n^E, G_n^E, h_n^E + \Delta h_n^E) - f_B(p_n^E, G_n^E, h_n^E)}{\Delta h_n^E} \qquad \textit{for a break}$$

$$= -\frac{\partial G}{\partial h_n^E} \qquad \textit{for a G-source}$$

$$= (\xi_n^E)^2 \left[\frac{1}{2} \left(-\frac{G_n^E}{\rho_n^E} \right)^2 \left(\frac{\partial \rho}{\partial h} \right)_n^E + \frac{1}{2} \left(\frac{\partial B}{\partial h} \right)_n^E - \frac{\partial p_{to}^+}{\partial h_n^E} \right]$$

$$- \frac{\kappa_n^E}{2} \left(\frac{\partial}{\partial h} \frac{\Phi^2}{\rho_f} \right)_n^E \qquad \textit{otherwise}$$

$$r_{41} = \frac{\partial (f_4)_n}{\partial p_{from}^+} = 0$$

$$r_{42} = \frac{\partial (f_4)_n}{\partial h_{from}^+} = \frac{\partial f_{n4}}{\partial h_n^A} \frac{\partial h_n^A}{\partial h_{from}^+}$$

$$= \left[-\left(\frac{G_n^A}{\rho_n^A} \right)^2 \left(\frac{\partial \rho}{\partial h} \right)_n^A + \left(\frac{\partial B}{\partial h} \right)_n^A - \frac{g}{2} \left(\frac{\partial}{\partial h} \rho L_{head} \right)_n^{av} \right.$$

$$\left. - \frac{1}{4} \left(\kappa_n^{av} + \frac{f_n^{av} L_n}{D_n} G_n^{av} \mid G_n^{av} \mid \right) \left(\frac{\partial}{\partial h} \frac{\Phi^2}{\rho_f} \right)_n^{av} \right] \frac{\partial h_n^A}{\partial h_{from}^+}$$

$$r_{43} = \frac{\partial (f_4)_n}{\partial p_{to}^+} = 0$$

$$r_{44} = \frac{\partial (f_4)_n}{\partial h_{to}^+} = \frac{\partial (f_4)_n}{\partial h_n^E} \frac{\partial h_n^E}{\partial h_{to}^+}$$

$$= \left[-\left(\frac{G_n^E}{\rho_n^E} \right)^2 \left(\frac{\partial \rho}{\partial h} \right)_n^E - \left(\frac{\partial B}{\partial h} \right)_n^E \right.$$

$$\left. - \frac{1}{4} \left(\kappa_n^{av} + \frac{f_n^{av} L_n}{D_n} G_n^{av} \mid G_n^{av} \mid \right) \left(\frac{\partial}{\partial h} \frac{\Phi^2}{\rho} \right)_n^{av} + \frac{g}{2} \left(\frac{\partial}{\partial h} \rho L_{head} \right)_n^{av} \right] \frac{\partial h_n^E}{\partial h_{to}^+}$$

$$r_{51}=\frac{\partial (f_5)_n}{\partial p^+_{from}}=0$$

$$r_{52}=\frac{\partial (f_5)_n}{\partial h^+_{from}}=\frac{\partial (f_5)_n}{\partial h^A_n}\frac{\partial h^A_n}{\partial h^+_{from}}=\frac{G^A_n}{L_n}\frac{\partial h^A_n}{\partial h^+_{from}}$$

$$r_{53}=\frac{\partial (f_5)_n}{\partial p^+_{to}}=0$$

and

$$r_{54}=\frac{\partial (f_5)_n}{\partial h^+_{to}}=\frac{\partial (f_5)_n}{\partial h^E_n}\frac{\partial h^E_n}{\partial h^+_{to}}=-\frac{G^E_n}{L_n}\frac{\partial h^E_n}{\partial h^+_{to}}$$

Thus, in general, matrices $\partial f_n/\partial x^+_{from}$ and $\partial f_n/\partial x^+_{to}$ have the following forms,

$$\frac{\partial f_n}{\partial x^+_{from}}=\begin{bmatrix} 0 & 0 \\ r_{21} & r_{22} \\ 0 & 0 \\ 0 & r_{42} \\ 0 & r_{52} \end{bmatrix} \qquad (A\text{-}3\text{-}1)$$

and

$$\frac{\partial f_n}{\partial x^+_{to}}=\begin{bmatrix} 0 & 0 \\ 0 & 0 \\ r_{33} & r_{34} \\ 0 & r_{44} \\ 0 & r_{54} \end{bmatrix} . \qquad (A\text{-}3\text{-}2)$$

(b) Matrix l_n

Let

$$\frac{\partial f^+_{from}}{\partial x_n}=\begin{bmatrix} (l_{11})_n & (l_{12})_n & (l_{13})_n & (l_{14})_n & (l_{15})_n \\ (l_{21})_n & (l_{22})_n & (l_{23})_n & (l_{24})_n & (l_{25})_n \end{bmatrix}$$

and

$$\frac{\partial f^+_{to}}{\partial x_n}=\begin{bmatrix} (l_{31})_n & (l_{32})_n & (l_{33})_n & (l_{34})_n & (l_{35})_n \\ (l_{41})_n & (l_{42})_n & (l_{43})_n & (l_{44})_n & (l_{45})_n \end{bmatrix} .$$

Differentiating Eqs.(2-3-9) to (2-3-14), we obtain components l_{ij} (i=1 ~

4 and j=1 ~ 5) as follows :

If the from-junction is normal, then

$$(l_{11})_n = A_n$$

$$(l_{21})_n = 0$$

and

$$(l_{25})_n = \frac{-\Delta t}{\Delta t + \tau_h^A} \qquad if\ (G_n^A)^{old} \leqq 0,$$

$$= 0 \qquad otherwise.$$

If the from-junction is a mixing junction, then

$$(l_{11})_n = A_n$$

$$(l_{21})_n = A_n h_n^A$$

and

$$(l_{25})_n = A_n G_n^A \frac{\partial h_n^A}{\partial h_n^{av}} \quad .$$

If the from-junction is a break, then

$$(l_{11})_n = 0$$

$$(l_{21})_n = 0$$

and

$$(l_{25})_n = 0 \quad .$$

If the to-junction is normal, then

$$(l_{33})_n = -A_n$$

$$(l_{43})_n = 0$$

and

$$(l_{45})_n = \frac{-\Delta t}{\Delta t + \tau_h^E} \qquad if\ (G_n^E)^{old} > 0,$$

$= 0$ *otherwise*.

If the to-junction is a mixing junction, then

$$(l_{33})_n = -A_n$$

$$(l_{43})_n = -A_n h_n^E$$

and

$$(l_{45})_n = -A_n G_n^E \frac{\partial h_n^E}{\partial h_n^{av}} \quad .$$

Thus, we can see that in general

$$\frac{\partial f_{from}^+}{\partial x_n} = \begin{bmatrix} l_{11} & 0 & 0 & 0 & 0 \\ l_{21} & 0 & 0 & 0 & l_{25} \end{bmatrix}_n \qquad (A\text{-}3\text{-}3)$$

and

$$\frac{\partial f_{to}^+}{\partial x_n} = \begin{bmatrix} 0 & 0 & l_{33} & 0 & 0 \\ 0 & 0 & l_{43} & 0 & l_{45} \end{bmatrix}_n \quad . \qquad (A\text{-}3\text{-}4)$$

(c) Matrix $(b_{ij})_n$ $\quad (i,j = to, from)$

Let

$$(J_n)^{-1} = \begin{bmatrix} (\gamma_{11})_n & (\gamma_{12})_n & (\gamma_{13})_n & (\gamma_{14})_n & (\gamma_{15})_n \\ (\gamma_{21})_n & (\gamma_{22})_n & (\gamma_{23})_n & (\gamma_{24})_n & (\gamma_{25})_n \\ (\gamma_{31})_n & (\gamma_{32})_n & (\gamma_{33})_n & (\gamma_{34})_n & (\gamma_{35})_n \\ (\gamma_{41})_n & (\gamma_{42})_n & (\gamma_{43})_n & (\gamma_{44})_n & (\gamma_{45})_n \\ (\gamma_{51})_n & (\gamma_{52})_n & (\gamma_{53})_n & (\gamma_{54})_n & (\gamma_{55})_n \end{bmatrix} \quad . \qquad (A\text{-}3\text{-}5)$$

Then, substituting Eqs.(A-3-1), (A-3-3) and (A-3-5) into Eq.(2-3-40), we obtain

$$(b_{from,from})_n =$$

$$\begin{bmatrix} l_{11}\gamma_{12}r_{21} & l_{11}(\gamma_{12}r_{22}+\gamma_{14}r_{42}+\gamma_{15}r_{52}) \\ (l_{21}\gamma_{12}+l_{25}\gamma_{52})r_{21} & l_{21}(\gamma_{12}r_{22}+\gamma_{14}r_{42}+\gamma_{15}r_{52})+l_{25}(\gamma_{52}r_{22}+\gamma_{54}r_{42}+\gamma_{55}r_{52}) \end{bmatrix}$$

Similarly, we obtain

$$(b_{from,to})_n =$$

$$\begin{bmatrix} l_{11}\gamma_{13}r_{33} & l_{11}(\gamma_{13}r_{34}+\gamma_{14}r_{44}+\gamma_{15}r_{54}) \\ (l_{21}\gamma_{13}+l_{25}\gamma_{53})r_{33} & l_{21}(\gamma_{13}r_{34}+\gamma_{14}r_{44}+\gamma_{15}r_{54})+l_{25}(\gamma_{53}r_{34}+\gamma_{54}r_{44}+\gamma_{55}r_{54}) \end{bmatrix}$$

$$(b_{to,from})_n =$$

$$\begin{bmatrix} l_{33}\gamma_{32}r_{21} & l_{33}(\gamma_{32}r_{22}+\gamma_{34}r_{42}+\gamma_{35}r_{52}) \\ (l_{43}\gamma_{32}+l_{45}\gamma_{52})r_{21} & l_{43}(\gamma_{32}r_{22}+\gamma_{34}r_{42}+\gamma_{35}r_{52})+l_{45}(\gamma_{52}r_{22}+\gamma_{54}r_{42}+\gamma_{55}r_{52}) \end{bmatrix}$$

and

$$(b_{to,to})_n =$$

$$\begin{bmatrix} l_{33}\gamma_{33}r_{33} & l_{33}(\gamma_{33}r_{34}+\gamma_{34}r_{44}+\gamma_{35}r_{54}) \\ (l_{43}\gamma_{33}+l_{45}\gamma_{53})r_{33} & l_{43}(\gamma_{33}r_{34}+\gamma_{34}r_{44}+\gamma_{35}r_{54})+l_{45}(\gamma_{53}r_{34}+\gamma_{54}r_{44}+\gamma_{55}r_{54}) \end{bmatrix}$$

A.4 Matrix m_j

If junction j is a normal junction, then Eqs.(2-3-9) and (2-3-10) give

$$m_j=\begin{bmatrix} 0 & 0 \\ 0 & 1 \end{bmatrix} .$$

If junction j is a break, then Eqs.(2-3-11) and (2-3-12) give

$$m_j=\begin{bmatrix} 1 & 0 \\ 0 & 1 \end{bmatrix} .$$

If junction j is a mixing junction, then Eqs.(2-3-13) and (2-3-14) give

$$m_j=\frac{V_j}{\Delta t}\begin{bmatrix} (\partial\rho/\partial p)_j^+ & (\partial\rho/\partial h)_j^+ \\ h_j^+(\partial\rho/\partial p)_j^+ & \rho_j^+ + h_j^+(\partial\rho/\partial h)_j^+ \end{bmatrix} .$$

A.5 Vectors $F_{j,from}$ and $F_{j,to}$

Substituting Eqs.(A-3-4) and (A-3-5) into Eq.(2-3-37a), we obtain

$$F_{j,from}=\begin{bmatrix} c_1 \\ c_2 \end{bmatrix}$$

where

$$c_1=(l_{33}\sum_{i=1}^{5}\gamma_{3i}f_i)_{from}$$

and

$$c_2=(l_{43}\sum_{i=1}^{5}\gamma_{3i}f_i+l_{45}\sum_{i=1}^{5}\gamma_{5i}f_i)_{from}\quad .$$

Similarly, substituting Eqs.(A-3-3) and (A-3-5) into Eq.(2-3-37b), we obtain

$$F_{j,to}=\begin{bmatrix} c_3 \\ c_4 \end{bmatrix}$$

where

$$c_3=(l_{11}\sum_{i=1}^{5}\gamma_{1i}f_i)_{to}$$

and

$$c_4=(l_{21}\sum_{i=1}^{5}\gamma_{1i}f_i+l_{45}\sum_{i=1}^{5}\gamma_{2i}f_i)_{to}\quad .$$

Appendix B Nomenclature

In the following, the symbols for use in this report will be shown along with their units, e.g., kcal/m^2/sec. In general, a unit written as A/B/C/..../H should be understood to be

$$\frac{A}{BC....H} \quad .$$

For example, we have

$$kcal/m^2/sec = \frac{kcal}{m^2 \times \text{sec}} \quad .$$

B.1 Alphabetic Symbols

a	Normalized shaft speed of hydraulic machine (-)
A	Cross-sectional flow area (m^2)
A_g	Flow area of the 3 x 3 fuel rod matrix (m^2)
A_v	Avogadro's number (-)
b	Normalized hydraulic torque of hydraulic machine (-)
c	Impurity concentration (ppm)
B	Momentum flux due to u_{rel} (kg/(sec^{2}m))
B	Matrix defined by Eq.(2-3-28)
B_{L_k}	Coupling matrix between junction group k and mixing junctions
B_{R_k}	Coupling matrix between junction group k and mixing junctions
BL	Percent blockage (-)
C	Matrix defined by Eq.(2-3-53)
c_c	Convertion ratio (-)
c_D	Discharge coefficient for critical flow (-)
c_{eff}	Discharge coefficient for non-critical flow(-)

c_p Specific heat under constant pressure (kcal/m^3/°c)

c_{VH} Sign of L_H (-)

$\tilde{c}$ $= c_B(1-x)$ (ppm)

d Diameter of bubble or droplet (m)

d_b Diameter of the burst rod node (m)

d_n Diameter of the non-burst rod node (m)

D Hydraulic diameter (m)

e $= r_{CL}^{ino} / r_R^o$

E_y Young's modules for cladding (kg/m/sec^2)

f Friction factor (-)

f Function vector defined by Eq.(2-3-15)

F Function vector defined by Eq.(2-3-29)

$(f_1^+)_j$ Mass conservation equation for junction j

$(f_2^+)_j$ Energy conservation equation for junction j

$(f_1)_n$ Mass conservation equation for node n

$(f_2)_n$ Momentum coupling equation at point A of node n

$(f_3)_n$ Momentum coupling equation at point E of node n

$(f_4)_n$ Momentum conservation equation for node n

$(f_5)_n$ Energy conservation equation for node n

f_B Function defined for a break by Eq.(2-2-89)

g Gravitational acceleration (m/sec^2)

g_M Critical mass velocity by Moody (kg/m^2/sec)

G Mass velocity (kg/m^2/sec)

G Function vector defined by Eq.(2-3-54)

Gr Grashof number (-)

G_t = 273 kg/m^2/sec (transition mass flux)

h Specific enthalpy (kcal/kg)

h_{gap} Gap conductivity without radiation (kcal/m^2/sec/°c)

h^{t}_{gap} Total gap conductivity (kcal/m^2/sec/$^\circ$c)

h_{rad} Radiative heat transfer coefficient between pellet and cladding (kcal/m^2/sec/$^\circ$c)

h_{tr} Heat transfer coefficient (kcal/m^2/sec/$^\circ$c)

h^{b}_{tr} Rod-to-rod rediative heat transfer coefficient for burst rod (kcal/m^2/sec/$^\circ$c)

h^{c}_{tr} Coefficient of heat transfer from cladding to coolant ($= h^{w-c}_{tr} + h^{cvn}_{tr}$) (kcal/m^2/sec/$^\circ$c)

h^{cs}_{tr} Coefficient of total heat transfer from non-burst cladding node (kcal/m^2/sec/$^\circ$c)

h^{cs*}_{tr} Coefficient of total heat transfer from burst cladding node (kcal/m^2/sec/$^\circ$c)

h^{cvn}_{tr} Convective or boiling or condensation heat transfer coefficient (kcal/m^2/sec/$^\circ$c)

h^{n}_{tr} Ro-to-rod radiative heat transfer coefficient for non-burst rod (kcal/m^2/sec/$^\circ$c)

h^{w-c}_{tr} Rod-to-coolant radiative heat transfer coefficient (kcal/m^2/sec/$^\circ$c)

$\mathcal{HC}^{F}_{Q}$ Head-discharge curve for positive speeds (-)

$\mathcal{HC}^{R}_{Q}$ Head-discharge curve for negative speeds (-)

$\mathcal{HC}^{F}_{W}$ Head-speed curve for forward flow (-)

$\mathcal{HC}^{R}_{W}$ Head-speed curve for reverse flow (-)

I Enthalpy flux due to u_{rel} (kcal/(m^{2}sec))

$\mathcal{I}$ Total enthalpy flux due to u_{rel} (kcal/sec)

I_m Moment of inertia (kg.m^2/rad^2)

J Number of junctions except boundary junctions (-)

J Jacobian matrix of thermal-hydraulic network

J_n Jacobian matrix associated with node n

k Loss coefficient (-)

l Neutron life (sec)

L Length of node (m)

L_H Height of node (m)

L_{head} Hydraulic machine head (m)

l_k Size of junction group k

L_n Coupling matrix between node n and junctionsl

l_p Fuel cell pitch (m)

l_w Wetted perimeter (m)

m Mass flow rate (kg/sec)

m_j Jacobian matrix of junction j

M Mass (kg)

M Jacobian matrix of junctions

M_h Two-phase head multiplier for hydraulic machine (-)

M_i Molecular weight of the i-th component of gap gas mixture

M_b Number of non-burst off-diagonal rods of the 3 x 3 rod matrix when the center rod is burst.

M_B Atomic weight of natural boron (g/mole)

M_n Number of non-burst off-diagonal rods of the 3 x 3

M_t Two-phase torque multiplier for hydraulic machine (-) rod matrix when the center rod is non-burst.

N_{gap} Mols of gas in fuel rod gap.

N Number of normal nodes including boundary nodes

n Normalized neutron density (-)

N_f Number of radial nodes in fuel pellet

N_R Number of radial nodes in fuel rod

N_b Number of non-burst diagonal rods when the center rod is burst

N_n Number of non-burst diagoanl rods when the center rod is not burst

$NPSH_R$ Required net positive suction head (m)

p Pressure (kgw/m^2)

p_{gc} Contact pressure between pellet and cladding

p_{head} Normalized hydraulic machine head (= L_{head}/L^r_{head}) (-)

p_{ref} Back pressure at break (ata)

Pr Prandtl number (-)

p_x Accumulator bottom pressure (ata)

q Number of chains with at least one normal junction

Q Heat transfer rate (kcal/sec)

q''' Power density (kcal/sec/m^3)

R_n Coupling matrix between node n and junctions

r_c Cladding thickness (m)

r^{in}_{CL} Cladding inner radius (m)

r_F Fuel pellet radius (m)

r_m Average clad radius (m)

r_{gap} Average fuel gap (m)

r_R Fuel rod diameter (m)

r^*_{Rmax} Maximum radius of burst rod (m)

R_{ACT} Normalized actinides decay heat (-)

Re Reynolds number (-)

Re_t Transition Reynolds number (-)

R_g Perfect gas constant (kcal/sec)

R_{FP} Normalized fission products decay heat (-)

R_n Jacobian matrix defined in Eq.(2-3-23)

R_{29} Normalized power decay from U^{239} (-)

R_{39} Normalized power decay from N_p^{239} (-)

S Heat transfer area (m^2)

s Plastic/burst hoop strain at middle point of clad (-)

s_{in} Plastic/burst strain of clad inner surface (-)

s_{int} Interfacial area between gas and liquid (m^2)

s_{out} Plastic/burst strain of clad outer surface (-)

s_p Elastic strain of cladding inner radius due to pressure change

s_t Elastic strain of cladding inner radius due to temperature change (m)

S_α Function of α defined in conjunction with Eq.(2-2-5)

T Temperature ($^\circ$c)

<T> Average Temperature ($^\circ$c)

T_b Coolant bulk temperature ($^\circ$c)

T_{burst} Burst temperature ($^\circ$c)

T_R^b Clad surface temperature of burst node ($^\circ$c)

T_R^n Clad surface temperature of non-burst node($^\circ$c)

u Velocity (m/sec)

u_{gj} Drift velocity (m/sec)

u_{rel} Relative velocity between vapor and liquid (m/sec)

v Specific volume (m^3/kg)

V Volume (m^3)

ω Normalized volumetric flow rate of hydraulic machine (-)

W Volumetric flow rate (m^3/sec)

x Mass quality (-)

$\boldsymbol{x}$ State vector defined by Eq.(2-3-1)

$\boldsymbol{x}_n$ State vector of normal node n

$\boldsymbol{x}_{N+1}$ Junctions vector defined by Eq.(2-3-3)

y_i Molecular fraction of component gas in gap or fission

yield of nuclide (-)

z Coordinate along initial coolant flow (m)

B.2 *Greek and Russian Symbols*

α Void fraction (-)

β Delayed neutron fraction (-)

β_i Delayed neutron fraction of the i-th group (-)

β_{sep} Separation efficiency of steam separator (-)E

γ Isentropic exponent (-)

γ^A Constriction factor at point A of a node (-)

γ^E Constriction factor at point E of a node (-)

γ_{T_c} Coolant temperature coefficient of reactivity $((^\circ C)^{-1})$

γ_{T_f} Fuel temperature coefficient of reactivity $((^\circ C)^{-1})$

γ_α Void coefficient of reactivity

$(\gamma_{ij})_n$ (i,j) component of the inverse of the node jacobian matrix J_n

Γ_{tot} Total reactivity ($)

Γ_{ex} External reactivity ($)

Γ_{T_c} Coolant temperature reactivity ($)

Γ_{T_f} Fuel temperature reactivity ($)

Γ_g Vapor generation rate (kg/m^3/sec)

Δh^r Rated enthalpy loss of hydraulic machine node (kcal/kg)

Γ_ρ Density reactivity ($)

Δh_{reac} Heat of metal-water reaction (kcal/kg)

ΔT_{sub} Subcooling ($^\circ$c)

ε Emissivity (-)

ε^A Inputted constriction factor at point A of a node (-)

ε^E Inputted constriction factor at point E of a node(-)

η Linear coefficient of thermal expansion ($^\circ c^{-1}$)

Θ Thickness of zircaloy reacted (m)

θ Clad thickness (m)

κ Quantity defined by Eq.(2-2-4) ($kg^2/m^4/sec^2$)

Λ Enthalpy flux (kcal/m^2/sec)

λ Thermal conductivity (kcal/m/$^\circ$c/sec)

or decay constant (sec^{-1})

μ Viscosity (kg/m/sec)

μ_p Poisson's ratio for cladding (-)

ξ^A Valve opening at point A of a node (-)

ξ^E Valve opening at point E of a node(-)

Ξ Heat source in the fuel rod (kcal/m^3/sec)

Π Normalized total power (-)

ρ Density (kg/m^3)

σ Surface tension (m/sec^2)

or microscopic cross section (barns)

σ_h Plastic hoop strain (kgw/m^2)

Σ_a Macroscopic absorption cross section of fissile material (cm^{-1})

Σ_f Macroscopic fission cross section of fissile material (cm^{-1})

τ Time constant (sec)

$\mathcal{T}e$ Electric torque (kg.m^2/sec^2/rad)

$\mathcal{T}_h$ Hydraulic torque (kg.m^2/sec^2/rad)

$\mathcal{T}_r$ Rated torque (kg.m^2/sec^2/rad)

$\mathcal{T}_Q^F$ Torque-discharge curve for positive speed (-)

$\mathcal{T}_Q^R$ Torque-discharge curve for negative speed (-)

T_w^F Torque-speed curve for forward flow (-)

T_w^R Torque-speed curve for reverse flow (-)

τ_e Normalized electric torque (-)

φ Heat flux (kcal/m^2/sec)

φ^b Rod-to-rod radiative heat flux from the burst rod (kcal/m^2/sec)

φ^n Rod-to-rod radiative heat flux from the non-burst rod (kcal/m^2/sec)

ϕ^2 Two-phase multiplier (-)

Φ_{ij} Quantity defined by Eq.(3-3-17) (-)

Ψ Momentum flux (kg/m/sec^2)

ψ_{ij} Quantity defined by Eq.(3-3-16)

ω Branching ratio at a mixing junction (-)

Ω Pump speed (rpm)

B.3 Subscripts

A Refers to A point of a node or a chain.

B Refers to boron.

ACC Refers to accumulator condition.

c Refers to equilibrium.

cd Refers to crack and dish.

CL Refers to cladding.

CLNT Refers to coolant.

core Refers to core.

CHF Refers to critical heat flux.

E Refers to E point of a node or a chain.

en Refers to pellet envelope.

ex Refers to external quantity.

eye Refers to pump "eye".

f Refers to liquid.

F Refers to fuel pellet or fuel pellet surface or film temperature.

feed Fefers to feed water line.

fg Refers to change in fluid property when codition changes from saturated water to saturated steam.

from Refers to from-node or from-junction

fs Refers to saturated liquid.

g Refers to vapor condition.

G Refers to accumulator gas.

gap Refers to gap between pellet and cladding.

gs Refers to saturated vapor.

inj Refers to injection flow.

int Refers to interfacial quantity.

j Refers to loop junction or axial clad node.

L Refers to accumulator liquid.

n Refers to loop node or radial fuel node.

N Refers to inertial flow.

M Refers to critical flow.

opn Refers to completely opened valve.

out Refers to outer surface.

R Refers to fuel rod surface or reverse flow.

s Refers to saturated value.

set Refers to prescribed value.

SG Refers to SG.

t Refers to mode transition.

to Refers to to-junction or to-node.

tot Refers to total.

lpl Refers to lower plenum of fuel rod.

upl Refers to upper plenum of fuel rod.

w Refers to wall condition.

zr Refers to zircaloy.

0 Refers to initial steady state condition.

B.4 Superscripts

A Refers to A point of a node or a chain.

b Refers to burst rod.

E Refers to E point of a node or a chain.

F Refers to forward flow.

G Refers to accumulator gas.

HS Refers to hydraulic source.

in Refers to inner surface.

int Refers to interfacial quantity.

L Refers to accumulator liquid.

n Refers to non-burst rod.

new Refers to present time.

old Refers to time which is one-time step past.

o Refers to initial steady state.

out Refers to outer surface.

r Refers to rated value.

R Refers to reverse flow.

* Refers to cladding condition after burst.

+ Refers to junction condition.

Appendix C Symbol Table for Plotter Output

The symbols of plotter output have the following format

XXX-YY

where XXX and YY stand for a variable and an index, respectively. Index YY is used to indicate the number of the node unless specified otherwise. In the following, the symbols as well as their units, the title along the abscissa, the default values for YM1 and YM2 (see subsection 6.2.3) and the type of the ordinate (1=linear and 2=logarithmic) will be shown.

***** NORMAL NODE DATA *****

Variable	UNIT	RANGE(MAX/MIN)		TYPE
1 PRA	PRESSURE(PASCAL)	2.000E+07	0.0	1
2 PRA	PRESSURE(PASCAL)	2.000E+07	0.0	1
3 PRA	PRESSURE(PASCAL)	2.000E+07	0.0	1
4 GLA	MASS FLUX (KG/SEC/M^2)	1.000E+05	-1.000E+05	1
5 GLE	MASS FLUX (KG/SEC/M^2)	1.000E+05	-1.000E+05	1
6 GLV	MASS FLUX (KG/SEC/M^2)	1.000E+05	-1.000E+05	1
7 HLA	ENTHALPY (KCAL/KG)	1.500E+03	0.0	1
8 HLE	ENTHALPY (KCAL/KG)	1.500E+03	0.0	1
9 HLV	ENTHALPY (KCAL/KG)	1.500E+03	0.0	1
10 RHA	DENSITY (KG/M^3)	1.000E+03	0.0	1
11 RHE	DENSITY (KG/M^3)	1.000E+03	0.0	1
12 RHV	DENSITY (KG/M^3)	1.000E+03	0.0	1
13 XLA	QUALITY (-)	2.000E+00	-1.000E+00	1
14 XLE	QUALITY (-)	2.000E+00	-1.000E+00	1
15 XLV	QUALITY (-)	2.000E+00	-1.000E+00	1
16 ALA	VOID FRACTION (-)	1.200E+00	-8.000E-01	1
17 ALE	VOID FRACTION (-)	1.200E+00	-8.000E-01	1
18 ALV	VOID FRACTION (-)	1.200E+00	-8.000E-01	1
19 QQQ	Q (KCAL/SEC/M***3)	1.000E+05	-1.000E+05	1
20 TMP	BULK TEMP (DEG)	1.500E+03	0.0	1

***** PUMP DATA *****

Variable	UNIT	RANGE(MAX/MIN)		TYPE
21 HDP	PUMP HEAD (M)	2.000E+02	0.0	1
22 AAA	PUMP SPEED	1.000E+01	-1.000E+01	1
23 BBB	PUMP TORQUE	1.000E+01	-1.000E+01	1
24 WWW	PUMP FLOW	1.000E+01	-1.000E+01	1

The variables 22 to 24 are relative values with respect to the steady

state values.

***** ACCUMULATOR DATA *****

Variable	UNIT	RANGE(MAX/MIN)		TYPE
25 PAC	PRESSURE (PASCAL)	2.000E+07	0.0	1
26 GAJ	MASS FLUX (KG/SEC)	5.000E+04	-5.000E+04	1
27 HAC	ENTHALPY (KCAL/KG	1.000E+03	0.0	1
28 VAG	GAS VOLUME (M^3)	2.000E+02	0.0	1
29 MAL	LIQUID MASW (KG)	2.000E+02	0.0	1

***** CORE AND FUEL DATA *****

Variable	UNIT	RANGE(MAX/MIN)		TYPE
30 QCR	RELATIVE POWER	2.000E+00	1.000E-03	2
31 PG1	PRESSURE (PASCAL)	2.000E+07	0.0	1
32 PG2	PRESSURE (PASCAL)	2.000E+07	0.0	1
33 HE1	HTR COEFF (KCAL/SEC/M^2/DEG)	1.000E+02	1.000E-03	2
34 HE2	HTR COEFF (KCAL/SEC/M^2/DEG)	1.000E+02	1.000E-03	2
35 HC1	HTR COEFF (KCAL/SEC/M^2/DEG)	1.000E+02	1.000E-03	2
36 HC2	HTR COEFF (KCAL/SEC/M^2/DEG)	1.000E+02	1.000E-03	2
37 HG1	HTR COEFF (KCAL/SEC/M^2/DEG)	1.000E+02	1.000E-03	2
38 HG2	HTR COEFF (KCAL/SEC/M^2/DEG)	1.000E+02	1.000E-03	2
39 LI1	ZR-REACTED IN (M)	1.000E-04	0.0	1
40 LI2	ZR-REACTED IN (M)	1.000E-04	0.0	1
41 LO1	ZR-REACTED OUT (M)	1.000E-04	0.0	1
42 LO2	ZR-REACTED OUT (M)	1.000E-04	0.0	1
43 QM1	Q-MW (KCAL/M^3)	1.000E+06	0.0	1
44 QM2	Q-MW (KCAL/M^3)	1.000E+06	0.0	1
45 TS1	CLAD SURFACE TEMP (DEG)	2.000E+03	0.0	1
46 TS2	CLAD SURFACE TEMP (DEG)	2.000E+03	0.0	1
47 TC1	FUEL CENTER TEMP (DEG)	2.000E+03	0.0	1
48 TC2	FUEL CENTER TEMP (DEG)	2.000E+03	0.0	1
49 STR	PLASTIC HOOP STRESS (KG/M^2)	1.000E+03	0.0	1
40 HST	HOOP STRAIN(-)	1.000E+00	0.0	1
51 BTE	BURST TEMP (DEG)	2.000E+03	0.0	1

Variables XX1 and XX2 refer to non-burst and burst rods, respectively. Heat transfer coefficients HC and HE refer to values obtained from correlations and values obtained by smoothing HC, respectively. For the core and fuel variables except variables 45 to 48, YY must be 01.

***** HEAT CONDUCTOR DATA *****

Variable	UNIT	RANGE(MAX/MIN)		TYPE
52 BHR	HTR COEFF (KCAL/SEC/M^2/DEG)	1.000E+02	1.000E-03	2

53 BHL	HTR COEFF (KCAL/SEC/M^2/DEG)	1.000E+02	1.000E-03	2
54 BTR	SURFACE TEMP (DEG)	2.000E+03	0.0	1
55 BTL	SURFACE TEMP (DEG)	2.000E+03	0.0	1

In variables 52 to 54, XXR and XXL stand for the right and left of the heat conductor, respectively, and index YY is to be used to show the heat conductor number. Plotting for fuel with gap can be made not by heat conductor variables 52-55, but by core and fuel variables 33-36 and 45-48.

Appendix D Control System Simulation Model

The objective of the control system simulation model (CSSM) is to determine the output of the control system, given the varying input and information characterizing the system. A control system may be divided into a number of fundamental control elements called the control blocks shown in Table D-1, where F_m, $L(t_i)$ and $Tr(t_i)$ mean the linear interpolator, the logical value of a condition specified by trip action data BB30, and the logical value of a trip specified by trip cntrol data BB04, respectively. In this table, symbols y and z stand for the dependent and independent variables, respectively. Symbol t is used instead of z when time is presumed as the independent variable.

The input of a control system are as follows ;

(1) minor edit variables

(2) trip control output , i.e.,

1.0 if trip output is FALSE

0.0 if trip output is TRUE

(3) time

and

(4) elapsed time after a trip condition was satified,

while the output of a control system is

(1) valve opening

(2) external heat input to coolant node

(3) hydraulic machine shaft speed

(4) hydraulic machine torque

(5) back pressure of hydraulic source or break

(6) reactivity or reactivity coefficient

(7) boron concentration of injected water

(8) heat source in heat slab.

(9) set point in trip action

(10) specific enthalpy of injected water

and

(11) external heat input to a mixing junction .

The Input specification of CSSM is shown in Table D-2. For interconnected blocks, the order in which the output of each block is calculated affects the numerical results. The order of computation is determined by the inputted order of the control block description cards , which contain the interconnection information.

In Table D-2, we note that

$$y=y_{max} \quad for \quad y>y_{max}$$

and

$$y=y_{min} \quad for \quad y<y_{min}$$

where y_{max} *and* y_{min} are inputs.

Parameter n ,i.e., INC2 in the control block description card for ITYPE=DLY is related to the manner in which DLY block stores the input values in the past T sec. That is to sample the input at fixed time intervals equal to (T/n) sec. and save each sample for T sec. As n increases, so does accuracy of the representaion of the past input at the cost of more storage.

The OUT block does not represent an actaul control element. It prints out the input or output of a specified control block at every time step for the purpose of debugging.

Table D-1 Models for Control Blocks

Symbol	Descriptive name	Mathematical definition	Numerical method in the code
ABS	*Absolute*	$y=\|x(z)\|$	$y_i=G\|x(z_i)\|$
DER	*Differentiator*	$y=G\frac{dx}{dz}$	$y_i=G\ \frac{x(z_i)-x(z_{i-1})}{z_i-z_{i-1}}$
DIV	*Divider*	$y=Gx_1(z)/x_2(z))$	$y_i=G\ x_1(z_i)/x_2(z_i)$
DLY	*Time delay*	$y(t)=y_0$ *for* $0\leqq t\leqq T$	
		$=Gx(t-T)$ *for* $t>T$	
EXT	*Extrapolator*		$y_i=y_{i-1}+G\frac{x(z_i)+x(z_{i-1})}{2}$
FNG	*Function generator*	$y=GF_m[\,x(z)\,]$	*linear interpolation*
FGT	*Time-function generator*	$y=GF_m[\,x(t)\,]$	*linear interpolation*
INT	*Integrator*	$y(t)=y_0+\int_0^z Gx(z')dz'$	$y_i=y_{i-1}+(z_i-z_{i-1})G\frac{x(z_i)+x(z_{i-1})}{2}$

Table D-1 Models for Control Blocks (Continued)

Symbol	Descriptive name	Mathematical definition	Numerical method in the code
IF	*Logical if controller*		$y_i = G\ x_1(t_i)$ *if* L_i *is true* $= G\ x_2(t_i)$ *if* L_i *is false*
LAG	*Lag compensation*	$y+\tau_2\frac{dy}{dt}=Gx(t)$	$y=\frac{Gx+\tau_2 y^{old}/\Delta t}{1+\tau_2/\Delta t}$
LLG	*Lead-lag*	$y+\tau_2\frac{dy}{dt}=G(x(t)+\tau_1\frac{dx}{dt})$	$y=\frac{G(x+\tau_1(x-x^{old})/\Delta t)\quad+\tau_2 y^{old}/\Delta t}{1+\tau_2/\Delta t}$
MUL	*Multiplier*	$y=x_1(z)x_2(z)$	$y_i=x_1(z_i)x_2(z_i)$
LN	*Natural logarithm*	$y=\ln[x(z)]$	
MAX	*Maximum*	$y=\max[x_1(z),x_2(z)]$	
MIN	*Minimum*	$y=\min[x_1(z),x_2(z)]$	
OUT	*Output*	(*Print out input and output of specified control block.*)	
SUM	*Weighted summer*	$y=G\ [g_1x_1(z)+g_2x_2(z)]$	

Table D-1 Models for Control Blocks (Continued)

Symbol	Descriptive name	Mathematical definition	Numerical method in the code
TIF	*Trip-if contoller*		$y_i = G\ x_1(t_i)$ *if* $Tr(t_i)$ *is on.* $= G\ x_2(t_i)$ *if* $Tr(t_i)$ *is off.*
VLM	*Velocity limiter*	$y = y_{down}$ *if* $Gx < y_{down}$ $= y_{up}$ *if* $Gx < y_{up}$ $= Gx$ *otherwise* where $y_{down} = y^{old} - \Delta t\, v_{down}$ $y_{up} = y^{old} + \Delta t\, v_{up}$.	
XPO	*Exponentation*	$y = x_1^{x_2}$	

Table D-2 Control Block Parameters

Symbol	INC1	INC2	INC3	INC4	GAIN	CP1	CP2	CIC	CMIN	CMAX
MUL	IDC for x_1	IDC for x_2	0	IDC for y_O	G	0.0	0.0	y_O	y_{min}	y_{max}
DIV	IDC for x_1	IDC for x_2	0	IDC for y_O	G	0.0	0.0	y_O	y_{min}	y_{max}
SUM	IDC for x_1	IDC for x_2	0	IDC for y_O	G	g_1	g_2	y_O	y_{min}	y_{max}
XPO	IDC for x_1	IDC for x_2	0	IDC for y_O	G	0.0	0.0	y_O	y_{min}	y_{max}
LN	IDC for x_1	0	0	IDC for y_O	G	0.0	0.0	y_O	y_{min}	y_{max}
ABS	IDC for x_1	0	0	IDC for y_O	G	0.0	0.0	y_O	y_{min}	y_{max}
MAX	IDC for x_1	IDC for x_2	0	IDC for y_O	G	0.0	0.0	y_O	y_{min}	y_{max}
MIN	IDC for x_1	IDC for x_2	0	IDC for y_O	G	0.0	0.0	y_O	y_{min}	y_{max}
VLM	IDC for x_1	0	0	IDC for y_O	G	v_{up}	v_{down}	y_O	y_{min}	y_{max}
DER	IDC for x_1	0	0	IDC for y_O	G	0.0	0.0	y_O	y_{min}	y_{max}
INT	IDC for x_1	0	0	IDC for y_O	G	0.0	0.0	y_O	y_{min}	y_{max}
EXT	IDC for x_1	0	0	IDC for y_O	G	0.0	0.0	y_O	y_{min}	y_{max}
FNG	IDC for x_1	m	0	IDC for y_O	G	0.0	0.0	y_O	y_{min}	y_{max}
FGT	0	m	0	IDC for y_O	G	0.0	0.0	y_O	y_{min}	y_{max}
DLY	IDC for x_1	0	n	IDC for y_O	G	T	0.0	y_O	y_{min}	y_{max}

Table D-2 Control Block Parameters (continued)

Symbol	INC1	INC2	INC3	INC4	GAIN	CP1	CP2	CIC	CMIN	CMA
LAG	IDC for x_1	0	0	IDC for y_O	G	0.0	τ_2	y_O	y_{min}	y_{max}
LLG	IDC for x_1	0	0	IDC for y_O	G	τ_1	τ_2	y_O	y_{min}	y_{max}
IF	IDC for x_1	IDC for x_2	m for L	IDC for y_O	G	0.0	0.0	y_O	y_{min}	y_{max}
TIF	IDC for x_1	IDC for x_2	m for Tr	IDC for y_O	G	0.0	0.0	y_O	y_{min}	y_{max}
OUT	IDC for x_1	n_{int}	0	0	0.0	0.0	0.0	0.	0.	0.

Appendix E Sample Input Data Set

E.1 Input Data for First Job

```
*****************************************************************
 -- 3,300 MW PWR NSSS (SPLIT DOWNCOMER NODING)
/---------------------------------------------------------------------
/ DATA TO BE CHECKED
/      HC DIMENSIONS
/      SCRAM LOGIC
/      TRIP  LOGIC
/      TEMPERATURE COEFFICIENT
/      CONTROL LOGIC OF FW ETC
/      HEAT CONDUCTORS
/      PZR SPRAY DUCT : DIVIDE N58 AND N59 INTO PLURAL NODES.
/      AC DUCT        : DIVIDE N60 AND N64 INTO PLURAL NODES.
/      CVCS DUCT      : ATTACH NODE TO J49 AND J57.
/ ************************************************
/                   NULL TRANSIENT        LBLOCA
/    SB0419 ION          0                3001
/    BB01   NPERT        1                 0
/---------------------------------------------------------------------
/
/   **** PROGRAM CONTROL DATA ****
BB01
/ LDMP NEDI NTC NTRP MTRP IOUT NPERT ICLAS LSEC IDPSTP DMPTM
  0    6    4   19   23   0    0     5      0      0   0.
/ NOCK
  0
/   **** MINOR EDIT DATA ****
BB02
PRA-44  GLE-44 GLA-13 GLE-31 GLE-50 GLE-64
/
/   **** TIME STEP CONTROL DATA ****
BB03
SB0301
/ E1    E2    E3
/ 0.2   0.2   100.
  -2
/ NMIN NMAJ NDMP NCHK    DTMAX    DTMIN    TLAST  EPSMX
SB0302
  180  100 100  0    1.0E-3    1.0E-6      0.5
SB0303
  120  100 100  0    4.0E-3    1.0E-6     20.0
SB0304
   60  80  50   0   64.0E-3    1.0E-6     40.0
SB0305
   80  100 50   0    6.0E-3    1.0E-6   1000.0
/
/   **** TRIP CONTROL DATA ****
BB04
/   IDTRP IZ1   IZ2   ION    IOFF  IOCS  DELAY
```

```
SB0401
401  2     1   0   3023     0     0     0.  / RCP-1 TRIP
SB0402
402  2     2   0   3023     0     0     0.  / RCP-1A TRIP
SB0403
403  4     1   0   3003 3004     0     0.  / PORV (PZR)
SB0404
404  4     2   0   3005 3006     0     0.  / SAFETY VALVES (PZR)
SB0405
405  4     4   0   3007 3008     0     0.  / SAFETY VALVE (LOOP-A)
SB0406
406  4     6   0   3009 3010     0     0.  / SAFETY VALVE (LOOP-B)
SB0407
407  4     3   0   3011 3012     0     0.  / SG 2NDRY RELIEF VALVE
SB0408
408  4     5   0   3013 3014     0     0.  / SG 2NDRY RELIEF VALVE
SB0409
409  4     8   0   3015     0     0  22.2  /HPCI VALVE OPENS.
SB0410
410  4    10   0   3015     0     0  22.2  /HPCI VALVE OPENS.
SB0411
411  4    18   0   3016     0     0   0.   /LPCI VALVE OPENS.
SB0412
412  4    19   0   3016     0     0   0.   /LPCI VALVE OPENS.
SB0413
413  4    13   0   3020     0     0   0.5  / FW VALVE CLOSES.
SB0414
414  4    14   0   3020     0     0   0.5  / FW VALVE CLOSES.
SB0415
415  4    15   0   3020     0     0   0.5  / MS VALVE CLOSES.
SB0416
416  4    21   0   3020     0     0  37.   /AUX FW VALVE OPENS.
SB0417
417  4    22   0   3020     0     0  37.   /AUX FW VALVE OPENS.
SB0418
418  3     0   0   3023     0     0   0.1  / REACTOR SCRAM
SB0419
/419  7    11   0      0     0     0   0.0  / COLD LEG BREAK
 419  7    11   0   3001     0     0   0.0  / COLD LEG BREAK
/
/  **** DENSITY DELAY TIME DATA ****
/BB05
/ NTAUD   DTAUD   ITAUD   ATAUD
/ 0       0.
/ 3       0.
/ 37      40      41
/ 100.    100.    100.
/ NTAUDJ  DTAUDJ  ITAUDJ  ATAUDJ
/ 0       0.
/ 1       0.
/ 58
/ 100.
/
/  **** PROBLEM OPTION DATA ****
BB07
/ NMODL IEM  NOPTF NOPTD ICHFOP1 ICHFOP2 IHTROP1 IHTROP  ISTM  EPS
  0     1    0     2     1       3       2       1       1     1.E-10
```

```
/  **** PROBLEM DIMENSION DATA ****
BB08
/ NNET NVOL  NJUNC NMIX NHYDS NPUMP NSHFT NACCM KROD NCTOT
  2    101   89    23   17    2     2     2     2    14
/ NCORE NSLB  NRGN NMESH NVLV  NSEP  NIMP NMAT NHSTG  NCI   NCB
  7     37    2    11    22    2     1    3     22    5     14    6
/  **** INITIAL LOOP-WISE THERMAL-HYDRAULICS DATA****
BB09
SB0901
/INET ICLNT   INLET LOOP     OUTLET LOOP     NADJ     QOUT
  1   0       0  0 0 0 0     1  2 0 0 0      1        8.E5  0.  0.  0.
/IVOL    GA            HA                BC(PPM)
/ 1       9.804E3       354.4             1.E3
  1       9.804E3       354.4             5.E2
SB0902
  2   0       1  1 0 0 0     0  0 0 0 0      2        0.    0.  0.  0.
  91    -508.8          224.8             0.
  92    -508.8          224.8             0.
/  **** NODE DATA ****
BB10
/ HOT LEG 2/3 LOOP : CALL THIS LOOP AS LOOP-B
SB1001
/INO  FJ TJ  INU INET IXCV PA(K)          AEFC     BZAIA   BZAIE   DH
/                         (ATM)          (M**2)                   (M)
  1   48 49    1   1    0  154.0454       0.430    1.      1.      0.0
/              L          LH             KFORA   KREVA   KFORE   KREV
/              (M)        (M)
               2.5        0.             -1.     -1.     -1.     -1.  0.
SB1002
  2   49  1    1   1    0  154.0305       0.430    1.      1.      0.0
               2.75       0.             -1.     -1.     -1.     -1.  0.
/ SG. INLET PLENUM (LOOP-B)
SB1003
  3    1  2    1   1    0  153.4832       2.898    1.      1.      1.92
               1.664      1.6            -1.     -1.     -1.     -1.  0.
/ SG. TUBES, LOWER INLET (LOOP-B)
SB1004
  4    2  3  3382  1    0  153.3428       3.017E-4 1.      1.      0.
               4.539      4.539          -1.     -1.     -1.     -1.  0.
/ SG. TUBES, MIDDLE INLET (LOOP-B)
SB1005
  5    3  4  3382  1    0  152.7604       3.017E-4  1.     1.      0.
               4.539      4.539          -1.     -1.     -1.     -1.  0.
/ SG. TUBES, UPPER INLET (LOOP-B)
SB1006
  6    4  5  3382  1    0  152.1714       3.017E-4  1.     1.      0.
               1.413      1.             -1.     -1.     -1.     -1.  0.
/ SG. TUBES, UPPER OUTLET (LOOP-B)
SB1007
  7    5  6  3382  1    0  152.0161       3.017E-4  1.     1.      0.
               1.413     -1.             -1.     -1.     -1.     -1.  0.
/ SG. TUBES, MIDDLE OUTLET (LOOP-B)
SB1008
  8    6  7  3382  1    0  152.0018       3.017E-4  1.     1.      0.
               4.539     -4.539          -1.     -1.     -1.     -1.  0.
/ SG. TUBES, LOWER OUTLET (LOOP-B)
SB1009
```

```
  9     7  8  3382  1    0  152.0549        3.017E-4  1.     1.       0.
                 4.539   -4.539          -1.   -1.   -1.   -1.   0.
/ SG. OUTLET PLENUM (LOOP-B)
SB1010
 10     8  9     1   1    0  152.06436       2.898   1.    1.       1.92
                 1.664   -1.6            -1.   -1.   -1.   -1.   0.
/ PUMP SUCTION (LOOP-B)
SB1011
 11     9 10     1   1    0  151.99404       0.487   1.    1.       0.0
                 7.327   -3.5            -1.   -1.   -1.   -1.   0.
/ PUMP (LOOP-B)
SB1012
 12    10 11     1   1    0  151.3539        0.192   1.    1.       0.351
                12.39     3.5             -1.    10.    -1.    10.    0.
/ COLD LEG (LOOP-B)
SB1013
 13    11 50     1   1    0  155.2586        0.383   1.    1.       0.
                0.144     0.0             -1.    -1.    -1.    -1.    0.
SB1014
 14    50 51     1   1    0  155.2485        0.383   1.    1.       0.
                3.        0.0             -1.    -1.    -1.    -1.    0.
SB1015
 15    51 52     1   1    0  155.2278        0.383   1.    1.       0.0
                3.144     0.              -1.   -1.   -1.   -1.   0.
SB1016
 16    48 57     3   1    0  154.0454        0.430     1.    1.       0.0
                2.5       0.              -1.   -1.   -1.   -1.   0.
/ HOT-LEG (LOOP-A)
SB1017
 17    57 12     3   1    0  154.0305        0.430     1.    1.       0.0
                2.75      0.              -1.   -1.   -1.   -1.   0.
/ SG. INLET PLENUM (LOOP-A)
SB1018
 18    12 13     3   1    0  153.4832        2.898     1.    1.       1.92
                1.664     1.6             -1.   -1.   -1.   -1.   0.
/ SG. TUBES, LOWER INLET (LOOP-A)
SB1019
 19    13 14  10146  1    0  153.3428        3.017E-4  1.    1.       0.
                4.539     4.539           -1.   -1.   -1.   -1.   0.
/ SG. TUBES, MIDDLE INLET (LOOP-A)
SB1020
 20    14 15  10146  1    0  152.7604        3.017E-4  1.    1.       0.
                4.539     4.539           -1.   -1.   -1.   -1.   0.
/ SG. TUBES, UPPER INLET (LOOP-A)
SB1021
 21    15 16  10146  1    0  152.1714        3.017E-4  1.    1.       0.
                1.413     1.              -1.   -1.   -1.   -1.   0.
/ SG. TUBES, UPPER OUTLET (LOOP-A)
SB1022
 22    16 17  10146  1    0  152.0161        3.017E-4  1.    1.       0.
                1.413    -1.              -1.   -1.   -1.   -1.   0.
/ SG. TUBES, MIDDLE OUTLET (LOOP-A)
SB1023
 23    17 18  10146  1    0  152.0018        3.017E-4  1.    1.       0.
                4.539   -4.539           -1.   -1.   -1.   -1.   0.
/ SG. TUBES, LOWER OUTLET (LOOP-A)
SB1024
```

```
24    18 19  10146 1   0   152.0549      3.017E-4  1.    1.      0.
               4.539   -4.539          -1.   -1.   -1.   -1.   0.
/ SG. OUTLET PLENUM (LOOP-A)
SB1025
 25   19 20    3   1   0  152.0644       2.898   1.      1.      1.92
               1.664   -1.6            -1.   -1.   -1.   -1.   0.
/ PUMP SUCTION (LOOP-A)
SB1026
 26   20 21    3   1   0  151.9940       0.487   1.      1.      0.
               7.327   -3.5            -1.   -1.   -1.   -1.   0.
/ PUMP (LOOP-A)
SB1027
 27   21 58    3   1   0  151.3539       0.192   1.      1.      0.351
              12.39     3.5            -1.    10.  -1.    10.   0.
/ COLD LEG (LOOP-A)
SB1028
 28   58 59    3   1   0  155.2485       0.383   1.      1.      0.
               3.144    0.             -1.   -1.   -1.   -1.   0.
SB1029
 29   59 61    3   1   0  155.2278       0.383   1.      1.      0.
               3.144    0.             -1.   -1.   -1.   -1.   0.
SB1030
 30   52 61    2   1   0  -5.            0.7     1.      1.      0.0
               6.09     0.             -1.   -1.   -1.   -1.   0.
/ DOWNCOMER (REACTOR VESSEL)
SB1031
 31   61 22    1   1   0  155.2068       1.86    1.      1.      0.192
               4.577   -8.994          -1.   -1.   -1.   -1.   0.
/ LOWER PLENUM
SB1032
 32   22 53    1   1   0  155.7456       3.645   1.      1.      0.152
               6.10     0.66           -1.   -1.   -1.   -1.   0.
/ NON-HEATED
SB1033
 33   53 23  50752 1   0  156.1509   0.8788E-4  1.      1.  1.1778E-2
               0.11     0.11           -1.   -1.   -1.   -1.   0.
/ LOWER CORE (REACTOR VESSEL)
SB1034
 34   23 24  50752 1   0  155.5714   0.8788E-4  1.      1.  1.1778E-2
               0.732    0.732          -1.   -1.   -1.   -1.   0.
SB1035
 35   24 54  50752 1   0  155.3624   0.8788E-4  1.      1.  1.1778E-2
               0.732    0.732          -1.   -1.   -1.   -1.   0.
/ MIDDLE CORE (REACTOR VESSEL)
SB1036
 36   54 25  50752 1   0  155.1488   0.8788E-4  1.      1.  1.1778E-2
               0.732    0.732          -1.   -1.   -1.   -1.   0.
SB1037
 37   25 26  50752 1   0  154.9312   0.8788E-4  1.      1.      0.
               0.732    0.732          -1.   -1.   -1.   -1.   0.
/ UPPER CORE (REACTOR VESSEL)
SB1038
 38   26 27  50752 1   0  154.6918   0.8788E-4  1.      1.  1.1778E-2
               0.732    0.732          -1.   -1.   -1.   -1.   0.
/ NON-HEATED
SB1039
 39   27 56  50752 1   0  154.4621   0.8788E-4  1.      1.  1.1778E-2
```

```
                0.11      0.11              -1.   -1.   -1.   -1.   0.
/ NON-HEATED
SB1040
 40   53 28     200 1   0  156.1509        0.8788E-4   1.    1.  1.1778E-2
                0.11      0.11              -1.   -1.   -1.   -1.   0.
/ LOWER CORE (REACTOR VESSEL)
SB1041
 41   28 29     200 1   0  155.5714        0.8788E-4   1.    1.  1.1778E-2
                0.732     0.732             -1.   -1.   -1.   -1.   0.
SB1042
 42   29 55     200 1   0  155.3624        0.8788E-4   1.    1.  1.1778E-2
                0.732     0.732             -1.   -1.   -1.   -1.   0.
/ MIDDLE CORE (REACTOR VESSEL)
SB1043
 43   55 30     200  1   0   155.1487989    0.8788E-4   1.    1.  1.1778E-2
                0.732     0.732             -1.   -1.   -1.   -1.   0.
SB1044
 44   30 31     200  1   0   154.9238       0.8788E-4   1.    1.  1.1778E-2
                0.732     0.732             -1.   -1.   -1.   -1.   0.
/ UPPER CORE (REACTOR VESSEL)
SB1045
 45   31 32     200  1   0   154.6919       0.8788E-4   1.    1.  1.1778E-2
                0.732     0.732             -1.   -1.   -1.   -1.   0.
/ NON-HEATED
SB1046
 46   32 56     200  1   0   154.4605       0.8788E-4   1.    1.  1.1778E-2
                0.11      0.11              -1.   -1.   -1.   -1.   0.
/ CORE CROSS FLOW
SB1047
 47   54 55     200  1   0  -0.01             9.08E-4   1.    1.       0.034
                0.1       0.0               -1.   -1.   -1.   -1.   0.
/ CORE BYPASS (REACTOR VESSEL)
SB1048
 48   53 56     1    1   0  154.7264778       1.7203    1.    1.       0.03
                3.88      3.88              -1.   -1.   -1.   -1.   0.
/ UPPER PLENUM
SB1049
 49   56 48     1    1   0  154.33615         9.29      1.    1.       0.305
                4.454     4.454             -1.   -1.   -1.   -1.   0.
SB1050
 50   52 37     1    1   0  155.2068          0.62      1.    1.       0.192
               4.577     -8.994             -1.   -1.   -1.   -1.   0.
SB1051
 51   37 53     1    1   0  155.7456          1.215     1.    1.       0.152
                6.1       0.66              -1.   -1.   -1.   -1.   0.
/ UPPER VOLUME (PRESSURIZER)
SB1052
 52   60 33     1    1 3120 -0.01             4.75      1.    1.       0.
                3.43     -3.43              -1.   -1.   -1.   -1.   0.
/ INLET SURGE LINE
/ MIDDLE VOLUME (PRESSURIZER)
SB1053
 53   33 34     1    1 3120 -0.01             4.75      1.    1.       0.
                3.43     -3.43              -1.   -1.   -1.   -1.   0.
/ LOWER VOLUME (PRESSURIZER)
SB1054
 54   34 35     1    1 3120 -0.01             4.75      1.    1.       0.
```

```
                3.43     -3.43              -1.    -1.    -1.    -1.    0.
/ OUTLET SURGE LINE
SB1055
 55    35 36     1     1 3120 -20.              0.0616   1.     1.       0.
                14.66     -4.255            10.     -1.    -1.    -1.       0.
SB1056
 56    36 57     1     1 3120 -20.              0.0616  1.     1.       0.
                14.66     -4.255            -1.     -1.    1.     1.       0.
SB1057
 57    49 50     1       1    0  -10.              1.15     0.0337  0.0337  0.0
/                2.E1      0.                  2.      2.    2.     2.       0.
                 1.E-9     0.                  2.      2.    2.     2.       0.
/ SPRAY LINE (LOOP-B)
SB1058
 58    51 60     1     1    0  -10.              5.94E-3  1.     1.       0.
                44.9      18.8              10.     -1.    -1.    -1.    0.
/ SPRAY LINE (LOOP-A)
SB1059
 59    59 60     1     1    0  -10.              5.94E-3  1.     1.       0.
                44.9      18.8              10.     -1.    -1.    -1.       0.
/ ACC DUCT
SB1060
 60    59 79     3     1    0  -10.              0.0388  1.      1.       0.
                5.E1      0.                -1.     -1.    10.    10.       0.
/               1.E-9     0.                -1.     -1.    10.    10.       0.
/ PI
SB1061
 61    59 63     3     1    0  -1.0              0.047   1.      1.       0.
                1.E1      0.                -1.     -1.    -1.    -1.    0.
SB1062
 62    63 71     1     1    0  -1.0              0.047   1.      1.       0.
                1.E1      0.                -1.     -1.    -1.    -1.    0.
SB1063
 63    63 72     1     1    0  -1.0              0.047   1.      1.       0.
                1.E1      0.                -1.     -1.    -1.    -1.    0.
/ ACC DUCT
SB1064
 64    51 78     1     1    0  -10.              0.0388  1.      1.       0.
                5.E1      0.                -1.     -1.    10.    10.       0.
/               1.E-9     0.                -1.     -1.    10.    10.       0.
/ PI
SB1065
 65    51 62     1     1    0  -1.0              0.047   1.      1.       0.
                1.E1      0.                -1.     -1.    -1.    -1.    0.
SB1066
 66    62 73     1     1    0  -1.0              0.047   1.      1.       0.
                1.E1      0.                -1.     -1.    -1.    -1.    0.
SB1067
 67    62 74     1     1    0  -1.0              0.047   1.      1.       0.
                1.E1      0.                -1.     -1.    -1.    -1.    0.
SB1068
 68    57 58     3     1    0    -10.             1.15     0.0337  0.0337  0.
                1.E-9     0.                  2.      2.    2.     2.       0.
/               20.       0.                  2.      2.    2.     2.       0.
/ PORV (PRESSURIZER)  (LOOP-A)
SB1069
 69    60 75     1     1    0  -1.0              0.0184  1.      1.       0.
```

```
                0.1       0.                  -1.    -1.   13.    13.      0.
/ SAFETY VALVES (PRESSURIZER)
SB1070
 70    60 76     1     1    0  -1.0              0.0184  1.      1.       0.
                0.1       0.0                 -1.    -1.   53.3   53.3   0.
SB1071
 71    57 80     3     1    0  -1.0              0.047   1.      1.       0.
                10.       0.                  -1.    -1.   -1.    -1.    0.
/ UPPER HEAD
SB1072
 72    48 77     1     1    0  -1.0              3.855   1.      1.       0.458
                3.658     3.658               -1.    -1.   -1.    -1.    0.
/ SG. DOWNCOMER (LOOP-A)
SB1073
 73    65 38     3     2    0  62.1502           1.0568  1.      1.       0.0152
                10.45    -10.45               -1.    -1.   -1.    -1.    0.
/ SG. RISER, LOWER REGION (LOOP-A)
SB1074
 74    38 39     3     2    0  62.7072           6.4242  1.      1.       0.0518
                3.45      3.45                -1.    -1.   -1.    -1.    0.
/ SG. RISER, MIDDLE REGION (LOOP-A)
SB1075
 75    39 40     3     2    0  62.585            6.4242  1.      1.       0.0518
                3.45      3.45                -1.    -1.   -1.    -1.    0.
/ SG. RISER, UPPER REGION (LOOP-A)
SB1076
 76    40 41     3     2    0  62.5065           6.4242  1.      1.       0.0518
                3.45      3.45                -1.    -1.   -1.    -1.    0.
/ SG. SEPERATOR INLET (LOOP-A)
SB1077
 77    41 64     3     2    0  62.438            6.4242  1.      1.       0.0518
                0.1       0.1                 -1.    -1.   100.0  -1.    0.
/ SG. RECIRCULATION PASS (LOOP-A)
SB1078
 78    64 65     3     2    0  62.1532714        0.7853  1.      1.       0.
                1.        0.                  -1.    -1.   -1.    -1.    0.
/ SG. STEAM DOME (LOOP-A)
SB1079
 79    64 47     3     2    0  62.1532714        8.7615  1.      1.       1.16
                6.77      6.77                -1.    -1.   -1.    -1.    0.
/ STEAM LINE (LOOP-A)
SB1080
 80    47 66     3     2    0  62.063076         0.4560  1.      1.       0.
              126.7     -29.75                -1.    -1.   -1.    -1.    0.
/ STEAM HEADER (LOOP-A)
SB1081
 81    66 70     3     2    0  62.043989         1.3705  1.      1.       0.661
                5.151     0.                  -1.    -1.   -1.    -1.    0.
/ SG. DOWNCOMER (LOOP-B)
SB1082
 82    67 42     1     2    0  62.1502           1.0568  1.      1.       0.0152
                10.45    -10.45               -1.    -1.   -1.    -1.    0.
/ SG. RISER, LOWER REGION (LOOP-B)
SB1083
 83    42 43     1     2    0  62.7072           6.4242  1.      1.       0.0518
                3.45      3.45                -1.    -1.   -1.    -1.    0.
/ SG. RISER, MIDDLE REGION (LOOP-B)
```

```
SB1084
 84    43 44     1    2    0  62.585          6.4242  1.       1.       0.0518
                3.45      3.45             -1.    -1.    -1.    -1.    0.
/ SG. RISER, UPPER REGION (LOOP-B)
SB1085
 85    44 45     1    2    0  62.5065         6.4242  1.       1.       0.0518
                3.45      3.45             -1.    -1.    -1.    -1.    0.
/ SG. SEPERATOR INLET (LOOP-B)
SB1086
 86    45 68     1    2    0  62.438          6.4242  1.       1.       0.0518
                0.1       0.1              -1.    -1.   100.    -1.    0.
/ SG. RECIRCULATION PASS (LOOP-B)
SB1087
 87    68 67     1    2    0  62.1532714      0.7853  1.       1.       0.
                1.        0.               -1.    -1.    -1.    -1.    0.
/ SG. STEAM DOME (LOOP-B)
SB1088
 88    68 46     1    2    0  62.1532714      8.7615  1.       1.       1.16
                6.77      6.77             -1.    -1.    -1.    -1.    0.
/ STEAM LINE (LOOP-B)
SB1089
 89    46 69     1    2    0  62.063076       0.4560  1.       1.       0.
              126.7     -29.75             -1.    -1.    -1.    -1.    0.
/ STEAM HEADER (LOOP-B)
SB1090
 90    69 70     1    2    0  62.043989       1.3705  1.       1.       0.661
                5.151     0.               -1.    -1.    -1.    -1.    0.
/                                ( FLOW AREA 3/4 TIMES AS PIUS77 )
/ SG. MAIN FEEDWATER (B-LINE)
SB1091
 91    67 84     1    2    0  62.10905127     0.92903   1.     1.       0.
               10.        0.               -1.    -1.    -1.    -1.    0.
/ SG. MAIN FEEDWATER (A-LINE)
SB1092
 92    65 85     3    2    0  62.10905127     0.92903 1.       1.       0.
               10.        0.               -1.    -1.    -1.    -1.    0.
/
/ STEAM LINE SAFETY VALVE (LOOP-A)
SB1093
 93    66 89     3    2    0  -1.               0.0184   1.       1.       0.
                0.1       0.0              -1.    -1.   74.45  74.45    0.
/ STEAM LINE RELIEF VALVES (LOOP-A)
SB1094
 94    66 81    15    2    0  -1.               0.0184   1.       1.       0.
                0.1       0.               -1.    -1.   18.6   18.6     0.
/ STEAM LINE RELIEF VALVES (LOOP-B)
SB1095
 95    69 83     5    2    0  -1.               0.0184   1.       1.       0.
                0.1       0.               -1.    -1.   18.6   18.6     0.
/ STEAM LINE SAFETY VALVE (LOOP-B)
SB1096
 96    69 82     1    2    0  -1.               0.0184   1.       1.       0.
                0.1       0.               -1.    -1.   74.45  74.45    0.
/ AUX FW
SB1097
 97    67 88     1    2    0  -1.               0.1      1.       1.       0.
                0.1       0.               -1.    -1.    -1.    -1.      0.
```

```
SB1098
 98    65 87     3     2    0  -1.              0.1       1.       1.       0.
                0.1       0.                -1.    -1.  -1.      -1.       0.
SB1099
 99    70 86     1     2    0  62.042319       1.3936    1.       1.       0.
                76.25     -6.1              -1.    -1.  -1.      -1.    0.
/
/  **** JUNCTION DATA ****
BB11
/ PRIMARY LOOP
/  JNO  JTP INET  IJU  A.OR.V     PRES          H0          BC
    1     1    1     1    0.        0.          0.         0.0
    2     1    1  3382    0.        0.          0.         0.0
    3     1    1  3382    0.        0.          0.         0.0
    4     1    1  3382    0.        0.          0.         0.0
    5     1    1  3382    0.        0.          0.         0.0
    6     1    1  3382    0.        0.          0.         0.0
    7     1    1  3382    0.        0.          0.         0.0
    8     1    1  3382    0.        0.          0.         0.0
    9     1    1     1    0.        0.          0.         0.0
   10     1    1     1    0.        0.          0.         0.0
   11     1    1     1    0.        0.          0.         0.0
   12     1    1     3    0.        0.          0.         0.0
   13     1    1 10146    0.        0.          0.         0.0
   14     1    1 10146    0.        0.          0.         0.0
   15     1    1 10146    0.        0.          0.         0.0
   16     1    1 10146    0.        0.          0.         0.0
   17     1    1 10146    0.        0.          0.         0.0
   18     1    1 10146    0.        0.          0.         0.0
   19     1    1 10146    0.        0.          0.         0.0
   20     1    1     3    0.        0.          0.         0.0
   21     1    1     3    0.        0.          0.         0.0
   22     1    1     1    0.        0.          0.         0.0
   23     1    1 50752    0.        0.          0.         0.0
   24     1    1 50752    0.        0.          0.         0.0
   25     1    1 50752    0.        0.          0.         0.0
   26     1    1 50752    0.        0.          0.         0.0
   27     1    1 50752    0.        0.          0.         0.0
   28     1    1   200    0.        0.          0.         0.0
   29     1    1   200    0.        0.          0.         0.0
   30     1    1   200    0.        0.          0.         0.0
   31     1    1   200    0.        0.          0.         0.0
   32     1    1   200    0.        0.          0.         0.0
   33     1    1     1    0.      153.53      500.        5.E2
   34     1    1     1    0.      153.59      500.        5.E2
   35     1    1     1    0.      153.65      500.        5.E2
   36     1    1     1    0.      153.756     450.        5.E2
   37     1    1     1    0.        0.          0.         0.0
   38     1    2     3    0.        0.          0.         0.
   39     1    2     3    0.        0.          0.         0.
   40     1    2     3    0.        0.          0.         0.
   41     1    2     3    0.        0.          0.         0.
   42     1    2     1    0.        0.          0.         0.
   43     1    2     1    0.        0.          0.         0.
   44     1    2     1    0.        0.          0.         0.
   45     1    2     1    0.        0.          0.         0.
   46     1    2     1    0.        0.          0.         0.
```

```
   47    1    2    3    0.          0.                  0.          0.
   48    4    1    1    0.5         0.                  0.          0.
   49    4    1    1    0.209       0.                  0.          0.
   50    4    1    1    0.18        0.                  0.          0.
   51    4    1    1    0.05        0.                  0.          0.
   52    4    1    1    0.18        0.                  0.          0.
   53    4    1    1    0.05        0.                  0.          0.
   54    4    1    1    0.01        0.                  0.          0.
   55    4    1    1    0.01        0.                  0.          0.
   56    4    1    1    0.1         0.                  0.          0.
   57    4    1    3    0.209       0.                  0.          0.
   58    4    1    3    0.18        0.                  0.          0.
   59    4    1    3    0.18        0.                  0.          0.
/  60    4    1    1    0.1       153.47519           310.          5.E2
   60    4    1    1    0.1       153.5656525         500.          5.E2
   61    4    1    3    0.18        0.                  0.          0.
   62    4    1    1    0.0616    155.2285995         200.          5.E2
   63    4    1    3    0.0616    155.2285995         200.          5.E2
/ SEPARATER MIXING JUNCTION NO.70 AT SG SECONDARY-A
   64    4    2    3    14.7        0.                  0.          0.
   65    4    2    3    0.323       0.                  0.          0.
   66    4    2    3    0.1         0.                  0.          0.
   67    4    2    1    0.323       0.                  0.          0.
/ SEPARATER MIXING JUNCTION NO.73 AT SG SECONDARY-B
   68    4    2    1    14.7        0.                  0.          0.
   69    4    2    1    0.1         0.                  0.          0.
   70    4    2    1    1.3         0.                  0.          0.
   71    7    1    1    0.        158.                100.          5.E2
   72    7    1    1    0.        158.                100.          5.E2
   73    7    1    1    0.        158.                100.          5.E2
   74    7    1    1    0.        158.                100.          5.E2
   75    7    1    1    0.        155.                300.          5.E2
   76    7    1    1    0.        155.                300.          5.E2
   77    7    1    1    0.        153.8084291         300.          5.E2
   78    5    1    1    0.        158.                250.          5.E2
   79    5    1    3    0.        158.                250.          5.E2
   80    7    1    3    0.          0.                350.          5.E2
   81    7    2    3    0.          0.                658.          0.
   82    7    2    1    0.          0.                658.          0.
   83    7    2    1    0.          0.                658.          0.
   84    7    2    1    0.         62.1322              0.          0.
   85    7    2    3    0.         62.1322              0.          0.
   86    7    2    1    0.         61.997               0.          0.
   87    7    2    3    0.          0.                 50.          0.
   88    7    2    1    0.          0.                 50.          0.
   89    7    2    3    0.          0.                658.          0.
/
/  **** MIXING JUNCTION DATA ****
BB12
/ UPPER PLENUM (REACTOR VESSEL)
SB1201
/ JNO    IDCQ      NOUT       N1       N2       N3       N4
/                             R1       R2       R3       R4
  48     0         3
                              1        16       72
                              0.25     0.75     0.
SB1202
```

```
  49      0          2
                                2          57
                                1.0        0.
SB1203
  50      0          1
                                14
                                1.0
SB1204
  51      0          4
                                15         58         64         65
                                1.         0.         0.         0.
SB1205
  52      0          2
                                30         50
                                0.         1.
/ LOWER PLENUM (REACTOR VESSEL)
SB1206
  53      0          3
                                33         40         48
                                254.       1.0        10.
SB1207
  54      0          2
                                36         47
                                1.0        0.0
SB1208
  55      0          1
                                43
                                1.0
SB1209
  56      0          1
                                49
                                1.0
SB1210
  57      0          3
                                17         68         71
                                1.0        0.         0.
SB1211
  58      0          1
                                28
                                1.0
SB1212
  59      0          4
                                29         59         60         61
                                1.         0.0        0.0        0.0
SB1213
  60   3120          3
                                52         70         69
                                1.0        0.         0.0
/ DOWNCOMER  TOP
SB1214
  61      0          1
                                31
                                1.0
SB1215
  62      0          2
                                66         67
                                0.         0.
```

```
SB1216
  63     0          2
                                62        63
                                0.        0.
SB1217
  64     0          2
                                78        79
                                0.75      0.25
SB1218
  65     0          3
                                73        92        98
                                1.0      -0.25      0.
SB1219
  66     0          3
                                81        94        93
                                1.0       0.        0.0
SB1220
  67     0          3
                                82        91        97
                                1.0      -0.25      0.
SB1221
  68     0          2
                                87        88
                                0.75      0.25
SB1222
  69     0          3
                                90        96        95
                                1.0       0.0       0.0
SB1223
  70     0          1
                                99
                                1.0
/
/  **** HYDRAULIC SOURCE DATA ****
BB13
/ ------ LPCI  ------
SB1301
/ NOPINJ IJ    IFPT  IHFLG  IDC   IDB   IDH   JPARA   HINJR        MHS
  1       71    1       0    3115   0     0       1      50.        283.
/ ------ HPCI  ------
SB1302
  2       72    1       0    3116   0     0       1      50.        89.
/ ------ CVCS BLEED ----
SB1303
  3       80    1       0     0     0     0       3      354.       -3.
/ ------ HPCI  ------
SB1304
  4       73    1       0    3117   0     0       1      50.        89.
/ ------ LPCI  ------
SB1305
  5       74    1       0    3118   0     0       1      50.        283.
/ ------ FEEDWATER FLOW (INTACT) -----
SB1306
  6       85    1       1    3109   0     0       3     225.    4.726905E2
/ ------ FEEDWATER FLOW (BROKEN) -----
SB1307
  7       84    1       1    3109   0     0       1     225.    4.726905E2
```

```
/ ------ TURBINE FLOW ------
SB1308
  8       86   1       -1   3108   0      0       1     655.   -1.8907612E3
/ ------ UPPER HEAD DEAD-END ---------
SB1309
  9       77   0        0      0    0      0       1     0.           0.
/ ------ PORV ------
SB1310
 10       75   2        0   3112    0      0       1     2.E2         0.
/ ------ SAFETY VALVE (PZR) -----
SB1311
 11       76   2        0   3112    0      0       1     2.E2         0.
/ ------ 2NDRY RELIEF VALVE (V3) ---
SB1312
 12       81   2        0   3112    0      0       3     2.E2         0.
/ ------ 2NDRY SAFETY VALVE (V4) ---
SB1313
 13       89   2        0   3112    0      0       3     2.E2         0.
/ ------ 2NDRY SAFETY VALVE (V6) ---
SB1314
 14       82   2        0   3112    0      0       1     2.E2         0.
/ ------ 2NDRY RELIEF VALVE (V5) ---
SB1315
 15       83   2        0   3112    0      0       1     2.E2         0.
/ ------ AUX FW   ---
SB1316
 16       87   1        0   3113    0      0       3     30.          19.44
SB1317
 17       88   1        0   3114    0      0       1     30.          19.44
/
/  **** PUMP DATA ****
BB14
SB1401
/SHAFT  TRIP MODE  IDC
 1       1          0
/OMEGAR OMEGAO OMEGAS IM      K1 K2 TAU        TORQR
 1190.  1190.  0.     3455.  5. 1. 15.519     30350.
SB1402
 2       1    0
 1190.  1190.  0.     3455.  5. 1. 15.519     30350.
BB15
SB1501
/MACHINE  SHFT  NODES   NODE   TBL   WR     HEADR  DELH  RHOR
 1        1     1
                        12     1     5.58   84.    0.    755.
SB1502
 2        2     1
                        27     1     5.58   84.    0.    755.
/
/  **** PUMP DATA TABLE ****
BB16
SB1601
/NPTB
   1
/IP1  HEAD-FLOW (POSITIVE SPEED)
 14
-1.00   3.55      -0.60   2.73      -0.32   2.20      -0.18   2.00
```

```
 0.00    1.79        0.11    1.72        0.22    1.64        0.34    1.49
 0.45    1.37        0.56    1.34        0.67    1.32        0.79    1.30
 0.90    1.18        1.00    1.00
/IP2  HEAD-FLOW (NEGATIVE SPEED)
 11
-1.00    0.00        0.00   -0.16        0.10   -0.12        0.20   -0.06
 0.28    0.00        0.40    0.09        0.60    0.31        0.70    0.42
 0.80    0.50        0.88    0.54        1.00    0.59
/IP3  HEAD-SPEED (POSITIVE FLOW)
 8
-1.00    0.00        0.00   -0.50        0.50    0.00        0.74    0.18
 0.81    0.37        0.89    0.64        0.99    0.97        1.00    1.00
/IP4
/IP4  HEAD-SPEED (NEGATIVE FLOW)
 14
-1.00    3.55       -0.89    3.20       -0.74    2.80       -0.60    2.47
-0.46    2.20       -0.20    1.73        0.00    1.40        0.37    0.80
 0.43    0.74        0.50    0.68        0.58    0.64        0.64    0.62
 0.70    0.61        1.00    0.59
/IP5  TORQUE-FLOW (POSITIVE SPEED)
 17
-1.00    2.98       -0.82    2.40       -0.60    1.87       -0.46    1.60
-0.34    1.40       -0.20    1.21       -0.10    1.10        0.00    1.01
 0.11    0.95        0.22    0.95        0.34    0.97        0.45    0.98
 0.56    0.99        0.67    1.03        0.79    1.08        0.90    1.06
 1.00    1.00
/IP6  TORQUE-FLOW (NEGATIVE SPEED)
 8
-1.00    0.00        0.00   -1.00        0.25   -0.60        0.40   -0.37
 0.50   -0.25        0.60   -0.16        0.80   -0.01        1.00    0.11
/IP7  TORQUE-SPEED (POSITIVE FLOW)
 8
-1.00    0.00        0.00   -0.60        0.50    0.00        0.74    0.33
 0.81    0.54        0.89    0.76        0.99    0.99        1.00    1.00
/IP8  TORQUE-SPEED (NEGATIVE FLOW)
 10
-1.00    2.98       -0.91    2.80       -0.80    2.60       -0.70    2.42
-0.60    2.25       -0.42    2.00        0.00    1.42        0.60    0.61
 0.80    0.35        1.00    0.11
/IP9  HEAD DIFFERENCE-FLOW  (POSITIVE SPEED)
  12
  -1.0   -1.15        -0.9   -1.24        -0.6    -2.8        -0.5   -2.9
  -0.4   -2.7          0.0    0.0          0.12    0.85        0.2    1.1
   0.5    1.02         0.7    1.0          0.9     0.95        1.0    1.0
/IP10  HEAD DIFFERENCE-FLOW  (NEGATIVE SPEED)
  4
  -1.0    0.0          0.0    0.0          0.5    -0.8         1.0   -1.46
/IP11  HEAD DIFFERENCE-SPEED  (POSITIVE FLOW)
  7
  -1.0    0.0          0.0    0.0          0.1    -0.02        0.2    0.0
   0.3    0.1          0.9    0.78         1.0     1.0
/IP12  HEAD DIFFERENCE-SPEED  (NEGATIVE FLOW)
  12
  -1.0   -1.15        -0.8   -0.5         -0.6    -0.2        -0.4    0.03
  -0.2    0.04         0.0    0.1          0.2     0.15        0.4    0.12
   0.6    0.05         0.8   -0.5          0.9    -0.9         1.0   -1.46
/IP13
```

```
  0
/IP14
  0
/IP15
  0
/IP16
  0
/IP17   HEAD MULTIPLIER
 13
  0.0  0.0    0.05 0.0     0.1  0.025     0.15  0.075   0.2  0.18
  0.3    0.475     0.4    0.625     0.5    0.74      0.6     0.82
  0.7    0.87      0.8    0.84      0.9    0.72      1.0     0.08
/IP18   TORQUE MULTIPLIER
 11
  0.0    0.0       0.1    0.0       0.20   0.13      0.3     0.24
  0.4    0.31      0.5    0.33      0.6    0.3       0.7     0.23
  0.8    0.16      0.9    0.08      1.0    0.0
/IP191 IP192   NPSHR
  2  2
        -1.      1.
   -1.   0.      0.
    1.   0.      0.
/   6     6
/ 0.0  0.2  0.4  0.6  0.8  1.0
/ 0.0  0.0  0.0  0.0  0.0  0.0  0.0
/ 0.2  0.0  3.0650E-5  7.7239E-5  1.3263E-4  1.9460E-4  2.6207E-4
/ 0.4  0.0  4.8660E-5  1.2261E-4  2.1053E-4  3.0996E-4  4.1602E-4
/ 0.6  0.0  6.3760E-5  1.6066E-4  2.7587E-4  4.0485E-4  5.4514E-4
/ 0.8  0.0  7.7239E-5  1.9463E-4  3.3419E-4  4.9044E-4  6.6037E-4
/ 1.0  0.0  8.9628E-5  2.2585E-4  3.8780E-4  5.6910E-4  7.6631E-4
SB1602
/NPTB
   2
/IP1
 13
-1.00   2.50      -0.90   2.28      -0.63   2.00      -0.55   1.74
-5.00   1.68      -0.42   1.60      -0.15   1.40       0.00   1.38
 0.25   1.38       0.35   1.35       0.65   1.20       0.80   1.10
 1.00   1.00
/IP2
 15
-1.00  -2.00      -0.68  -1.50      -0.45  -1.00      -0.28  -0.40
-0.23  -0.27      -0.13  -0.20       0.00   0.00       0.15   0.05
 0.35   0.20       0.55   0.30       0.70   0.40       0.86   0.60
 0.96   0.80       0.99   0.90       1.00   1.00
/IP3
 11
-1.00  -2.00      -0.75  -1.94      -0.50  -1.80      -0.12  -1.20
 0.00  -1.02       0.10  -0.90       0.37  -0.50       0.50  -0.25
 0.80   0.40       0.85   0.60       1.00   1.00
/IP4
 12
-1.00   2.50      -0.90   2.28      -0.63   2.00      -0.55   1.74
-0.50   1.68      -0.42   1.60      -0.15   1.40       0.00   1.30
 0.30   1.10       0.50   1.00       0.75   0.88       1.00   1.00
/IP5
 13
```

```
-1.00   2.50      -0.80   2.00      -0.60   1.45      -0.46   1.15
-0.30   0.95      -1.30   0.80       0.00   0.80       0.23   0.80
 0.35   0.87       0.50   0.93       0.60   0.95       0.80   0.96
 1.00   1.00
/IP6
 10
-1.00  -2.00      -0.30  -1.50      -0.18  -1.35      -0.07  -1.00
 0.00  -0.92       0.30  -0.60       0.42  -0.40       0.50  -0.05
 0.75   0.25       1.00   0.57
/IP7
 12
-1.00  -2.00      -0.25  -1.80      -0.12  -1.50      -0.08  -1.40
 0.00  -1.00       0.13  -0.80       0.30  -0.60       0.40  -0.40
 0.50   0.19       0.56   0.20       0.90   0.80       1.00   1.00
/IP8
 12
-1.00   2.50      -0.65   2.15      -0.40   1.79      -0.30   1.61
-0.13   1.50       0.00   1.44       0.10   1.40       0.22   1.20
 0.33   1.10       0.50   1.00       0.80   0.80       1.00   0.57
/IP9
  12
  -1.0   -1.15      -0.9  -1.24      -0.6   -2.8      -0.5   -2.9
  -0.4   -2.7        0.0   0.0        0.12   0.85       0.2    1.1
   0.5    1.02       0.7   1.0        0.9    0.95       1.0    1.0
/IP10
  4
  -1.0    0.0        0.0   0.0        0.5   -0.8        1.0   -1.46
/IP11
  7
  -1.0    0.0        0.0   0.0        0.1   -0.02       0.2    0.0
   0.3    0.1        0.9   0.78       1.0    1.0
/IP12
  12
  -1.0   -1.15      -0.8  -0.5       -0.6   -0.2       -0.4    0.03
  -0.2    0.04       0.0   0.1        0.2    0.15       0.4    0.12
   0.6    0.05       0.8  -0.5        0.9   -0.9        1.0   -1.46
/IP13
  0
/IP14
  0
/IP15
  0
/IP16
  0
/IP17
 13
  0.0  0.0    0.05 0.0     0.1  0.025     0.15  0.075   0.2   0.18
  0.3    0.475     0.4     0.625     0.5     0.74        0.6     0.82
  0.7    0.87      0.8     0.84      0.9     0.72        1.0     0.08
/IP18
 11
  0.0    0.0       0.1     0.0       0.20    0.13        0.3     0.24
  0.4    0.31      0.5     0.33      0.6     0.3         0.7     0.23
  0.8    0.16      0.9     0.08      1.0     0.0
/IP191 IP192
 2  2
         -1.      1.
```

```
   -1.     0.      0.
    1.     0.      0.
/   6      6
/ 0.0  0.2  0.4  0.6  0.8  1.0
/ 0.0  0.0  0.0  0.0  0.0  0.0  0.0
/ 0.2  0.0  3.0650E-5  7.7239E-5  1.3263E-4  1.9460E-4  2.6207E-4
/ 0.4  0.0  4.8660E-5  1.2261E-4  2.1053E-4  3.0996E-4  4.1602E-4
/ 0.6  0.0  6.3760E-5  1.6066E-4  2.7587E-4  4.0485E-4  5.4514E-4
/ 0.8  0.0  7.7239E-5  1.9463E-4  3.3419E-4  4.9044E-4  6.6037E-4
/ 1.0  0.0  8.9628E-5  2.2585E-4  3.8780E-4  5.6910E-4  7.6631E-4
/
/  **** ACCUMULATOR DATA ****
BB17
SB1701
/V    J  NPARA ISTC ENT(WATER) CROSS SEC  VT      V(AIR)  PRS PSET B
  100 79  3    0    50.        2.E1      33.3      10.     46. 60.  2.1E3
SB1702
/ V   J   NPARA  ENT(WATER)    CROSS SEC  VT      V(AIR)  PRS PSET B
  101 78  1    0    50.        2.E1      33.3      10.     46. 60.  2.1E3
/
/  **** BREAK POINT DATA ****
BB18
/ IBJ  IDCTB C2A  CDA  CEA      C2E   CDE  CEE
  11   3110  0.8  0.6  0.6      0.8   0.6  0.6
/ KU(DIS) KU(SUC) KD(DIS)  KD(SUC) TUK  TLK
    1.      1.       1.       1.    1.   1.
/  **** SPECIFIC ENTHALPY OF INITIALLY STAGNANT DATA ****
BB19
/NODE   HE
SB1901
 68    150.
SB1902
 57    150.
SB1903
 59    300.
SB1904
 58    300.
SB1905
 70    300.
SB1906
 69    300.
SB1907
 72    350.
SB1908
 60    250.
SB1909
 61    250.
SB1910
 62    250.
SB1911
 63    250.
SB1912
 64    250.
SB1913
 65    250.
SB1914
 66    250.
```

```
SB1915
 67     250.
SB1916
 94     650.
SB1917
 93     650.
SB1918
 96     650.
SB1919
 95     650.
SB1920
 71     350.
SB1921
 97      30.
SB1922
 98      30.
/
/  **** CORE DATA ****
BB20
SB2001
/ IROD
      1
/          NROD  NVB NVT NSB NST IGAP IQMW
          50752  33  39  1   7   1     1
SB2002
/ IROD
      2
/          NROD  NVB NVT NSB NST IGAP IQMW
            200  40  46  8   14  1     1
BB21
/IDC1  IREAC2 IDC2     IREAC3 IDC3     IREAC4 IDC4     IREAC5 IDC5    NF
 3111    0     0          0      0         0      0         0      0      0
/ L
  2.377E-5
/ RAMDA(J) - BETA(J)
  0.0124      0.0212E-2 0.0305      0.1402E-2  0.111       0.1254E-2
  0.301       0.2529E-2 1.13        0.0736E-2  3.00        0.0269E-2
/ CR           AMACRO  FMACRO      FLUX
  0.6          0.1     0.04        5.E13
/*** DENSITY REACTIVITY ****
         13
/ RHO/RHO(0)    REACTIVITY
         0.     -140.
         0.2     -90.35
         0.4     -42.26
         0.6     -20.12
         0.7     -13.16
         0.8      -7.734
         0.9      -3.448
         0.95     -1.63
         1.        0.
         1.1       2.82
         1.2       5.14
         1.3       7.07
         1.4       8.685
/***  FUEL TEMP - TEMP COEF *******
  2
```

```
/ TMP      REAC COEFFICIENT
  50.     -0.0036
  2280.   -0.0036
/
/***  COOLANT TEMP - TEMP COEF *******
  2
/ TMP      REAC COEFFICIENT
  50.     0.0
  2280.   0.0
/
/
/   **** M - W REACTION ****
BB22
SB2201
/ NN
  2
/ IROD
  1  2
/ HR            K1              K2              LOUT            LIN
  1.54E03       0.775E-04       2.29E04         1.E-7           1.E-7
/
/   **** FUEL GAP DATA ****
BB23
SB2301
/ NN
  2
/ IROD
  1  2
/ MOL           PGC             RGAP            VPL             VOPR            VCR
  5.7E-4        0.0             9.48E-5         5.493E-6        0.0             0.0
/ VCD           TPLC            ENF             ECL             RAMDA
  0.0           0.0             0.9             0.75            0.0
/ HE            XE              KR              AIR             N2
  0.887         0.0355          0.0063          0.0             0.0712
/ H2            H2O
  0.0           0.0
/
/   **** CLAD BURST DATA ****
BB24
SB2401
/ NN
  2
/ IROD
  1  2
/ NI MI
  2  2
/ A             C               B               D               E
  5.00E7        6.96E-08        2.87E4          2.86E-03        1.15E0
/ A0            A1              A2              A3              A4
  1.528E0       1.49E-07        2.0E-08         1.25E-16        1.85E-01
/ A             B               SBURST          BLM             PCORE
/ 8.0E09        3.3E-03         0.1             0.6             1.43E-2
/ A             B               SBURST          BLM
  8.0E09        3.3E-03         0.1             0.6
/
/   **** HEAT SLAB DATA ****
BB26
```

```
/************ AVERAGE CHANNEL ********************
SB2601
/ SLBN1 SLBN2 GEOMT KSLB NSLB NRGN  RI          RO          TSINK COEF DE
  1     7     2     1    50752 2    0.          4.75E-3 0.    0.    0.
/ RGN1  IMAT  NMESH IP             WDTH
  1     -1    7     0              4.025E-3
  2     -2    4     0              6.400E-4
/ COOLANT   COOLANT   IDCL  IDCR  CONDUCTOR  HTRCV  XLH    SGHFL
/ NODE(IN)  NODE(OUT)                LENGTH
  0         33        0     0     0.1        0.     3.71
                                                    PWRD(0)  PWRD(R)
/                                                   0.       0.
                                                    0.       0.
  0         34        0     0     0.732      0.     3.294
                                                    5.565E4  0.
                                                    0.       0.
  0         35        0     0     0.732      0.     2.562
                                                    10.57E4  0.
                                                    0.       0.
  0         36        0     0     0.732      0.     1.83
                                                    10.57E4  0.
                                                    0.       0.
  0         37        0     0     0.732      0.     1.098
                                                    10.57E4  0.
                                                    0.       0.
  0         38        0     0     0.732      0.     0.466
                                                    5.565E4  0.
                                                    0.       0.
  0         39        0     0     0.1        0.     0.05
                                                    0.       0.
                                                    0.       0.

/
/*************** HOT CHANNEL *********************************
SB2608
/ SLBN1 SLBN2 GEOMT KSLB NSLB NRGN      RI          RO          TEMP    C
/ SLBN1 SLBN2 GEOMT KSLB NSLB NRGN  RI          RO          TSINK COEF DE
  8     14    2     1      200  2    0.          4.75E-3 0.    0.    0.
/ RGN1  IMAT  NMESH IP             WDTH
  1     -1    7     0              4.025E-3
  2     -2    4     0              6.400E-4
/ COOLANT   COOLANT   IDCL  IDCR  CONDUCTOR  HTRCV  XLH    SGHF
/ NODE(IN)  NODE(OUT)                LENGTH
  0         40        0     0     0.1        0.     3.71
                                                    0.       0.
                                                    0.       0.
  0         41        0     0     0.732      0.     3.294
                                                    7.23E4   0.
                                                    0.       0.
  0         42        0     0     0.732      0.     2.562
                                                    13.75E4  0.
                                                    0.       0.
  0         43        0     0     0.732      0.     1.83
                                                    13.75E4  0.
                                                    0.       0.
  0         44        0     0     0.732      0.     1.098
                                                    13.75E4  0.
                                                    0.       0.
```

```
0          45         0      0      0.732      0.      0.466
                                                 7.23E4  0.
                                                 0.      0.
0          46         0      0      0.1        0.      0.05
                                                 0.      0.
                                                 0.      0.

/ SG. TUBES
SB2616
 15    20     2    2    3382   1   9.820E-3  1.112E-2  0.     0. 0.
  1     1     5    0               1.30E-3
  4    83               0      0      4.82      0.      9.58
                                                 0.      0.
  5    84               0      0      4.82      0.      4.76
                                                 0.      0.
  6    85               0      0      2.35      0.      1.175
                                                 0.      0.
  7    85               0      0      2.35      0.      1.175
                                                 0.      0.
  8    84               0      0      4.82      0.      4.76
                                                 0.      0.
  9    83               0      0      4.82      0.      9.58
                                                 0.      0.

/ SG. TUBES
SB2619
 21    26     2    2   10146   1   9.820E-3  1.112E-2  0.     0.  0.
  1     1     5    0               1.30E-3
 19    74               0      0      4.82      0.      9.58
                                                 0.      0.
 20    75               0      0      4.82      0.      4.76
                                                 0.      0.
 21    76               0      0      2.35      0.      1.175
                                                 0.      0.
 22    76               0      0      2.35      0.      1.175
                                                 0.      0.
 23    75               0      0      4.82      0.      4.76
                                                 0.      0.
 24    74               0      0      4.82      0.      9.58
                                                 0.      0.

/
SB2620
 27     0     2    0        1   1     1.88      1.938     0.     0. 270.
  1     2     4    0               0.0572
  31    49               0      0      2.202     0.      0.94
                                                 0.      0.

SB2621
 28     0     2    0        1   1     1.88      1.938     0.     0. 270.
  1     2     4    0               0.0572
 31     48               0      0      4.27      0.      2.135
                                                 0.      0.

SB2622
 29     0     2    0        1   2     2.198     2.418     0.     0. 270.
  1     2     4    0               0.00397
  2     3     5    0               0.216
  0     31               0      0      0.793     0.      0.3965
                                                 0.      0.
                                                 0.      0.

SB2623
```

```
30      0       2       0       1    2      2.198      2.418      0.      0. 270.
 1      2       4       0                   0.00397
 2      3       5       0                   0.216
 0       31              0       0          1.269      0.    7.4275
                                                 0.          0.
                                                 0.          0.

SB2624
31      0       1       0       1    1      6.         0.356      0.      0. 270.
 1      2       5       0                   0.0356
 0      31      0       0                   6.         0.    3.793
                                                 0.          0.

SB2629
32      0       2       0      50    1      0.         5.E-2      0.      0.  0.
 1      1       4       0                   5.E-2
 0      54      0       0                   2.3        0.     1.15
                                                 0.          0.

SB2630
33      0       2       0       1    2      2.198      2.418      0.      0.  90.
 1      2       4       0                   0.00397
 2      3       5       0                   0.216
 0       50              0       0          0.793      0.    0.3965
                                                 0.          0.
                                                 0.          0.

SB2631
34      0       2       0       1    2      2.198      2.418      0.      0.  90.
 1      2       4       0                   0.00397
 2      3       5       0                   0.216
 0       50              0       0          1.269      0.    7.4275
                                                 0.          0.
                                                 0.          0.

SB2632
35      0       1       0       1    1      6.         0.356      0.      0.  90.
 1      2       5       0                   0.0356
 0      50      0       0                   6.         0.    3.793
                                                 0.          0.

SB2633
36      0       2       0       1    1      1.88       1.938      0.      0.  90.
 1      2       4       0                   0.0572
 50     49              0       0           2.202  0.     0.94
                                                 0.          0.

SB2634
37      0       2       0       1    1      1.88       1.938      0.      0.  90.
 1      2       4       0                   0.0572
 50     48              0       0          4.27       0.    2.135
                                                 0.          0.

/
/  **** MATERIAL DATA ****
BB27
SB2701
  1
  INCONEL
  2
/ TEMP (C) - DENSITY (NON DIMENSION)
  20.0        1.0
  1000.0      1.0
  8
/ TEMP (C) - VOLUMETRIC HEAT CAPACITY (KCAL/K/M**3)
```

```
 93.3        917.82
 204.4       964.00
 232.2       971.87
 260.0       979.72
 287.8       987.74
 315.6       994.70
 426.7       1028.34
 537.8       1078.61
  3
/ TEMP (C) - THERMAL CONDUCTIVITY (KCAL/S/K/M)
  100.0      0.0041365
  385.0      0.0045502
  1000.0     0.0074457
SB2702
 2
 STAINLESS STEEL ( 18CR 8NI )
 2
 20.0 7820.0  1000.0 7820.0
 2
 20.0 0.118   1000.0 0.118
 5
 20.0 3.5E-3  100.0 3.8E-3  200.0 4.0E-3  400.0 4.7E-3  600.0 5.5E-3
/
SB2703
  3
  MN-MO-NI-STEEL
  2
/ TEMP (C) - DENSITY (NON DIMENSION)
  20.0       1.0
  1000.0     1.0
  5
/ TEMP (C) - VOLUMETRIC HEAT CAPACITY (KCAL/K/M**3)
   75.0      2.999E2
  225.0      3.071E2
  275.       3.217E2
  325.0      3.313E2
  375.       3.458E2
  4
/ TEMP (C) - THERMAL CONDUCTIVITY (KCAL/S/K/M)
    0.       0.0124
  100.       0.01219
  200.       0.0117
  300.       0.01021
/
/ *** STEAM SEPARATOR DATA  ***
BB28
/ J     NMIX  NFS    TAU
SB2801
  64     79   78     1.
SB2802
  68     88   87     1.
/
/  **** VALVE DATA ****
BB29
SB2901
/ VLVNO VLVTP VLVND
  1     -2    69     0     1.     1.  / PORV (PZR)
```

```
SB2902
  2     -2     70      0      1.      1.  / SAFETY VALVE (PZR)
SB2903
  3     -2     94      0      1.      1.  / RELIEF VALVE (LOOP-A)
SB2904
  4     -2     93      0      1.      1.  / SAFETY VALVE (LOOP-A)
SB2905
  5     -2     95      0      1.      1.  / RELIEF  VALVE (LOOP-B)
SB2906
  6     -2     96      0      1.      1.  / SAFETY VALVE (LOOP-B)
SB2907
  7     -1     60      0      1.      1.  / ACC CHECK VALVE
SB2908
  8     -2     63      0      0.      0.  / HPCI CONTROL VALVE
SB2909
  9     -1     64      0      5.      5.  / ACC CHECK VALVE
SB2910
  10    -2     66      0      1.      0.  / HPCI CONTROL VALVE
SB2911
/ 11     2     68      0      1.      1.  / FICTITIOUS VALVE
  11    -2     68      0      1.      1.  / FICTITIOUS VALVE
SB2912
/ 12     2     57      0      1.      1.  / FICTITIOUS VALVE
  12    -2     57      0      1.      1.  / FICTITIOUS VALVE
SB2913
  13     2     92      0      1.      1.  /  FW VALVE
SB2914
  14     2     91      0      1.      1.  /  FW VALVE
SB2915
  15     2     99      0      1.      1.  /  MAIN STEAM VALVE
SB2916
  16    -2     59      0      1.      1.  / SPRAY CONTROL VALVE
SB2917
  17    -2     58      0      1.      1.  / SPRAY CONTROL VALVE
SB2918
  18    -2     62      0      1.      1.  / LPCI CONTROL VALVE
SB2919
  19    -2     67      0      1.      1.  / LPCI CONTROL VALVE
SB2920
  20    -2     71      0      1.      1.  / CVCS BLEED VALVE
SB2921
  21    -2     98      0      5.      5.  / AUX FW
SB2922
  22    -2     97      0      5.      5.  / AUX FW
/
/  **** LOGICAL CONDITION DATA ****
BB30
/      IDSIG   IX1   IX2  IY1  IY2  SETPT
SB3001
 3001  1       0     0    0    0           / TIME OF ACCIDENT OCCURRENCE
                                   0.01    /
SB3002
 3002 -2      99     0    0    0             / MS LINE PRESS LOW
                                   40.       /
SB3003
 3003  2      52     0    0    0             / PORV (PZR) OPEN : 2350 PSIA
                                   159.91    / PORV (PZR) OPEN : 2350 PSIA
```

```
SB3004
 3004 -2     52     0    0    0                    / PORV (PZR) CLOSE : 2330 PSIA
                                        158.55     / PORV (PZR) CLOSE : 2330 PSIA
SB3005
 3005  2     52     0    0    0                    / SAFETY VALVES (PZR) OPEN: 250
                                        170.11     / SAFETY VALVES (PZR) OPEN: 250
SB3006
 3006 -2     52     0    0    0                    / SAFETY VALVE (PZR) CLOSE: 250
                                        170.11     / SAFETY VALVE (PZR) CLOSE: 250
SB3007
 3007  2     80     0    0    0                  / 2NDRY SAFETY VALVE (A) OPEN : 1
                                         74.85   / 2NDRY SAFETY VALVE (A) OPEN : 1
SB3008
 3008 -2     80     0    0    0                  / 2NDRY SAFETY VALVE (A) CLOSE: 1
                                         68.05   / 2NDRY SAFETY VALVE (A) CLOSE: 1
SB3009
 3009  2     89     0    0    0                  / 2NDRY SAFETY VALVE (B) OPEN: 11
                                         74.85   / 2NDRY SAFETY VALVE (B) OPEN: 11
SB3010
 3010 -2     89     0    0    0                  / 2NDRY SAFETY VALVE (B) CLOSE: 1
                                         68.05   / 2NDRY SAFETY VALVE (B) CLOSE: 1
SB3011
 3011  2     80     0    0    0                   / 2NDRY RELIEF VALVE OPENS.
                                         66.      / 2NDRY RELIEF VALVE OPENS.
SB3012
 3012 -2     80     0    0    0                   / 2NDRY RELIEF VALVE CLOSES.
                                         64.      / 2NDRY RELIEF VALVE CLOSES.
SB3013
 3013  2     89     0    0    0                   / 2NDRY RELIEFVALVE OPENS.
                                         66.      / 2NDRY RELIEFVALVE OPENS.
SB3014
 3014 -2     89     0    0    0                   / 2NDRY RELIEF VALVE CLOSES.
                                         64.      / 2NDRY RELIEF VALVE CLOSES.
SB3015
 3015 -2     52     0    0    0                   / PZR PRESS  < 123.8 ATA
                                        123.8     /
SB3016
 3016 -2     52     0    0    0                   / PZR PRESS  < 10 ATA
                                         10.      /
SB3017
 3017 -8     14     0    0    0                   / COLD LEG G LOW
                                        0.85E4    /
SB3018
 3018 -8     28     0    0    0                   / COLD LEG G LOW
                                        0.85E4    /
SB3019
 3019 -9   3017     0 3018 0                       / 3017 OR 3018
                                          0.      /
SB3020
 3020 -9   3002     0 3015 0                       / 3002 OR 3015
                                          0.      / ECCS ACTUATION OR MSL ISOLATIO
SB3021
 3021 -9   3019     0 3020 0                       / 3002 OR 3015 OR 3017 OR 3018
                                          0.      /
SB3022
 3022  4     0     0    0    0                     / REACTOR POWER  >  1.15
                                         1.15     /
```

```
SB3023
3023  -9  3021    0  3022 0          / 3002 OR 3015 OR 3017 OR 3018
                              0.     / OR 3022 -- (SCRAM CONDITION)

BB31
/**** CONTROL INPUT DATA
SB3101
TMP   -3101    49    1.          /CORE OUTLET TMP
SB3102
CONS  -3102     0    1.          /CONSTANT ( ONE )
SB3103
TRTM  -3103   418    1.          /TIME AFTER SCRAM
SB3104
CONS  -3104     0    0.          /CONSTANT (ZERO)
SB3106
AAA   -3105     1    1.          /MCP1 SPEED
//
/ITYPE IDC INC1 INC2 INC3 INC4 GAIN CP1 CP2 CIC CMIN CMAX
//
// ***** MS FLOW RATE  *****
//
SB3116
FGT  3107  0   3201   0   0   1.   0.  0. 1. -1.E10 1.E10
//
//  (SET ZERO IF 3020 IS SATISFIED.)
//
SB3117
IF   3108 -3104  3107 3020 0    1.   0.  0. 1. -1.E10 1.E10
//
// *****  FW *****      (DELAYED MS FLOW RATE)
//
SB3118
LAG   3109 3108   0    0   0    1.   0. 100.  1. -1.E10 1.E10
//
// *****  CONTAINMENT PRESSURE IN LBLOCA *********
//
SB3119
FGT   3110  0   3208   0   0    1.   0.  0. 1. -1.E10 1.E10
//
// *****  SCRAM REACTIVITY *********
//
SB3120
FNG   3111 -3103 3207   0   0    1.   0.  0. 0. -1.E10 1.E10
//
// *****  ATMOSPHERIC PRESSURE  *********
//
SB3121
FGT   3112  0   3209   0   0    1.   0.  0. 1. -1.E10 1.E10
//
// *****  AUX FW   *********
SB3122
TIF 3113 -3102 -3104  416  0    1.   0.  0. 0. -1.E10 1.E10 /AUX FW
SB3123
TIF 3114 -3102 -3104  417  0    1.   0.  0. 0. -1.E10 1.E10 /AUX FW
//
// *****  LPCI   *********
SB3124
TIF 3115 -3102 -3104  411  0    1.   0.  0. 0. -1.E10 1.E10 /AUX FW
```

```
SB3125
TIF 3118 -3102 -3104  412  0    1.   0.  0. 0. -1.E10 1.E10 /
//
// *****  HPCI   *********
SB3126
TIF 3116 -3102 -3104  409  0    1.   0.  0. 0. -1.E10 1.E10 /
SB3127
TIF 3117 -3102 -3104  410  0    1.   0.  0. 0. -1.E10 1.E10 /
//
// *****  PZR HEATER TRIP *****
SB3128
IF  3119 -3104 -3102 3023  0    1.   0.  0. 1. -1.E10 1.E10 /
SB3129
LAG 3120  3119   0    0    0    1.   0.  2. 1. -1.E10 1.E10 /
//
BB32
SB3201
 ******  MS FLOW RATE  ****
/     (BEFORE ISOLATION OF MS LINE)
  3201 3
/ TIME (SEC)  RELATIVE FLOW RATE
  0.            1.
  1.            1.
  10000.        1.
SB3204
*******  DUMMY  *******
  3204   2
/ TIME (SEC)  RELATIVE FLOW RATE
  0.           1.
  1.E4         1.
SB3205
*******  DUMMY  ******
  3205   2
/ TIME (SEC)  RELATIVE FLOW RATE
  0.          1.
  1.E4        1.
/
SB3207
****  SCRAM REACTIVITY ******
  3207   10
/ TIME AFTER SCRAM SIGNAL IS GENERATED     REACTIVITY
  0.0                                       0.0
  0.05                                      0.0
  1.0                                      -0.24
  1.5                                      -0.6
  2.0                                      -2.05
  2.2                                      -4.11
  2.4                                      -7.37
  2.7                                      -8.15
  3.0                                      -8.42
  1.E3                                     -8.42
SB3208
**** CONTAINMENT PRESSURE IN LBLOCA ***
  3208  4
/       TIME(S)   PRESSURE(ATA)
        0.        1.
        7.5       2.7
```

```
        15.         4.
        10000.      4.
SB3209
**** ATMOSPHERIC PRESSURE  ***
  3209  2
/       TIME(S)    PRESSURE(ATA)
        0.          1.
        1.E4        1.
BEND
END
```

E.2 Input Data for Restart Job

```
/
/  **** PROGRAM CONTROL DATA ****
BB01
/ LDMP NEDI NTC NTRP MTRP IOUT NPERT ICLAS LSEC IDPSTP DMPTM
  2    6    4   19   23   0    0      5      0     0    0.
/ NOCK
  0
/  **** MINOR EDIT DATA ****
BB02
PRA-44  GLE-44 GLA-13 GLE-31 GLE-50 GLE-64
/
/  **** TIME STEP CONTROL DATA ****
BB03
SB0301
/ E1   E2   E3
/ 0.2  0.2  100.
  -2
/ NMIN NMAJ NDMP NCHK   DTMAX    DTMIN    TLAST  EPSMX
SB0302
  180  100 100  0   1.0E-3   1.0E-6     0.5
SB0303
  120  100 100  0   4.0E-3   1.0E-6    20.0
SB0304
   60  80  50   0  64.0E-3   1.0E-6    40.0
SB0305
   80  100 50   0   6.0E-3   1.0E-6  1000.0
/
/  **** TRIP CONTROL DATA ****
BB04
/  IDTRP IZ1  IZ2  ION   IOFF  IOCS  DELAY
SB0401
401  2     1    0   3023    0     0    0.  / RCP-1 TRIP
SB0402
402  2     2    0   3023    0     0    0.  / RCP-1A TRIP
SB0403
403  4     1    0   3003 3004     0    0.  / PORV (PZR)
SB0404
404  4     2    0   3005 3006     0    0.  / SAFETY VALVES (PZR)
SB0405
405  4     4    0   3007 3008     0    0.  / SAFETY VALVE (LOOP-A)
SB0406
406  4     6    0   3009 3010     0    0.  / SAFETY VALVE (LOOP-B)
SB0407
```

```
407  4      3    0    3011 3012      0    0.    / SG 2NDRY RELIEF VALVE
SB0408
408  4      5    0    3013 3014      0    0.    / SG 2NDRY RELIEF VALVE
SB0409
409  4      8    0    3015    0      0   22.2   /HPCI VALVE OPENS.
SB0410
410  4     10    0    3015    0      0   22.2   /HPCI VALVE OPENS.
SB0411
411  4     18    0    3016    0      0    0.    /LPCI VALVE OPENS.
SB0412
412  4     19    0    3016    0      0    0.    /LPCI VALVE OPENS.
SB0413
413  4     13    0    3020    0      0    0.5   / FW VALVE CLOSES.
SB0414
414  4     14    0    3020    0      0    0.5   / FW VALVE CLOSES.
SB0415
415  4     15    0    3020    0      0    0.5   / MS VALVE CLOSES.
SB0416
416  4     21    0    3020    0      0   37.    /AUX FW VALVE OPENS.
SB0417
417  4     22    0    3020    0      0   37.    /AUX FW VALVE OPENS.
SB0418
418  3      0    0    3023    0      0    0.1   / REACTOR SCRAM
SB0419
/419  7     11    0       0    0      0    0.0   / COLD LEG BREAK
 419  7     11    0    3001    0      0    0.0   / COLD LEG BREAK
BEND
END
```